

The effects of green tea, green rooibos and  
their major flavonoids (EGCG and aspalathin)  
on testicular cell health *in vitro*

by

Robin Alvin Booysen

---



UNIVERSITY *of the*  
WESTERN CAPE

*A thesis submitted in partial fulfilment of the requirements  
for the degree of **Doctor Philosophiae**  
in the Department of Medical Bioscience,  
University of the Western Cape.*

**Supervisor:** Prof. TK Monsees  
**Co-supervisor:** Dr SH Adbul-Rasool

May 2021

<http://etd.uwc.ac.za/>



UNIVERSITY *of the*  
WESTERN CAPE

Copyright © 2021  
University of the Western Cape  
All rights reserved

# Dedication

---

During the course of this project I have lost six family members and, in reflection of the years spent on this project, I can't help but think of them. I also can't help but think of the rest of my deceased family, who won't be able to celebrate this victory with me.

This project was emotionally draining on me and has pushed me near a breaking point multiple times. Despite the many challenges that I have faced, I eventually completed it and so I want to dedicate this thesis to my deceased family:



Mr Joël Phillipus Ballem (1969-2021)  
Mr Ashley Edwin Booysen (1963-2021)  
Miss Chricenda Murray (1992-2019)  
Miss Mischka Jade Xena Solomons (2005-2017)  
Mr David Hamy Ballem (1929-2017)  
Mrs Marina Everina Ballem (1935-2015)  
Mr Mervin Ernest Booysen (1953-2013)  
Mrs Gaynor Janine Jansen van Rensburg (1977-2002)  
Mrs Winifred Martha Booysen (1926-2000)  
Mrs Gloria Mary van Wyk (1950-1999)  
Mr Ernest Booysen (1925-1990)  
Baby: Naomi Booysen, Jnr (1983)

None of you will ever read this dedication, but I do it in memory of you. I love all of you and I wish that you were still here with me.

# Declaration

---

I, **Robin Alvin Booysen**, declare that ***The effects of green tea, green rooibos and their major flavonoids (EGCG and aspalathin) on testicular cell health in vitro*** is my own work, that it has not been submitted for any degree or examination in any other university, and that all the sources I have used or quoted have been indicated and acknowledged by complete references.

Robin Alvin Booysen

31 May 2021

Full Name

Date



UNIVERSITY *of the*  
WESTERN CAPE

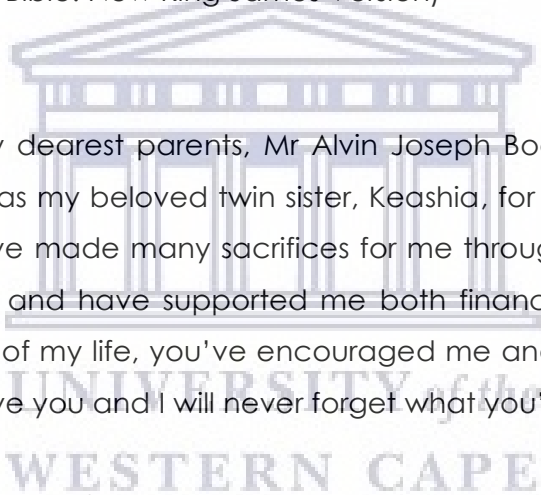
# Acknowledgements

---

...Blessed be the name of God forever and ever, For wisdom and might are His.  
And He changes the times and the seasons; He removes kings and raises up kings;  
He gives wisdom to the wise and knowledge to those who have understanding.  
He reveals deep and secret things; He knows what is in the darkness, and light dwells  
with Him.

'I thank You and praise You, O God of my fathers; You have given me wisdom and  
might...'

**Daniel 2: 20-23** (The Holy Bible: New King James Version)



I would like to thank my dearest parents, Mr Alvin Joseph Booysen and Mrs Naomi Levina Booysen, as well as my beloved twin sister, Keashia, for always supporting me with my studies. You have made many sacrifices for me throughout my life, more so than anybody else has, and have supported me both financially and emotionally. During the lowest points of my life, you've encouraged me and consoled me. Thank you for your support; I love you and I will never forget what you've done for me.

I also thank my supervisors, Prof. Thomas Monsees and Dr Sahar Abdul-Rasool for their guidance and expert help in completing this thesis. When my project was met with challenges, you were patient and helped me to get through those times. Thank you especially for your help during the final stages of this project.

I would like to thank the following people for allowing me the use their equipment during this project. Prof. Charlene Africa (NanoDrop™ 2000), Prof. David Fisher (Millicell® volt-ohmmeter), Prof. Donovan Hiss (Glomax®-Multi Detection System), Prof. Ralf Henkel (analytical balance, pH meter), Prof. Mervin Meyer (POLARstar® Omega microplate reader, BD Accuri™ C6 flow cytometer and other lab equipment), Mrs Eloise Braaf (freeze-drier), the Institute for Microbial Biotechnology and Metagenomics (Light Cycler® 480 II), as well as Ms Bianca Sansom and the Genomics Unit of the South African Medical Research Council (QuantStudio™ 7 Flex).

I also thank the following people for helping me with some practical aspects of this project: Miss Tarryn Webber for help with the MTT assay, flow cytometry, the testosterone trials and general lab assistance; Mr Radwan Abdulgader for general lab assistance; Mrs Eurinah Koeras for help with cell culture maintenance; Miss Sameera Slahudeen for help with the qPCR and Miss Janet Olugbodi for help with some of the flow cytometry.

I would like to thank the following people for technical advice with specific assays: Dr Bronwyn Kirby-McCullough for guidance with qPCR optimisation and execution; Dr Nicole Sibuyi and Mr Thomson Msiska for help with flow cytometry; Miss Bianca Gordon for help with AGE photography and NanoDrop™ 2000; Mr Dewald Schoeman for help with ImageJ densitometry; Dr Olufemi Alamu for help with TEER.

I thank Mr Freddy Williams from Winelands Pork in Bellville for donating the boar testes used in the primary culture experiment, and for ensuring that the testes were freshly excised when I received them.

I also wish to thank the University of the Western Cape's Department of Medical Bioscience, at large, for their general assistance in any research related issues. Thank you for lending me resources while I awaited my deliveries, thank you for helping me to resolve problems and thank you for any advice that you've given me.

The financial assistance of the National Research Foundation (NRF) towards this research is hereby acknowledged. Opinions expressed and conclusions arrived at are those of the author and not necessarily to be attributed to the NRF.

# Abstract

---

The testes play a central role in the male reproductive system, as they represent the sites of male sex steroidogenesis and of spermatogenesis. Leydig cells, located at the testicular interstitium, produce predominantly testosterone upon stimulation with either chorionic gonadotropin (CG) or luteinising hormone by a series of enzymatic modifications of cholesterol. Sertoli cells respond to testosterone and follicle stimulating hormone to secrete inhibin and facilitate spermatogenesis by additional activities like maintaining Sertoli cell barrier (SCB) integrity and lactate secretion. Ultimately the Leydig cells, Sertoli cells etc. all work together to confer male *fertility*. However, infertility occurs globally; leading to the pursuit of treatment, including herbal medicines.

Tea and rooibos are popular health drinks with global reach. Both have a green/unfermented form, which are said to possess potent health-beneficial properties. Polyphenols, and especially the flavonoids: epigallocatechin gallate (EGCG, from green tea) and aspalathin (from green rooibos), are held as primarily responsible for their health benefits. These flavonoids are known antioxidants that can interact with proteins, carbohydrates and fats, making them bioactive compounds of interest to health sciences. However, research on the effects of these teas and flavonoids on male reproduction are scarce and sometimes conflicting. Hence, this thesis aimed to determine some of the mechanisms by which green tea, green rooibos, EGCG and aspalathin affect model Leydig and Sertoli cells *in vitro*.

The murine TM3 (Leydig) and TM4 (Sertoli) cell lines were cultured *in vitro* and exposed to varying concentrations of green tea, green rooibos, EGCG or aspalathin for 24 hours. Thereafter, the cells were assayed for oxidoreductase activity (by MTT: 3-(4,5-dimethylthiazol-2-yl)-2,5-diphenyltetrazolium bromide), morphological alterations (light microscopy), mitochondrial membrane potential ( $\Delta\Psi_m$  by tetramethylrhodamine ethyl ester) and reactive oxygen species (by chloromethyl 2',7'-dichlorodihydrofluorescein diacetate). TM3 cells, as well as boar testes *ex vivo*, were assayed for hCG-stimulated and unstimulated testosterone secretion. TM3 cells were assayed for mRNA expression of selected genes involved in steroidogenesis; namely *Lhcgr*, *Star*, *Tspo*, *Cyp11a1*, *Cyp17a1* and *Hsd17b3*, as well as for *Gapdh* as a housekeeping gene. TM4 cells were

also assayed for inhibin B secretion, lactate secretion and SCB integrity (by transepithelial electrical resistance).

Within the tested concentration range of the teas and flavonoids used in this study, no cytotoxic effects were observed in Leydig or Sertoli cells. The experimental data further suggest that both green tea and green rooibos increase mitochondrial activity, resulting in lower cytosolic NADH, consequently decreasing oxidoreductase activity of Sertoli cells. Furthermore, lactate secretion was slightly reduced in Sertoli cells exposed to the teas. Contrary to this, their major flavonoids, EGCG and aspalathin did not exert the same responses. Sertoli cells exposed to EGCG or aspalathin showed a significant decrease in oxidoreductase activity without affecting lactate secretion or the SCB.

In Leydig cells, both EGCG and aspalathin induced slight decreases in  $\Delta\Psi_m$  without affecting oxidoreductase activity. However, the flavonoids altered steroidogenic gene expression. EGCG increased both basal and hCG-stimulated *Tspo* expression, as well as stimulated *Star* expression. In contrast, aspalathin did not affect *Star* expression, but increased both basal and stimulated *Tspo* expression. All in all, these data suggest that both EGCG and aspalathin exerted pro-steroidogenic effects on Leydig cells.

The murine TM3 (Leydig) and TM4 (Sertoli) cell lines are often used to investigate the effects of plant extracts on testicular functions. Several authors reported testosterone secretion in TM3 cells, and the TM3 cell population used here also proved to produce testosterone before the start of this study. However, in the interim, the cell physiology seems to have changed. As it turned out, both the TM3 and TM4 cell lines seemed to display a divergent physiology. The mRNA from some critical steroidogenic genes (i.e. *Lhcgr*, *Cyp11a1* and *Hsd17b3*) could not be detected in the TM3 cells via PCR. That could explain why those cells were unresponsive to hCG. The TM4 cells did not secrete detectable levels of inhibin B either, indicating aberrant physiology for Sertoli cells.

## Keywords

---

Green tea, Green rooibos, Epigallocatechin gallate (EGCG), Aspalathin, Leydig cell, TM3 cell, Sertoli cell, TM4 cell, Steroidogenesis, Energy metabolism.



# Table of Contents

---

<b>Title</b>	<b>Page</b>
Dedication.....	ii
Declaration.....	iii
Acknowledgements.....	iv
Abstract .....	vi
Keywords .....	vii
Table of Contents .....	viii
List of Figures.....	xiii
List of Tables.....	xviii
List of Abbreviations .....	xix
<b>Chapter 1: Introduction &amp; Literature review .....</b>	<b>2</b>
<b>1.1. A brief overview of the male reproductive system .....</b>	<b>3</b>
<b>1.2. Testicular anatomy and histology .....</b>	<b>4</b>
<b>1.3. Leydig cells .....</b>	<b>6</b>
<b>1.3.1 Steroids .....</b>	<b>6</b>
<b>1.3.2 Hypothalamus-pituitary-testis axis.....</b>	<b>8</b>
<b>1.3.3 Leydig cell signal transduction .....</b>	<b>8</b>
1.3.3.1 Protein kinase A pathway .....	8
1.3.3.2 Arachidonic acid pathway .....	9
1.3.3.3 Calcium and other ions in Leydig cell signalling.....	9
<b>1.3.4 Mitochondria and steroidogenesis .....</b>	<b>12</b>
1.3.4.1 Testosterone biosynthesis .....	14
<b>1.4. Sertoli cells .....</b>	<b>16</b>
<b>1.4.1 Sertoli cell signal transduction .....</b>	<b>17</b>
1.4.1.1 Follicle stimulating hormone and Sertoli cell signalling .....	18
1.4.1.2 Testosterone and Sertoli cell signalling .....	18
<b>1.4.2 Spermatogenesis and the Sertoli cell barrier .....</b>	<b>19</b>
<b>1.5. Infertility and some African cultural beliefs .....</b>	<b>21</b>

---

1.6. Herbal Medicine .....	22
1.6.1 Tea .....	22
1.6.2 Rooibos .....	24
1.7. Plant polyphenols.....	26
1.7.1 Flavonoids .....	26
1.7.2 Polyphenols as antioxidants .....	28
1.7.2.1 Polyphenols as direct antioxidants .....	29
1.7.2.2 Polyphenols as indirect antioxidants .....	30
1.7.3 Polyphenols as pro-oxidants .....	30
1.7.3.1 ROS in cell signalling, a role for anti- and pro-oxidants .....	30
1.7.4 Polyphenol bioavailability and interactions with other biomolecules ....	32
1.7.4.1 Polyphenols and lipids .....	32
1.7.4.2 Polyphenols and proteins.....	32
1.7.4.3 Polyphenols and carbohydrates.....	33
1.7.4.4 Polyphenols in plasma .....	33
1.7.5 Male reproductive system studies with green tea, rooibos and EGCG ..	34
1.8. Aims and objectives of this thesis.....	42
Chapter 2: Materials & Methods .....	44
2.1 List of materials .....	45
2.2 Sample preparation .....	48
2.2.1 Green tea and green rooibos preparation .....	48
2.2.2 EGCG and aspalathin preparation .....	49
2.3 Cell culture .....	50
2.3.1 Cell maintenance .....	50
2.3.2 Trypsinisation .....	50
2.3.3 Subculturing and freezing .....	50
2.3.4 Cell counting for experiments .....	51
2.4 MTT (and photo microscopy) experiments .....	52
2.4.1 MTT principle .....	52
2.4.2 Cell seeding and treatment.....	52
2.4.3 Photo microscopy .....	53
2.4.4 MTT assay.....	53

---

2.5 TMRE experiments.....	<b>54</b>
2.5.1 TMRE principle.....	54
2.5.2 Cell seeding and treatment.....	54
2.5.3 TMRE assay.....	55
2.6 CM-H <sub>2</sub> DCFDA experiments.....	<b>56</b>
2.6.1 CM-H <sub>2</sub> DCFDA principle.....	56
2.6.2 ROS assay by flow cytometry.....	56
2.6.3 ROS assay trials by microplate reader.....	57
2.7 Leydig cell testosterone secretion experiments.....	<b>59</b>
2.7.1 TM3 cell testosterone secretion experimets.....	59
2.7.1.1 Forty eight hour experiment with complete medium.....	59
2.7.1.2 Twenty four hour experiment with complete medium.....	59
2.7.1.3 Forty eight hour experiment with plain medium.....	59
2.7.2 Boar testis testosterone secretion experiment.....	60
2.7.3 Testosterone ELISA.....	61
2.8 Steroidogenic mRNA expression experiments.....	<b>62</b>
2.8.1 Primer design.....	62
2.8.2 Cell seeding and treatment.....	62
2.8.3 RNA extraction.....	64
2.8.4 Reverse transcription.....	65
2.8.5 Conventional polymerase chain reaction.....	66
2.8.6 Agarose gel electrophoresis.....	67
2.8.7 Densitometry measurements.....	68
2.8.8 qPCR optimisation.....	69
2.8.9 Gel clean-up and qPCR standard curve generation.....	70
2.8.10 Real time qPCR.....	70
2.8.11 Calculation of the Pfaffl ratio.....	71
2.9 Inhibin B secretion experiments.....	<b>72</b>
2.9.1 Cell seeding and treatment.....	72
2.9.2 Inhibin B ELISA.....	72
2.10 Lactate secretion experiments.....	<b>73</b>
2.10.1 Lactate assay principle.....	73
2.10.2 Cell seeding and treatment.....	73

---

2.10.3 Lactate assay procedure .....	74
2.10.4 Calculation of lactate concentration .....	75
2.11 TEER experiments .....	<b>76</b>
2.11.1 TEER principle .....	76
2.11.2 Plate preparation and cell seeding .....	76
2.11.3 TEER readings .....	77
2.11.4 Cell treatment .....	77
2.11.5 TEER calculations .....	78
2.12 Statistical Analysis .....	<b>79</b>
Chapter 3: Results .....	<b>80</b>
3.1 MTT assay .....	<b>81</b>
3.2 Photo microscopy .....	<b>90</b>
3.2.1 TM3 cell morphology .....	90
3.2.2 TM4 cell morphology .....	100
3.3 TMRE assay .....	<b>105</b>
3.4 CM-H <sub>2</sub> DCFDA assays .....	<b>110</b>
3.4.1 CM-H <sub>2</sub> DCFDA assay by flow cytometry .....	110
3.4.2 CM-H <sub>2</sub> DCFDA assay trial by plate reader .....	115
3.5 Leydig cell testosterone secretion trials .....	<b>117</b>
3.6 AGE results from PCRs for steroidogenic gene expression .....	<b>122</b>
3.6.1 Conventional PCR AGE results .....	122
3.6.2 qPCR AGE results .....	129
3.7 Quantitative PCR assay for steroidogenic gene expression .....	<b>132</b>
3.8 TM4 cell inhibin B secretion .....	<b>136</b>
3.9 TM4 cell lactate secretion .....	<b>138</b>
3.10 TEER assay .....	<b>142</b>
Chapter 4: Discussion .....	<b>144</b>
4.1 Choosing concentrations for <i>in vitro</i> testicular cell studies .....	<b>145</b>
4.2 The effects of green tea on testicular cell physiology .....	<b>147</b>
4.2.1 Effects of green tea on Leydig cell health .....	147
4.2.1.1 TM3 cells and testosterone .....	148

---

4.2.1.2 Boar testis primary culture .....	149
4.2.1.3 Challenges of using flow cytometry .....	149
4.2.1.4 Leydig cell mitochondrial membrane potential.....	152
4.2.1.5 Flaw in the ROS assay .....	153
<b>4.2.2 Effects of green tea on Sertoli cell health .....</b>	<b>154</b>
4.2.2.1 The MTT assay and mitochondria.....	154
4.2.2.2 Green tea and Sertoli cell energy metabolism.....	155
4.2.2.3 Green tea and Sertoli cell ROS.....	156
4.2.2.4 Problems with the TM4 cell model .....	156
<b>4.3 The effects of EGCG on testicular cell physiology .....</b>	<b>158</b>
<b>4.3.1 Effects of EGCG on Leydig cell health .....</b>	<b>158</b>
4.3.1.1 Aberrant TM3 cell gene expression .....	159
<b>4.3.2 Effects of EGCG on Sertoli cell health .....</b>	<b>161</b>
<b>4.4 The effects of green rooibos on testicular cell physiology.....</b>	<b>163</b>
<b>4.4.1 Effects of green rooibos on Leydig cell health .....</b>	<b>163</b>
<b>4.4.2 Effects of green rooibos on Sertoli cell health .....</b>	<b>164</b>
<b>4.5 The effects of aspalathin on testicular cell physiology .....</b>	<b>165</b>
<b>4.5.1 Effects of aspalathin on Leydig cell health .....</b>	<b>165</b>
<b>4.5.2 Effects of aspalathin on Sertoli cell health .....</b>	<b>167</b>
<b>Chapter 5: Conclusions &amp; Recommendations.....</b>	<b>170</b>
5.1 General conclusions .....	171
5.2 Recommendations.....	172
<b>List of References .....</b>	<b>174</b>
<b>Appendices .....</b>	<b>196</b>



# List of Figures

---

Title	Page
<b>Chapter 1</b>	
<b>Figure 1.1.</b> Illustration of a human sagittal section, showing the organs of the male reproductive system. ....	4
<b>Figure 1.2.</b> Photograph showing a transverse section of a human testis. ....	5
<b>Figure 1.3.</b> The human seminiferous tubule in cross-section. ....	6
<b>Figure 1.4.</b> Diagram showing representatives of the main steroid classes. ....	7
<b>Figure 1.5.</b> Scematic diagram showing Leydig cell signal transduction. ....	11
<b>Figure 1.6.</b> Scematic diagram showing steroidogenesis in Leydig cells. ....	15
<b>Figure 1.7.</b> Illustrations of the Sertoli cell. ....	17
<b>Figure 1.8.</b> Photographs of the green tea plant, tea leaves and tea. ....	23
<b>Figure 1.9.</b> Photographs of the rooibos plant, tea leaves and teas. ....	25
<b>Figure 1.10.</b> Diagram showing the classification of polyphenols, with subdivisions of the flavonoids. ....	27
<b>Figure 1.11.</b> Diagram showing the structures of flavonoids, including EGCG and aspalathin. ....	28
<b>Figure 1.12.</b> Diagram showing the pro-oxidant pathway for catecholic (or pyrogallolic) polyphenols, by use of copper(II) ions. ....	31
<b>Chapter 2</b>	
<b>Figure 2.1.</b> Diagram illustrating the principle of using TMRE to measure mitochondrial membrane potential. ....	54
<b>Figure 2.2.</b> Diagram illustrating the principle of how CMH <sub>2</sub> DCFDA reacts to signal ROS levels within cells. ....	57
<b>Figure 2.3.</b> Diagram showing an overview of the lactate assay principle. ....	73
<b>Figure 2.4.</b> Schematic diagram showing the apparatus used to test for transepithelial electrical resistance. ....	76

Chapter 3

<b>Figure 3.1.</b>	Graph showing the effects of green tea on TM3 cell oxidoreductase activity, both with and without hCG. ....	82
<b>Figure 3.2.</b>	Graph showing the effects of green rooibos on TM3 cell oxidoreductase activity, both with and without hCG. ....	83
<b>Figure 3.3.</b>	Graph showing the effects of EGCG on TM3 cell oxidoreductase activity, both with and without hCG. ....	84
<b>Figure 3.4.</b>	Graph showing the effects of aspalathin on TM3 cell oxidoreductase activity, both with and without hCG. ....	85
<b>Figure 3.5.</b>	Graph showing the effects of green tea on TM4 cell oxidoreductase activity.....	86
<b>Figure 3.6.</b>	Graph showing the effects of green rooibos on TM4 cell oxidoreductase activity.....	87
<b>Figure 3.7.</b>	Graph showing the effects of EGCG on TM4 cell oxidoreductase activity.....	88
<b>Figure 3.8.</b>	Graph showing the effects of aspalathin on TM4 cell oxidoreductase activity.....	89
<b>Figure 3.9.</b>	Photomicrographs showing TM3 cell morphology after treatment with green tea. ....	91
<b>Figure 3.10.</b>	Photomicrographs showing TM3 cell morphology after treatment with green tea and hCG.....	92
<b>Figure 3.11.</b>	Photomicrographs showing TM3 cell morphology after treatment with green rooibos.....	94
<b>Figure 3.12.</b>	Photomicrographs showing TM3 cell morphology after treatment with green rooibos and hCG. ....	95
<b>Figure 3.13.</b>	Photomicrographs showing TM3 cell morphology after treatment with EGCG. ....	96
<b>Figure 3.14.</b>	Photomicrographs showing TM3 cell morphology after treatment with EGCG and hCG. ....	97
<b>Figure 3.15.</b>	Photomicrographs showing TM3 cell morphology after treatment with aspalathin.....	98
<b>Figure 3.16.</b>	Photomicrographs showing TM3 cell morphology after treatment with aspalathin and hCG. ....	99

---

<b>Figure 3.17.</b> Photomicrographs showing TM4 cell morphology after treatment with green tea. ....	101
<b>Figure 3.18.</b> Photomicrographs showing TM4 cell morphology after treatment with green rooibos.....	102
<b>Figure 3.19.</b> Photomicrographs showing TM4 cell morphology after treatment with EGCG.....	103
<b>Figure 3.20.</b> Photomicrographs showing TM4 cell morphology after treatment with aspalathin.....	104
<b>Figure 3.21.</b> Graph showing the effects of green tea and green rooibos on the mitochondrial membrane potential of TM3 cells.....	106
<b>Figure 3.22.</b> Graph showing the effects of EGCG and aspalathin on the mitochondrial membrane potential of TM3 cells.....	107
<b>Figure 3.23.</b> Graph showing the effects of green tea and green rooibos on the mitochondrial membrane potential of TM4 cells.....	108
<b>Figure 3.24.</b> Graph showing the effects of EGCG and aspalathin on the mitochondrial membrane potential of TM4 cells.....	109
<b>Figure 3.25.</b> Graph showing the effects of green tea and green rooibos on TM3 cell intracellular ROS, as determined by flow cytometry.....	110
<b>Figure 3.26.</b> Graph showing the effects of EGCG on TM3 cell intracellular ROS, as determined by flow cytometry.....	111
<b>Figure 3.27.</b> Graph showing the effects of aspalathin on TM3 intracellular ROS, as determined by flow cytometry.....	112
<b>Figure 3.28.</b> Graph showing the effects of green tea and green rooibos on TM4 cell intracellular ROS, as determined by flow cytometry.....	113
<b>Figure 3.29.</b> Graph showing the effects of EGCG and aspalathin on TM4 cell intracellular ROS, as determined by flow cytometry.....	114
<b>Figure 3.30.</b> An overview of results from the TM3 cell trials for ROS determination by microplate reader.....	115
<b>Figure 3.31.</b> Representative graphs from the trial ROS assay by microplate reader. ....	116
<b>Figure 3.32.</b> Graph showing the levels of TM3 cell testosterone secretion after 48 hours with complete medium.....	118
<b>Figure 3.33.</b> Graph showing the levels of TM3 cell testosterone secretion after 24 hours with complete medium.....	119



<b>Figure 3.34.</b> Graph showing the levels of TM3 cell testosterone secretion in the absence of sera.....	120
<b>Figure 3.35.</b> Graphs showing the results from the experiment with the crude boar testes extracts.....	121
<b>Figure 3.36.</b> Conventional PCR results for <i>Gapdh</i> gene expression.....	122
<b>Figure 3.37.</b> Photograph showing the AGE results for <i>Lhcgr</i> gene expression..	123
<b>Figure 3.38.</b> Conventional PCR results for <i>Star</i> gene expression. ....	124
<b>Figure 3.39.</b> Conventional PCR results for <i>Tspo</i> gene expression. ....	125
<b>Figure 3.40.</b> Photograph showing the AGE results for <i>Cyp11a1</i> gene expression. ....	126
<b>Figure 3.41.</b> Conventional PCR results for <i>Cyp17a1</i> gene expression.....	127
<b>Figure 3.42.</b> Photograph showing the AGE results for <i>Hsd17b3</i> gene expression. ....	128
<b>Figure 3.43.</b> Photograph showing a representative AGE result for <i>Gapdh</i> after qPCR.....	129
<b>Figure 3.44.</b> Photographs showing representative AGE results for <i>Star</i> and <i>Tspo</i> after qPCR. ....	130
<b>Figure 3.45.</b> Photograph showing a representative AGE result for <i>Cyp17a1</i> after qPCR.....	131
<b>Figure 3.46.</b> Graph showing the effects of hCG, EGCG and aspalathin on <i>Star</i> relative gene expression. ....	132
<b>Figure 3.47.</b> Graph showing the effects of hCG, co-treated with EGCG or aspalathin on <i>Star</i> relative gene expression.....	133
<b>Figure 3.48.</b> Graph showing the effects of hCG, EGCG and aspalathin on <i>Tspo</i> relative gene expression. ....	134
<b>Figure 3.49.</b> Graph showing the effects of hCG, co-treated with EGCG or aspalathin on <i>Tspo</i> relative gene expression. ....	135
<b>Figure 3.50.</b> Graph showing the effects of green tea and green rooibos on inhibin B secretion by TM4 cells.....	136
<b>Figure 3.51.</b> Graph showing the effects of EGCG and aspalathin on inhibin B secretion by TM4 cells. ....	137
<b>Figure 3.52.</b> Graph showing the effects of green tea and green rooibos on lactate secretion by TM4 cells. ....	138

<b>Figure 3.53.</b>	Graph showing the effects of EGCG and aspalathin on lactate secretion by TM4 cells. ....	140
<b>Figure 3.54.</b>	Graph showing the effects of EGCG on TM4 cell transepithelial electrical resistance over a 72 hour period. ....	142
<b>Figure 3.55.</b>	Graph showing the effects of aspalathin on TM4 cell transepithelial electrical resistance over a 72 hour period. ....	143
<b>Appendices</b>		
<b>Figure I.</b>	Graph showing a standard curve used for testosterone quantitation via ELISA. ....	197
<b>Figure II.</b>	Graph showing the standard curve used for inhibin B quantitation via ELISA. ....	197
<b>Figure III.</b>	Representative scatter plots and histograms showing the gating strategy for TM3 cell ROS determination. ....	198
<b>Figure IV.</b>	Representative scatter plots and histograms showing the gating strategy for TM4 cell ROS determination. ....	199
<b>Figure V.</b>	Graphic representation of the <i>Gapdh</i> gene features. ....	200
<b>Figure VI.</b>	Graphic representation of the <i>Lhcgr</i> gene features. ....	202
<b>Figure VII.</b>	Graphic representation of the <i>Star</i> gene features. ....	204
<b>Figure VIII.</b>	Graphic representation of the <i>Tspo</i> gene features. ....	208
<b>Figure IX.</b>	Graphic representation of the <i>Cyp11a1</i> gene features. ....	210
<b>Figure X.</b>	Graphic representation of the <i>Cyp17a1</i> gene features. ....	212
<b>Figure XI.</b>	Graphic representation of the <i>Hsd17b3</i> gene features. ....	214
<b>Figure XII.</b>	Graph showing the standard curve used for <i>Gapdh</i> quantitation by qPCR. ....	216
<b>Figure XIII.</b>	Graph showing the standard curve used for <i>Star</i> quantitation by qPCR. ....	216
<b>Figure XIV.</b>	Graph showing the standard curve used <i>Tspo</i> quantitation by qPCR. ....	217
<b>Figure XV.</b>	Graph showing a melting curve for <i>Gapdh</i> qPCR. ....	217
<b>Figure XVI.</b>	Graph showing a melting for <i>Star</i> qPCR. ....	218
<b>Figure XVII.</b>	Graph showing a melting curve for <i>Tspo</i> qPCR. ....	218
<b>Figure XVIII.</b>	Photographs of the apparatus used for measuring transepithelial electrical resistance. ....	219

# List of Tables

---

Title	Page
<b>Chapter 1</b>	
<b>Table 1.1.</b> Table showing an overview of studies on the protective effects of EGCG, green tea, green rooibos and rooibos on the mammalian male reproductive system against various physiological insults <i>in vivo</i> . .....	36
<b>Chapter 2</b>	
<b>Table 2.1.</b> Table showing the primer sequences, predicted product lengths and melting temperatures used for amplifying the target genes of interest by PCR. ....	63
<b>Table 2.2.</b> Table showing the makeup of the mastermix used to perform the reverse transcription reaction .....	65
<b>Table 2.3.</b> Table showing the makeup of the mastermix used to perform the conventional PCR.....	66
<b>Table 2.4.</b> Table showing the makeup of the mastermix used to perform the qPCR.....	69

# List of Abbreviations

---

%	percent(age)
[Ca <sup>2+</sup> ] <sub>i</sub>	cytosolic calcium ion concentration
°C	degrees Celsius (centigrade)
µg	microgram(s)
µl	microliter(s)
µM	micro molar (i.e. micromoles per litre)
µm	micrometre(s)
ΔCt	change in cycle threshold
ΔΨ <sub>m</sub>	mitochondrial membrane potential(s)
Ω	ohm(s)
3βHSD	3 β-hydroxysteroid dehydrogenase
17βHSD	17 β-hydroxysteroid dehydrogenase (protein)
AA	arachidonic acid
ABP	androgen binding protein
AGE	agarose gel electrophoresis
AR	androgen receptor
ATAD3	ATPase family AAA domain containing protein 3A
ATP	adenosine triphosphate
BLAST	basic local alignment search tool
bp	base pair(s)
BSA	bovine serum albumin
Ca <sup>2+</sup>	calcium ion
cAMP	cyclic adenosine monophosphate
CCCP	carbonyl cyanide 3-chlorophenylhydrazone
cDNA	complementary deoxyribonucleic acid
CG	chorionic gonadotropin
Cl <sup>-</sup>	chloride anion
cm	centimetre(s)
CM-H <sub>2</sub> DCFDA	chloromethyl 2',7'-dichlorodihydrofluorescein diacetate
CO <sub>2</sub>	carbon dioxide
CREB	cAMP response-element binding protein

## List of Abbreviations

---

Ct	cycle threshold
<i>Cyp11a1</i>	murine gene or mRNA for CYP11A1
CYP11A1	cytochrome P450 11A1 (protein)
<i>Cyp17a1</i>	murine gene or mRNA for CYP17A1
CYP17	cytochrome P450c17 (protein)
CYP19A1	cytochrome p450 19A1 or aromatase (protein)
DAG	diacylglycerol
DCF	2',7'-dichlorofluorescein
DMEM:F12	Dulbeco's modified eagles medium:Ham's F12 medium mix, 1:1.
DMSO	dimethyl sulfoxide
DNA	deoxyribonucleic acid
dNTP	deoxynucleoside triphosphate
e.g.	<i>exempli gratia</i> (for example)
EDC	endocrine disrupting compound/chemical
EDTA	ethylenediaminetetraacetic acid
EGCG	(-)-epigallocatechin gallate
ELISA	enzyme-linked immunosorbent assay
EPOX	epoxygenase
ER	endoplasmic reticulum
ES	ectoplasmic specializations
FBS	fetal bovine serum
FSH	follicle stimulating hormone
FSHR	follicle stimulating hormone receptor
<i>g</i>	g-force
g	gram(s)
<i>Gapdh</i>	murine gene or mRNA for GAPDH
GAPDH	glyceraldehyde 3-phosphate dehydrogenase (protein)
GnRH	gonadotropin releasing hormone
GOI	gene of interest
GPT	glutamic pyruvate transaminase
Gy	gray(s)
H <sub>2</sub> O <sub>2</sub>	hydrogen peroxide
HAT	hydrogen atom transfer
hCG	chorionic gonadotropin from human urine
HPT	hypothalamus-pituitary-testis (axis)

HS	horse serum
<i>Hsd17b3</i>	murine gene or mRNA for 17 $\beta$ HSD
i.e.	<i>id est</i> (that is)
IMM	inner mitochondrial membrane
IP <sub>3</sub>	inositol 1,4,5-triphosphate
K <sup>+</sup>	potassium ion
kg	kilogram(s)
l	litre(s)
LD	lipid droplet
LDH	lactate dehydrogenase
LH	luteinizing hormone
<i>Lhcgr</i>	murine gene or mRNA for LHCGR
LHCGR	luteinizing hormone/chorionic gonadotropin receptor
LOX	lipoygenase
M	molar (i.e. moles per litre)
MAM	mitochondria-associated membrane
mg	milligram(s)
MgCl <sub>2</sub>	magnesium chloride
mIU	milli international unit(s)
ml	millilitre(s)
mM	milli molar (i.e. milli moles per litre)
mm	millimetre(s)
mRNA	messenger ribonucleic acid
MTT	3-(4,5-dimethylthiazol-2-yl)-2,5-diphenyltetrazolium bromide
n	number of samples
NAD <sup>+</sup>	nicotinamide adenine dinucleotide
NADH	reduced nicotinamide adenine dinucleotide
NADPH	reduced nicotinamide adenine dinucleotide phosphate
NaOH	sodium hydroxide
NCBI	National Center for Biotechnology Information
ng	nanogram(s)
nl	nanolitre(s)
nm	nanometre(s)
O <sub>2</sub> <sup>-</sup>	superoxide anion
OH <sup>-</sup>	hydroxyl radical

## List of Abbreviations

---

OMM	outer mitochondrial membrane
P	probability (value)
PAGE	polyacrylamide gel electrophoresis
PBS	phosphate buffered saline
PCR	polymerase chain reaction
pen-strep	penicillin-streptomycin mixture
pH	potential for hydrogen
PKA	protein kinase A
pmol	pico mole(s)
qPCR	quantitative (real-time) polymerase chain reaction
RNA	ribonucleic acid
RO	reverse-osmosis
ROS	reactive oxygen species
rpm	revolutions per minute
RT	reverse transcription
SCB	Sertoli cell barrier
SET	single electron transfer
<i>Star</i>	murine gene or mRNA for StAR
StAR	steroidogenic acute regulatory protein
T75	75 cm <sup>2</sup> surface area (cell culture flask)
TBE	tris-boric acid-ethylenediaminetetraacetic acid
TEER	transepithelial/transendothelial electrical resistance
T <sub>m</sub>	melting temperature
TMRE	tetramethylrhodamine ethyl ester
<i>Tspo</i>	murine gene or mRNA for TSPO
TSPO	transduceosome translocator protein
V	volt(s)
VDAC1	voltage-dependent anion channel 1
ZIP9	zinc regulated transporter-and iron regulated transporter-like protein 9



---

(This page was intentionally left blank)



UNIVERSITY *of the*  
WESTERN CAPE



# Chapter 1

---

## Introduction & Literature review



UNIVERSITY *of the*  
WESTERN CAPE

## 1.1. A brief overview of the male reproductive system

The male reproductive system is comprised of the external genitalia (scrotum and penis), the internal principal organs (testis, epididymis, vas deferens, ejaculatory duct and urethra) and the accessory glands (prostate gland, seminal vesicle and the bulbourethral gland); see [Figure 1.1](#). The scrotum primarily serves to protect the testis from the external environment and to help regulate testicular temperature (together with the spermatic cord).

The testes produce the male gametes, i.e. spermatozoa, and the male sex steroids i.e. androgens. Androgens facilitate spermatogenesis and permit the development of masculine characteristics. Spermatozoa arise from germ cells (spermatogonia) in the seminiferous tubules, together with the help of Sertoli (sustentacular) cells. Once formed, spermatozoa enter the epididymis, where they mature and await ejaculation.

During coitus, spermatozoa travel via the vas deferens to the ejaculatory duct. The prostate gland and seminal vesicles supplement the sperm with a medium (seminal plasma) conducive to sperm functioning and protection (e.g., it contains antioxidants to protect sperm against oxidative stress). The spermatozoa and this medium together is known as semen. The semen exits the male's body via the urethra and enters the female reproductive tract during coitus. This process is facilitated by a penile erection, which permits the efficient delivery of sperm to the female reproductive system; as well as bulbourethral gland secretions, which lubricate the penile (spongy) urethra. Additionally, the urethra and penis permit the passage of urine out of the body.

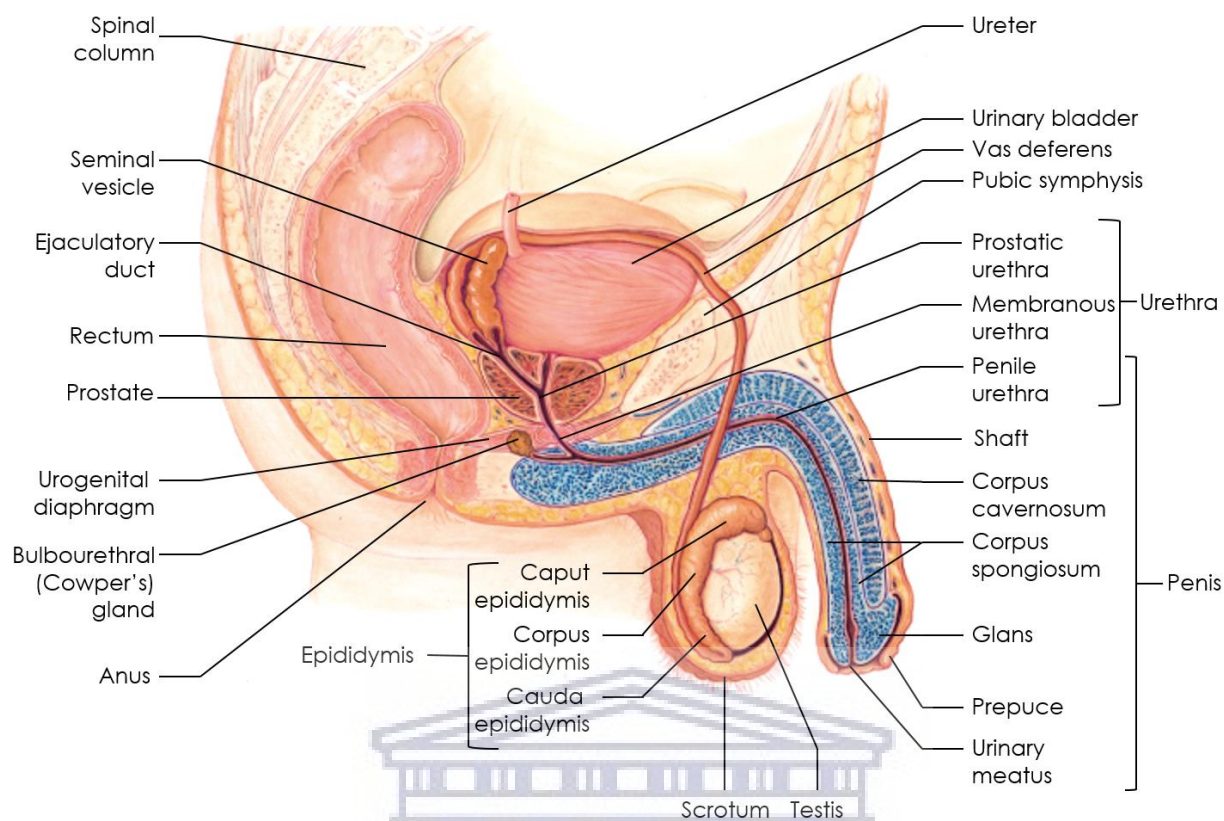


**Figure 1.1. Illustration of a human sagittal section, showing the organs of the male reproductive system** (adapted from [www.s3.amazonaws.com](http://www.s3.amazonaws.com), 2015).

## 1.2. Testicular anatomy and histology

The primary specialised reproductive tissues in the testis are the seminiferous tubules and the Leydig cells. The testis divides into lobules by fibrous septa. Each lobule holds approximately four highly folded seminiferous tubules, which empty into the epididymis via the rete testis (see [Figure 1.2](#)).

Seminiferous tubules are composed of the spermatogenic tissue and the supporting cells (Sertoli cells and myoid cells). The outermost layer of the seminiferous tubules is composed of the myoid layer (myoid cells, also known as peritubular cells), followed by the basement membrane. The spermatogonia (germ cells) and Sertoli cells rest on the basement membrane in the basal compartment of the seminiferous tubules. However, Sertoli cells protrude into the adluminal compartment as well. The separation of the two seminiferous tubule compartments is provided by the inter-Sertoli cell tight junctions, which form the Sertoli cell barrier (SCB; formerly known as the blood-testis barrier) (Hess and França, 2005). Deep to the Sertoli cell barrier are the spermatocytes

(primary and secondary), spermatids and spermatozoa (in the lumen), in that order. These cells present at various stages of differentiation within the seminiferous tubule (see Figure 1.3).

The Leydig cells are located in the interstitium, between seminiferous tubules, and are consequently also known as interstitial cells (see Figure 1.3). Additionally, the interstitium contains fibroblasts, blood vessels, lymphatics, nerves and connective tissue (Weinbauer *et al.*, 2010).

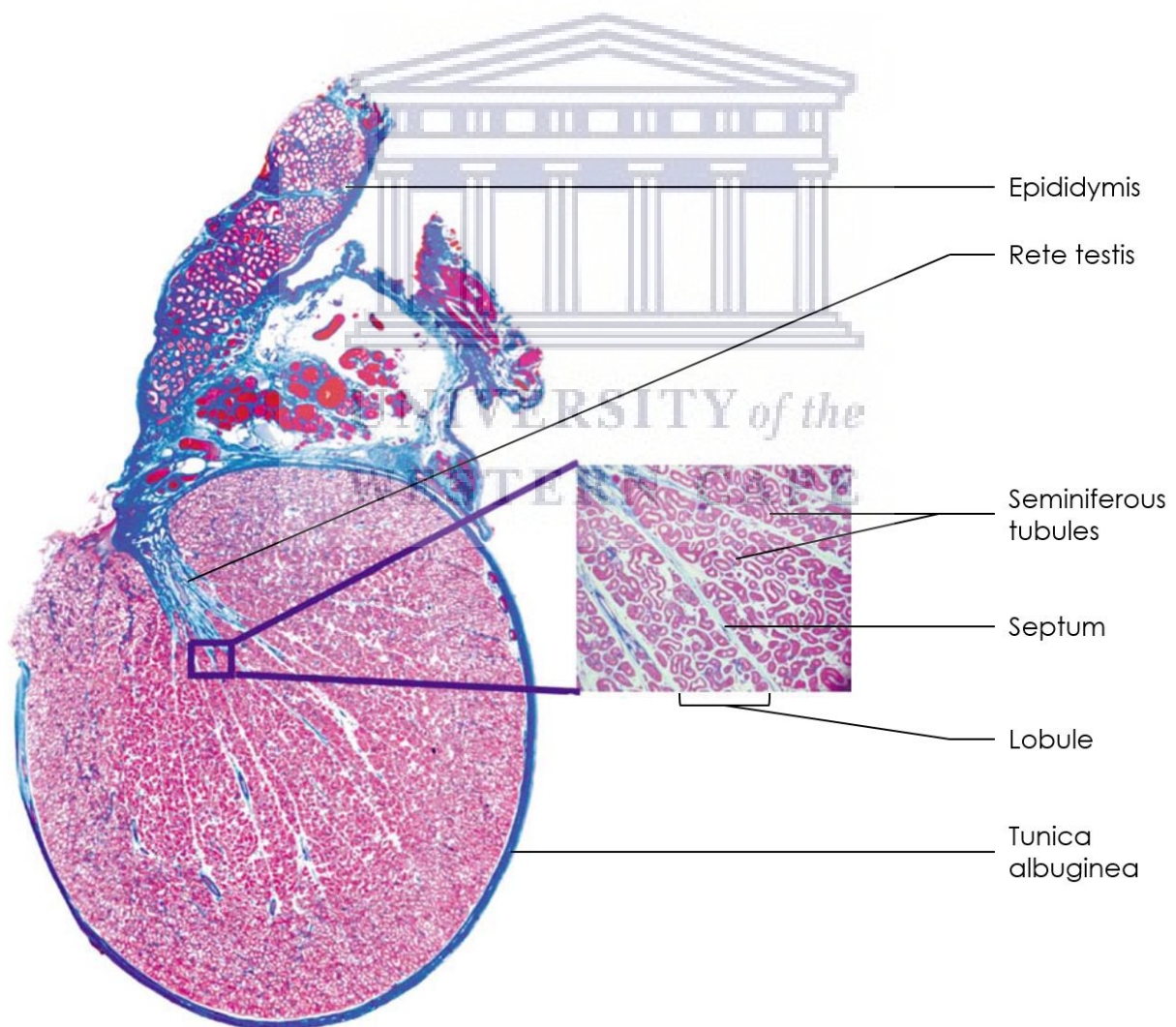


**Figure 1.2. Photograph showing a transverse section of a human testis** (adapted from Weinbauer *et al.*, 2010).

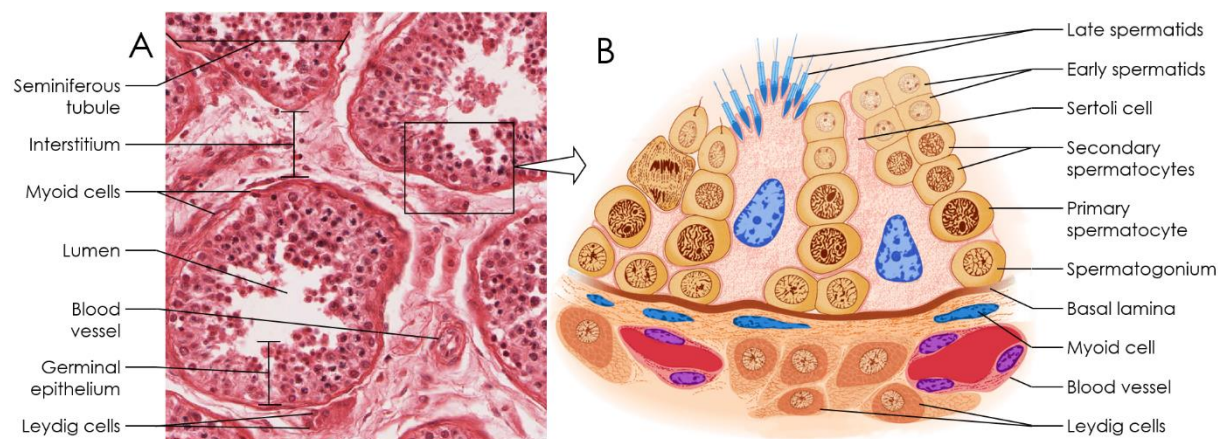


**Figure 1.3. The human seminiferous tubule in cross-section.** **A:** Photomicrograph of the germinal epithelium in cross-section. The tissue was stained by haematoxylin and eosin, and viewed at 200 × magnification (adapted from [www.virtualslides.med.umich.edu](http://www.virtualslides.med.umich.edu), 2015); **B:** Illustration of the germinal epithelium in cross-section (adapted from Barrett *et al.*, 2012).

### 1.3. Leydig cells

The primary sites for steroidogenesis in the male reproductive system are the Leydig cells. Leydig cells often localise around interstitial blood vessels, but may occur as solitary cells (Bloom and Fawcett, 1968; Young and Heath, 2000). Adult Leydig cells have an abundance of smooth endoplasmic reticulum (ER) and mitochondria with cylindrical cristae, which is characteristic of steroidogenic tissues (Bloom and Fawcett, 1968; Young and Heath, 2000; Weinbauer *et al.*, 2010). Interstitial cells are quite large and have large nuclei, sometimes even being bi-nucleated (Bloom and Fawcett, 1968; Zhang, 1999; Young and Heath, 2000). Additionally, Leydig cells possess lipid droplets and crystals of Reinke; the latter, being unique to humans and wild bush rats, having an unknown function (Bloom and Fawcett, 1968; Young and Heath, 2000; Weinbauer *et al.*, 2010). The Leydig cells produce primarily androgens (mostly testosterone) upon stimulation with luteinizing hormone (LH) or chorionic gonadotropin, but can produce other steroids as well.

#### 1.3.1 Steroids

Steroids form a special class of hormone that is derived from cholesterol and is produced in the primary steroidogenic tissues, which are the adrenals (zona fasciculata and zona glomerulosa), the ovaries in females (theca cells, granulosa cells and corpus luteum) and the testes in males (Leydig cells). The steroid classes include

glucocorticoids, mineralocorticoids, progestins, androgens and estrogens (refer to Figure 1.4). Each class of steroid acts via its specific receptor in its target tissues (e.g. androgens act via the androgen receptor: AR), and despite their similar structure, produce very different physiological outcomes (Hinson *et al.*, 2010).

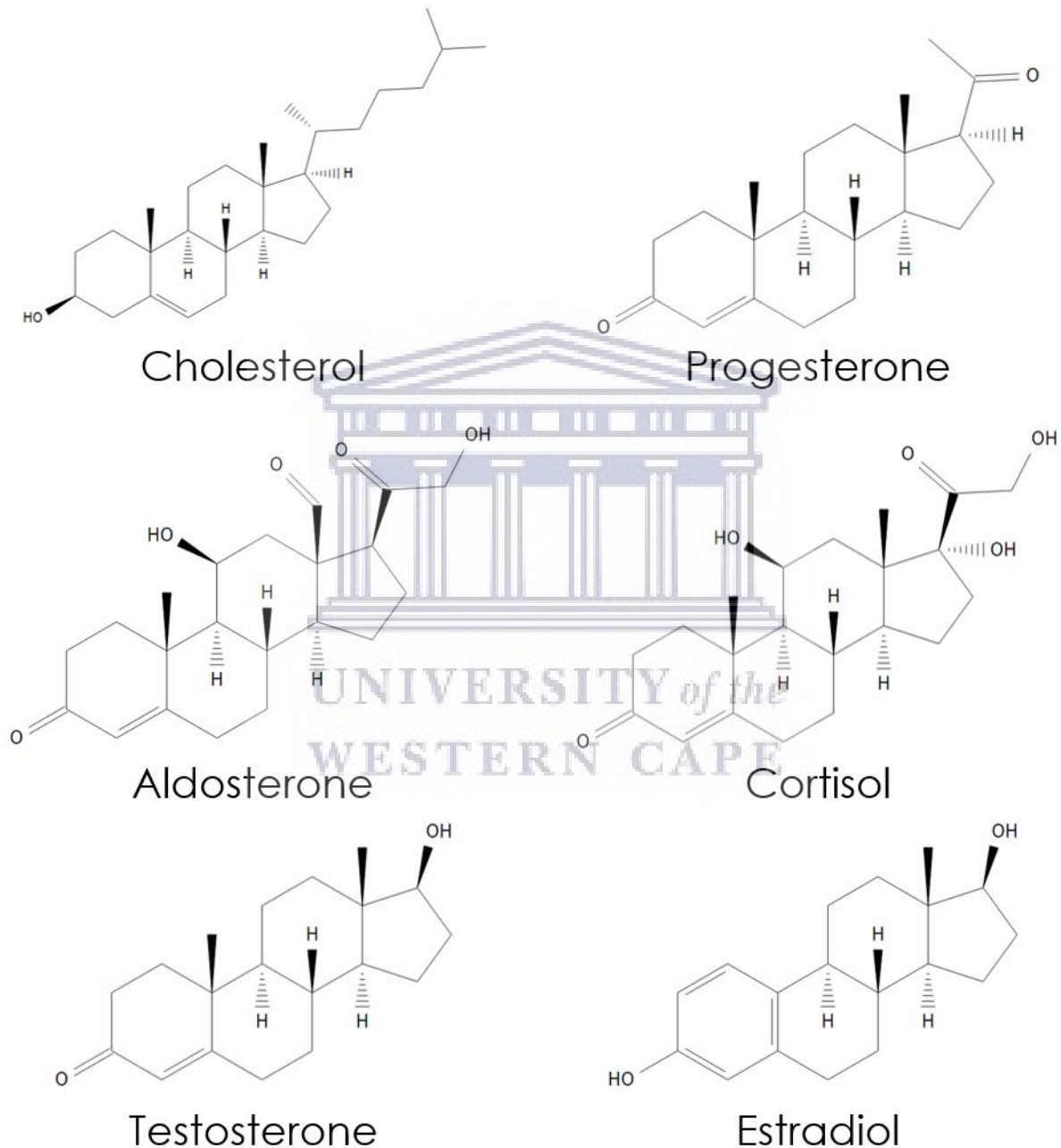


**Figure 1.4. Diagram showing representatives of the main steroid classes.** Cholesterol is the precursor of all steroids. Progesterone is a progestin, aldosterone is a mineralocorticoid, cortisol is a glucocorticoid, testosterone is an androgen and estradiol is an estrogen. Chemical structures were drawn using 'Structure Editor' (<https://scifinder.cas.org>).

### 1.3.2 Hypothalamus-pituitary-testis axis

Leydig cell steroidogenesis is under the control of the hypothalamus-pituitary-testis (HPT) axis. The hypothalamus firstly produces pulsatile secretions of gonadotropin releasing hormone (GnRH). The GnRH travels to the pituitary gland via the hypophyseal portal system and stimulates the pituitary gland to release LH and follicle stimulating hormone (FSH) into the general circulation. Both LH and FSH are also secreted in pulses, because of the GnRH pulses. Once at the testis, FSH acts on Sertoli cells, which consequently secrete inhibin. Inhibin provides negative feedback, by inhibiting FSH secretion. LH acts on the Leydig cells, causing them to secrete testosterone, which inter alia provides negative feedback by inhibiting GnRH secretion.

### 1.3.3 Leydig cell signal transduction

Once at the Leydig cell, LH binds to the LH/chorionic gonadotropin receptor (LHCGR), which is a transmembrane guanosine triphosphate-binding protein receptor. The LH-LHCGR interaction causes a conformational change in the receptor, which permits the initiation of the signal transduction pathways that lead to acute and chronic steroidogenesis. The acute (nongenomic) reactions cause a release of steroids within a few minutes of LH stimulation, whereas chronic (genomic) reactions are only fully active in the order of hours (Hattangady *et al.*, 2012). The acute reactions simply involve the activation of enzymes that permit the transport of cholesterol to the mitochondrial matrix and inactivation of steroidogenesis inhibitors. The chronic reactions add to the acute reactions by activating gene transcription, translation and post-translational modification of proteins involved in steroidogenesis. Thus, chronic reactions increase the cells' capacity for steroidogenesis. Although these two groups of reactions induce steroidogenesis on different time scales, they appear to be interlinked (see [Figure 1.5](#)).

#### 1.3.3.1 Protein kinase A pathway

In adult Leydig cells, chronic steroidogenesis is responsible for most of the testosterone synthesized upon LH stimulation (Stocco *et al.*, 2005). The LH-LHCGR interaction activates adenylate cyclase, which converts adenosine triphosphate (ATP) to cyclic adenosine monophosphate (cAMP). The rise in cytosolic cAMP concentration that follows, permits the activation of protein kinase A (PKA). PKA phosphorylates various downstream proteins (directly and indirectly), including transcription factors, like CREB (cAMP response-element binding protein), and proteins that are not involved in transcription but still are required for steroidogenesis, like StAR (steroidogenic acute

regulatory protein) (Stocco *et al.*, 2005). Phosphorylation of StAR activates it, thus permitting acute steroidogenesis. PKA also activates Plin1 and hormone sensitive lipase to catalyse the formation of cholesterol from cholesteryl esters in cytosolic lipid droplets (Kraemer *et al.*, 2013). The activated transcription factors permit transcription of multiple specific genes that play roles in steroidogenesis, such as the gene for StAR; this permits chronic steroidogenesis. StAR, together with other transduceosome and metabolon proteins, permits the movement of cholesterol from the cytosolic compartment to the mitochondrial matrix, where the initial steroidogenic enzyme resides (Issop *et al.*, 2013). This process is the rate-limiting step in steroidogenesis.

### 1.3.3.2 Arachidonic acid pathway

Another cascade involved in steroidogenic signal transduction is the arachidonic acid (AA) pathway. The high cytosolic cAMP concentration, which follows LH-LHCGR interaction, also causes the release of AA from phospholipids in the cell. AA release is likely due to the action of phospholipase A<sub>2</sub> and/or PKA, and possibly through other pathways as well (Wang *et al.*, 2002; Stocco *et al.*, 2005). Phospholipase A<sub>2</sub> is also directly activated by the LHCGR reaction, though. Alternatively, AA release could be mediated by ART1st (arachidonic acid related thioesterase involved in steroidogenesis), which requires cAMP for its activation (Maloberti *et al.*, 2007).

Arachidonic acid is metabolised via three pathways, namely the lipoxygenase (LOX), the epoxygenase (EPOX) and the cyclooxygenase pathways. The cyclooxygenase pathway appears to tonically inhibit steroidogenesis, whereas the LOX and EPOX pathways help increase steroidogenesis (Stocco *et al.*, 2005). Additionally, both the LOX and EPOX pathways require LH stimulation for activation and work synergistically with the PKA pathway to induce steroidogenesis (Wang *et al.*, 2002; Stocco *et al.*, 2005).

### 1.3.3.3 Calcium and other ions in Leydig cell signalling

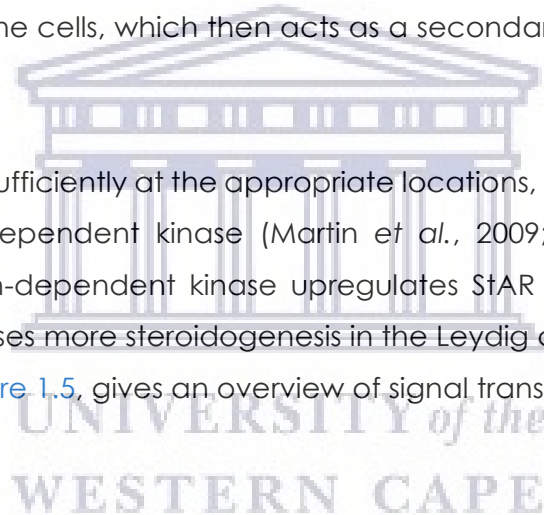
In addition, steroidogenesis signalling appears to involve ions (calcium ion: Ca<sup>2+</sup>; potassium ion: K<sup>+</sup> and chloride anion: Cl<sup>-</sup>) and their membrane channels. Upon LH stimulation, Leydig cells increase the cytosolic Ca<sup>2+</sup> concentration ([Ca<sup>2+</sup>]<sub>i</sub>), presumably via the activation of phospholipase C, which would convert phosphatidylinositol 4,5-bisphosphate to diacylglycerol (DAG) and IP<sub>3</sub> (inositol 1,4,5-triphosphate). DAG can activate protein kinase C which, like PKA, phosphorylates



various substrates (Khan *et al.*, 1995; Stocco *et al.*, 2005). Some DAG could also be converted to AA via DAG lipase and monoacylglycerol lipase (Khan *et al.*, 1995).

On the other hand, the IP<sub>3</sub> would then activate ligand-gated Ca<sup>2+</sup> channels (IP<sub>3</sub> channels, which also are L-type channels: long lasting voltage-activated Ca<sup>2+</sup> channels, i.e. high voltage-activated Ca<sup>2+</sup> channels), which would cause an increase in cytosolic Ca<sup>2+</sup> concentration (Stocco *et al.*, 2005). Although this pathway is active in adult Leydig cells, it is not the primary mechanism for the rise in [Ca<sup>2+</sup>]<sub>i</sub>. According to Costa *et al.* (2010), the IP<sub>3</sub> pathway is only secondary to the activity of ryanodine receptors (another L-type channel) in the endoplasmic reticulum (ER). Studies by Ramnath *et al.* (1997), Panesar and Chan (2005), Costa and Varanda (2007), Chaves and Veranda (2008), Pandey *et al.* (2010) and Matzkin *et al.* (2013) collectively show how voltage-dependent ion channels interplay with one another to affect the [Ca<sup>2+</sup>]<sub>i</sub> at specific locations in the cells, which then acts as a secondary messenger in Leydig cell signalling.

Once [Ca<sup>2+</sup>]<sub>i</sub> increases sufficiently at the appropriate locations, it activates calmodulin and Ca<sup>2+</sup>/calmodulin-dependent kinase (Martin *et al.*, 2009; Abdou *et al.*, 2013). Calcium ion/calmodulin-dependent kinase upregulates StAR levels via the NURR77 protein; this, in turn, causes more steroidogenesis in the Leydig cell (Martin *et al.*, 2009; Abdou *et al.*, 2013). [Figure 1.5](#), gives an overview of signal transduction in Leydig cells.



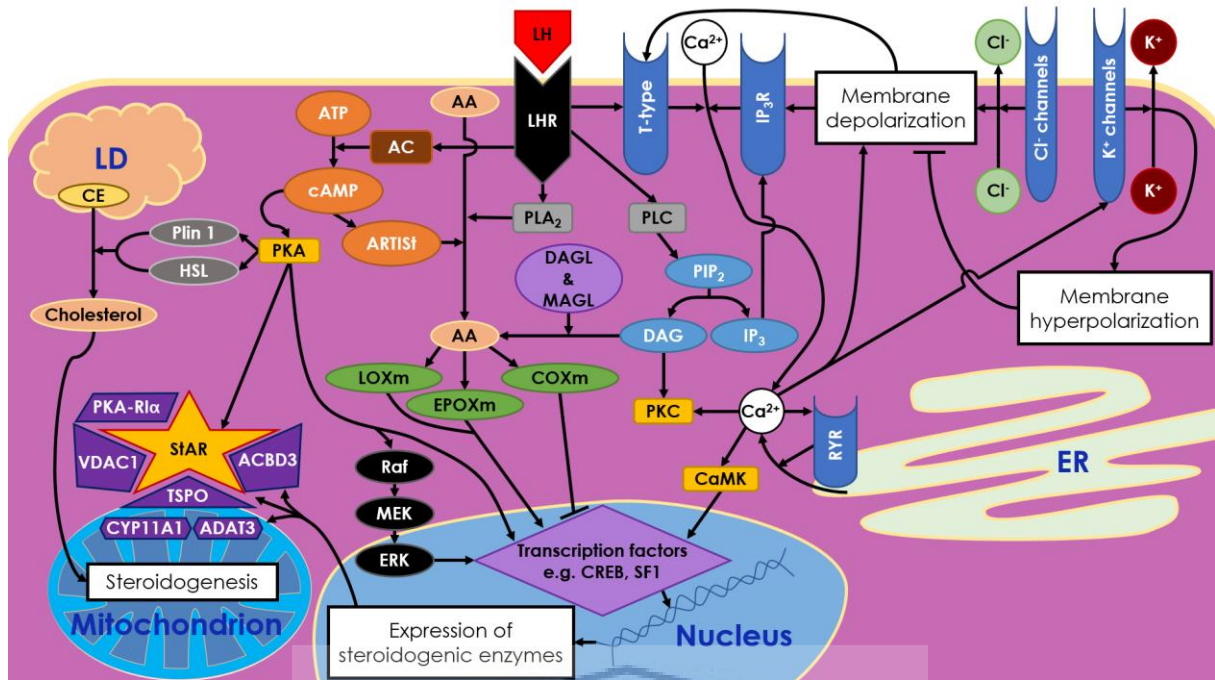


**Figure 1.5. Schematic diagram showing Leydig cell signal transduction.** AA: arachidonic acid; AC: adenylate cyclase; ACBD3: acyl-CoA binding domain-containing 3; ARTIST: arachidonic acid related thioesterase involved in steroidogenesis; ATAD3: ATPase family AAA domain containing 3A; ATP: adenosine triphosphate;  $\text{Ca}^{2+}$ : calcium ion; CaMK:  $\text{Ca}^{2+}$ /calmodulin-dependent kinase; cAMP: cyclic adenosine monophosphate; CE: cholesteryl esters;  $\text{Cl}^-$ : chloride anion; COXm: cyclooxygenase metabolites; CREB: cAMP response-element binding protein; CYP11A1: cytochrome P450 11A1; DAGL: diacylglycerol lipase; EPOXm: epoxygenase metabolites; ER: endoplasmic reticulum; ERK: extracellular-signal regulated kinase; HSL: hormone sensitive lipase;  $\text{IP}_3$ : inositol 1,4,5-triphosphate;  $\text{IP}_3\text{R}$ :  $\text{IP}_3$  receptor;  $\text{K}^+$ : potassium ion; LD: lipid droplet; LH: luteinizing hormone; LHR: LH receptor; LOXm: lipoxygenase metabolites; MAGL: monoacylglycerol lipase; MEK: mitogen activated protein kinase kinase; PKA: protein kinase A; PKA-R1 $\alpha$ : PKA regulatory subunit I alpha; PKC: protein kinase C;  $\text{PIP}_2$ : phosphatidylinositol 4,5-bisphosphate;  $\text{PLA}_2$ : phospholipase  $\text{A}_2$ ; PLC: phospholipase C; RYR: ryanodine receptor; SF-1: steroidogenic factor 1; StAR: steroidogenic acute regulatory protein; TSPO: transduceosome translocator protein; T-type: transient (low voltage activated)  $\text{Ca}^{2+}$  channel; VDAC1: voltage-dependent anion channel 1. This figure is based primarily on Stocco *et al.* (2005), but additional information came from Khan *et al.* (1995), Ramnath *et al.* (1997), Manna *et al.* (1999), Wang *et al.* (2002), del Corso and Varanda (2003), Panesar and Chan (2005), Costa and Varanda (2007), Maloberti *et al.* (2007), Chaves and Veranda (2008), Martin *et al.* (2009), Costa *et al.* (2010), Pandey *et al.* (2010), Abdou *et al.* (2013), and Matzkin *et al.* (2013).

### 1.3.4 Mitochondria and steroidogenesis

The mitochondrial matrix contains the initial steroidogenic enzyme, namely cytochrome P450 11A1 (CYP11A1; also called cytochrome P450 side-chain cleavage enzyme), which is associated with the inner mitochondrial membrane (IMM). The transfer of cholesterol from the mitochondrial outer membrane (OMM) to the IMM is crucial for steroidogenesis, as it is the rate-limiting step of steroidogenesis. Thus, mitochondria play a key role in steroidogenesis. However, the mitochondrial participation in adult Leydig cell steroidogenesis is dependent on a number of factors, such as its membrane potential, its activity in ATP synthesis,  $\text{Ca}^{2+}$  signalling within mitochondria, the pH gradient between the mitochondrial membranes and the activity of reactive oxygen species (ROS) (Hales *et al.*, 2005).

The transfer of cholesterol to the IMM was historically attributed to the steroidogenic acute regulatory (StAR) protein. However, it has recently become evident that StAR is only part of a larger complex (termed the transduceosome) which accumulates cholesterol at the OMM (Issop *et al.*, 2013). According to Issop *et al.* (2013), the transduceosome includes the transduceosome translocator protein (TSPO, formerly known as the peripheral benzodiazepine receptor), voltage-dependent anion channel 1 (VDAC1), acyl-CoA binding domain-containing protein 3 (ACBD3), PKA regulatory subunit I alpha (PKA-R1 $\alpha$ ) and StAR, of course. The actual transportation of cholesterol is believed to occur via the metabolon, which contains TSPO and VDAC1 (like the transduceosome), but includes ATAD3 (ATPase family AAA domain containing protein 3A) and CYP11A1 (Issop *et al.*, 2013). Nonetheless, StAR may be required to activate the metabolon (Issop *et al.*, 2013).

Upon LH stimulation, mitochondria change shape and localize in the perinuclear region of the Leydig cell (Poderoso *et al.*, 2013). The positional and morphological changes in mitochondria are likely due to cytoskeletal actions (Poderoso *et al.*, 2013). Mitochondria also associate with the ER through mitochondria-associated membranes (MAMs), which may also play a role in mitochondrial kinetics (Issop *et al.*, 2013; Poderoso *et al.*, 2013; van Vliet *et al.*, 2014). MAMs are thought to provide a portal for  $\text{Ca}^{2+}$  from the ER to the mitochondria (Issop *et al.*, 2013; van Vliet *et al.*, 2014). Additionally, the closer association between mitochondria and the ER, mediated by MAMs, likely facilitates the transportation of pregnenolone from the mitochondria to the ER (Issop *et al.*, 2013; van Vliet *et al.*, 2014).

As with the ER, mitochondria also associate with cytosolic lipid droplets (LDs). The lipid droplets serve as a storage form of cholesterol since they are rich in sterol esters (Issop *et al.*, 2013). LDs also associate with the mitochondrial-associated ER, forming a LERMIT (LD-ER-mitochondria) association (Issop *et al.*, 2013). Thus, mitochondrial plasticity may play a very important role in stimulated steroidogenesis.

The mitochondrial electron transport chain produces a hydrogen ion concentration gradient (and thus, a differential pH) between the OMM and IMM. The hydrogen ion gradient is responsible for the mitochondrial membrane potential ( $\Delta\Psi_m$ ), which is essential for ATP synthesis during oxidative phosphorylation. However, this process also (as well as other mitochondrial processes like steroidogenesis) produces ROS, which can damage various cellular structures and even cause apoptosis. A study conducted by Hales *et al.* (2005) revealed how disrupting  $\Delta\Psi_m$  and inhibiting ATP synthesis (the latter producing high ROS levels) could restrain Leydig cell steroidogenesis.

High mitochondrial  $\text{Ca}^{2+}$  levels can also induce apoptosis, by altering mitochondrial membrane permeability and subsequent mitochondrial rupture. Nonetheless, mitochondrial  $\text{Ca}^{2+}$  is essential for steroidogenesis (Hales *et al.*, 2005). According to Hales *et al.* (2005), low mitochondrial  $\text{Ca}^{2+}$  levels inhibits steroidogenesis, likely via stopping ATP synthesis. Hales *et al.* (2005) reason that, since the tricarboxylic acid cycle enzymes and electron transport chain proteins require  $\text{Ca}^{2+}$  to function, the absence of mitochondrial  $\text{Ca}^{2+}$  would cease ATP production and thus steroidogenesis as well (steroidogenesis and StAR phosphorylation require ATP). Furthermore, the transducesome may also require ATP and  $\text{Ca}^{2+}$ , since it contains an ATPase (ATAD3) and an ion transporter (VDAC); adding to ATP's importance in steroidogenesis (Issop *et al.*, 2013).

The role of mitochondria is central to steroidogenesis. This explains why mitochondrial movement and association with the ER and LDs are required. Nonetheless, mitochondria are only needed for the first step of androgen and estrogen steroidogenesis.

### 1.3.4.1 Testosterone biosynthesis

Androgen and estrogen steroidogenesis both start in the mitochondria, but end in the smooth ER. At the inner mitochondrial membrane, CYP11A1 converts cholesterol to pregnenolone. Thereafter pregnenolone translocates to the ER (likely with the aid of MAMs), where the remaining steroidogenic enzymes reside (Weinbauer *et al.*, 2010). According to Miller and Archus (2011), Leydig cells primarily convert pregnenolone to 17-hydroxypregnenolone, before producing dehydroepiandrosterone, both catalysed by cytochrome P450c17 (CYP17). Thereafter, dehydroepiandrosterone could either be converted into 4-androstenedione or 5-androstenediol via 3  $\beta$ -hydroxysteroid dehydrogenase (3 $\beta$ HSD) or 17 $\beta$ HSD, respectively. The final step in testosterone production is catalysed by 3 $\beta$ HSD from 5-androstenediol or by 17 $\beta$ HSD3 from 4-androstenedione.

Once formed, testosterone passively exits the Leydig cell and associates with interstitial androgen binding protein (ABP), from Sertoli cells, or enters the blood vessels in the vicinity (Dong and Hardy, 2004). In the blood, most testosterone (98%) associates with the plasma proteins, ABP and albumin, the remainder is free in plasma (Dong and Hardy, 2004; Weinbauer *et al.*, 2010). Often testosterone is irreversibly converted to dihydrotestosterone by 5 $\alpha$  reductase in a target tissue, such as the prostate (Dong and Hardy, 2004; Weinbauer *et al.*, 2010). Refer to [Figure 1.6](#) for an overview of Leydig cell steroidogenesis.

UNIVERSITY of the  
WESTERN CAPE

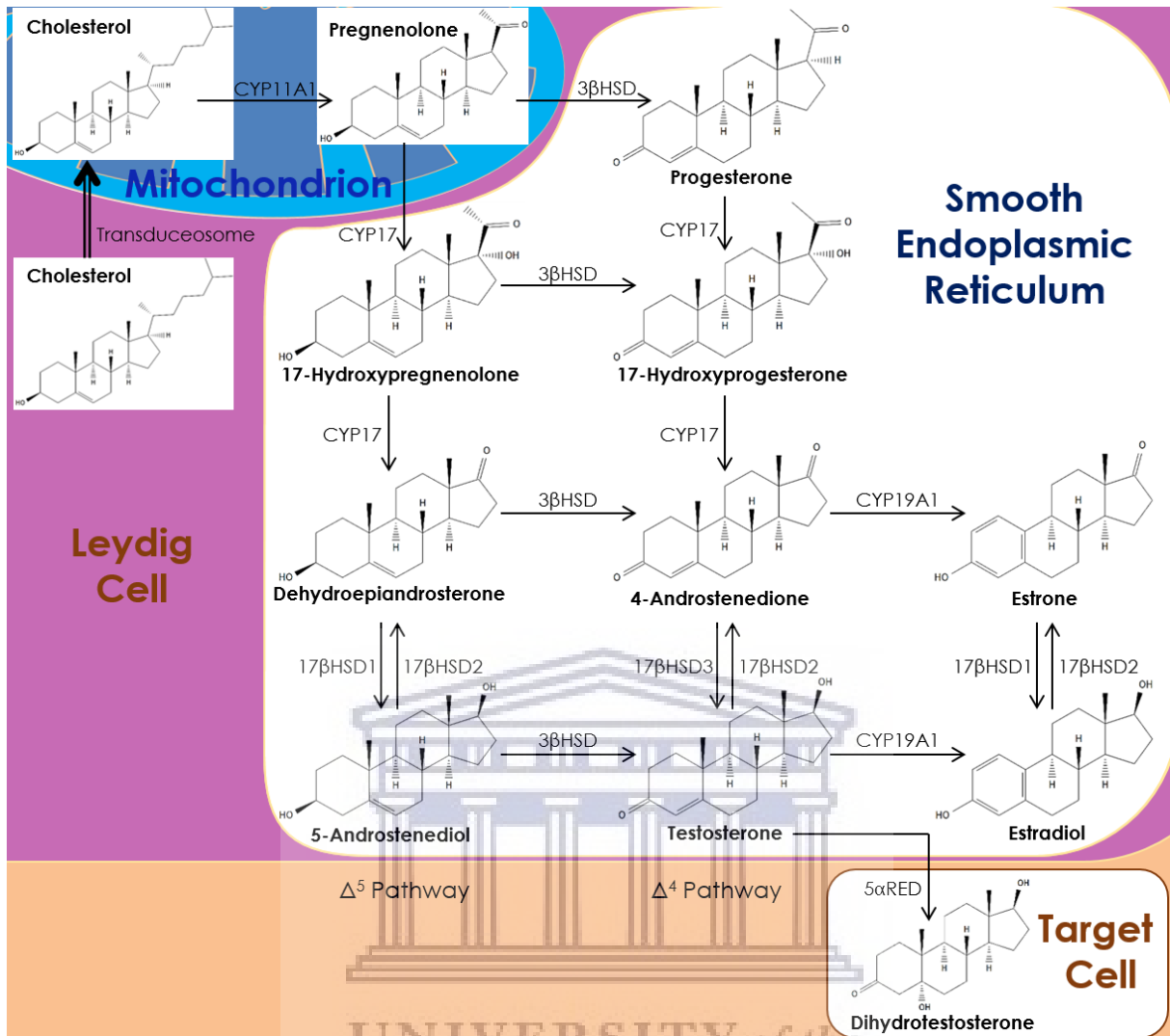


**Figure 1.6. Schematic diagram showing steroidogenesis in Leydig cells.** The  $\Delta^4$  and  $\Delta^5$  pathways are most active in humans, but human Leydig cells primarily use the  $\Delta^5$  pathway to synthesize testosterone (Dong and Hardy, 2004; Weinbauer *et al.*, 2010; Miller and Archus, 2011). 3βHSD: 3 β-hydroxysteroid dehydrogenase; 5αRED: 5α reductase; 17βHSD: 17 β-hydroxysteroid dehydrogenase; CYP11A1: cytochrome P450 11A1; CYP17: cytochrome P450c17; CYP19A1: aromatase. Chemical structures were drawn using 'Structure Editor' (<https://scifinder.cas.org>).

## 1.4. Sertoli cells

Sertoli cells are sustentacular cells that perform several functions which are essential for spermatogenesis. Sertoli cells wrap cytoplasmic projections around, and are intimately connected to, the spermatogonia and the developing spermatozoa (spermatocytes, spermatids and spermatozoa). Essentially, Sertoli cells aid spermatogenesis by nourishing and structurally supporting the developing spermatozoa, as well as providing them with paracrine (and endocrine) support and the Sertoli cell barrier (Hess and França, 2005; Weinbauer *et al.*, 2010).

As mentioned, Sertoli cells rest on the basal membrane of each seminiferous tubule, and form the Sertoli cell barrier (SCB) via tight junctions between adjacent Sertoli cells. Adult Sertoli cells have large oval nuclei, with a tripartite nucleolus, which are usually found close to the basement membrane (Bloom and Fawcett, 1968; Young and Heath, 2000; Hess and França, 2005). The Sertoli cells have many mitochondria of variable shapes; however, Sertoli cell mitochondria have tubular cristae and are usually orientated parallel to the cell's long axis (Bloom and Fawcett, 1968; Hess and França, 2005).

Sertoli cells also have abundant smooth ER and cytoskeletal filaments (microtubules, intermediate filaments and actin filaments) (Bloom and Fawcett, 1968; Hess and França, 2005; Weinbauer *et al.*, 2010; Vogl *et al.*, 2011). The ER and cytoskeleton form ectoplasmic specialisations (ES), where actin filaments are sandwiched between the plasma membrane and ER (Vogl *et al.*, 2011). Ectoplasmic specialisations allow for adhesion between adjacent Sertoli cells as well as between Sertoli cells and spermatids (Vogl *et al.*, 2011).

Nonetheless, Sertoli cells have few rough ER and Golgi apparatus (Bloom and Fawcett, 1968; Hess and França, 2005; Weinbauer *et al.*, 2010). Additionally, Sertoli cells have lysosomes and lipid droplets; human Sertoli cells also contain Charcot-Böttcher crystals (Bloom and Fawcett, 1968; Young and Heath, 2000; Hess and França, 2005). All of the cytological features present in Sertoli cells play roles in their function. [Figure 1.7](#) illustrates adult Sertoli cells.

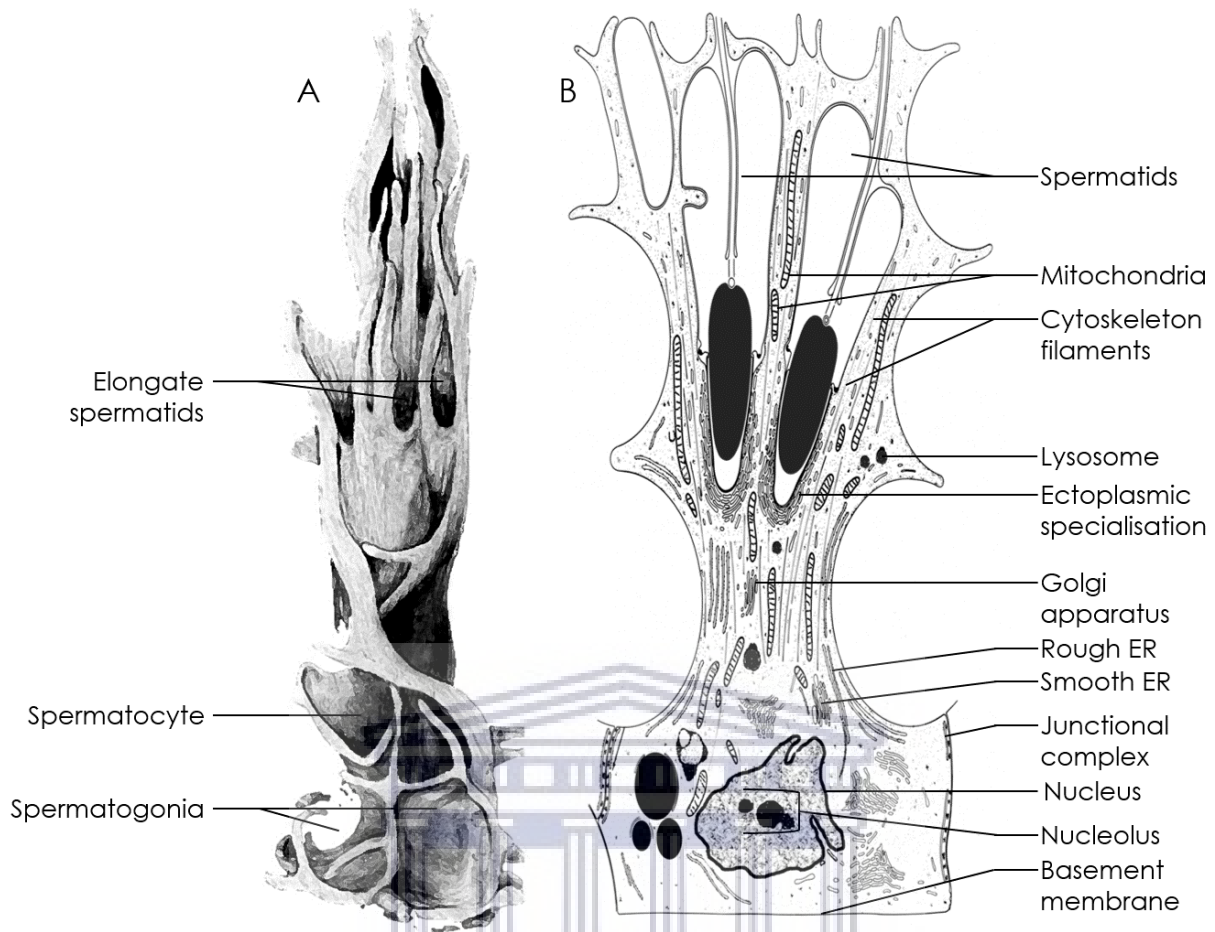


**Figure 1.7. Illustrations of the Sertoli cell** (adapted from Hess and França, 2005). **A:** A rat Sertoli cell, showing the cytoplasmic projections that surround the developing spermatozoa. **B:** A Sertoli cell in longitudinal section (cross-section of the seminiferous tubule) showing some of its cytoplasmic features. ER: endoplasmic reticulum.

#### 1.4.1 Sertoli cell signal transduction

Sertoli cells form part of the HPT axis, by secreting inhibin in response to FSH stimulation. Inhibin, in turn, provides negative feedback by inhibiting pituitary secretion of GnRH. In addition, Sertoli cells secrete androgen binding protein (ABP), which retains high testicular testosterone levels (Hinson *et al.*, 2010). Furthermore, testosterone is also required for proper Sertoli cell function (Sharpe, 2005; Ge *et al.*, 2011; Buldan *et al.*, 2016). Nevertheless, some Sertoli cell signal transduction commences on the interaction between FSH and the FSH receptor (FSHR) on the Sertoli cell membrane. Sertoli cells activate multiple signal transduction pathways due to FSH (and testosterone) stimulation.



### 1.4.1.1 Follicle stimulating hormone and Sertoli cell signalling

The FSH-FSHR interaction causes adenylate cyclase activation, which increases cytosolic cAMP levels, similar to the LH-LHCGR interaction in Leydig cells (Tindall *et al.*, 1981). Once more, as in Leydig cells, cAMP activates PKA, which appears to be the main mediator of Sertoli cell response to FSH stimulation (Weinbauer *et al.*, 2010). Additionally, cytosolic cAMP (increasing in response to FSH) can activate phosphoinositide 3-kinase in Sertoli cells (Meroni *et al.*, 2002; Walker and Cheng, 2005). Subsequently, phosphoinositide 3-kinase activates protein kinase B; this pathway is believed to mediate Sertoli cell secretion of lactate, which is the energy source for the spermatogenic series (Walker and Cheng, 2005).

### 1.4.1.2 Testosterone and Sertoli cell signalling

Testosterone signalling in the Sertoli cell appears to occur via two modes, which is the classic androgen receptor (AR)-mediated response and the non-classic response. For the classic response, testosterone passively diffuses across the cell membrane to enter the cytosol. Thereafter testosterone interacts with an intracellular AR. This interaction uncouples the AR from heat shock proteins, which tonically inhibit AR activity. The active AR then translocates to the nucleus, where it forms a dimer (with another nuclear androgen-AR complex) and (with the help of cofactors) mediates transcription of appropriate genes via interacting with androgen response elements. The classic testosterone response takes at least 30 minutes to affect gene transcription and in the order of hours to affect protein levels (Walker, 2009).

Additionally, testosterone could activate non-classical actions either via the classical AR or a membrane AR. In the first scenario, the activated ARs interact with Src kinase resulting in its phosphorylation (Walker, 2009; Walker and Cheng, 2005). Src kinase would phosphorylate the epidermal growth factor receptor, which initiates the mitogen-activated protein kinase pathway (Walker, 2009; Walker and Cheng, 2005). Ultimately, the mitogen-activated protein kinase pathway would phosphorylate CREB (cAMP response-element binding protein) (Walker, 2009; Walker and Cheng, 2005). In both non-classical signalling pathways, CREB would mediate a genomic response to testosterone.

Recently, however, it has been demonstrated that ZIP9 (zinc regulated transporter-and iron regulated transporter-like protein 9) acts as a membrane testosterone receptor for Sertoli cell signalling (Bulldan *et al.*, 2016). In their study, Bulldan *et al.* (2016) showed

that a Sertoli cell line (93RS2) that lacks the classical AR, could still be stimulated by testosterone. Furthermore, Buldan *et al.* (2016) showed that testosterone stimulation of 93RS2 Sertoli cells resulted in the phosphorylation of Erk1/2, ATF-1 and CREB within minutes. After three days of exposure to testosterone, there was an upregulation of mRNA (messenger ribonucleic acid) and protein expression of claudin-1 and -5 (Buldan *et al.*, 2016). The claudins are an important group of proteins that play a role in SCB formation (Krause *et al.*, 2008), so their upregulation to testosterone stimulation is to be expected. Lastly, Buldan *et al.* (2016) demonstrated that exposing the cells to small interfering RNA against ZIP9 caused a loss of the aforementioned responses. This presents strong evidence that ZIP9 is a testosterone receptor and may even be solely responsible for the non-classical response to testosterone.

Nonetheless, Sertoli cells synthesize various proteins in response to hormonal stimulation. These proteins could be hormones themselves (e.g. inhibin), carrier proteins (e.g. ABP), structural proteins (e.g. claudins) or enzymes (e.g. lactate dehydrogenase). Additionally, hormonal signals to Sertoli cells could also activate or inactivate specific enzymes. Hence, this communication makes it possible for the Sertoli cell to maintain its cytology, physiology and function as the nurse of the developing spermatozoa.

#### **1.4.2 Spermatogenesis and the Sertoli cell barrier**

During spermatogenesis, germ cells divide and a subset of their daughter cells (Type B spermatogonia) mature into spermatozoa. During that process, the Type B spermatogonia migrate from the basal compartment of the seminiferous tubule to the lumen, which are on either end of the SCB. Hence, the Sertoli cells must disassemble the SCB on the luminal side and reassemble the SCB on the basal side of leptotene spermatocytes (Mruk and Cheng, 2015).

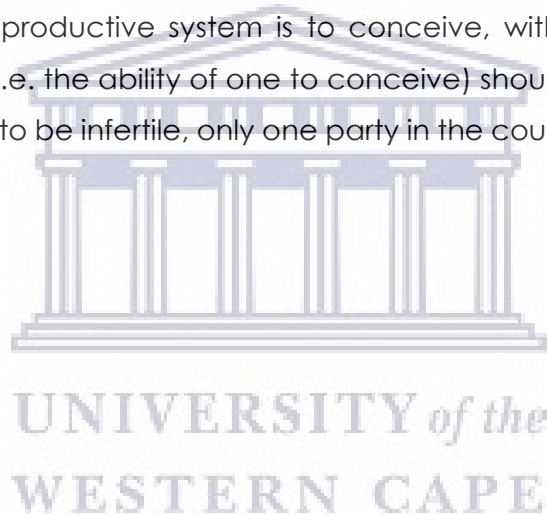
There are four different junction types in the SCB; namely tight junctions, ectoplasmic specializations (ES), desmosome-like junctions and gap junctions (For reviews see Kopera *et al.*, 2010 as well as Mruk and Cheng, 2015). These structures coexist and cooperate to produce the SCB.

Tight junctions are believed to play the most important role in SCB integrity and they can be found between preleptotene and pachytene spermatocytes. Tight junctions connect adjacent Sertoli cells and contain structural proteins including occludin,

claudins and tricellulin as well as scaffolding proteins like zona occludens which connect the tight junction to their actin cytoskeletons (Mruk and Cheng, 2015).

There are two types of ectoplasmic specialisations, based on their location in the Sertoli cell. Basal ES connect Sertoli cells to each other at the basal compartment, and are associated with the desmosome-like junctions (Kopera *et al.*, 2010). On the other hand, apical ES connect the Sertoli cells with the elongating/elongated spermatids but are not associated with desmosome-like junctions (Kopera *et al.*, 2010). Lastly, gap junctions are simply membrane channels that permit inter-Sertoli cell communication (Mruk and Cheng, 2015).

Taken together, both Leydig and Sertoli cells play essential roles in the HPT axis and indirectly in spermatogenesis; which itself is essential for conception. Ultimately, the purpose of the male reproductive system is to conceive, with the help of a fertile female. Hence, fertility (i.e. the ability of one to conceive) should be viewed as a trait of a 'couple'. However, to be infertile, only one party in the couple needs have fertility issues.



## 1.5. Infertility and some African cultural beliefs

The World Health Organisation defines infertility as the inability of a couple to conceive after a year of regular coitus, without the use of contraception (Rowe *et al.*, 1993). According to Mascarenhas *et al.* (2012), this phenomenon affects around 12.4 % of couples globally, which amounted to approximately 97 million people in 2010. Half of all infertility cases have a male factor to them, which could be caused by anything from chromosomal abnormalities, such as Klinefelter's syndrome to mechanical infertility such as a failure to ejaculate (Iammarrone *et al.*, 2003). Additionally, almost half of all male factor infertility cases are classified as idiopathic, having no known cause (Iammarrone *et al.*, 2003).

Couples who struggle to conceive often endure psychological distress with a reduction in social status, especially in Black-African cultures<sup>1</sup> (Sewpaul, 1999; Dyer *et al.*, 2004; Dyer, 2008; Gerrits *et al.*, 2017; Aiyenigba *et al.*, 2019). Many Black-African cultures place a lot of value on children because they see marriage as a union of two clans, but the union requires a new generation i.e. children (Sewpaul, 1999). In Black-African cultures, the status of women is often heavily dependent on how many children they have; furthermore, children contribute to the wealth of a family, which adds to their desirability (Sewpaul, 1999; Aiyenigba *et al.*, 2019). Infertile couples are often mocked and blamed for their infertility, because of the cultural belief that infertility is a punishment for some wrongdoing (Sewpaul, 1999; Dyer *et al.*, 2004). This places a lot of stress on marriages, and can even predispose the affected woman to domestic violence; whether she is the 'infertile' party, or not (Dyer *et al.*, 2004; Gerrits *et al.*, 2017; Aiyenigba *et al.*, 2019). Consequently (as with any health ailment), many Africans who struggle to conceive seek treatment, especially women (Dyer *et al.*, 2002; Dyer, 2008; Gerrits *et al.*, 2017).

---

**1:** This chapter uses the term 'Black-African' to refer to what is internationally known as 'Bantu'. The term 'Bantu' is generally considered as offensive in parts of Southern Africa, due to the former, *Apartheid*, South African government's policies that associated the term 'Bantu' with inferiority. I am well aware that this term is not uniquely identifiable as *Bantu*, though. There are five major indigenous African ethnic divisions, including the Pygmy people of central Africa; the latter also being a black and African population but is not *Bantu* (Diamond, 2005).

---

### 1.6. Herbal Medicine

Approximately 60% of the global population use plants as a form of medicine, and plants form a very important part of traditional medicine (World Health Organization: WHO, 2002; James *et al.*, 2018). In Africa, as much as 80% of the population use traditional medicine to treat illness, mainly because of accessibility and cultural acceptability (WHO, 2002; WHO, 2013; James *et al.*, 2018). In Africa, allopathic medical experts often have to serve larger groups of people than practitioners of traditional medicine do (WHO, 2002; WHO, 2013). Furthermore, allopathic physicians are typically located in cities, and their treatments are more expensive than traditional medicine, making them less accessible to especially the rural poor (WHO, 2002; James *et al.*, 2018). These factors, together with the Black-African cultural view that traditional medicine is as acceptable as allopathic medicine, make traditional medicine usage the norm in many regions of Africa (Sewpaul, 1999; WHO, 2002).

Traditional medicine typically involves the use of plants and/or plant products as medicines, i.e. herbal medicine (WHO, 2002; James *et al.*, 2018). There are hundreds of plants around the world that have proven beneficial and/or harmful effects on human health (Duke *et al.*, 2002). Many of these plants have been used in traditional medicine for centuries, but haven't yet been fully validated as true medicines (WHO, 2002). Tea and rooibos are examples of commonly consumed herbal medicines. The medicinal properties of plants are due to the actions of the phytochemicals they contain, e.g. polyphenols (Blair, 1907; Duke *et al.*, 2002).

#### 1.6.1 Tea

The beverage that is known as tea<sup>2</sup> (see Figure 1.8-B) is the aqueous extract from the dried leaves (sometimes the buds and stems are included) of the plant *Camelia sinensis* (family Theaceae); and is a widely consumed beverage, second only to water world-wide (Ruxton, 2008; Schneider and Segre, 2009; Das *et al.*, 2008; Khan and Mukhtar, 2007; Awoniyi *et al.*, 2012). Historically, tea was used in traditional Oriental medicine for various ailments, but it has since gained popularity as a health drink (Mukhtar and Ahmad, 2000; Zhu *et al.*, 2006).

---

**2:** To avoid confusion, in this thesis the term *tea* is used to refer to the beverage; whereas the term *tea leaves* refers to the harvested and processed plant material that is used to make *tea*. Additionally, some of the experiments described in this thesis were performed with a reconstituted *green tea*, which is also referred to as *green tea*. Lastly, the term *teas* may have been used in reference to tea and one or more tisanes (herbal teas) as a group.

---

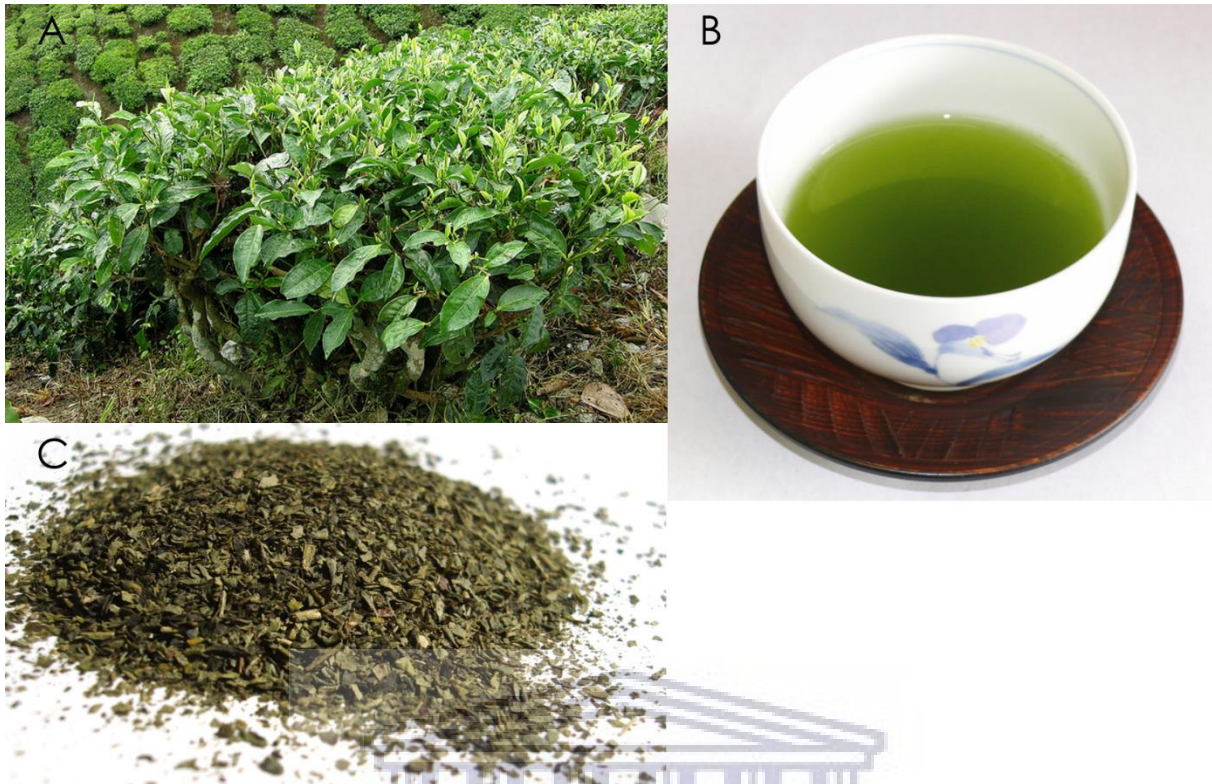


**Figure 1.8. Photographs of the green tea plant, tea leaves and tea.** **A:** *Camelia sinensis*, the tea bush (from [www.maultasch.us](http://www.maultasch.us), 2016); **B:** a cup of brewed green tea (from [www.wordpress.com](http://www.wordpress.com), 2016); **C:** processed green tea leaves (from [www.nexcesscdn.net](http://www.nexcesscdn.net), 2016).

Green tea accounts for approximately 20% of the global tea consumption, and is reported to afford more pronounced health benefits than black tea does (Rio *et al.*, 2004; Khan and Mukhtar, 2007; Das *et al.*, 2008). Green tea leaves (see [Figure 1.8-C](#)) are produced by immediately steaming or pan-frying the harvested leaves (Yang *et al.*, 2011; Cooper *et al.*, 2005; Khan and Mukhtar, 2007). This is done to prevent oxidation (also known as fermentation) of the plant material, and thus retain its green colour (oxidation of harvested leaves produces oolong and eventually black tea leaves) (Yang *et al.*, 2011; Cooper *et al.*, 2005; Khan and Mukhtar, 2007). During the fermentation process, the phytochemical composition of the tea leaves, and consequently the tea, changes. The primary phytochemicals in green tea leaves (and tea) are the catechins, which are converted to theaflavins and thearubigins during fermentation, thus producing black tea leaves (Crespy and Williamson, 2004).

The catechins (flavan-3-ols) are the most prominent flavonoids, and indeed polyphenols, in green tea. Green tea catechins include, amongst others, (+)-catechin, (-)-epicatechin, (-)-catechin gallate, (-)-epicatechin gallate, (-)-epigallocatechin and

(-)-epigallocatechin gallate (EGCG) (Wang *et al.*, 2003; Liang *et al.*, 2001; Yang *et al.*, 2007). However, green tea was also reported to contain flavonols, hydroxycinnamate quinic esters, theaflavins, caffeine, various amino acids (e.g. theanine, glutamic acid, threonine, etc.) and low levels of heavy metals and trace elements (Liang *et al.*, 2001; Shen and Chen, 2008; Rio *et al.*, 2004; Yang *et al.*, 2007).

Factors like climate (where the plant is grown), harvesting practices, storage conditions, brewing time, etc. all impact on the final composition of the brewed tea (Velayutham *et al.*, 2008). Consequently, studies that have evaluated tea composition have shown variation amongst similar tea samples (Rio *et al.*, 2004; Wang *et al.*, 2003). Nonetheless, it is well accepted that the most abundant flavonoid in green tea is EGCG which accounts for up to 55% of its total catechins (Velayutham *et al.*, 2008); see [Figure 1.11-B](#). EGCG is also reported to be one of the primary molecules that provide the health benefits of green tea (Johnson *et al.*, 2012).

Tea has many health benefits associated with it, such as inter alia antioxidant activity, anticancer activity, cardio-protective activity, anti-diabetic activity, neuroprotective activity, antibacterial activity and antiviral activity (Tan *et al.*, 2008; Zaher *et al.*, 2008; Awoniyi *et al.*, 2011; Duffy *et al.*, 2001; Cooper *et al.*, 2005; Narotzki *et al.*, 2012). However, many of the health benefits afforded to tea are related to the antioxidant activity of the tea polyphenols like EGCG (Zaveri, 2006; Das *et al.*, 2008; Velayutham *et al.*, 2008).

### 1.6.2 Rooibos

The rooibos<sup>3</sup> tisane (herbal tea) is another popular health drink (see [Figure 1.9](#)). Rooibos is produced from the leaves and stems of *Aspalathus linearis* (family Fabaceae), a leguminous shrub endemic to the Cederberg region of the Western Cape in Southern Africa (Joubert and de Beer, 2011). The Khoi-San people used rooibos as an herbal medicine, and it has historically been used to treat infantile colic (van Wyk, 2008), as a general health drink and to improve appetite (Van Wyk and Gorelik, 2017). Rooibos is becoming increasingly popular in Europe, Japan and North America due to its health benefits and lack of caffeine (Joubert *et al.*, 2008; Joubert and de Beer, 2011).

---

**3:** To avoid confusion, in this thesis the term *rooibos* is used to refer to the beverage; whereas the term *rooibos tea leaves* refers to the harvested and processed plant material that is used to make *rooibos*. Additionally, some of the experiments described in this thesis were performed with a reconstituted *green rooibos*, which is also referred to as *green rooibos*.

---

Like tea, rooibos is also sold in a fermented (red) and unfermented (green) form, but only the fermented form was historically used; hence its name (*rooibos* means 'red bush' in the Afrikaans language) (Joubert and de Beer, 2011). The preparation of green and red rooibos tea leaves is similar to that of tea (tea leaves), and like tea, the oxidation process changes the biochemical composition of the tea leaves, and thus the tisane (Joubert *et al.*, 2008; Joubert and de Beer, 2011).

The major phenolic compounds in rooibos are dihydrochalcones (e.g. aspalathin and nothofagin), flavones (e.g. orientin and iso-orientin) and flavonols (e.g. rutin) (Joubert and de Beer, 2011). Aspalathin (see [Figure 1.11-C](#)) is the most abundant polyphenol in green rooibos and, together with aspalanin (another dihydrochalcone), appears to be unique to rooibos (Joubert and de Beer, 2011).

Rooibos is reported to possess antioxidant activity, hypoglycaemic activity, anti-tumorigenic activity, cardio-protective activity and anti-mutagenic activity (von Gadow *et al.*, 1997; Muller *et al.*, 2012; Marnewick *et al.*, 2005; Pantsi *et al.*, 2011; van der Merwe *et al.*, 2006). Many of the health benefits of rooibos are likely due to its major flavonoid, aspalathin.

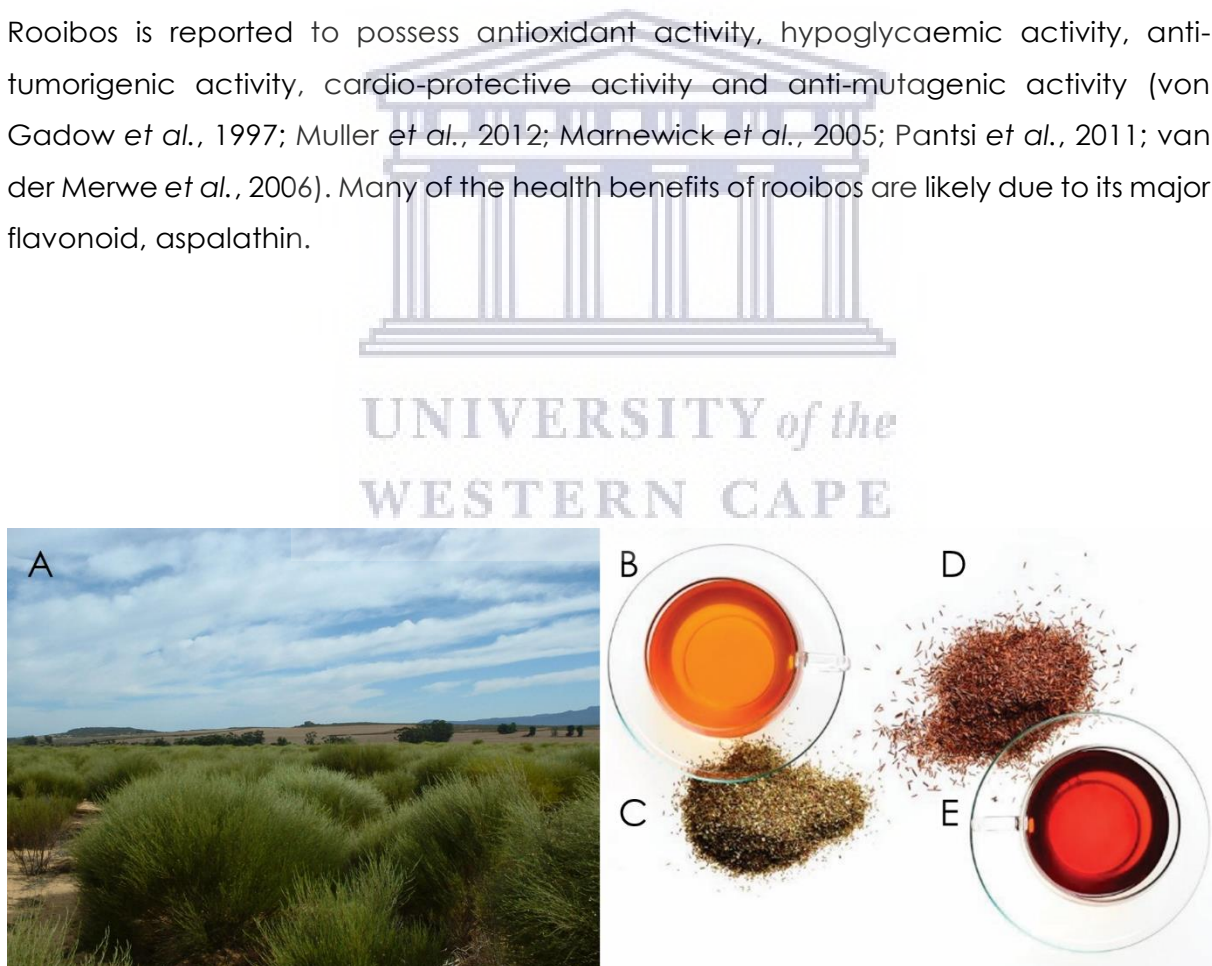


**Figure 1.9. Photographs of the rooibos plant, tea leaves and teas.** **A:** *Aspalathus linearis*, the rooibos bush (from [www.tumblr.com](http://www.tumblr.com), 2016); **B:** a cup of brewed green rooibos; **C:** processed green rooibos tea leaves; **D:** processed red rooibos tea leaves; **E:** a cup of brewed red rooibos (B-D are all from [www.gulliverstea.com](http://www.gulliverstea.com), 2016).



### 1.7. Plant polyphenols

The word *polyphenol* is made up of three parts; namely *poly-* (meaning many), *-phen-* (from the term phenyl ring, which is also known as a benzene ring) and *-ol* (i.e. containing a hydroxyl group). Thus, polyphenols are a vast group of biomolecules that should feature at least two benzene rings, each containing at least one hydroxyl group, in their structures. Historical definitions of polyphenols excluded all simple phenolic compounds that possess many similarities to the 'classic polyphenols' (Quideau *et al.*, 2011; Ferrazzano *et al.*, 2011). Consequently, many authors broaden their definitions of polyphenols to even include molecules that only contain one benzene ring (Quideau *et al.*, 2011; Sandoval-Acuña *et al.*, 2014; Tsao, 2010). According to Quideau *et al.* (2011), the simplest phenolic compounds should be excluded from the class of polyphenols, since one phenol group is insufficient to denote them as polyphenols. Consequently, Quideau *et al.* (2011) proposed their own definition for polyphenols as "*plant secondary metabolites derived exclusively from the shikimate-derived phenylpropanoid and/or the polyketide pathway(s), featuring more than one phenolic ring and being devoid of any nitrogen-based functional group in their most basic structural expression*". Additionally, Quideau *et al.* (2011) subcategorized polyphenols into chlorogenic acids, tannins, labiataetannins and flavanoids/flavonoids (see [Figure 1.10](#)).

#### 1.7.1 Flavonoids

The *Flavonoids* is a class of polyphenol that is often found in medicinal plants. Flavonoids are characterized by the presence of at least two phenyl rings (the A and B rings), which are often linked by a three-carbon chain to form a six-member ring (C ring) with the A ring (Raj Narayana *et al.*, 2001; Bravo, 1998). In addition, flavonoids contain at least one hydroxyl group in its structure and an oxygen heteroatom in the C ring, when the C ring is present (see [Figure 1.11-A](#)).

As previously mentioned, many of the health benefits associated with herbal medicines are attributed to their polyphenol content. However, the flavonoids appear to be the most important class of polyphenol in medicinal plants.

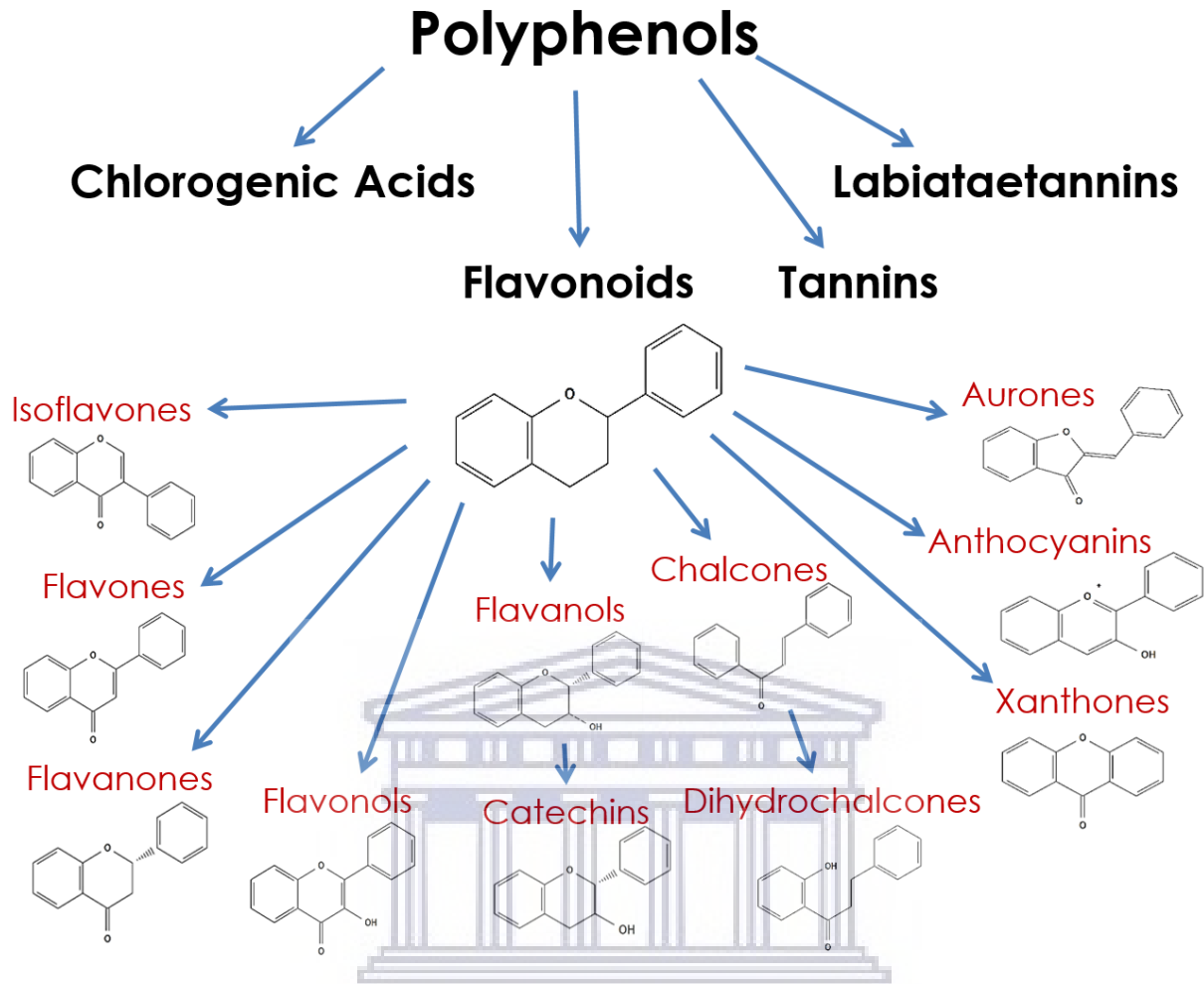


**Figure 1.10.** Diagram showing the classification of polyphenols, with subdivisions of the flavonoids (based on Quideau *et al.*, 2011. Additional information comes from: Bravo, 1998; Raj Narayana *et al.*, 2001; Tsao, 2010; Sandoval-Acuña *et al.*, 2014). Chemical structures were drawn using 'Structure Editor' (<https://scifinder.cas.org>).

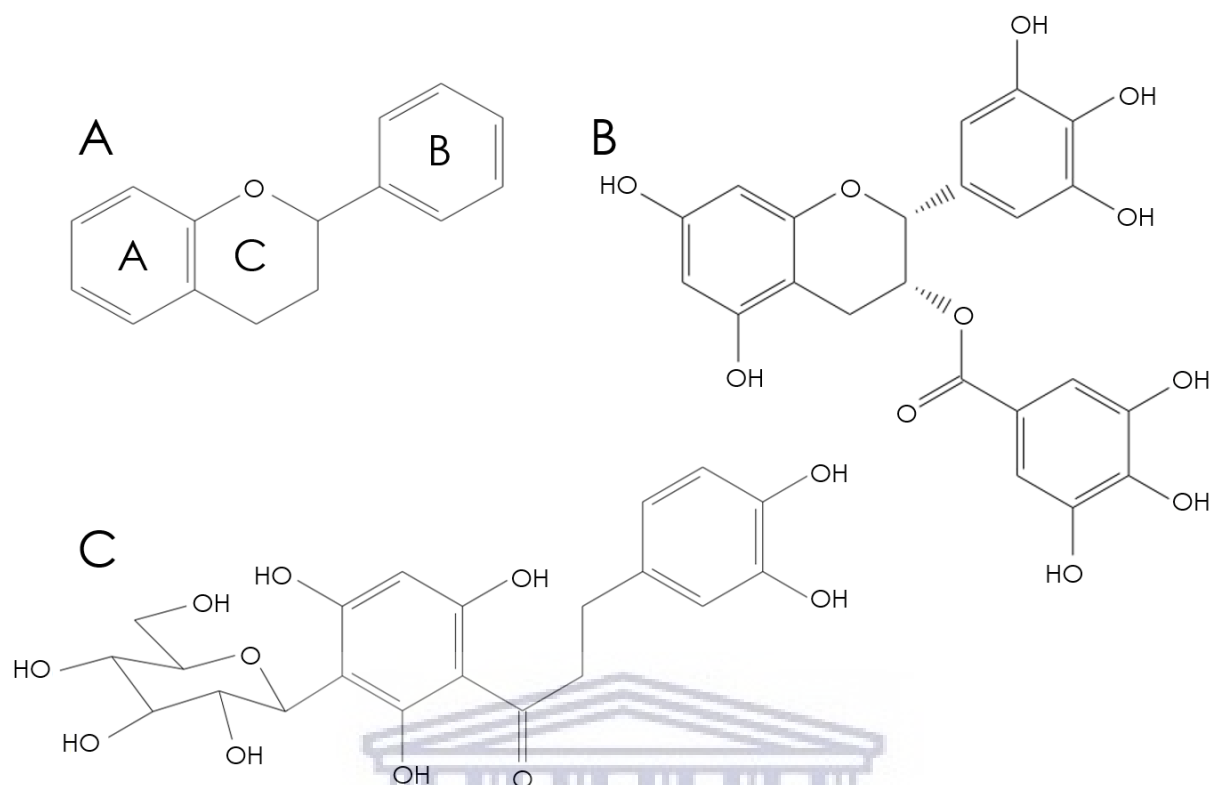


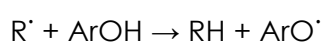
**Figure 1.11. Diagram showing the structures of flavonoids, including EGCG and aspalathin** (Bravo, 1998; Sandoval-Acuña *et al.*, 2014). **A:** the basic structure of flavonoids, showing the locations of the A, B and C rings; **B:** the structure of EGCG; **C:** the structure of aspalathin. Chemical structures were drawn using 'Structure Editor' (<https://scifinder.cas.org>).

### 1.7.2 Polyphenols as antioxidants

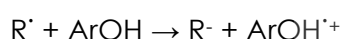
Probably the best known physiological effect of polyphenols is their antioxidant activity. Polyphenols can provide both direct and indirect antioxidant activity. Using the direct method, polyphenols scavenge reactive oxygen species (ROS) and stabilize them. Polyphenols can also act indirectly, by increasing the activity/expression of other antioxidants within cells, such as glutathione, or by inactivating/lowering ROS-producing enzymes. Additionally, polyphenols can chelate metal ions, which would otherwise catalyse free radical formation (Bravo, 1998).

### 1.7.2.1 Polyphenols as direct antioxidants

Polyphenols are thought to provide their direct antioxidant actions via two main reactions, namely the hydrogen atom transfer (HAT) reaction and the single electron transfer (SET) reaction (Bravo, 1998; Quideau *et al.*, 2011; Bentes *et al.*, 2011). As can be deduced from its name, the HAT reaction involves the donation of a proton (from the polyphenol) to a free radical. In this process, the polyphenol forms a phenoxy radical, which must be stable to stop the progression of a radical chain reaction (Bravo, 1998; Quideau *et al.*, 2011; Bentes *et al.*, 2011). The HAT reaction is represented as follows, where R<sup>•</sup> represents the free radical and ArOH represents the polyphenol (antioxidant):



During the SET reaction, the polyphenol donates an electron to a free radical. Once more, a phenoxy radical is formed in the process. The SET reaction is shown below:



Tea catechins use both HAT and SET reactions for free radical scavenging (Wright *et al.*, 2001). The B ring of tea flavonoids usually contains one or more hydroxyl groups (with low bond dissociation energies), which are reported to provide the direct ROS scavenging abilities of tea (Valcic *et al.*, 1999; Quideau *et al.*, 2011). Consequently, EGCG (which possesses three hydroxyl groups in its B ring) is reported to be the most potent antioxidant of all the tea polyphenols (Wright *et al.*, 2001).

Computational work carried out by Bentes *et al.* (2011), indicated that dihydrochalcones also use both HAT and SET reactions. Furthermore, the presence of hydroxyl groups at the C2, C6 and C4' locations determines the antioxidant activity of the dihydrochalcones (Bentes *et al.*, 2011). Aspalathin possesses hydroxyl groups at these locations, making it a potent antioxidant amongst the dihydrochalcones.

### 1.7.2.2 Polyphenols as indirect antioxidants

One indirect mechanism for the antioxidant activity of tea polyphenols involves activation of the natural antioxidant defence system. For example, tea consumption was shown to upregulate the natural antioxidant glutathione in rat testis and sperm (Awoniyi *et al.*, 2011; Awoniyi *et al.*, 2012). According to Sandoval-Acuña *et al.* (2014), the observed increase in innate antioxidant enzymes is often due to activation of the Keap1/Nrf2/ARE (Kelch ECH-associating protein 1/NF-E2-related factor 2/antioxidant response elements) pathway. Another indirect antioxidant mechanism of polyphenols involves the inhibition or antagonisation of ROS-forming enzymes, such as NADPH (reduced nicotinamide adenine dinucleotide phosphate) oxidase, xanthine oxidase and monoamine oxidase (Sandoval-Acuña *et al.*, 2014).

### 1.7.3 Polyphenols as pro-oxidants

Under specific conditions, however, polyphenols may instead act as pro-oxidants; this may be an important route for some of the reported anticancer activity of polyphenols (Quideau *et al.*, 2011; León-González *et al.*, 2015). At high concentration and pH, polyphenols could act via a SET reaction and reduce metal ions, such as copper(II) ions; eventually leading to the formation of the superoxide anion ( $O_2^-$ ), hydrogen peroxide ( $H_2O_2$ ) and hydroxyl radicals ( $OH^-$ ), as shown in [Figure 1.12](#). Cancer cells often have higher levels of these transition metals, making them particularly susceptible to this mode of ROS production by polyphenols (León-González *et al.*, 2015). According to León-González *et al.* (2015), certain polyphenols could alternatively (or concomitantly) increase cytosolic ROS levels by affecting the ROS-producing enzymes like NADPH oxidase.

#### 1.7.3.1 ROS in cell signalling, a role for anti- and pro-oxidants

ROS were previously thought of as harmful, unwanted, byproducts of aerobic respiration. Recently, however, researchers have realised that ROS may well function as cell signalling molecules (Reczek and Chandel, 2015; Kang *et al.*, 2015). Although healthy cells produce various ROS, they predominantly produce  $H_2O_2$ . Hydrogen peroxide is a relatively stable ROS and typically produces reversible interactions with cellular components (Reczek and Chandel, 2015; Kang *et al.*, 2015).

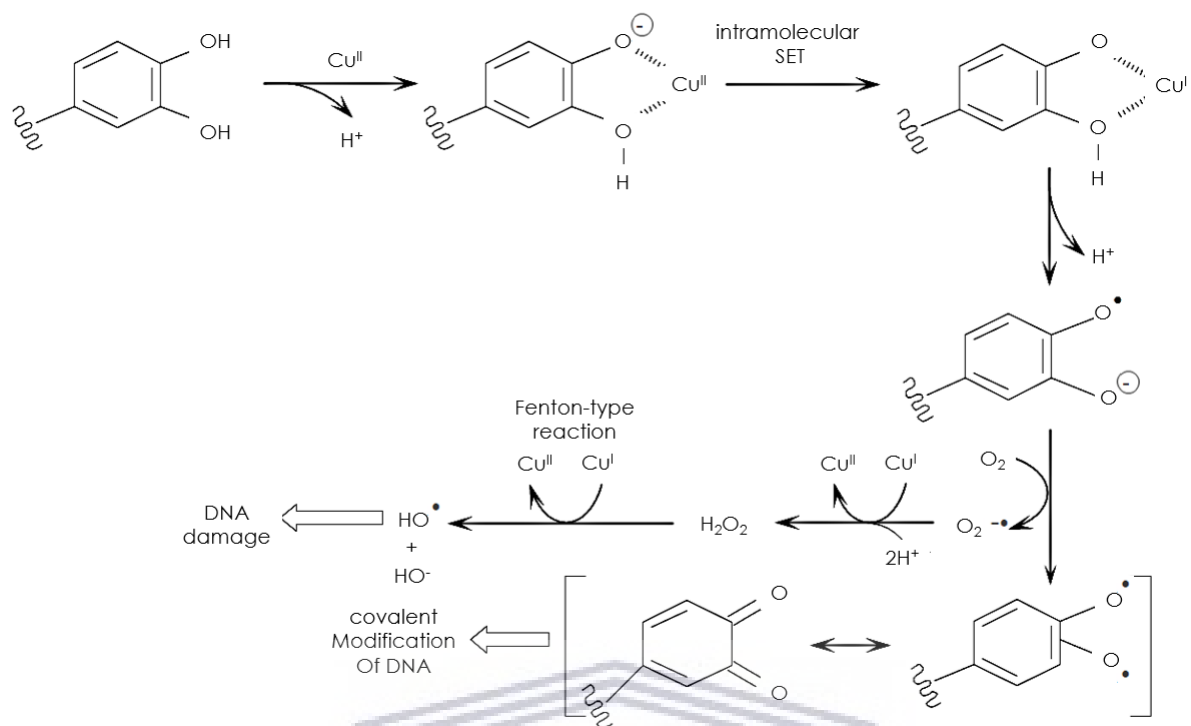


**Figure 1.12. Diagram showing the pro-oxidant pathway for catecholic (or pyrogallolic) polyphenols, by use of copper(II) ions** (redrawn from Guideau *et al.*, 2011). Chemical structures were drawn using 'Structure Editor' (<https://scifinder.cas.org>).

Hydrogen peroxide preferentially targets cysteine residues in proteins, usually forming either disulfide or sulfenicamide bonds (Reczek and Chandel, 2015; Kang *et al.*, 2015). These chemical bonds would, in turn, alter the structure of the affected protein, which could either inactivate or activate the protein in question (Reczek and Chandel, 2015; Kang *et al.*, 2015). The enzymes glutaredoxin and thioredoxin can undo the protein modifications of H<sub>2</sub>O<sub>2</sub>, returning the cell to its previous state (Reczek and Chandel, 2015; Kang *et al.*, 2015). Thus, antioxidants and (pro-oxidants), like polyphenols, could alter cell signalling by affecting H<sub>2</sub>O<sub>2</sub> levels and thus, specific protein activities.

### **1.7.4 Polyphenol bioavailability and interactions with other biomolecules**

Bioavailability refers to the capacity of a chemical agent to reach and affect its target tissue. This encompasses the absorption of the molecule into the circulation via the gastrointestinal tract, the entry of the molecule into the interstitial fluid and sometimes the entry of the molecule into specific cells, together with the actions of said agent on the relevant tissue. Additionally, the stability of the molecule(s) in each of these phases also impacts its bioavailability.

Since the major source of polyphenols in humans is ingestion of plant materials and plant-derived products, polyphenols are generally ingested together with other biomolecules such as carbohydrates, lipids and proteins (also of plant origin). The article by Jakobek (2015) reviews how polyphenols interact with proteins, carbohydrates and lipids in the alimentary canal. Although Jakobek (2015) focuses on how polyphenols interact with biomolecules in the alimentary canal, these interactions are likely to be similar to how the polyphenols would interact with the same classes of biomolecules in plasma and even within cells.

#### **1.7.4.1 Polyphenols and lipids**

According to Jakobek (2015), polyphenols cause an aggregation of lipid droplets in digestive juices, which in turn inhibits lipase activity. The lower lipase activity, *inter alia*, causes a reduction in lipid absorption, resulting in anti-lipogenic effects (Jakobek, 2015). Furthermore, the polyphenol-lipid interaction also preserves the polyphenols along the alimentary canal, as they are rendered inaccessible to catalytic enzymes. This plays a role in providing antioxidant environments in the small intestine.

#### **1.7.4.2 Polyphenols and proteins**

Polyphenols also interact with proteins by hydrophobic and/or hydrophilic bonds, which can subsequently be supplemented by hydrogen bonds (Jakobek, 2015; Chanphai *et al.*, 2018). The polyphenol's traits determine its binding affinity for proteins. High molecular weight polyphenols and those with many hydroxyl groups have the highest affinity for proteins amongst polyphenols (Jakobek, 2015; Chanphai *et al.*, 2018). Additionally, polyphenols with flexible structures are less specific in their protein substrates than less flexible polyphenols (Jakobek, 2015).

Once complexed with a polyphenol, a protein may change shape due to blockage of hydrophobic sites by the polyphenol (Jakobek, 2015; Chanphai *et al.*, 2018). It should be noted that the complexed protein may be an enzyme and this polyphenol-enzyme complexation likely inhibits enzyme activity (Jakobek, 2015; Martinez-Gonzalez *et al.*, 2017). Nonetheless, a polyphenol-protein interaction may also contribute to the preservation of polyphenols throughout the alimentary canal (Jakobek, 2015).

#### **1.7.4.3 Polyphenols and carbohydrates**

The polyphenol-carbohydrate interaction depends on the polyphenol's hydrophobicity and molecular weight, as well as the carbohydrate's structure (Amoako and Awika, 2016). Carbohydrates that have hydrophobic pockets capture free polyphenols and consequently reduce the bioavailability of that polyphenol and preserve it in the alimentary canal, as with lipid- and protein-polyphenol interactions (Jakobek, 2015). On the other hand, some carbohydrates could instead increase polyphenol bioavailability due to its (the carbohydrate's) activity on the digestive system (Jakobek, 2015). Furthermore, polyphenol-carbohydrate interactions could inhibit the formation of polyphenol-protein interactions; compounding the effects of polyphenols on mammalian physiology (Jakobek, 2015).

#### **1.7.4.4 Polyphenols in plasma**

Although much research is conducted to determine the physiological actions of polyphenols in mammals, usually only a small proportion of the consumed polyphenols can be detected in plasma. For example, Del Rio *et al.* (2010) discovered that approximately 7% of consumed polyphenols could become bioavailable to humans who ingest 500 ml of tea. However, a study by Breiter *et al.* (2011), showed that human participants who drank 500 ml of rooibos had a maximal plasma aspalathin level only 0.17% of what they consumed. It was also noted that there was much variation in plasma flavonoid levels between participants, though (Breiter *et al.*, 2011).

Once in plasma, the polyphenols are subject to various factors such as interactions with other biomolecules (e.g plasma proteins), hepatic (phase I and phase II) metabolism and elimination in urine or bile (Crozier *et al.*, 2010). Nonetheless, despite the physiological systems geared at eliminating polyphenols from the body, they can be taken up by and/or associate with various cell types (Lambert and Yang, 2003; Spencer *et al.*, 2004). Once associated with a target cell, polyphenols may well affect the physiology of that cell.



### **1.7.5 Male reproductive system studies with green tea, rooibos and EGCG**

There are few investigations on the health effects of green tea and EGCG on the male reproductive system, but there are fewer on rooibos and only one (to my knowledge) on aspalathin (Webber, 2018). Most studies investigated the protective effects of the infusions (green tea or rooibos) or flavonoids on the male mammalian reproductive system *in vivo*; see Table 1.1 for an overview. According to Table 1.1, green tea, EGCG and rooibos, administered either before, during or after exposure to a physiological insult (such as arsenic, irradiation or testicular occlusion), either attenuates or completely counteracts the insult as determined by measurements of antioxidant activity, expression of various genes, sperm quality, testicular histology, etc.

Nonetheless, there are studies on the effects of green tea, rooibos and EGCG alone on the male mammalian reproductive system. Once more, most studies on male reproduction investigate green tea or its constituents and few people study rooibos. In 2002, Satoh *et al.* published their findings that a green tea extract (Polyphenone-60) caused an increase in plasma LH and testosterone levels in male rats; indicating a positive activity on male reproduction. Another research group (Yu *et al.*, 2010) found that various green tea catechins (including EGCG) also caused an increase in male rat plasma testosterone levels. However, these findings are not universal. Opuwari and Monsees (2020) found no change in plasma testosterone levels of rats fed green tea compared to tap water. Studies by Chandra *et al.* (2011) and by Das and Karmakar (2015) both found that green tea causes a reduction in male rat testosterone levels. These studies were supported by *in vitro* experiments that showed the same trend (Figueiroa *et al.*, 2009; Abuaniza, 2013; Opuwari and Monsees, 2015). The conflict in published data indicates a need to better understand the mechanisms involved in green tea's effects on testosterone secretion and/or biosynthesis.

An investigation, by Opuwari and Monsees (2014), showed that green rooibos produced no effects on male rat serum testosterone levels, but increased sperm concentration, viability and motility. Conventional red rooibos also increased sperm viability but increased spontaneous acrosome reaction as well (Opuwari and Monsees, 2014). Furthermore, rooibos and green rooibos both appeared to reduce seminiferous tubule diameter as well as the germinal epithelium height in rats, indicating a mixed effect on male reproduction. Another study by Opuwari and Monsees (2015) showed that rooibos and green rooibos both decreased testosterone secretion by TM3 Leydig cells (*in vitro*). Although the decrease in TM3 cell testosterone

secretion disagrees with their *in vivo* study, it was a monoculture and so the interaction with other organs and tissues are missing from the *in vitro* model, making the *in vivo* study more relevant. A Master's thesis by Abuaniza (2013), showed that *ex vivo* mouse minced testis culture with rooibos produced no change in testosterone secretion, just like the *in vivo* study of Opuwari and Monsees (2014).

*In vitro* studies are useful to investigate the mechanisms by which phytochemicals affect testosterone production and release. Various studies have used TM3 cells to assess the effects of substances on testosterone secretion (Opuwari and Monsees, 2015; Gonçalves *et al.*, 2018; Leisegang and Henkel, 2018; Masuku *et al.*, 2020), which is why the TM3 model was chosen for this thesis. Unfortunately, Webber (2018) together with this thesis, discovered that TM3 Leydig cells seem to have ceased testosterone production, even upon hCG stimulation. However, Webber (2018) also found that both EGCG and aspalathin cause mitochondrial depolarization of Leydig cells without inducing apoptosis. Clearly, more research is needed to better understand how rooibos produced the noted responses in the work by Opuwari and Monsees (2014, 2015).



**Table 1.1.** Table showing an overview of studies on the protective effects of EGCG, green tea, green rooibos and rooibos on the mammalian male reproductive system against various physiological insults *in vivo*.

Treatment	Model	Delivery	Dose(s)	Insult	Insult dose	Treatment exposure type	Effects	Reference
EGCG	Mouse, <i>in vivo</i>	IP injection	50 mg/kg	Testicular vascular occlusion	60 min	Post-trauma treatment	Protects WRT apoptosis markers, DNA damage and seminiferous tubule morphometry.	Al-Ajmi <i>et al</i> (2013)
EGCG	Mouse, <i>in vivo</i>	IP injection	50 mg/kg	Irradiation	2.0 Gy total	Pre- and post-trauma treatment	Protects WRT testis weight, seminiferous tubule histology, apoptosis markers, steroidogenesis (inhibitory), SCB and Sertoli gene expression. Attenuated damage WRT sperm quality parameters, impregnation rate and LPO.	Ding <i>et al</i> (2015)
EGCG	Mouse, <i>in vivo</i>	IP injection	40 mg/kg	di-(2-ethylhexyl) phthalate, orally	400 mg/kg	Co-treatment	Protects WRT body weight, testosterone levels and sperm deformity index. Attenuates damage WRT testis histology, spermatogenic apoptosis and aromatase expression.	Ge <i>et al</i> (2015)
EGCG	Mouse, <i>in vivo</i>	IP injection	20 mg/kg	Arsenic, orally	200 ppm	Co-treatment	Protects WRT sperm concentration, sperm motility, sperm membrane integrity, sperm $\Delta\Psi_m$ , LPO, GSH activity, SOD activity, CAT activity, testosterone and testicular histology	Guvvala <i>et al</i> (2017)

							damage. Attenuates damage WRT sperm kinematics.	
EGCG	Rat, <i>in vivo</i>	IP injection	50 mg/kg	Testicular vascular occlusion	60 min	Post- trauma treatment	Protects WRT seminiferous tubule morphometry, DNA damage, inflammation markers, apoptosis and inflammation marker gene expression.	Al-Maghrebi <i>et al</i> (2012)
EGCG	Rat, <i>in vivo</i>	IP injection	80 mg/kg	Lead acetate trihydrate	50 mg/kg	Co- treatment	Protects WRT testis weight, CYP19 expression, LPO, SOD activity GPx activity, CAT activity and testicular histology damage. Attenuates WRT sperm concentration, sperm motility Seminal vesicle weight, epididymis weight, testosterone levels and estrogen levels. EGCG alone increased CYP19 expression compared to the control.	Hassan <i>et al</i> (2019)
EGCG	Rat, <i>in vivo</i>	Oral	40 mg/kg	NaF, orally	25 mg/kg	Pre-trauma treatment	Protects WRT ROS levels, MMP, non-enzymatic antioxidant levels, inflammatory cytokine expression, NQO-1 expression, HO-1 expression, Bcl-2 expression, Cas-3 expression and Cyt-c expression. Attenuates damage WRT OS markers,	Thangapandiyan and Miltonprabu (2015)

EGCG	Rat, <i>in vivo</i>	Oral	150 mg/kg	Testicular vascular occlusion	4 hours	Post- trauma treatment	3 $\beta$ HSD activity, 17 $\beta$ HSD activity, testosterone levels, sperm concentration, viability, abnormal sperm prevalence, enzymatic antioxidant activities, NRF2 expression, Keap-1 expression, $\gamma$ -GCS expression, Bad expression and testis histology. EGCG alone increased $\Delta\Psi_m$ .	Protects WRT testicular histology. Attenuates damage WRT SOD activity.	Sugiyama <i>et al</i> (2012)
Green rooibos	Rat, <i>in vivo</i>	Drinking	2% aqueous extract	t-butyl hydroperoxide injection	Not specified	Pre-trauma and co- treatment	Decreased SOD activity		Awoniyi <i>et al</i> (2011)
Green rooibos	Rat, <i>in vivo</i>	Drinking	2% aqueous extract	t-butyl hydroperoxide injection	300 $\mu$ M/kg	Pre-trauma and co- treatment	Increased epididymal sperm motility and concentration, CAT activity, SOD activity and GSH levels even with induced OS.		Awoniyi <i>et al</i> (2012)
Green tea	Mouse, <i>in vivo</i>	Gavage	250 mg/kg	Cyclophosphamide injection	100 mg/kg	Pre-trauma treatment	Protects WRT testicular LPO, GPx activity (testicular and epididymal), testicular GST activity and epididymal 17 $\beta$ HSD activity. Attenuates damage WRT testicular protein carbonyl levels, DNA damage index and sperm concentration.		Zanchi <i>et al</i> (2015)

Green tea	Rat, <i>in vivo</i>	Drinking	2% aqueous extract	t-butyl hydroperoxide injection	Not specified	Pre-trauma and co- treatment	Decreased LPO, increased SOD activity.	Awoniyi <i>et al</i> (2011)
Green tea	Rat, <i>in vivo</i>	Drinking	2% aqueous extract	t-butyl hydroperoxide injection	300 $\mu$ M/kg	Pre-trauma and co- treatment	Increased SOD activity.	Awoniyi <i>et al</i> (2012)
Green tea	Rat, <i>in vivo</i>	Drenched	100 mg/kg	Streptozotocin injection	60 mg/kg	Post- trauma treatment	Attenuates damage WRT LH levels. Green tea alone increased testosterone and FSH levels.	Al-Zamely and Al- Maraby (2014)
Green tea	Rat, <i>in vivo</i>	Gavage	40 mg/kg	Interferon $\alpha$ -2 $\beta$ (delivery method not stated)	7.500 units	Co- treatment	Protects WRT testicular histology and SOD activity.	Rezk <i>et al</i> (2014)
Green tea	Rat, <i>in vivo</i>	Drinking	2% aqueous extract	Benzo(a)pyrene injection	50 mg/kg	Pre- and post- trauma treatment	Protects WRT, testis weight, sperm motility, sperm concentration and testosterone levels.	Eldebaky <i>et al</i> (2015)
Green tea	Rat, <i>in vivo</i>	Drinking	2% aqueous extract	Nicotine, S-3-(1- methyl-2-pyrrolidinyl) pyridine injection	1 mg/kg BW	Co- treatment	Protects WRT body weight, relative testicular weight, LPO, GSH levels, SOD activity, CAT activity, sperm concentration, sperm motility, testosterone levels and testicular histology.	Mosbah <i>et al</i> (2015)
Green tea	Rat, <i>in vivo</i>	Drinking	1.5% aqueous extract	CdCl <sub>2</sub> injection	1.5 mg/kg	Post- trauma treatment	Protects WRT sperm motility. Attenuates damage WRT sperm concentration, testosterone levels and testicular histology.	Mahmoudi <i>et al</i> (2018)

Green tea	Rat, <i>in vivo</i>	Gavage	70 mg/kg	CdCl <sub>2</sub> , orally	3 mg/kg	Co-treatment	Protects WRT organ weight, sperm concentration, hypercholesterolemia, AR expression loss and caspase activation. Increased SOD and GSH activity, whilst decreasing CAT activity.	Abdelrazek <i>et al</i> (2016)
Green tea methanolic extract	Mouse, <i>in vivo</i>	Gavage	500 and 750 mg/kg	Testicular heat stress	20 min scrotal exposure to 42°C	Pre-, co- and post-trauma treatment	Protected against heat stress WRT sperm concentration, motility and membrane integrity.	Abshenas <i>et al</i> (2011)
Green tea methanolic extract	Rat, <i>in vivo</i>	IP injection	30 mg/kg	Malathion	150 mg/kg	Co-treatment	Protects WRT LPO and testicular histology. Green tea alone increased total antioxidant capacity.	Nahid <i>et al</i> (2016)
Green tea supplement	Rat, <i>in vivo</i>	Drinking	1% in water	t-butyl hydroperoxide injection	Not specified	Pre-trauma and co-treatment	Decreased SOD activity, increased GSH levels.	Awoniyi <i>et al</i> (2011)
Green tea supplement	Rat, <i>in vivo</i>	Drinking	1% in water	t-butyl hydroperoxide injection	300 µM/kg	Pre-trauma and co-treatment	Increased CAT activity	Awoniyi <i>et al</i> (2012)
Rooibos	Rat, <i>in vivo</i>	Drinking	2% aqueous extract	t-butyl hydroperoxide injection	Not specified	Pre-trauma and co-treatment	Decreased LPO, increased SOD activity.	Awoniyi <i>et al</i> (2011)
Rooibos	Rat, <i>in vivo</i>	Drinking	2% aqueous extract	t-butyl hydroperoxide injection	300 µM/kg	Pre-trauma and co-treatment	Increased epididymal sperm motility and concentration, CAT activity, SOD activity and GSH levels even with induced OS.	Awoniyi <i>et al</i> (2012)

Rooibos	Rat, <i>in vivo</i>	Drinking	2% aqueous extract	Streptozotocin injection	50 mg/kg	Post- trauma treatment	Rooibos alone could not improve sperm quality parameters.	Ayeleso <i>et al</i> (2014)
Rooibos supplement	Rat, <i>in vivo</i>	Drinking	1% in water	t-butyl hydroperoxide injection	Not specified	Pre-trauma and co- treatment	Decreased ROS levels, increased SOD activity.	Awoniyi <i>et al</i> (2011)
Rooibos supplement	Rat, <i>in vivo</i>	Drinking	1% in water	t-butyl hydroperoxide injection	300 $\mu$ M/kg	Pre-trauma and co- treatment	Increased CAT activity	Awoniyi <i>et al</i> (2012)

17 $\beta$ -HSD: 17 $\beta$  hydroxysteroid dehydrogenase; AR: androgen receptor; Bad: BCL2 associated agonist of cell death; Bcl-2: B cell lymphoma 2; Cas-3: caspase-3; CAT: catalase; CYP19: cytochrome p450 protein 19 (aromatase); Cyt-c: cytochrome C; DNA: deoxyribonucleic acid; EGCG: epigallocatechin gallate; FSH: follicle stimulation hormone; GPx: glutathione peroxidase; GSH: glutathione; HO-1: heme oxygenase 1; IP: intraperitoneal; Keap-1: kelch-like ECH-associated protein 1; LH: luteinizing hormone; LPO: lipid peroxidation; NQO-1: NAD(P)H quinone dehydrogenase 1; NRF2: nuclear factor erythroid 2-related factor 2; OS: oxidative stress; ROS: reactive oxygen species; SCB: Sertoli cell Barrier; SOD: superoxide dismutase; WRT: with respect to;  $\gamma$ -GCS: gamma-glutamylcysteine synthetase;  $\Delta\Psi_m$ : mitochondrial membrane potential.



UNIVERSITY of the  
WESTERN CAPE



## 1.8. Aims and objectives of this thesis

One can tell, from the literature presented here, that medicinal plants show a lot of potential as future allopathic medicines. They are reported to show various health-promoting effects and likely produce these effects via the polyphenols they contain, amongst others. Polyphenols show antioxidant activity and can interact with proteins, carbohydrates and lipids to produce additional physiological effects. Green tea and green rooibos both produce some effects on the male reproductive system, but conflicting research findings indicate a need for more studies.

To that end, this thesis aims to clarify how green tea and green rooibos extracts, as well as the flavonoids: EGCG (the major polyphenol of green tea) and aspalathin (the major polyphenol of green rooibos) affect the physiology of testicular cells. This study employed TM3 cells and TM4 cells as murine models of Leydig and Sertoli cells respectively.

This thesis specifically addresses the following topics:

- 1) How green tea, green rooibos, EGCG and aspalathin affect general physiological markers of testicular cells.
  - The effects of the teas and flavonoids on the oxidoreductase activity in TM3 and TM4 cells.
  - The effects of the teas and flavonoids on the morphology of TM3 and TM4 cells.
  - The effects of the teas and flavonoids on the mitochondrial membrane potential ( $\Delta\Psi_m$ ) of TM3 and TM4 cells.
  - The effects of the teas and flavonoids on intracellular levels of reactive oxygen species in TM3 and TM4 cells.
  
- 2) How EGCG and aspalathin affect Leydig cell steroidogenesis.
  - The effects of the flavonoids on TM3 cell testosterone secretion.
  - The effects of the flavonoids on TM3 cell *Lhcgr* (mRNA for LHCGR).
  - The effects of the flavonoids on TM3 cell *Star* (mRNA for StAR).
  - The effects of the flavonoids on TM3 cell *Tspo* (mRNA for TSPO).
  - The effects of the flavonoids on TM3 cell *Cyp11a1* (mRNA for CYP11A1).
  - The effects of the flavonoids on TM3 cell *Cyp17a1* (mRNA for CYP17A1).
  - The effects of the flavonoids on TM3 cell *Hsd17b3* (mRNA for 17 $\beta$ HSD3).

- 3) How green tea, green rooibos, EGCG and aspalathin affect specific Sertoli cell functions.
- The effects of the teas and flavonoids on TM4 cell inhibin B secretion.
  - The effects of the teas and flavonoids on lactate secretion by TM4 cells.
  - The effects of the flavonoids on transepithelial electrical resistance (TEER) of TM4 cells.



UNIVERSITY *of the*  
WESTERN CAPE

# Chapter 2

---

## Materials & Methods



UNIVERSITY *of the*  
WESTERN CAPE

## 2.1 List of materials

**Department of Molecular & Cell Biology, University of Cape Town, South Africa:**

Primers for conventional PCR (see [Table 2.1](#))

**DRG Instruments GmbH, Germany:**

Testosterone ELISA kit

**Elabscience®, USA:**

Inhibin B ELISA kit

**Fanorgen Biotech corp., Taiwan:**

Tri-RNA reagent

**Five Roses®, South Africa:**

Green tea teabags

**GeneDirex, Taiwan:**

Novel Juice

**Gibco, UK:**

Phosphate buffered saline (PBS)

**Inqaba Biotech Industries (Pty) Ltd, South Africa:**

PAGE-purified primers for qPCR (see [Table 2.1](#))

**Kimix Chemicals and Laboratory Suppliers cc, South Africa:**

Ethanol

Various plastic consumables

**Life Technologies™, USA:**

Chloromethyl 2',7'-dichlorodihydrofluorescein diacetate (CM-H<sub>2</sub>DCFDA)

Hoechst 33342

Tetramethylrhodamine ethyl ester (TMRE)

MicroAmp® Fast Optical 96-well Reaction Plate (0.1 ml)



**Lonza, Belgium:**

Dulbecco's modified Eagle's medium:Ham's F12 medium mix, 1:1 (DMEM:F12)  
Foetal bovine serum (FBS)  
Horse serum (HS)  
Penicillin-streptomycin (pen-strep)  
Trypsin- ethylenediaminetetraacetic acid (trypsin-EDTA)

**Merck, Germany:**

Chloroform  
Dimethyl sulfoxide (DMSO)  
Ethanol for molecular biology  
Hydrogen peroxide (H<sub>2</sub>O<sub>2</sub>)  
Millicell® 0.45 µm standing cell culture plate inserts  
Sodium hydroxide (NaOH)

**New England Biolabs Inc., USA:**

Luna® Universal qPCR Mater Mix

**Promega Corporation, USA:**

100 bp (base pair) DNA ladder  
Agarose powder  
Boric acid for molecular biology  
Deoxynucleoside triphosphate (dNTP)  
Ethidium bromide  
Ethylenediaminetetraacetic acid (ETDA) for molecular biology  
GoTaq® G2 Flexi DNA Polymerase PCR kit  
Tris base for molecular biology  
Wizard® SV Gel and PCR Clean-Up System

**Qiagen GmbH, Germany:**

Nuclease-free water

**Raybiotech, USA:**

Follicle stimulating hormone (FSH)



**Rooibos Ltd, South Africa:**

Green rooibos tea leaves

**Sigma-Aldridge, USA:**

3-(4,5-dimethylthiazol-2-yl)-2,5-diphenyltetrazolium bromide (MTT)

Amphotericin B

Aspalathin

Bovine serum albumin (BSA)

Carbonyl cyanide 3-chlorophenylhydrazone (CCCP)

Chorionic gonadotropin from human urine (hCG)

Collagenase type I

Deoxyribonuclease

Epigallocatechin gallate (EGCG)

Glutamic pyruvate transaminase (GTP)

Isopropanol

Lactate dehydrogenase (LDH)

L-glutamic acid

Sodium L-lactate

Soybean trypsin inhibitor

Trypan blue

$\beta$ -Nicotinamide adenine dinucleotide hydrate ( $\beta$ -NAD)



UNIVERSITY of the  
WESTERN CAPE

**SPL Life Sciences, Korea:**

Black flat-bottomed 96-well plates for cell culture

Clear flat-bottomed 96-well plates for cell culture

**Takara, China:**

PrimeScript™ RT reagent kit (Perfect Real Time)

**Whatman®, UK:**

200 nm pore syringe filters

Whatman® cellulose filter paper

**Wuxi NEST Biotechnology Co.,Ltd, China:**

PCR tubes

Various cell culture plastic consumables

## 2.2 Sample preparation

### 2.2.1 Green tea and green rooibos preparation

Tea bags for green tea (Five Roses®; Bryanston, South Africa) were purchased from a local supermarket and green rooibos tea leaves were kindly donated by Rooibos Ltd (Clanwilliam, South Africa) (see the footnotes <sup>2</sup> on page 22 and <sup>3</sup> on page 24 for my semantics of *green tea* and *green rooibos*). The dried tea leaves were stored at room temperature, in a dark container until needed. Both the green tea and green rooibos were prepared in the same manner.

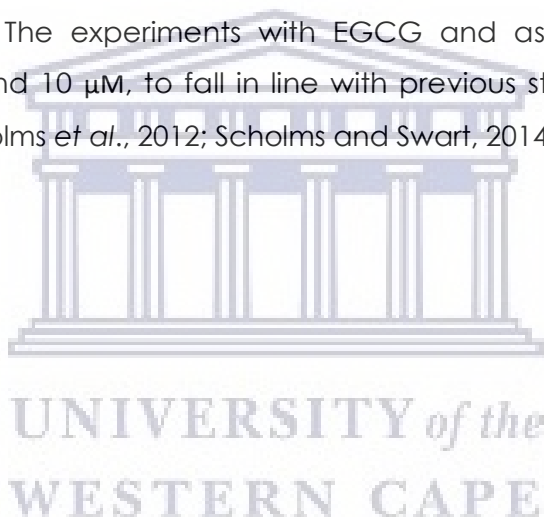
Tap water was brought to the boil, before immediately being measured and mixed with the tea leaves of either green tea or green rooibos at a concentration of 50 g/l (i.e. a five percent solution). Then, the tea leaves and water was continuously mixed for five minutes on a magnetic stirrer. Thereafter, the tea/tisane solution was strained through two layers of clean muslin cloth. Next, the solutions were sequentially passed through Whatman® cellulose filter paper (Whatman®, UK), numbers four and one, using a vacuum-powered Büchner funnel. The solutions were then centrifuged at maximum speed (4 180 ×g) for 10 minutes, and their supernatants were collected for freeze-drying. The respective tea solutions were then frozen at -20°C overnight, before being freeze-dried. After freeze-drying, the powders produced were weighed before being stored at -20°C in airtight containers that were protected from light until needed.

On the day of an experiment, just prior to use, the freeze-dried powders were allowed to reach room temperature, before being weighed out into sterile test tubes as needed. Next the appropriate volumes of prepared complete media (see [section 2.3.1](#) for details about complete media) were added to the test tubes and allowed to mix thoroughly, producing reconstituted teas. Thereafter, the reconstituted teas were passed through 200 nm pore (sterile) filters (Whatman®, UK) under sterile conditions. Finally, the sterile reconstituted teas were diluted as needed before being used in the experiments described further in this chapter. The experiments with green tea and green rooibos focussed on concentrations of 50 and 200 µg/ml, to fall in line with previous studies (Abuaniza, 2013; Opuwari and Monsees, 2015).

### 2.2.2 EGCG and aspalathin preparation

The EGCG and aspalathin samples used for these experiments were purchased, in powder form, from Sigma-Aldridge (USA) and were solubilised in dimethyl sulfoxide (DMSO) (Merck, Germany) to produce stock solutions of 20 mM each. These were then sterile filtered using 200 nm pore syringe filters and stored in aliquots at -20°C until needed.

On the day of an experiment, just prior to use, aliquots of EGCG and/or aspalathin stock solutions were allowed to thaw at room temperature. Next, the flavonoids were diluted further as needed with appropriate volumes of sterile DMSO under sterile conditions. Finally, the DMSO-flavonoid solutions were mixed with appropriate volumes of complete media to produce the desired flavonoid concentrations, whilst producing a DMSO concentration of 0.5 %. These were then used in the experiments as described further in this chapter. The experiments with EGCG and aspalathin focussed on concentrations of 0.1 and 10  $\mu\text{M}$ , to fall in line with previous studies (Figueiroa *et al.*, 2009; Yu *et al.*, 2010; Scholms *et al.*, 2012; Scholms and Swart, 2014; Mugari, 2015).





## 2.3 Cell culture

### 2.3.1 Cell maintenance

TM3 Leydig cells and the TM4 Sertoli cells (both from *Mus musculus*) were purchased from ATCC® (CRL-1714™ and CRL-1715™, respectively), and both cell-lines were cultured in the same way. They were maintained in a complete medium (10 ml per flask) made up of Dulbecco's modified Eagle's medium:Ham's F12 medium mix, 1:1 (DMEM:F12; Lonza, Belgium) supplemented, by volume, with five percent foetal bovine serum (FBS; Lonza, Belgium), 10 % horse serum (HS; Lonza, Belgium) and one percent penicillin-streptomycin (pen-strep; Lonza, Belgium). The cells were cultivated in T75 (75 cm<sup>2</sup> surface area) cell culture flasks (NEST, China) and were incubated under humid conditions at 37°C with five percent CO<sub>2</sub>. The cells were monitored daily for confluence levels, changes in media pH and signs of microbial contamination. The media was usually replaced daily, unless the cell density was too low to cause a noticeable change in media colour. Both TM3 and TM4 cells were maintained like this until they reached at least 80 % confluency before being trypsinised. Cell passage numbers of 30 to 55 were used for experimentation.

### 2.3.2 Trypsinisation

For trypsinisation, firstly the old media was discarded and the cells were washed once with 5 000 µl of sterile phosphate buffered saline solution (PBS; Gibco, USA). Thereafter, 2 000 µl of trypsin-EDTA solution (Lonza, Belgium) was added to the flask, and this was placed in the incubator (37°C) for approximately two minutes. Next, the cells would be examined under microscope (at 100 × magnification) to confirm detachment. If cells were not satisfactorily detached, the flask would be struck on the side a few times to aid detachment. Once enough cells were detached from the flask, the trypsin would be inactivated by the addition of 4 000 µl of complete media, followed by mixing. This gave an initial cell suspension that was used for either subculturing, freezing or experimentation.

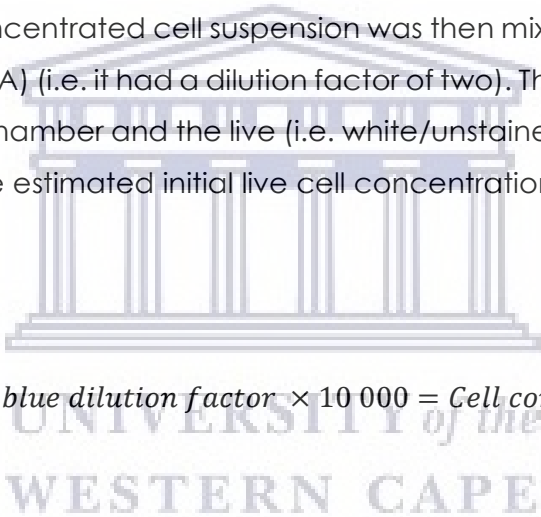
### 2.3.3 Subculturing and freezing

For subculturing, a proportion of the cell suspension (usually 1 000 µl) was transferred to a new flask. The new flask was then topped up (to 10 ml) with more complete medium before returning to a humidified incubator at 37°C with five percent CO<sub>2</sub>.

For freezing, the cell suspension (from trypsinisation) was instead transferred to a 15 ml centrifuge tube and centrifuged at 120 xg for five minutes. Thereafter the supernatant was carefully discarded and the cells were resuspended in 3000 µl of freezing medium (complete medium supplemented by volume with five percent DMSO) and transferred to cryogenic vials (cryovials) (NEST, China). The cryovials were held at -20°C for 30 minutes before being transferred to a polystyrene foam box placed at -80°C. Cryovials remained at -80°C for at least 20 hours before being transferred to liquid nitrogen for long-term storage.

### **2.3.4 Cell counting for experiments**

After trypsinisation, the cell suspension was transferred to a 15 ml centrifuge tube and centrifuged at 120 xg for five minutes (as for freezing). The supernatant was carefully discarded and the cell pellet was resuspended in 2 000 µl of complete medium. Next, a 20 µl sample of the concentrated cell suspension was then mixed with 20 µl of trypan blue (Sigma-Aldridge, USA) (i.e. it had a dilution factor of two). This was then transferred to a haemocytometer chamber and the live (i.e. white/unstained) cells were counted under a microscope. The estimated initial live cell concentration was then calculated as follows:


$$\frac{\text{Live cells counted}}{\text{Chambers counted}} \times \text{trypan blue dilution factor} \times 10\,000 = \text{Cell concentration [cells/ml]}$$

After determining the cell concentration, the cell suspension was diluted with complete medium (as needed) for the experiment at hand.

## 2.4 MTT (and photo microscopy) experiments

### 2.4.1 MTT principle

Measuring the reduction of the chromogen MTT (3-(4,5-dimethylthiazol-2-yl)-2,5-diphenyltetrazolium bromide) by living cells to its formazan is widely used for assessing cell viability. Dead cells would not produce formazan from MTT and so would produce lower absorbance readings (between 500 and 600 nm) than living cells would. As such, the amount of formazan detected (in an MTT assay) can indicate the amount of living cells in a test vessel. If one were to control how many living cells are used in an MTT assay, one could thus assess the viability of the cells in question.

Of course, there is the caveat that a test substance which affects cell proliferation and/or specific enzyme activities could influence MTT results. As such, the MTT is well complimented by the microscopic evaluation of cells being tested. Microscopy can show how densely cells are packed, as well as their morphology, which can also indicate cell viability.

### 2.4.2 Cell seeding and treatment

TM3 and TM4 cells were treated in the same way for the MTT assay. Once cells were confluent enough, they were trypsinised, centrifuged and counted as described in [section 2.3](#). Next the cells were diluted to a cell concentration of 20 000 per millilitre and seeded at 200  $\mu$ l/well into clear, sterile, flat-bottomed 96-well cell culture plates (SPL Life Sciences, Korea). Thereafter, the cells were incubated overnight at 37°C with five percent CO<sub>2</sub> in a humid incubator, to allow cell attachment and recovery from trypsinisation.

After the recovery period, the supernatants were discarded and replaced with appropriate treatments in complete medium. Cells were either treated with no compounds (complete medium only), a vehicle control (0.5 % DMSO in complete medium), a cell death positive control (10 % DMSO in complete medium), or either reconstituted green tea or green rooibos (25  $\mu$ g/ml, 50  $\mu$ g/ml, 100  $\mu$ g/ml, 200  $\mu$ g/ml or 400  $\mu$ g/ml; TM3 experiments included 800  $\mu$ g/ml as well) in complete medium or with either aspalathin or EGCG (0.1  $\mu$ M, 5  $\mu$ M, 10  $\mu$ M, 50  $\mu$ M or 100  $\mu$ M for TM3 cells; 0.5  $\mu$ M, 5  $\mu$ M or 10  $\mu$ M for TM4 cells, all with 0.5 % DMSO total) in complete medium. In addition, TM3 cells were also cultured either in the presence or absence of human chorionic gonadotropin (hCG; Sigma-Aldridge, USA) at a concentration of 125 mIU/ml (IU:

international units). Cells were exposed to these treatments for 24 hours at 37°C with five percent CO<sub>2</sub> in a humid incubator.

#### **2.4.3 Photo microscopy**

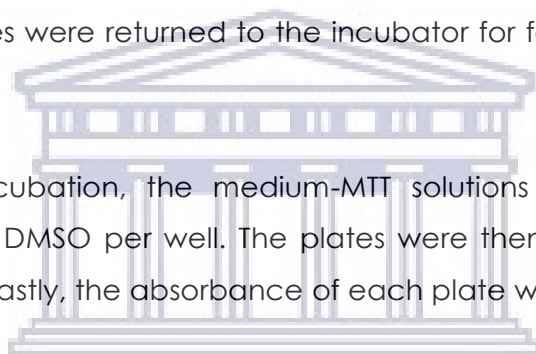
Once the treatment times had elapsed, random wells from each treatment were viewed under a light microscope and photographed for qualitative morphology analysis.

#### **2.4.4 MTT assay**

Thereafter, the supernatants were discarded. The cells were then washed with 100 µl of sterile PBS per well and were followed up with the addition of 200 µl of fresh complete medium per well. Next, 20 µl of 3-(4,5-dimethylthiazol-2-yl)-2,5-diphenyltetrazolium bromide (MTT; Sigma-Aldridge, USA) stock solution (1000 µg/ml in PBS) was added to each well and the plates were returned to the incubator for four hours (humid, 37°C with five percent CO<sub>2</sub>).

After the four hour incubation, the medium-MTT solutions were discarded and replaced with 100 µl of DMSO per well. The plates were then held in the dark and agitated for 5 minutes. Lastly, the absorbance of each plate was read at 560 nm and 750 nm and recorded.

To calculate the percentage of oxidoreductase activity, the absorbance readings at 750 nm was subtracted from that of the 560 nm reading. The percentage oxidoreductase activity was calculated on the assumption that the negative control treatments (i.e. medium or vehicle) produced 100 % oxidoreductase activity for the respective experiments (i.e. teas or flavonoids).



UNIVERSITY of the  
WESTERN CAPE

## 2.5 TMRE experiments

### 2.5.1 TMRE principle

Tetramethylrhodamine, ethyl ester (TMRE) is a cationic, cell permeable fluorescent probe. Since active mitochondria maintain a negative membrane potential, they also attract the TMRE probe. Subsequently, TMRE can accumulate in these mitochondria and their fluorescence can be detected. If mitochondria were to depolarize, the TMRE would leach out (or not accumulate there as much) and a decrease in relative fluorescence would be observed. Figure 2.1 shows an illustration of the TMRE principle.

### 2.5.2 Cell seeding and treatment

For the TMRE assay, cells were trypsinised, centrifuged and counted as described in section 2.3. The cells were seeded at 10 000 cells per well in a volume of 100  $\mu$ l per well into sterile black 96-well plates (SPL Life Sciences, Korea). After allowing cell attachment overnight (in a humid incubator at 37°C with five percent CO<sub>2</sub>), 80  $\mu$ l of the supernatant was removed and replaced with either no compounds (complete medium only), a vehicle control (0.5 % DMSO in complete medium), complete medium-reconstituted green tea or complete medium-reconstituted green rooibos (50  $\mu$ g/ml, or 200  $\mu$ g/ml) or with either aspalathin or EGCG (0.1  $\mu$ M or 10  $\mu$ M in complete medium with 0.5 % DMSO). Next, the cells were allowed a 24 hour exposure to these treatments at 37°C in a humidified incubator with five percent CO<sub>2</sub>.

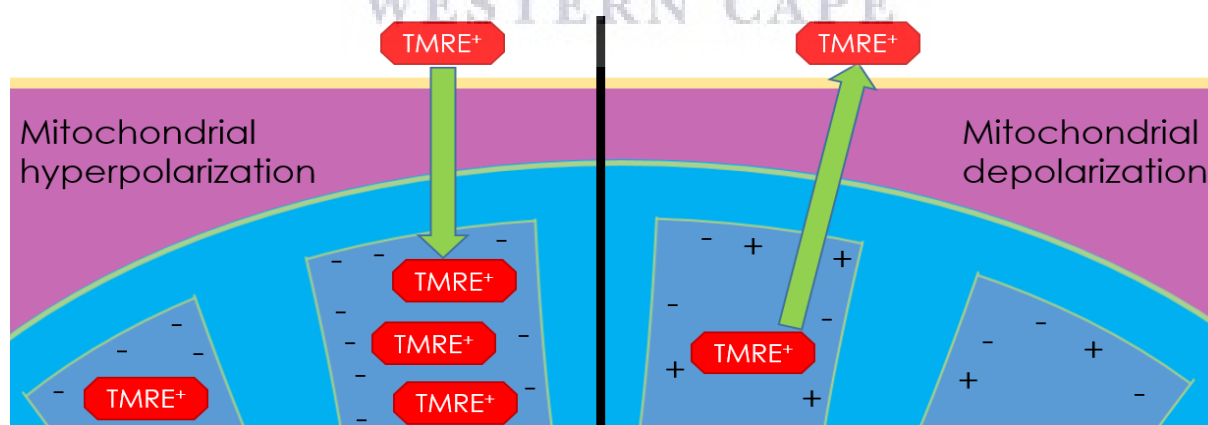


**Figure 2.1. Diagram illustrating the principle of using TMRE to measure mitochondrial membrane potential.** TMRE is membrane permeable and positively charged. TMRE is attracted to the negative charge of hyperpolarized mitochondria and accumulates there, giving a fluorescent signal. When a mitochondrion becomes depolarized, TMRE passively diffuses out of the mitochondria. Alternatively, depolarized mitochondria will not accumulate TMRE.

An additional treatment was added as a positive control for depolarization, namely medium with carbonyl cyanide 3-chlorophenylhydrazone (CCCP; Sigma-Aldrich, USA). However, the CCCP treatment only lasted for 60 minutes (to prevent cell death) and so was added to the appropriate wells an hour before the other treatments were complete. Furthermore, to mitigate the effects of changing media on the experiment; the CCCP-treated cells only received 10  $\mu$ l of a concentrated CCCP solution to produce the final concentration of 20  $\mu$ M when diluted with the medium already present in the wells.

### **2.5.3 TMRE assay**

After the exposure period, 80  $\mu$ l (90  $\mu$ l for the CCCP-treated cells) of the supernatant was replaced with 80  $\mu$ l of PBS to wash each well. Thereafter, the PBS from each well was replaced with 80  $\mu$ l of the TMRE-Hoechst label solution (500 nM TMRE with 4 000 ng/ml Hoechst 33342 in PBS). Blanks were included in the plate for each treatment (i.e. additional treated cells), and those wells received PBS instead of the label solution. This was incubated for 30 minutes (in a humid incubator at 37°C with five percent CO<sub>2</sub>) to allow labelling.

After labelling, 80  $\mu$ l of the supernatant from each well was replaced with a PBS solution containing 0.2 % BSA (bovine serum albumin; Sigma-Aldridge, USA). Finally, the plate's fluorescence was measured on a Glomax®-Multi Detection System Model E7031 (Promega Corporation, USA) plate reader using a green fluorescence filter kit (excitation at 525 nm and emission at 580 nm - 640 nm) for TMRE followed, by a violet fluorescence filter kit (excitation at 365nm and emission at 410 nm - 460 nm) for Hoechst.

To calculate relative fluorescence, the fluorescence reading of the blank for each sample was subtracted from that of each labelled well of that sample. Next, the blank subtracted TMRE readings were divided by the blank subtracted Hoechst readings to give an indication of fluorescence per unit of cell population.

## 2.6 CM-H<sub>2</sub>DCFDA experiments

### 2.6.1 CM-H<sub>2</sub>DCFDA principle

The nonfluorescent leucodye chloromethyl-2',7'-dichlorodihydrofluorescein diacetate (CM-H<sub>2</sub>DCFDA) can passively diffuse into cells where intracellular esterase can cleave its acetate groups. The deacetylation makes the probe more polar and thus less membrane permeable. Furthermore, the chloromethyl group reacts with thiols within the cell to aid in its retention. Thereafter, the probe can be oxidised by various intracellular ROS to produce the fluorophore 2',7'-dichlorofluorescein (DCF). DCF fluorescence can then be quantified by a fluorescence instrument, like a fluorescence microscope, a fluorometer or a flow cytometer. [Figure 2.2](#) illustrated how the CMH<sub>2</sub>DCFDA probe works. The higher the DCF fluorescent signal, the greater the ROS levels in the cells under study. Alternatively, a cell population with high ROS levels would have a high proportion of cells that exhibit DCF fluorescence.

### 2.6.2 ROS assay by flow cytometry

The ROS assay, by flow cytometry, was performed according to Webber (2018); and both the TM3 and TM4 cells were treated in the same manner for this assay. The cells were trypsinised and enumerated as described in [section 2.3](#). Cells were seeded into 12 well plates (NEST, China) at a concentration of 100 000 cells per well (1000 µl/well) in complete medium and were allowed 24 hours of recovery in a humid incubator at 37°C and 5 % CO<sub>2</sub>. After the recovery period, the cells were exposed to the following treatments for 24 hours (humid, 37°C and 5 % CO<sub>2</sub>): a negative control (complete medium), vehicle control (0.5 % DMSO in complete medium), positive control (100 µM of H<sub>2</sub>O<sub>2</sub> in complete medium), green tea (50 µg/ml or 200 µg/ml), green rooibos (50 µg/ml or 200 µg/ml), EGCG (0.1 µM or 10 µM; TM3 cells received 5 µM and 100 µM as well) in DMSO at 0.5% or aspalathin (0.1 µM or 10 µM; TM3 cells received 5 µM and 100 µM as well) in DMSO at 0.5%.

After the treatment time, the supernatants were discarded and the cells were washed with 500 µl of PBS per well. Next, each well received 200 µl of trypsin-EDTA and were given 60 seconds to detach (humid, 37°C and 5 % CO<sub>2</sub>). Thereafter, the trypsin was inactivated by the addition of 200 µl of complete medium. The floors of the wells were flushed a few times to aid the cell detachment, and the cell suspensions were transferred to 1.5 ml centrifuge tubes. The cells were then centrifuged at 260 ×g for five minutes.

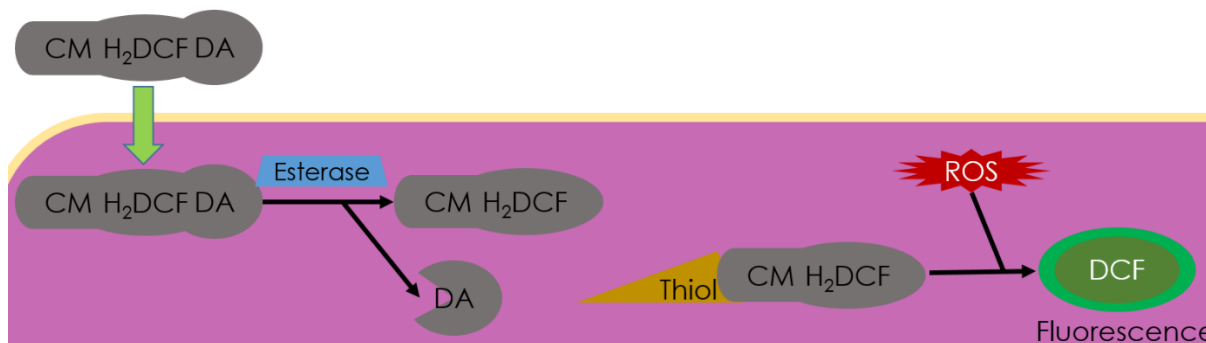


**Figure 2.2. Diagram illustrating the principle of how CMH<sub>2</sub>DCFDA reacts to signal ROS levels within cells.**

The nonfluorescent CMH<sub>2</sub>DCFDA passively enters the cell, where its acetate groups are cleaved to retain it in the cell. Additionally, thiols within the cell bind to the CM group. ROS interact with the probe to form DCF which is fluorescent.

Next, the supernatants were discarded and each cell pellet was resuspended in 400  $\mu$ l of CM-H<sub>2</sub>DCFDA label solution (10  $\mu$ M in PBS). The preparation of the labelling solution, the labelling procedure and the subsequent steps were all done under low light to minimise photobleaching. The cells were labelled for 30 minutes under humid conditions at 37°C and with 5 % CO<sub>2</sub>. Thereafter, 10 000 events were quantified using a BD Accuri™ C6 flow cytometer for DCF fluorescent cells. The filters used were for excitation wavelengths of 492 to 495 nm, and for emission wavelengths of 517 to 527 nm. The gating was performed using the BD Accuri™ 6C software, version 1.0.264.21. See [Appendices III](#) and [IV](#) for representative scatter plots and histograms of the blank control (unlabelled cells), negative control and positive control (100  $\mu$ M H<sub>2</sub>O<sub>2</sub>).

### 2.6.3 ROS assay trials by microplate reader

After reviewing the flow cytometry data for the CM-H<sub>2</sub>DCFDA assay, and after the success in using the microplate reader in the TMRE assay, it was decided to attempt the CM-H<sub>2</sub>DCFDA using the plate reader as well.

A number of trials were conducted in order to determine whether a greater difference could be realised between the controls, by varying the concentration of H<sub>2</sub>O<sub>2</sub> used. An attempt was also made to determine the optimal concentration of the fluorescent probe (CM-H<sub>2</sub>DCFDA) for labelling. Tests were performed to determine whether reducing the amount of wash steps could retain enough cells for labelling, without producing excessive background fluorescence. Furthermore, the background fluorescence and autofluorescence of the cells were also determined in order to establish the detection limit for DCF with the setup being used.



The TM3 cells were trypsinised and enumerated as described in [section 2.3](#). The cells were seeded into black 96-well cell culture plates (SPL, Korea) as described for the TMRE assay. After the 24 hour recovery period, the cells were treated with varying concentrations of H<sub>2</sub>O<sub>2</sub> (in complete medium) to act as a positive control (0 µM, 1 µM, 5 µM, 10 µM, 50 µM, 100 µM, 1000 µM, 2000 µM or 4000 µM). The cells were given a 24 hour exposure to these treatments under humid conditions, 5 % CO<sub>2</sub> and 37°C.

After the treatment period, the supernatants were discarded, the wells were washed at least once with PBS (initially four wash steps were used), which was followed by the addition of a label solution. Various label solutions were used, and all label solutions (and assay procedures that followed), were prepared/performed under low light to protect the fluorescent probes. The label solutions were prepared in PBS with Hoechst 33342 (4 000 ng/ml) and CM-H<sub>2</sub>DCFDA (1 µM, 5 µM, 10 µM, 20 µM or 30 µM). Cells were given a 30 minute label period at 37°C, 5 % CO<sub>2</sub> and humidity.

After labelling, the label solution was carefully discarded and replaced with PBS containing 0.2 % BSA. Finally, the fluorescence of each well was measured using a Glomax®-Multi Detection System Model E7031 (Promega Corporation, USA). The violet filter kit was used for Hoechst (excitation: 365 nm, emission: 410 - 460 nm) and the blue filter kit (excitation: 490, emission: 510 - 570 nm) was used for DCF.



UNIVERSITY of the  
WESTERN CAPE

## 2.7 Leydig cell testosterone secretion experiments

### 2.7.1 TM3 cell testosterone secretion experiments

A trial was performed on TM3 Leydig cells to determine whether they still produced testosterone upon hCG stimulation.

#### 2.7.1.1 Forty eight hour experiment with complete medium

Once TM3 cells were confluent enough in culture, they were trypsinised, enumerated, diluted and seeded into 96-well cell culture plates (SPL Life Sciences, Korea) at a cellular density of 12 500 cells per millilitre (200  $\mu$ l/well). After 24 hours of recovery from trypsinisation, the cells were exposed to either no hCG, 60 mIU/ml (i.e. 12 mIU/well) or 180 mIU/ml (i.e. 36 mIU/well) in complete medium for another 48 hours. Thereafter, the supernatants were removed and used for testosterone determination by enzyme-linked immunosorbent assay (ELISA).

#### 2.7.1.2 Twenty four hour experiment with complete medium

Once TM3 cells were confluent enough in culture, they were trypsinised, enumerated, diluted and seeded into 96-well plates (SPL Life Sciences, Korea) as described for the MTT assay (section 2.4.2). After 24 hours of recovery from trypsinisation, the cells were exposed to either no hCG, 60 mIU/ml (i.e. 12 mIU/well) hCG, 120 mIU/ml (i.e. 24 mIU/well) hCG, 180 mIU/ml (i.e. 36 mIU/well) hCG or 240 mIU/ml (i.e. 48 mIU/well) hCG in complete medium for another 24 hours. Thereafter, the supernatants were removed and their testosterone levels were determined by ELISA.

#### 2.7.1.3 Forty eight hour experiment with plain medium

After reviewing the results from the first TM3 testosterone secretion trial, a few modifications were made. Once TM3 cells in culture reached at least 80 % confluency, they were trypsinised, centrifuged and enumerated as described. Thereafter the cells were seeded at 22 500 /ml (200  $\mu$ l/well), followed by a 24 hour humid incubation at 37°C with five percent CO<sub>2</sub>.

After the first 24 hour incubation, the supernatants were replaced with medium containing half the sera concentrations of complete medium (i.e. 1.25 % FBS and 2.5 % HS). Cells were exposed to these conditions for another 24 hours in the incubator (humid, 37°C with five percent CO<sub>2</sub>). After the second 24 hour incubation, the supernatants were replaced with plain DMEM:F12 medium (i.e. without sera). Once

more the cells were given 24 hours of exposure to this treatment at 37°C with five percent CO<sub>2</sub> in a humid incubator.

After the third 24 hour incubation, the supernatants were replaced with fresh batches of plain medium, either with or without hCG at different concentrations. Cells were treated with either zero mIU/ml, 62.5 mIU/ml (i.e. 12.5 mIU/well) or 125 mIU/ml (i.e. 25 mIU/well) of hCG for 48 hours (humid, 37°C with five percent CO<sub>2</sub>). Thereafter the supernatants were assayed for testosterone concentrations by ELISA.

### **2.7.2 Boar testis testosterone secretion experiment**

After noting that TM3 cells were unresponsive to hCG treatment, a primary culture of boar testis from a local abattoir (Winelands Pork, Bellville) was attempted in the hopes of replacing the TM3 cell model for the testosterone secretion studies. An enzymatic isolation of testes cells was performed using a modified protocol from Moundipa *et al.* (2005).

Testes from a freshly slaughtered boar were removed from the carcass and immediately transferred to sterile PBS in an ice bath and transported to the lab within 30 minutes. Once at the lab, one testis was chosen for the experiment. The testis was washed under tap water to remove all blood. Next, the epididymis, all fat and other connective tissues were removed. The testis weight was then determined to be 604 g. Thereafter, the testis was wiped down with a 70 % ethanol solution (Kimix Chemicals and Laboratory Suppliers cc, South Africa) and transferred to a sterile laminar flow cabinet. The testis capsule was removed and an 11 g block of testis tissue was washed twice with an antimicrobial medium (complete medium with one percent pen-strep and one percent amphotericin B; Sigma-Aldridge, USA). Next the testis block was transferred to 5 000 µl of fresh antimicrobial medium and minced.

Thereafter, 20 ml of dissociation medium was added to the testis mince and was incubated at 37°C under agitation for either 20 or 30 minutes (both periods were used to increase the likelihood of a successful dissociation). The dissociation medium consists of DMEM:F12 medium, 1.5 % BSA (Sigma-Aldridge, USA), 1 000 µg/ml collagenase type I (Sigma-Aldridge, USA), 200 µg/ml soybean trypsin inhibitor (Sigma-Aldridge, USA) and 20 µg/ml deoxyribonuclease (Sigma-Aldridge, USA). Next, the digestates were topped up with 20 ml of DMEM:F12 medium each and allowed to settle for 15 minutes at room temperature. Thereafter the supernatants were removed and temporarily stored

before repeating the digestion process (i.e. from addition of the dissociation medium until the removal of the supernatant).

The supernatants from the digestions were pooled (the 20 minute digested tissue was pooled separately from the 30 minute digested cells) and was centrifuged at 180 xg for 10 minutes. Thereafter, the supernatants were discarded and the cell pellets were resuspended in 5 000 µl of DMEM:F12 medium. This centrifugation and suspension step was repeated two more times.

Some cells were then transferred to 96-well plates (SPL Life Sciences, Korea) at a density of 4 000 /well (200 µl/well) and were allowed 24 hours to recover at 37°C, five percent CO<sub>2</sub> under humid conditions. Next, the old media was discarded and replaced with either fresh complete medium (negative control) or complete medium with hCG at 125 mIU/ml (testosterone secretion positive control). Cells were given a 24 hour treatment, at 37°C, five percent CO<sub>2</sub> under humid conditions.

After the 24 hour treatment, the supernatants were used for testosterone determination via ELSIA, whereas the cells that received the 30 minute digestion period (from day one) were used in an MTT assay. The MTT assay is described in [section 2.4.4](#).

### **2.7.3 Testosterone ELISA**

A testosterone ELISA (DRG Instruments GmbH, Germany) was performed on supernatants from the testosterone production trials according to the manufacturer's instructions. In brief, the given standards, and select supernatants from the abovementioned trials were transferred to appropriate microtiter wells. Next, the enzyme conjugate was added to all wells, followed by a 60 minute incubation at room temperature on a plate shaker (600 revolutions per minute: rpm). Thereafter the plates were washed at least four times with wash buffer and then dried before the addition of the substrate solution to all wells. After a 15 minute incubation (at room temperature) in the dark, the stop solution was added to all wells and the plate was read at 450 nm (within 10 minutes of adding the stop solution).

Lastly a standard curve plot was produced from the standards, and this was used to calculate the testosterone concentrations in the supernatants tested. [Appendix I](#) shows a representative standard curve from a testosterone ELSIA used in these experiments.

## 2.8 Steroidogenic mRNA expression experiments

### 2.8.1 Primer design

Before undertaking any molecular biology experiments, a primer pair was designed for each gene of interest (GOI). The GOIs were luteinizing hormone/chorionic gonadotropin receptor (*Lhcgr*), steroidogenic acute regulatory protein (*Star*), transduceosome translocator protein (*Tspo*), cytochrome P450 11A1 (*Cyp11a1*), cytochrome P450 17A1 (*Cyp17a1*), 17 $\beta$ -hydroxysteroid dehydrogenase 3 (*Hsd17b3*) and glyceraldehyde-3-phosphate dehydrogenase (*Gapdh*) as a housekeeping gene.

All primer pairs were designed using the National Center for Biotechnology Information (USA) gene database for *Mus musculus* (2016), which can be accessed at <https://www.ncbi.nlm.nih.gov/gene>. Using the primer BLAST (basic local alignment search tool), primers were designed for mRNA of each GOI, and it was ensured that all the primers cross over exon-exon junctions. For more information on the primers, see [Table 2.1](#). For the full cDNA sequences (from mRNA) of the GOIs, as well as the locations of the primers on those sequences, see [Appendices V-XI](#).

The primers (used for the conventional polymerase chain reaction: PCR) were synthesized by the University of Cape Town's Molecular and Cell Biology Department (Cape Town, South Africa). For the qPCR (quantitative PCR) assays, a different set of primers (ones that were successful in conventional PCR) were synthesized and purified using polyacrylamide gel electrophoresis (PAGE) by Inqaba Biotech Industries (Pty) Ltd (Pretoria, South Africa). All primers were diluted to produce 100  $\mu$ M stock solutions in nuclease-free water (Qiagen GmbH, Germany) that were stored at -20°C until required.

### 2.8.2 Cell seeding and treatment

TM3 cells were cultured as described in [section 2.3.1](#). After trypsinisation and enumeration ([sections 2.3.2](#) and [2.3.4](#)), TM3 cells were seeded in T75 cell culture flasks (NEST, China) at a density of four million cells per flask, in 5 000  $\mu$ l of complete medium per flask. Cells were allowed a 24 hour recovery period under humid conditions with five percent CO<sub>2</sub> at 37°C.

**Table 2.1.** Table showing the primer sequences, predicted product lengths and melting temperatures used for amplifying the target genes of interest by PCR.

Gene	Product size	Gene Bank Accession Number	Primer Sequence (5'-3')	T <sub>m</sub> (°C)	PCR type used
Gapdh	252 bp	NM_001289726.1	F: AACTCAGGAGAGTGTTTCCTCG	59.7	c
			R: TGATGGGCTTCCCGTTGATG	60.39	
Gapdh	97 bp		F: GTCCCAGCTTAGGTTTCATCAGGT	61.96	q
			R: CCAATACGGCCAAATCCGTTT	59.94	
Lhcgr	281 bp	NM_013582.2	F: AGAAGCTAATGCCITTTGACA	54.95	c
			R: CATAACAGTTTCAGCGTGATG	54.83	
Star	254 bp	NM_011485.4	F: AGTATTGACCTGAAGGGGT	54.83	c & q
			R: TTACCAGTCAGTCCTAGTGT	54.82	
Tspo	217 bp	NM_009775.4	F: AACATCAGTTGCAATCACCA	55.84	c & q
			R: TATGTAGGAGCCATACCCCAT	57.42	
Cyp11a1	241 bp	NM_019779.3	F: GGGTCCTGTTTAAGAGTTCA	54.59	c
			R: CGCTCCCCAAATATAACACT	55.21	
Cyp17a1	241 bp	NM_007809.3	F: TGATATGTCAGGAAGCCAAC	55.13	c & q
			R: GGAAAAATCTTCAACCACGG	55.17	
Hsd17b3	251 bp	NM_008291.3	F: TATTCAGGTGCTGACCCCTTA	58.16	c
			R: TGTGCGTTTGAGGTAATCT	55.3	

T<sub>m</sub>: melting temperature; bp: base pairs; F: forward primer; R: reverse primer; c: conventional PCR; q: qPCR.

After the 24 hour recovery period, the old media was discarded and replaced with 5 000 µl of fresh complete medium (per flask), either with or without hCG at 125 mIU/ml (Sigma-Aldridge, USA), as well as their respective treatments. Since the flavonoids (EGCG and aspalathin) were solubilised in DMSO, all treatments were given approximately the same levels of DMSO to allow for the determination of the effects that these flavonoids have on the cells. Hence, the treatments used were as follows: negative control (complete medium with 0.5 % DMSO and without hCG), presumptive positive control (complete medium with 0.5 % DMSO and with hCG), 10 µM aspalathin (with 0.5 % DMSO and either with or without hCG), and 10 µM EGCG (with 0.5 % DMSO and either with or without hCG). These were once more incubated at 37°C, five percent CO<sub>2</sub> and under humid conditions for 24 hours before proceeding to RNA extraction.

### 2.8.3 RNA extraction

All steps that followed the 24 hour treatments were done under non-sterile conditions. The old treatment media were discarded and each flask was washed with 5 000  $\mu$ l of sterile PBS. The PBS from each flask was also discarded and replaced with 3 000  $\mu$ l of ice cold tri-RNA reagent (Fanorgen Biotech corp., Taiwan). Each flask's floor was flushed a few times with the tri-RNA reagent until all of the cells were visibly detached, as evidenced by the drifting of a blanket of cells to the bottom of the flask. Thereafter, each one millilitre of tri-RNA-cell lysate was transferred to an appropriately labelled 2 000  $\mu$ l PCR tube. Those tubes were then vortexed for 60 seconds, followed by an incubation at room temperature for five minutes.

Next, 200  $\mu$ l of chloroform (Merck, Germany) was added to each PCR tube before being vortexed for another 15 seconds and incubated for five more minutes at room temperature. The mixtures were then separated by centrifugation at 12 000  $\times$ g for 30 seconds. Thereafter, 500  $\mu$ l of the upper clear supernatant from each tube was transferred to appropriately labelled 1 500  $\mu$ l PCR tubes. Next, 500  $\mu$ l of isopropanol (Sigma-Aldridge, USA) was added to each (1 500  $\mu$ l) PCR tube and thoroughly mixed. These were allowed to precipitate overnight at  $-20^{\circ}\text{C}$ .

The next day, each tube was centrifuged at 12 000  $\times$ g for 10 minutes and the supernatants were carefully discarded. Thereafter 1 000  $\mu$ l of an 80 % molecular biology grade ethanol (Merck, Germany) solution (in autoclaved reverse osmosis water: RO water) was added to each pellet and this was vortexed for one minute. These were then centrifuged for five minutes at 7 500  $\times$ g. Once more, each supernatant was carefully removed and discarded; care was taken to avoid allowing the pellets to dry. Immediately thereafter, the RNA pellets were resuspended in 100  $\mu$ l of nuclease-free water (Qiagen GmbH, Germany).

Where possible, the final step of RNA purification and the reverse transcription reaction would take place on the same day; but when not, the RNA samples would be stored at  $-20^{\circ}\text{C}$  for fewer than five days. When necessary, the RNA samples were thawed before determining its concentration by NanoDrop™ 2000 (Thermo scientific, USA) spectrophotometer. Next, each RNA sample was diluted to 150 ng/ $\mu$ l and then heat treated at  $90^{\circ}\text{C}$  for five minutes before being shock-cooled in an ice bath for five minutes. These prepared RNA samples were immediately used for cDNA synthesis.

### 2.8.4 Reverse transcription reaction

The reverse transcription (RT) reaction was performed using the Takara PrimeScript™ RT reagent kit (Perfect Real Time) (Takara, China) according to the manufacturer's instructions. A mastermix of RT reagents was prepared according to Table 2.2, below:

**Table 2.2.** Table showing the makeup of the mastermix used to perform the reverse transcription reaction (taken from the manufacturer: Takara, China).

Reagent	Initial Concentration	Final Concentration
5 × PrimeScript Buffer	5 ×	1 ×
PrimeScript RT Enzyme Mix I	20 ×	1 ×
Oligo dT Primer	50 µM	25 pmol
Random hexamers	100 µM	50 pmol

Once the mastermix was prepared, it was separated into aliquots of 3 500 nl into labelled PCR tubes. Thereafter the thawed RNA samples were added to the appropriate tubes and diluted with nuclease-free water to a final RNA concentration of 100 ng/µl such that each tube held 10 µl of RT mix (i.e. the RNA together with the nuclease-free water amounted to 6 500 nl in total per tube).

Next, the RT mixtures were placed in a thermocycler and given the following temperature fluctuations: 37°C for 15 minutes (reverse transcription), 85°C for five seconds (heat inactivation of reverse transcriptase) and 4°C for five minutes. Once the RT reaction was complete, the synthesized complementary DNA (cDNA) samples were assessed by NanoDrop™ 2000 for purity and concentration before being stored at -20°C until needed. For long-term storage (i.e. longer than 30 days), the cDNA was stored at -80°C.



### 2.8.5 Conventional polymerase chain reaction

The polymerase chain reaction was performed using the GoTaq® G2 Flexi DNA Polymerase PCR kit (Promega Corporation, USA) according to the manufacturer's instructions. Briefly, 2 000 nl of the thawed cDNA was transferred to PCR tubes containing Buffer, MgCl<sub>2</sub> (1 000 µM final), deoxynucleoside triphosphate (dNTP; Promega Corporation, USA; 200 µM final) Taq (*Thermus aquaticus*) polymerase (1.25 u final) and 200 nM (final) of each the forward and reverse primer. Table 2.3 provides a breakdown of the mastermix components. Additionally, a no template control (NTC) was included in the sample set; it consisted of nuclease-free water instead of a cDNA sample. Next, the PCR tubes were transferred to a thermocycler for 40 PCR cycles. However, this was preceded by a 180 second exposure at 95 °C for denaturation.

The PCR cycles started with a 45 second exposure to 95°C for denaturation, followed by 45 seconds at the appropriate annealing temperatures and another 45 seconds at 72°C for extension. The annealing temperatures used were 55°C for *Gapdh*; 50°C for *Star*, *Cyp11a1*, *Cyp17a1* and *Lhcgr*; and 52°C for *Hsd17b3* and *Tspo*.

**Table 2.3.** Table showing the makeup of the mastermix used to perform the conventional PCR (taken from the manufacturer: Promega Corporation, USA).

Reagent	Initial Concentration	Final Concentration
Water	N/A	N/A
Buffer	5 ×	1 ×
MgCl <sub>2</sub>	25 mM	1 mM
dNTPs	10 mM	0.2 mM
Taq polymerase	5 u/µl	1.25 u
Forward Primer	100 µM	0.2 µM
Reverse Primer	100 µM	0.2 µM

N/A: not applicable.

### **2.8.6 Agarose gel electrophoresis**

Both the conventional PCRs and qPCRs (see [sections 2.8.5](#) and [2.8.10](#)) were followed by an agarose gel electrophoresis (AGE) of the amplicons, to confirm the specificity of each PCR for the GOIs. Both AGEs (from conventional and qPCR) were performed similarly, with the exception of the well sizes and visualisation systems used.

For the conventional PCR AGE, large wells that could handle 24  $\mu$ l were used whereas smaller wells that could handle 12  $\mu$ l were used for the qPCR AGE. The conventional PCR AGE also used the GeneDirex (Taiwan) visualisation system, while the qPCR AGEs used ethidium bromide and a standard transilluminator. Both AGEs are described here.

Firstly, a 10  $\times$  TBE (Tris, boric acid and EDTA) buffer was prepared and subsequently diluted to 1  $\times$  with RO water. The 10  $\times$  TBE buffer was prepared as follows: 54 g of Tris base (Promega Corporation, USA) was added to 27.5 g of boric acid (Promega Corporation, USA) and 4 650 mg of EDTA (Promega Corporation, USA) and made up to 500 ml using RO water.

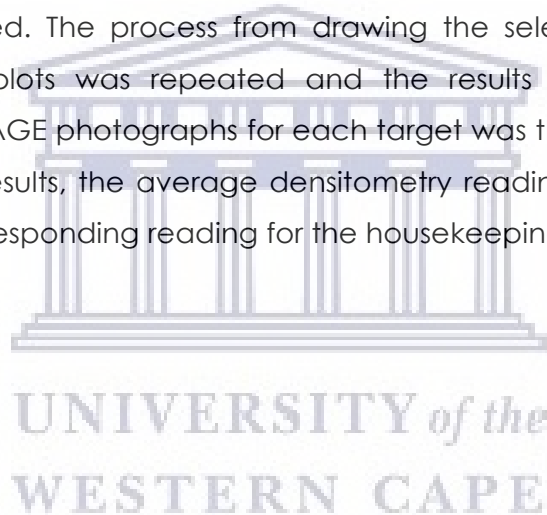
A 1.5 % agarose gel was prepared as follows: 2 250 mg of agarose powder (Promega Corporation, USA) was mixed with 150 ml of TBE buffer. This was heated in a microwave oven at high power for two minutes. For the qPCR's AGE, 3 000  $\mu$ l of ethidium bromide (Promega Corporation, USA) was added to the unset hot gel. Next, the 1.5 % agarose-TBE solution was allowed to cool slightly before casing into a gel mould (for either PCR type). The gel was allowed to set at room temperature for approximately 45 minutes before transferring the gel to the electrophoresis chamber and slightly submerging the gel in TBE buffer.

Once the conventional PCR was complete, 20  $\mu$ l of each PCR-amplicon was mixed with 700 nl of Novel Juice (GeneDirex, Taiwan), before transferring to the appropriate wells in the gel. Alternatively, the qPCR products were loaded directly into the (ethidium bromide-containing) gel at 10  $\mu$ l per well. Additionally, a 100 bp (base pair) DNA ladder (Promega Corporation, USA) was included in each gel; here 5 000 nl of the DNA ladder was mixed with 700 nl of Novel Juice before transferring to its allocated well in the gel. For the qPCR the DNA ladder was loaded neat into the appropriate well (also 5 000 nl).

The gel was exposed to a 100 V for 150 minutes before visualisation. Either gel was cooled in ice before transferring to an appropriate transilluminator. For conventional PCR, the gel was transferred to a BLook™ transilluminator (GeneDirex, Taiwan) and viewed in the dark. For the qPCR, the gel was transferred to a standard ultraviolet transilluminator. The gels were photographed as record of the experimental results.

### **2.8.7 Densitometry measurements**

Once the AGE photographs were captured, the densitometry of the bands were measure using the ImageJ software (National Institutes of Health, USA), according to the webpage of the Diamantina Institute, University of Queensland (2018). Briefly, selection boxes were placed around each of the bands in one photograph. The selection boxes were then used to generate density plots. Next, the peak of each density plot was sealed off with a straight line. Finally, the area under the peak was quantified and recorded. The process from drawing the selection boxes until the quantification of the plots was repeated and the results were averaged. The densitometry from two AGE photographs for each target was then averaged as well. To normalise the PCR results, the average densitometry reading for each treatment was divided by the corresponding reading for the housekeeping gene (i.e. Gapdh).



### 2.8.8 qPCR optimisation

Only the GOIs from successful conventional PCRs were used for qPCR; namely *Star*, *Tspo*, *Cyp17a1* and *Gapdh*. Only the PAGE-purified primers, and only cDNA from the vehicle control and presumptive positive control (as well as a NTC; see [section 2.8.2](#)) were used for qPCR optimisation.

All qPCRs were performed using the Luna® Universal qPCR Mater Mix (New England Biolabs Inc., USA) kit, according to the manufacturer's instructions. A mastermix was prepared for each GOI (see [Table 2.4](#)), and then mixed with the cDNA in a MicroAmp® Fast Optical 96-well Reaction Plate (Applied Biosystems® by Life Technologies™, USA). The qPCRs were performed using the QuantStudio™ 7 Flex Real-Time PCR System (Applied Biosystems, by Thermo Fisher Scientific, Singapore).

**Table 2.4.** Table showing the makeup of the mastermix used to perform the qPCR (taken from the manufacturer: New England Biolabs, USA).

Reagent	Initial Concentration	Final Concentration
Water	N/A	N/A
Master Mix (from kit)	2 ×	1 ×
Forward Primer	100 μM	0.2 μM
Reverse Primer	100 μM	0.2 μM

N/A: not applicable.

Each qPCR started with a pre-denaturation at 95°C for 180 seconds. Then the PCR proceeded with 44 cycles as follows: five seconds at 95°C for denaturation and 30 seconds at the annealing temperature of choice (see [section 2.8.10](#)). Each qPCR was also followed by a high resolution melt curve.

Each, the cDNA concentrations, annealing temperatures, annealing times and primer concentrations were varied during the qPCR optimisation. The specificity of the PCR for the GOI was confirmed by post-PCR high density melt curve analysis and AGE ([section 2.8.6](#)). For the annealing temperatures, at least a 10°C range within 5°C of the predicted  $T_m$  (melting temperature) was used for each GOI. Where needed, the amplification time may have been extended from 30 second to 40 second, in an

attempt to improve amplification. When necessary, the primer concentrations were lowered when trying to decrease non-specific amplification. The lowest annealing temperatures that reliably produced the desired PCR products, without non-specific amplification, was selected for the experimental qPCRs.

### **2.8.9 Gel clean-up and qPCR standard curve generation**

In order to assess the PCR efficiency, a standard curve was generated for each of the GOIs that were assessed by qPCR. During the optimisation steps for the qPCR, some of the PCR amplicons were confirmed to be the correct molecular weight by AGE (as described in [section 2.8.6](#)). Thereafter the bands corresponding to the correct molecular weight were quickly excised by scalpel, under UV light, and weighed. Next, the amplicons were purified from the gel using the Wizard® SV Gel and PCR Clean-Up System (Promega Corporation, USA), according to the manufacturer's instructions.

Briefly, each agarose slice was mixed with an equal volume of Gel Binding Buffer and incubated at 65°C for 10 minutes under constant agitation. Thereafter, the melted gel was transferred to an SV Minicolumn assembly and centrifuged at 16 000 xg for 60 seconds. Then the liquid in the collection tube was discarded. Next, the Membrane Wash Solution (diluted with 95 % molecular biology-grade ethanol) was added to the SV Minicolumn. The SV Minicolumn assembly was, once more, centrifuged at 16 000 xg for one minute and the collected liquid was discarded; this step was repeated. Then, the Minicolumn was transferred to a clean PCR tube and 50 µl of nuclease-free water was placed on the membrane, followed by a one minute incubation at room temperature. The SV Minicolumn-PCR tube assembly was then centrifuged at 16 000 xg for one minute and the collected amplicon DNA was stored at -20°C until needed.

To generate a standard curve, an aliquot of the purified amplicon DNA was subjected to a 10-fold serial dilution in nuclease-free water (Qiagen GmbH, Germany). At least five dilutions of the appropriate amplicon DNA was included (in duplicate) in each qPCR run.

### **2.8.10 Real time qPCR**

The changes to the qPCR protocol, during optimisation, were unsuccessful at removing non-specific amplification when present. Consequently, the actual experimental qPCRs were performed as described in [section 2.8.8](#). Additionally, the qPCRs that showed non-specific amplification were for *Gapdh* and *Cyp17a1*. The *Cyp17a1* qPCR

was thus abandoned, and a new primer set for *Gapdh* was designed (shown in Table 2.1), ordered (PAGE-purified), optimised and used for qPCR.

Each qPCR included an NTC and at least five standards from section 2.8.9 (see Appendices XII-XIV for the qPCR standard curves). Additionally, the cDNA samples were tested in triplicate. The qPCR annealing temperatures used were 55°C for *Gapdh*, 54°C for *Star* and 48°C for *Tspo*. Once more, the qPCR amplicons were subjected to a high resolution melt curve analysis (see Appendices XV-XVII) and an AGE.

### 2.8.11 Calculation of the Pfaffl ratio

The Ct (cycle threshold) values were determined by the QuantStudio™ Real-Time PCR System Version 1.3 software (Thermo Fisher Scientific, USA). The Pfaffl ratio was determined according to Pfaffl (2004). For the standards, the log cDNA concentration was plotted on a straight line graph, against the Ct values. The efficiency was calculated by the following formula:

$$E = 10^{(-1/slope)}$$

Where **E** is the efficiency value and **slope** is the slope the from the standard curve graph equation.

Next the efficiency corrected  $\Delta Ct$  (change in Ct) values was calculate for each gene of interest, as follows:

$$E^{\Delta Ct} = E^{Ct_{vehicle} - Ct_{sample}}$$

Where **Ct<sub>vehicle</sub>** is the mean Ct value of the negative control sample and **Ct<sub>sample</sub>** is the mean Ct value of a given sample.

Finally, the normalised relative fold expression (i.e. Pfaffl ratio) was calculated as follows:

$$Pfaffl\ ratio = (E_{target}^{\Delta Ct_{target}}) \div (E_{reference\ gene}^{\Delta Ct_{reference\ gene}})$$

Here the **target** refers to either *Star* or *Tspo* (when appropriate) and the **reference gene** referers to *Gapdh*.

## 2.9 Inhibin B secretion experiments

### 2.9.1 Cell seeding and treatment

Once TM4 cells in culture were confluent enough, they were trypsinised and enumerated as described in [section 2.3](#). Next the cells were seeded into clear 96-well cell culture plates (SPL Life Sciences, Korea) at 10 000 cells per well in a volume of 100  $\mu$ l per well. After the 24 hour recovery from trypsinisation, the supernatants were discarded and replaced with one of the treatments used (200  $\mu$ l per well). Cells were exposed to either complete medium (negative control), 0.5 % DMSO in complete medium (vehicle control), FSH in medium at 125 mIU/ml (presumptive positive control), green tea (50  $\mu$ g/ml, 100  $\mu$ g/ml or 200  $\mu$ g/ml), green rooibos (50  $\mu$ g/ml, 100  $\mu$ g/ml or 200  $\mu$ g/ml), EGCG and 0.5 % DMSO in complete medium (0.1  $\mu$ M, 5  $\mu$ M or 10  $\mu$ M) or aspalathin and 0.5 % DMSO in complete medium (0.1  $\mu$ M, 5  $\mu$ M or 10  $\mu$ M). The cells were exposed to these treatments for 24 hours at 37°C, 5 % CO<sub>2</sub> and under humid conditions. Once the treatment period had elapsed, the supernatants were collected and their inhibin B levels were quantified by ELISA.

### 2.9.2 Inhibin B ELISA

The Inhibin B ELISA (Elabscience, USA) was performed according to the manufacturer's instructions. Briefly, all standards were prepared and 100  $\mu$ l of each standard and treatment was transferred to the appropriate wells. This was followed by a 90 minute incubation at 37°C. Next the wells were aspirated empty and each received 100  $\mu$ l of biotinylated detection antibody. The ELISA plate was once more incubated at 37°C, but for 60 minutes this time. Next, the wells were all decanted and washed six times with wash buffer. After the wash, the horseradish peroxidase conjugate was added to all wells at 100  $\mu$ l each, and the plate was allowed 30 minutes at 37°C. After the 30 minute incubation, the plate was decanted once more and washed seven times with wash buffer. Thereafter, 90  $\mu$ l of substrate solution was added to all wells. This was followed by a 20 minute incubation in the dark and at room temperature. Next, the reaction was halted by the addition of 50  $\mu$ l stop solution to each well. The absorbance of the plate was then read at 450 nm, and the concentrations of inhibin B in the samples was calculated using the standards as reference. [Appendix II](#) shows the standard curve from the inhibin B ELISA of this experiment.

## 2.10 Lactate secretion experiments

### 2.10.1 Lactate assay principle

The lactate assay used in this thesis is based on the conversion of lactate to pyruvate and NADH (reduced nicotinamide adenine dinucleotide) by the enzyme lactate dehydrogenase (LDH). The NADH is subsequently quantified by reading its absorbance at 340 nm. Due to their stoichiometry, the final NADH concentration is indicative of the initial lactate concentration; see [Figure 2.3](#) for an overview.

### 2.10.2 Cell seeding and treatment

The experiments for lactate secretion were performed exactly as described for the inhibin B secretion experiment (see [section 2.9.1](#)), but an additional cell death control was included (10 % DMSO in complete medium). Furthermore, after the treatment period had elapsed, the supernatants were heat inactivated by exposure to 95°C for five minutes. They were subsequently placed in an ice bath for five minutes, before being stored at -20°C until needed.

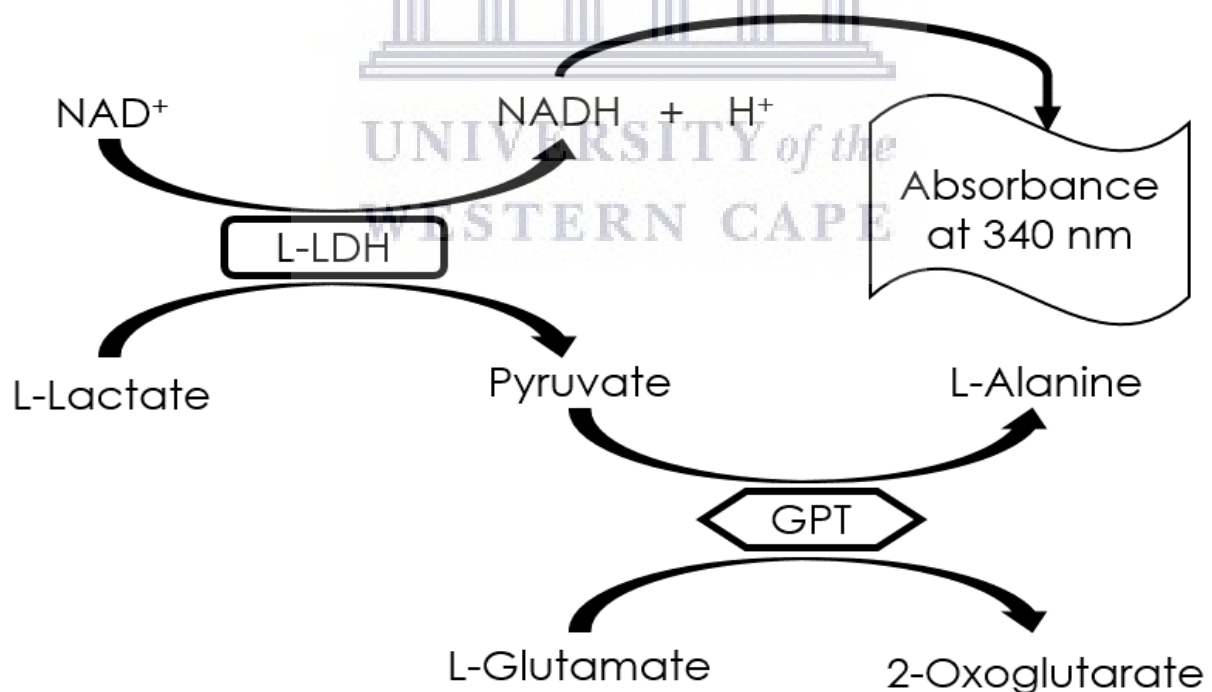


**Figure 2.3. Diagram showing an overview of the lactate assay principle.** Firstly, L-LDH converts L-lactate and NAD<sup>+</sup> (nicotinamide adenine dinucleotide) to pyruvate and NADH + H<sup>+</sup>. Thereafter, the pyruvate is converted to L-alanine by GPT, in the presence of L-glutamate which is converted to 2-oxoglutarate. This latter step captures the pyruvate, allowing the first reaction to proceed in the indicated direction. The Absorbance of NADH is measured at 340 nm to determine the initial L-lactate concentration.



### 2.10.3 Lactate assay procedure

On the day of assay, all lactate experimental samples were thawed, resuspended and diluted as one part sample with two parts plain DMEM:F12 medium (i.e. giving a dilution factor of 3). Next, 10  $\mu$ l of each diluted sample was transferred to appropriate wells of a clear flat-bottomed 96-well plate (SPL Life Sciences, Korea). The assay included two standard solutions of sodium L-lactate (80 mg/l and 160 mg/l; Sigma-Aldridge, USA) that were prepared in plain DMEM:F12 medium as well as blanks (plain DMEM:F12 medium). Since the standards were not diluted, their dilution factor was 1.

A glutamate buffer solution was then prepared by dissolving L-glutamic acid (Sigma-Aldridge, USA) in a 1 M solution of NaOH (Merck, Germany), producing a glutamate concentration of 0.52 M. This glutamate buffer was then used to produce a pre-LDH reaction mixture: 0.121 M glutamate, 0.666 mM  $\beta$ -NAD (Sigma-Aldridge, USA), 7 units/ml glutamic pyruvate transaminase (GPT; Sigma-Aldridge, USA) in autoclaved RO water. Thereafter, 80  $\mu$ l of the pre-LDH reaction mixture was added to each well. The plates were allowed a 10 minute incubation on a plate shaker (600 rpm) at room temperature. Then, the plate's absorbance, at 340 nm, was recorded as the T10 value.

Next the LDH stock (Sigma-Aldridge, USA) was diluted in a 1 % BSA (Sigma-Aldridge, USA) solution to a concentration of 210 units/ml. Then 10  $\mu$ l of the LDH solution was added to each well (except for the blanks) to produce a final LDH concentration of 21 units/ml. The plate was once more incubated at room temperature on a plate shaker (600 rpm), but for 120 minutes this time. Finally, the plate's absorbance was measured at 340 nm; this was recorded as the T120 value.

#### 2.10.4 Calculation of lactate concentration

The concentration of lactate was determined using an adaptation of the Lambert-Beer equation, as described by Hohorst (1957).

$$c = \frac{V \times MW}{\epsilon \times d \times v \times 1000} \times D$$

Here, **c** is the lactate concentration of the sample (in g/l), **V** is the final volume in each well in millilitres (i.e. 0.1 ml), **MW** is the molecular weight of lactate (i.e. 90 g/mol), **ε** is the extinction coefficient of NADH at 340 nm (i.e. 6.3 l/mmol/cm) (Bergmeyer, 1975; McComb et al., 1976), **d** is the path length that light travels through the sample, **v** is the volume of sample placed into each well (i.e. 0.01 ml). To determine **D**, one firstly calculates the ΔA value, which is the difference between the T10 and T120 readings of each sample (i.e. ΔA = T120<sub>absorbance</sub> - T10<sub>absorbance</sub>). Then one subtracts the ΔA value of each sample from that of the average for the blanks (i.e. **D** = ΔA<sub>sample</sub> - ΔA<sub>blank</sub>).

The path length was estimated to be 0.301 cm. This was based on the known volume used in each well (0.1 ml) and the diameter of the wells (6.5 mm). To simplify the calculation, all wells were assumed to be perfectly cylindrical and the meniscus effect was ignored.

To compensate for the complication of the meniscus effect, the standards were used to determine a correction factor for the equation. Using the formula above and the standards, the correction factor was determined to be 2, approximately.

Lastly, to make the results easy to read, the unit for lactate concentration was converted from g/l to mg/l. Hence the formula used to determine the actual lactate concentration of the samples is as follows:

$$c = \frac{0.1 \text{ ml} \times 90 \text{ g/mol}}{6.3 \text{ l/mmol/cm} \times 0.301 \text{ cm} \times 0.01 \text{ ml} \times 1000} \times D \times 1000 \times 2 \times \text{dilution factor}$$

## 2.11 TEER experiments

### 2.11.1 TEER principle

The measurement of a transepithelial electrical resistance (TEER) provides a simple method for assessing the integrity of a biological barrier. The rationale behind this assay is that an intact barrier would act like a resistor in a circuit when an electrical current is applied across it. The more complete the barrier the greater the resistance it would produce. As such a drop in TEER would indicate that the barrier was compromised. Figure 2.4 provides a schematic overview of the apparatus used to measure TEER in these experiments. Appendix XVIII provides photographs of the actual apparatus used to measure TEER in these experiments.

### 2.11.2 Plate preparation and cell seeding

Before trypsinisation of TM4 cells, 12-well cell culture plates (NEST, China) were prepared by the addition of 1 000  $\mu$ l of complete medium to each well. Thereafter, Millicell® 0.45  $\mu$ m standing cell culture plate inserts (Merck, Germany) were placed into appropriate wells under sterile conditions. Each insert was visually inspected for damage and no damaged inserts were used.

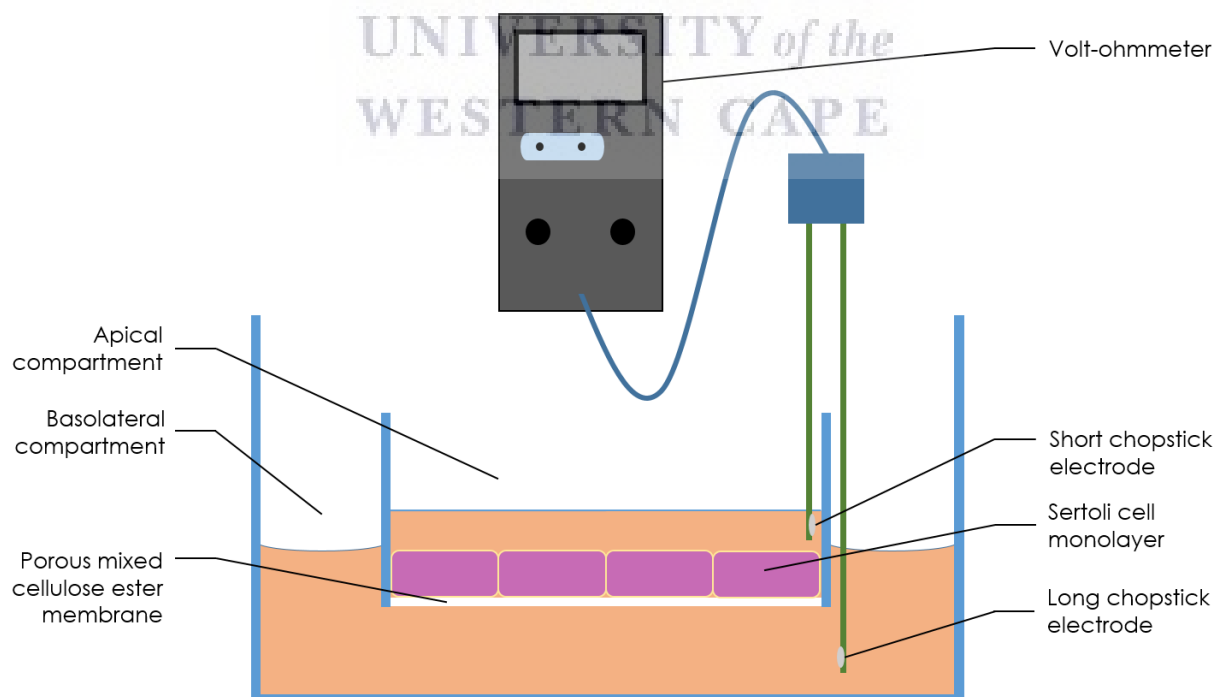


**Figure 2.4. Schematic diagram showing the apparatus used to test for transepithelial electrical resistance.** This illustration is not to scale.

After the trypsinisation of TM4 cells (see [section 2.3](#)), they were seeded into the Millicell® inserts at a density of 60 000 cells per insert (400 µl/insert). There were inserts included that did not receive cells, but received complete medium instead; these served as the blanks for the experiments. Thereafter the 24 well plates were incubated in a humid environment at 37°C and 5 % CO<sub>2</sub>. The insert transepithelial electrical resistance was monitored daily (the measurement procedure is described in [section 2.11.3](#)) to assess cell confluence, since microscopic examination was not possible. The spent medium was also replaced daily.

### **2.11.3 TEER readings**

Firstly the chopstick electrodes from a Millicell® volt-ohmmeter were placed in a 70 % ethanol solution (Kimix Chemicals and Laboratory Suppliers cc, South Africa) for 15 minutes to stabilise them. Thereafter, they were placed in fresh complete medium (at room temperature) for another 15 minutes under sterile conditions. In the meantime, all spent media was replaced with fresh complete medium (i.e. 1000 µl in the wells and 400 µl in the inserts) and the cells were allowed 30 minutes to reach room temperature in the laminar flow cabinet.

Thereafter the chopstick electrodes of the Millicell® volt-ohmmeter were positioned such that the shorter electrode was within the insert and the longer electrode was outside (but within the well). The electrodes were held in place with the aid of a burette stand and clamp (see [Appendix XVIII](#)). Care was taken to ensure that there were no air bubbles in the well-insert system. Then the resistance was measured using the 2000 Ω setting. The transepithelial electrical resistance of each well was taken four times, once in each the twelve O'clock, three O'clock, six O'clock and nine O'clock positions of the insert. The average of the highest two reading from each insert-well system was used to calculate TEER.

### **2.11.4 Cell treatment**

Once it was determined that the cells had formed a confluent barrier within the inserts, the actual experiments were initiated. After reading the TEER, the media of the wells was replaced once more, but with fresh media containing the appropriate treatments. The media within the inserts were not changed, as they represented the luminal compartment of the testes. On the other hand, the wells represented the basal compartment which is the direction from which blood sera would interact with the Sertoli cells *in vivo*.

The treatments used were EGCG and aspalathin at 0.1  $\mu\text{M}$ , 5  $\mu\text{M}$  and 10  $\mu\text{M}$  (with 0.5 % DMSO in complete medium), as well as a negative control (0.5 % DMSO in complete medium). The cells were then allowed an initial 24 hours of treatment at 37°C, 5 %  $\text{CO}_2$  in humidity.

After each 24 hour treatment period, the TEER readings were again taken as described (section 2.11.3). However, when the spent treatment-media was removed, the wells were washed once with sterile PBS (1 000  $\mu\text{l}$  per well), before adding fresh medium for the readings. After the readings were taken, the media in the wells was replaced with fresh treatment-media. The cells were then returned to the incubator (humid, 37°C, 5 %  $\text{CO}_2$ ) for another 24 hours. TEER readings were taken after 24 hours, 48 hours and 72 hours of total treatment.

### 2.11.5 TEER calculations

To calculate TEER, one firstly calculates the average resistance of each well-insert and subtracts the average resistance of the blank from that (i.e. those data are blank-corrected). Next, one simply multiplies the blank-corrected resistance by the surface area of the insert to give TEER.

However, during the experiments described here, the initial resistance readings showed a fair amount of variability between inserts, even before any treatments were administered. Hence, it was decided that the data needed normalisation to their respective readings on Day 0 (i.e. the day that treatment commenced). However, to retain the ability to compare treatments with one another, the Day 0 readings also needed normalization to the readings from the Vehicle treatment (on Day 0). As such, a correction factor was incorporated into the resistance calculation. The correction factor was calculated by dividing the blank-corrected reading of the Vehicle treatment on Day 0 by that of the blank-corrected sample of Day 0.

$$TEER_{A \text{ of Day } B} = (R_{A \text{ of Day } B} - R_{Blank \text{ of Day } B}) \times \left( \frac{R_{Vh \text{ of Day } 0} - R_{Blank \text{ of Day } 0}}{R_{A \text{ of Day } 0} - R_{Blank \text{ of Day } 0}} \right) \times Area$$

Here TEER is expressed as normalised  $\Omega \times \text{cm}^2$ , **A** is the variable for a specific sample, **B** is the variable for a specific day, **R** is the resistance ( $\Omega$ ), **Day 0** is the day that treatment commenced and the **Area** is the surface area of the insert (i.e. 0.6  $\text{cm}^2$ ).

## 2.12 Statistical Analysis

All quantitative data were compiled and stored in Microsoft® Excel® spreadsheet documents. The statistical analyses were performed using MedCalc® Statistical Software version 14.8.1 (MedCalc Software bvba, Ostend, Belgium; <http://www.medcalc.org>; 2014). Data were queried for outliers using the Turkey outlier test, after which all outliers were excluded. All normally distributed data were compared using student's t-test, whereas data that were not normally distributed were compared using the Mann-Whitney test.



# Chapter 3

---

## Results



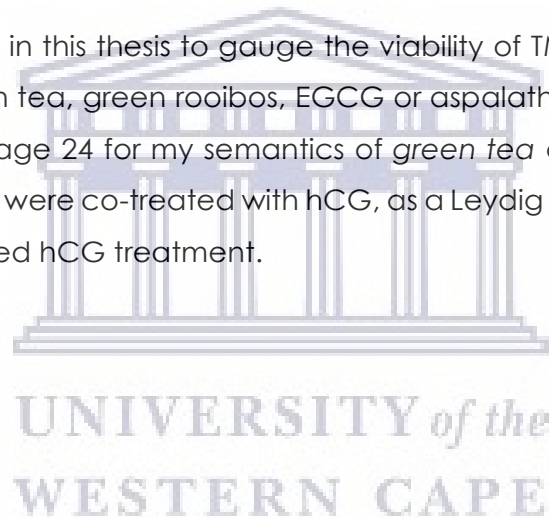
UNIVERSITY *of the*  
WESTERN CAPE

### 3.1 MTT assay

The MTT assay provides an indirect estimate of cell viability by quantifying the absorbance of formazan crystals that resulted from reduction of the MTT dye in living cells.

According to Berridge *et al.* (2005), MTT is reduced predominantly by intracellular oxidoreductases and provides a reasonably robust estimation of cell viability. However, MTT assay data can be skewed if a test substance increases the number of live cells in test vessels (more cells reduce more MTT) or the activity of MTT-reducing enzymes. This is why it is important to confirm MTT data by microscopy; as it can show cell density and morphology, which can indicate cellular stress.

The MTT assay was used in this thesis to gauge the viability of TM3 and TM4 cells after exposure to either green tea, green rooibos, EGCG or aspalathin (see the footnotes <sup>2</sup> on page 22 and <sup>3</sup> on page 24 for my semantics of *green tea* and *green rooibos*). In addition, some TM3 cells were co-treated with hCG, as a Leydig cell stimulant; whereas the TM4 cells did not need hCG treatment.





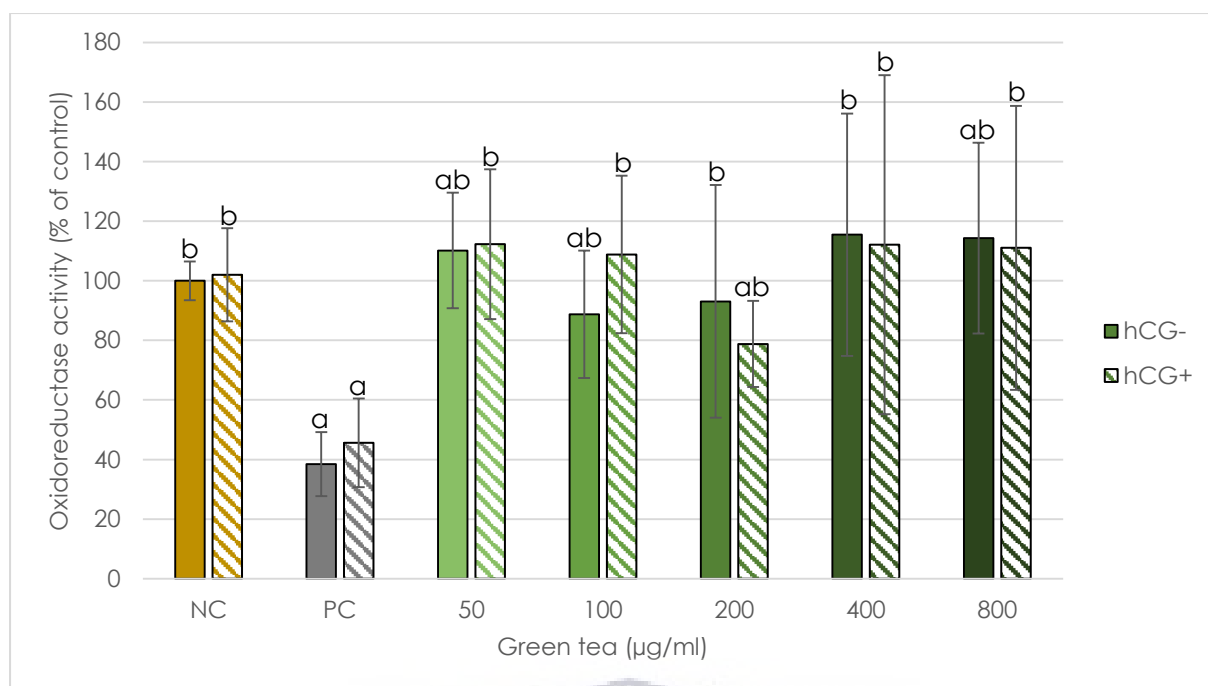


**Figure 3.1. Graph showing the effects of green tea on TM3 cell oxidoreductase activity, both with and without hCG.** The cells were treated for 24 hours with either a control or green tea reconstituted in media, either with hCG at 125 mIU/ml or without hCG. The percentage oxidoreductase activity was calculated under the assumption that the **NC** treatment produced 100 % activity. **NC**: negative control (i.e. complete medium), **PC**: positive control (i.e. 10 % DMSO), **hCG-**: without hCG, **hCG+**: with hCG. Data are represented as means  $\pm$  standard deviations. A P value of less than 0.05 was considered significant; a: significantly different to **NC**, b: significantly different to **PC**;  $n \geq 6$ .

Both the 50  $\mu\text{g/ml}$  and the 800  $\mu\text{g/ml}$  green tea samples, without hCG, produced significantly higher oxidoreductase activities than the negative control did, at 110.2 %  $\pm$  19.4 % and 114.3 %  $\pm$  32 %, respectively (see Figure 3.1). Furthermore, the 100  $\mu\text{g/ml}$  green tea sample, without hCG, showed 88.7 %  $\pm$  21.4 % oxidoreductase activity, and the 200  $\mu\text{g/ml}$  green tea sample with hCG showed 78.8 %  $\pm$  14.4 % oxidoreductase activity; both of which were significantly lower than the negative control. No other green tea treatments showed any significant differences to the negative control. On the other hand, the negative controls showed significantly higher oxidoreductase activity than the (cell death) positive control (10 % DMSO), which confirms the validity of this MTT assay. Additionally, all green tea samples tested produced significantly higher oxidoreductase activities ( $P < 0.05$ ) than the positive control.

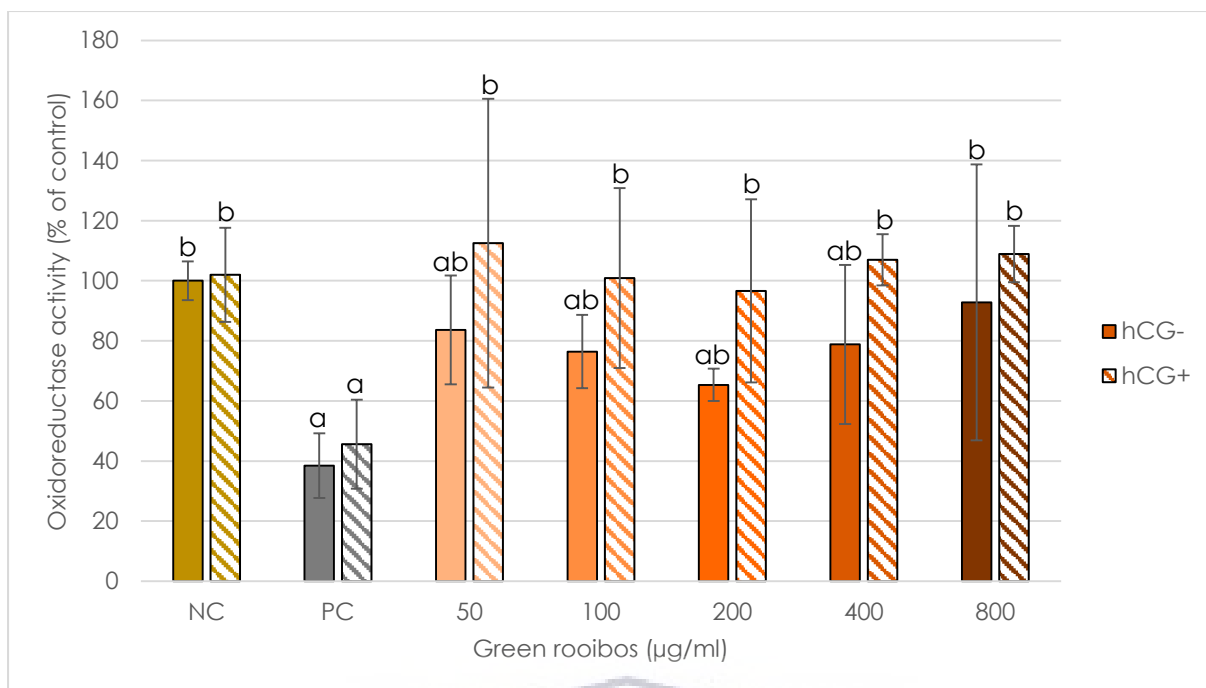


**Figure 3.2. Graph showing the effects of green rooibos on TM3 cell oxidoreductase activity, both with and without hCG.** The cells were treated for 24 hours with either a control or green rooibos reconstituted in media, either with hCG at 125 mIU/ml or without hCG. The percentage oxidoreductase activity was calculated under the assumption that the **NC** treatment produced 100 % activity. **NC**: negative control (i.e. complete medium), **PC**: positive control (i.e. 10 % DMSO), **hCG-**: without hCG, **hCG+**: with hCG. Data are represented as means  $\pm$  standard deviations. A P value of less than 0.05 was considered significant; a: significantly different to **NC**, b: significantly different to **PC**;  $n \geq 18$ .

The results from the 50 µg/ml, 100 µg/ml, 200 µg/ml and 400 µg/ml green rooibos samples without hCG were all significantly lower than the negative control ( $P < 0.05$ ), with values of 83.7 %  $\pm$  18.1 %, 76.4 %  $\pm$  12.2 %, 65.4 %  $\pm$  5.4 % and 78.8 %  $\pm$  26.5 % respectively (Figure 3.2). On the other hand, the green rooibos treatments with hCG were statistically no different to the negative control. Lastly, all green rooibos treatments (i.e. with and without hCG) gave oxidoreductase activities that were significantly higher than the corresponding positive control ( $P < 0.05$ ).

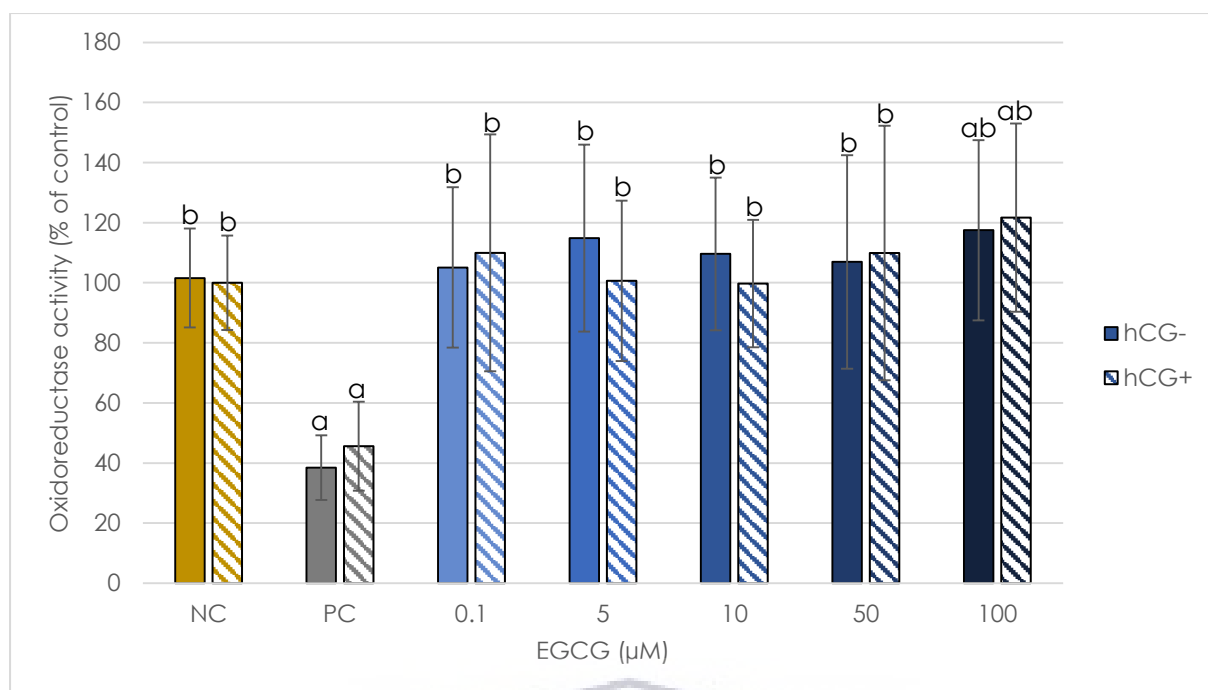


**Figure 3.3. Graph showing the effects of EGCG on TM3 cell oxidoreductase activity, both with and without hCG.** The cells were treated for 24 hours with either a control or EGCG (and 0.5 % DMSO) in media, either with hCG at 125 mIU/ml or without hCG. The percentage oxidoreductase activity was calculated under the assumption that the **NC** treatment produced 100 % activity. **NC**: negative control (i.e. 0.5 % DMSO), **PC**: positive control (i.e. 10 % DMSO), **hCG-**: without hCG, **hCG+**: with hCG. Data are represented as means  $\pm$  standard deviations. A P value of less than 0.05 was considered significant; a: significantly different to **NC**, b: significantly different to **PC**;  $n \geq 21$ .

Only the 100  $\mu\text{M}$  EGCG treatments, both with and without hCG, showed activities that were significantly higher than the negative control ( $P < 0.05$ ) at 121.7 %  $\pm$  31.3 % and 117.5 %  $\pm$  30 % respectively (Figure 3.3). No other EGCG treatment showed statistical differences to the corresponding negative control (i.e. with or without hCG). Moreover, the negative control and the (cell death) positive control were significantly different ( $P < 0.05$ ), indicating a valid MTT assay. Lastly, the oxidoreductase activities of all EGCG treated samples were significantly higher than the cell death positive control ( $P < 0.05$ ).

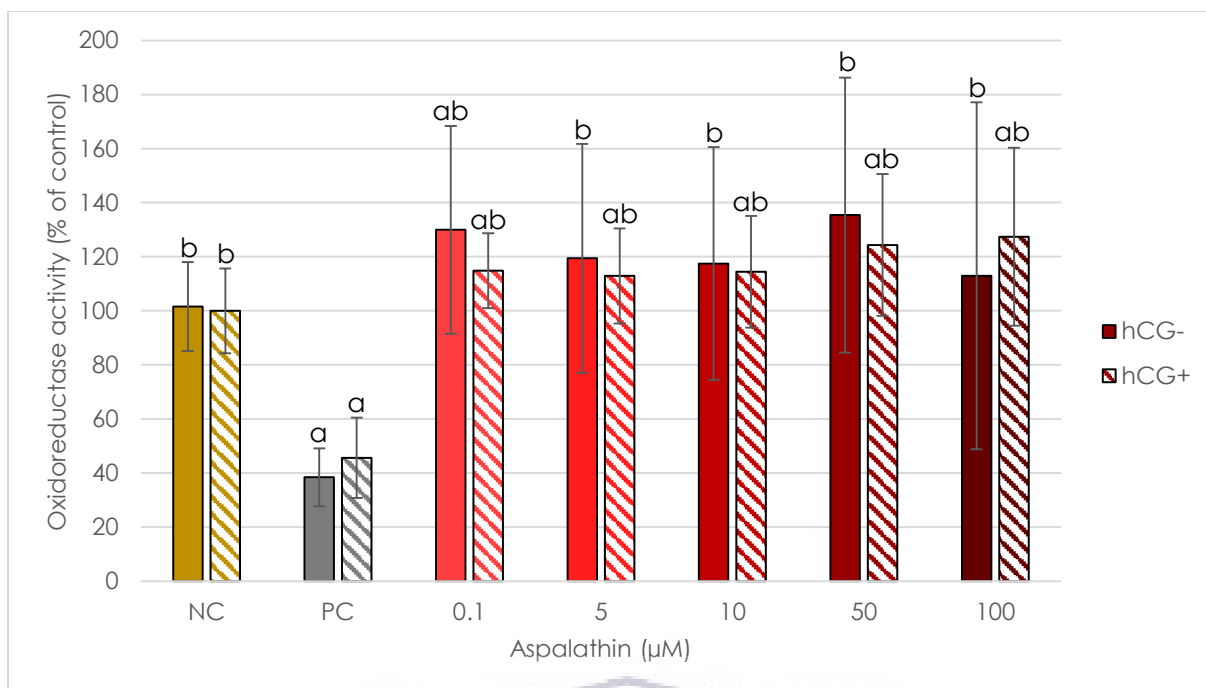


**Figure 3.4. Graph showing the effects of aspalathin on TM3 cell oxidoreductase activity, both with and without hCG.** The cells were treated for 24 hours with either a control or aspalathin (and 0.5 % DMSO) in media, either with hCG at 125 mIU/ml or without hCG. The percentage oxidoreductase activity was calculated under the assumption that the **NC** treatment produced 100 % activity. **NC**: negative control (i.e. 0.5 % DMSO), **PC**: positive control (i.e. 10 % DMSO), **hCG-**: without hCG, **hCG+**: with hCG. Data are represented as means  $\pm$  standard deviations. A P value of less than 0.05 was considered significant; a: significantly different to **NC**, b: significantly different to **PC**;  $n \geq 20$ .

Of the treatments without hCG, only the 0.1  $\mu\text{M}$  aspalathin sample produced significantly higher results than the negative control group, at 130 %  $\pm$  38.4 % (Figure 3.4). On the other hand, all of the aspalathin treatments with hCG produced higher oxidoreductase activities than the corresponding negative control. Those values were 114.8 %  $\pm$  13.9 %, 112.9 %  $\pm$  17.6 %, 114.4 %  $\pm$  20.7 %, 124.4 %  $\pm$  26.3 % and 127.4 %  $\pm$  33 % for 0.1  $\mu\text{M}$ , 5  $\mu\text{M}$ , 10  $\mu\text{M}$ , 50  $\mu\text{M}$  and 100  $\mu\text{M}$  respectively. Lastly, both negative controls (i.e. with and without hCG), as well as all of the aspalathin samples tested, gave significantly higher results than the (cell death) positive control did ( $P < 0.05$ ).

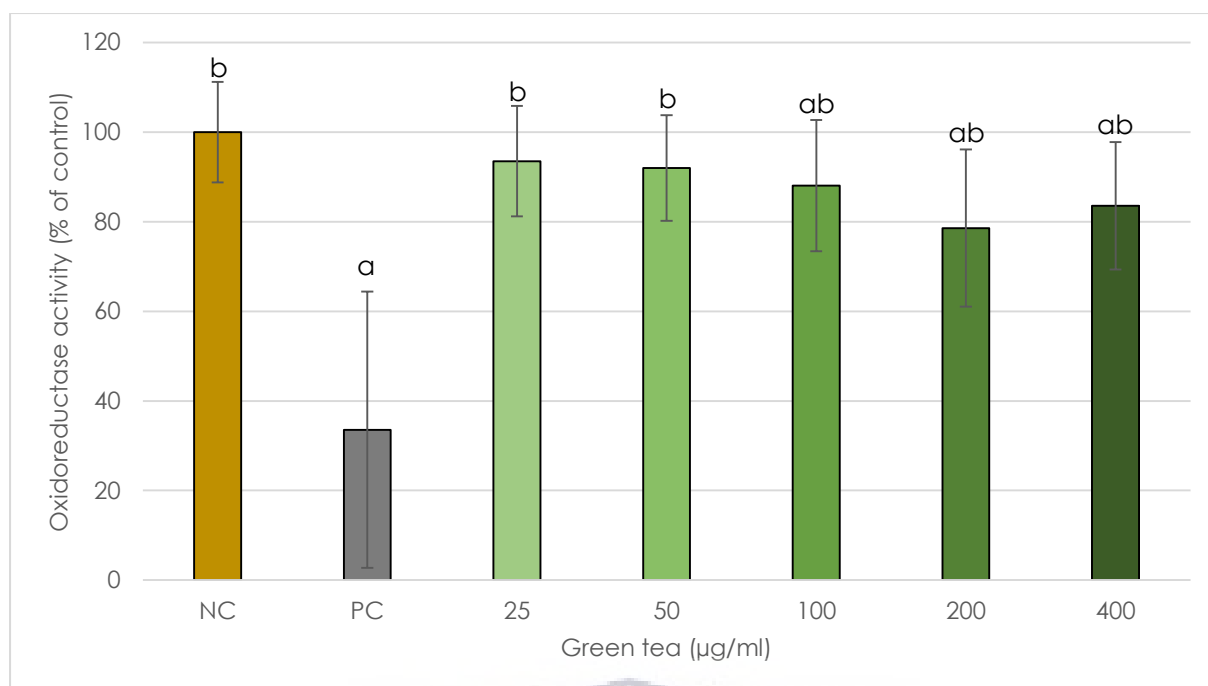


**Figure 3.5. Graph showing the effects of green tea on TM4 cell oxidoreductase activity.** The cells were treated for 24 hours with either a control or green tea reconstituted in media. The percentage oxidoreductase activity was calculated under the assumption that the **NC** treatment produced 100 % activity. **NC**: negative control (i.e. complete medium), **PC**: positive control (i.e. 10 % DMSO). Data are represented as means  $\pm$  standard deviations. A P value of less than 0.05 was considered significant; a: significantly different to **NC**, b: significantly different to **PC**;  $n \geq 14$ .

In [Figure 3.5](#), there were no significant differences between the oxidoreductase activities of TM4 cells given either 25 µg/ml or 50 µg/ml green tea treatments and the negative control. The 100 µg/ml, 200 µg/ml and the 400 µg/ml treatments showed results of 88 %  $\pm$  14.7 %, 78.6 %  $\pm$  17.5 % and 83.5 %  $\pm$  14.2 % respectively; all of which were significantly lower than the negative control ( $P < 0.05$ ). However, the negative control gave significantly higher readings than the (cell death) positive control (i.e. DMSO treatment) did ( $P < 0.05$ ), which validates this assay. All green tea treatments also showed higher MTT results than the DMSO treatment.

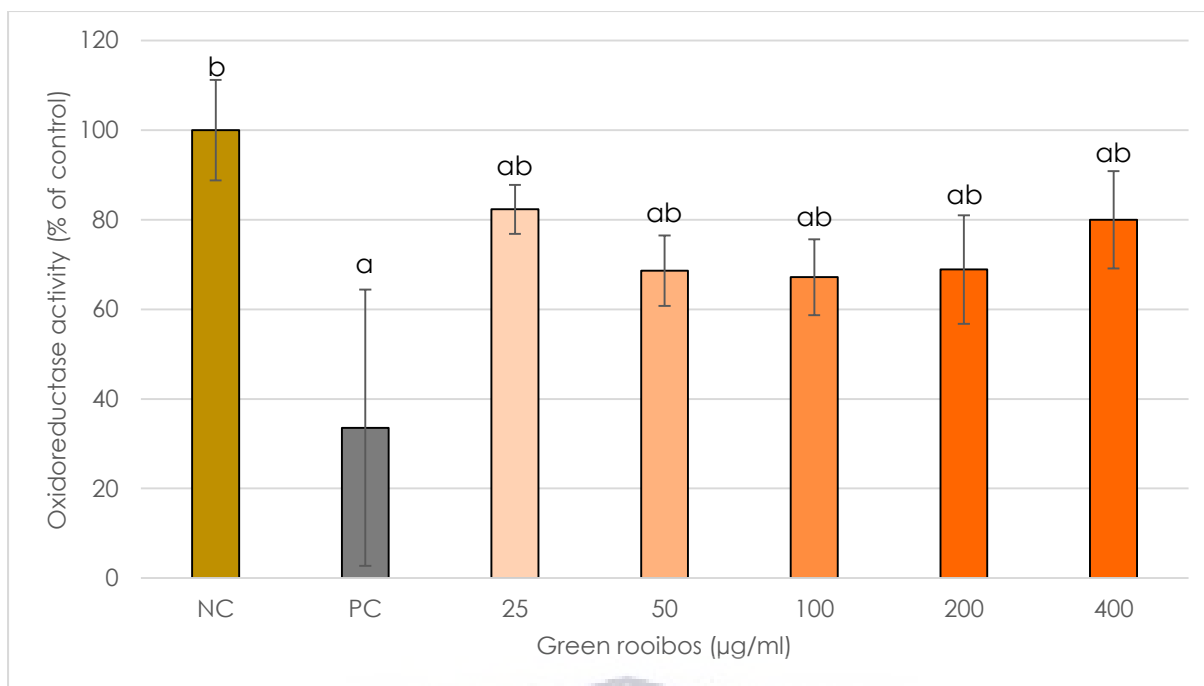


**Figure 3.6. Graph showing the effects of green rooibos on TM4 cell oxidoreductase activity.** The cells were treated for 24 hours with either a control or green rooibos reconstituted in media. The percentage oxidoreductase activity was calculated under the assumption that the **NC** treatment produced 100 % activity. **NC**: negative control (i.e. complete medium), **PC**: positive control (i.e. 10 % DMSO). Data are represented as means  $\pm$  standard deviations. A P value of less than 0.05 was considered significant; a: significantly different to **NC**, b: significantly different to **PC**;  $n \geq 13$ .

According to Figure 3.6, all green rooibos treatments tested produced data that were significantly different to both controls ( $P < 0.05$ ); they were lower than the negative control, whilst being higher than the (cell death) positive control. The lowest oxidoreductase activity (apart from the positive control) was noted in the cells treated with 100  $\mu\text{g/ml}$  green rooibos ( $67.2 \% \pm 8.5 \%$ ) whilst the 25  $\mu\text{g/ml}$  treatment gave the highest activity ( $82.3 \% \pm 5.4 \%$ ).

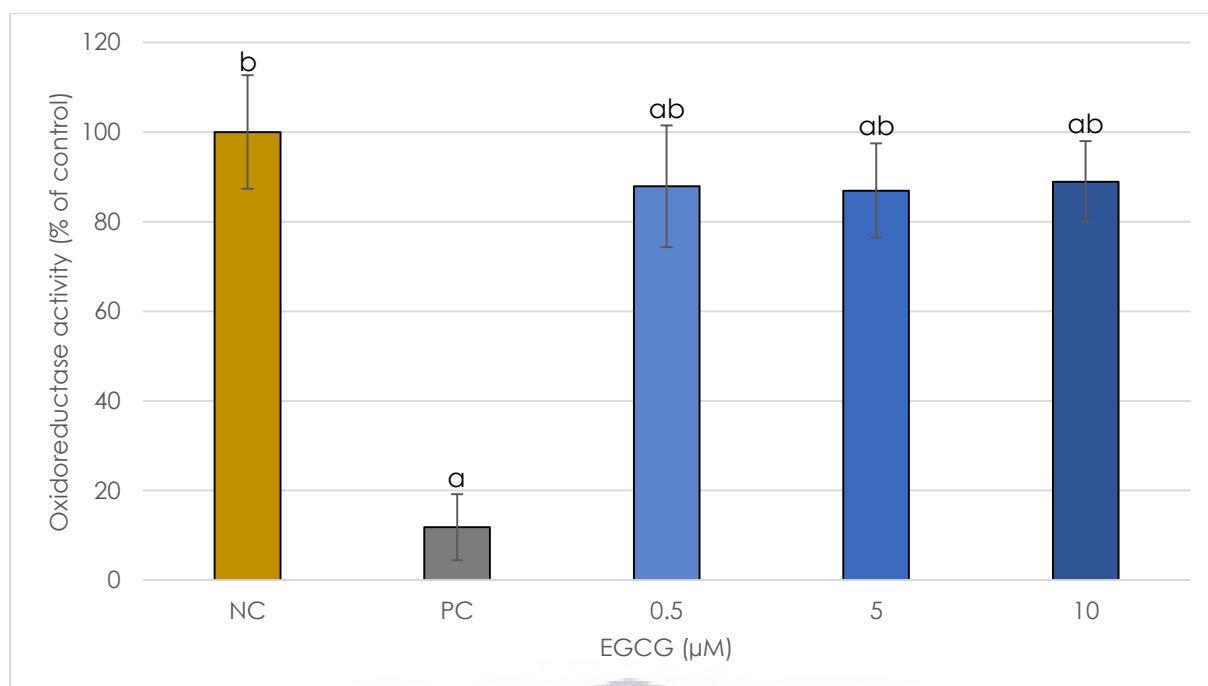


**Figure 3.7. Graph showing the effects of EGCG on TM4 cell oxidoreductase activity.** The cells were treated for 24 hours with either a control or EGCG (and 0.5 % DMSO) in media. The percentage oxidoreductase activity was calculated under the assumption that the **NC** treatment produced 100 % activity. **NC**: negative control (i.e. 0.5 % DMSO), **PC**: positive control (i.e. 10 % DMSO). Data are represented as means  $\pm$  standard deviations. A P value of less than 0.05 was considered significant; a: significantly different to **NC**, b: significantly different to **PC**;  $n \geq 13$ .

All three of the EGCG treatments produced significantly lower oxidoreductase activities than the negative control ( $P < 0.05$ ). The results from the TM4 cell MTT experiment on EGCG treatments were 87.9 % ( $\pm 13.5$  %), 86.9 % ( $\pm 10.5$  %) and 88.9 % ( $\pm 9.1$  %) for 0.5  $\mu\text{M}$ , 5  $\mu\text{M}$  and 10  $\mu\text{M}$  respectively (Figure 3.7). On the other hand, the negative control showed significantly higher MTT results than the (cell death) positive control ( $P < 0.05$ ), supporting the assay's validity. Additionally, all three of the EGCG treatments produced significantly higher oxidoreductase activities than the positive control ( $P < 0.05$ ).

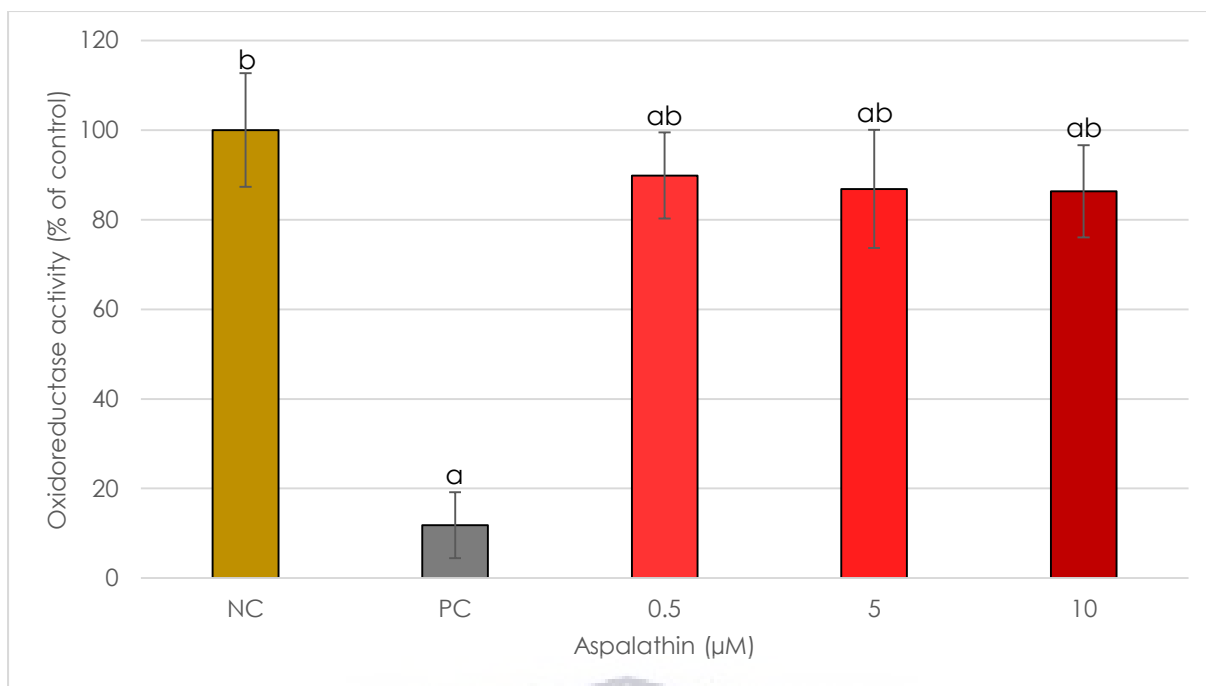


**Figure 3.8. Graph showing the effects of aspalathin on TM4 cell oxidoreductase activity.** The cells were treated for 24 hours with either a control or aspalathin (and 0.5 % DMSO) in media. The percentage oxidoreductase activity was calculated under the assumption that the **NC** treatment produced 100 % activity. **NC**: negative control (i.e. 0.5 % DMSO), **PC**: positive control (i.e. 10 % DMSO). Data are represented as means  $\pm$  standard deviations. A P value of less than 0.05 was considered significant; a: significantly different to **NC** treatment, b: significantly different to **PC**;  $n \geq 14$ .

As shown in [Figure 3.8](#), all aspalathin treatments produced a significant decline in oxidoreductase activity compared to the negative control ( $P < 0.05$ ). Aspalathin gave oxidoreductase activities of 89.9 % ( $\pm 9.6$  %), 86.9 % ( $\pm 13.2$  %) and 86.3 % ( $\pm 10.3$  %) for 0.5  $\mu\text{M}$ , 5  $\mu\text{M}$  and 10  $\mu\text{M}$  treatments respectively. The data from all aspalathin treatments were also significantly higher than those from the cell death positive control ( $P < 0.05$ ).



### 3.2 Photo microscopy

The microscopic study of cells *in vitro* provides a fair amount of information to cell biologists. Using microscopy, one can confirm the presence of cells in test vessels, their attachment to the vessels (for adherent cells) as well as their density. These factors can be very useful if one were to acquire very low signals from cell-based assays. However, another informative consideration is the morphology of the cells being studied.

It is well known that form and function are interrelated traits in biology, including in cell biology. Different tissues have developed different structures and even cytological features that assist those cells in achieving their functions. As such, morphological examinations of cells in culture has long been used to gauge the wellbeing of said cells. An article by Walton (1975) even provides a checklist for rating cellular injury after examining the cells by electron microscopy. Although it provides a much lower resolution than electron microscopy, standard light microscopy can still give good insight into the health status of cells under study. Here, only photomicrographs at 100 × magnification are shown, as they are adequate to assess cell morphology and the higher magnification photos did not reveal anything new. In addition, they show relatively large subsets of the treatment groups that reveal general cell morphology.

#### 3.2.1 TM3 cell morphology

According to [Figure 3.9](#), TM3 cells that were exposed to either 50 µg/ml, 100 µg/ml, 200 µg/ml or 400 µg/ml of green tea (without hCG) showed little difference in shape to the media treated cells (i.e. the negative control). After all of those treatments, observation showed cells that were well formed with elongated bodies that resembled stretched triangles to spindles; this is a normal, healthy morphology for TM3 cells.

There were clusters of cells in all treatment groups where the cells were so densely packed together that their shapes were hard to discern, but appeared to be deformed and squashed. In those clusters, the cells seemed to be stressed due to space constraints. However, along the edges of those clusters, where there was more space for growth, the cells showed good morphology. These cell clusters could have resulted from cells not fully separating from each other during the trypsinisation and plating process. This is a normal occurrence for TM3 cells, although not desirable.

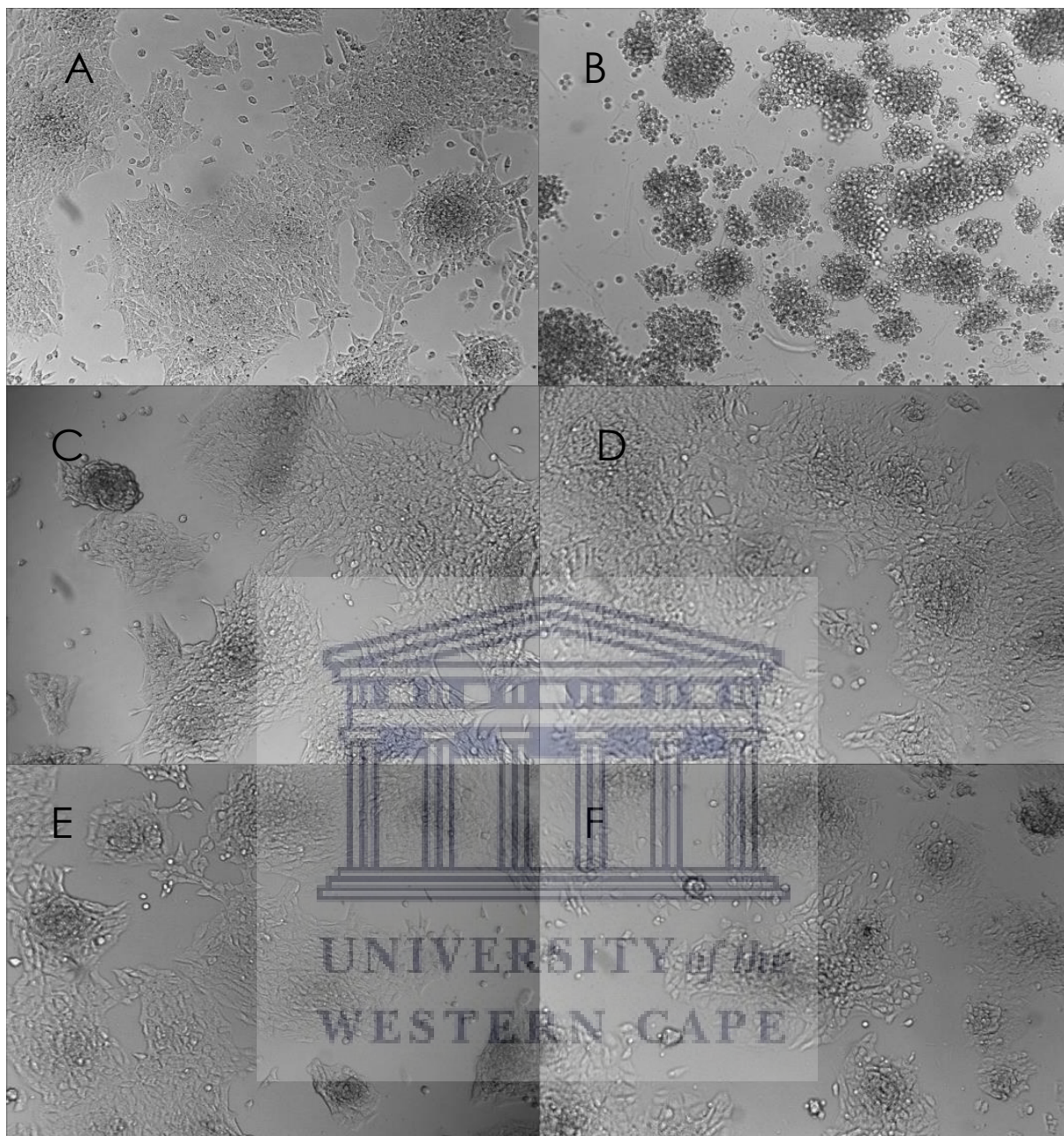


**Figure 3.9. Photomicrographs showing TM3 cell morphology after treatment with green tea.** Cells were exposed for 24 hours to controls or varying concentrations of reconstituted green tea (without hCG). **A:** negative control (i.e. complete medium); **B:** cell death positive control (i.e. 10 % DMSO); **C:** 50  $\mu\text{g/ml}$  green tea; **D:** 100  $\mu\text{g/ml}$  green tea; **E:** 200  $\mu\text{g/ml}$  green tea; **F:** 400  $\mu\text{g/ml}$  green tea. Magnification = 100  $\times$ .

On the other hand, the cell death positive control groups showed very different morphologies to the other studied groups. Instead of having stretched spindle shapes, those cells were all rounded and shrunken. In addition, most (if not all) of the cells from the DMSO treatment appeared to be detached from the culture wells.

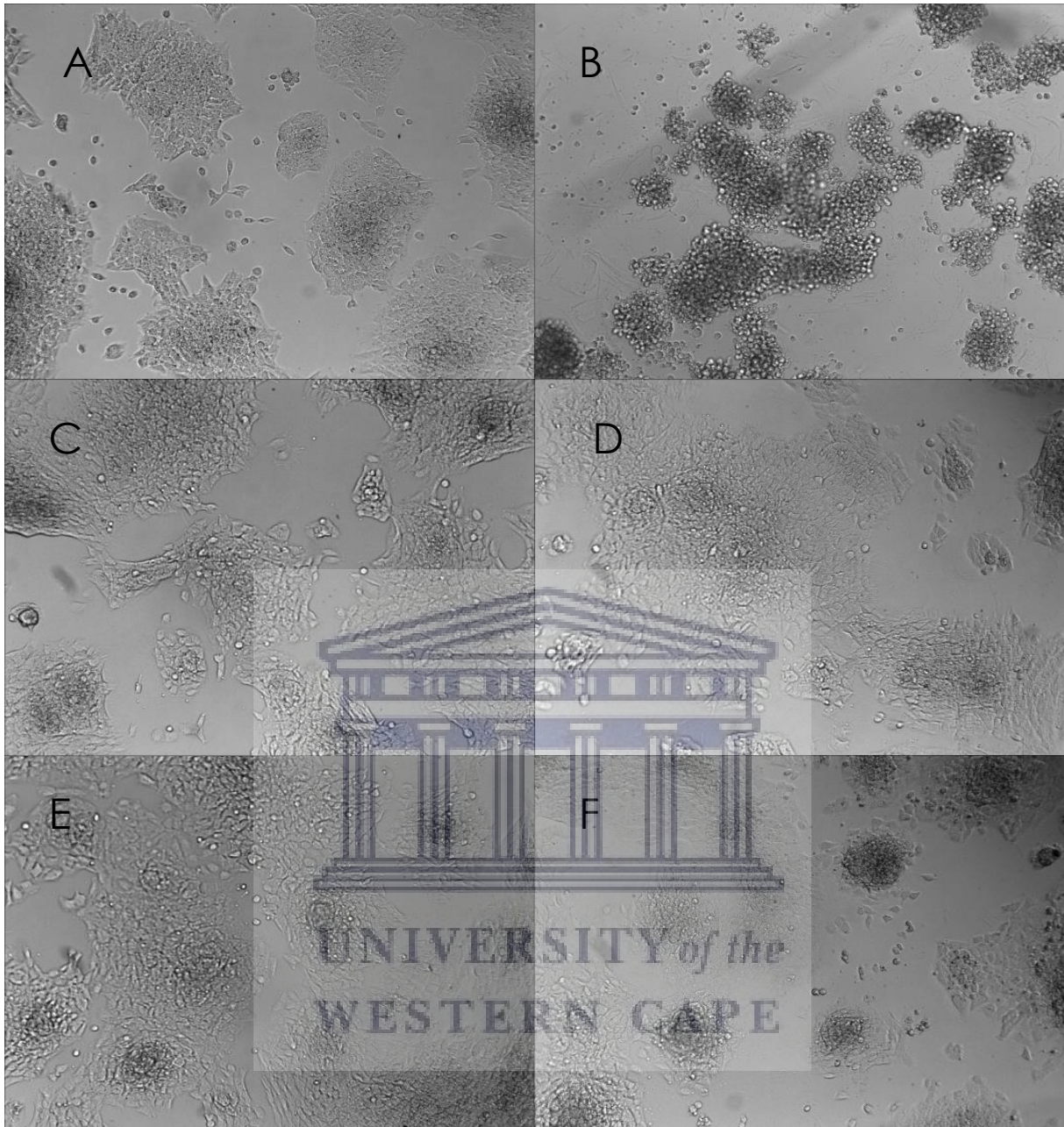


**Figure 3.10. Photomicrographs showing TM3 cell morphology after treatment with green tea and hCG.** Cells were exposed for 24 hours to controls or varying concentrations of reconstituted green tea as well as hCG at 125 mIU/ml. **A:** negative control (i.e. complete medium); **B:** cell death positive control (i.e. 10 % DMSO); **C:** 50 µg/ml green tea; **D:** 100 µg/ml green tea; **E:** 200 µg/ml green tea; **F:** 400 µg/ml green tea. Magnification = 100 ×.

Figure 3.10 shows basically the same morphology as Figure 3.9. All treatments with green tea produced no real differences in morphology compared with the negative control cells (or each other). Here, the TM3 cells were co-treated with green tea and hCG in an attempt to stimulate the TM3 cells. The cells that received hCG were no different to those that received the same treatments without hCG (compare Figure 3.9 to 3.10).



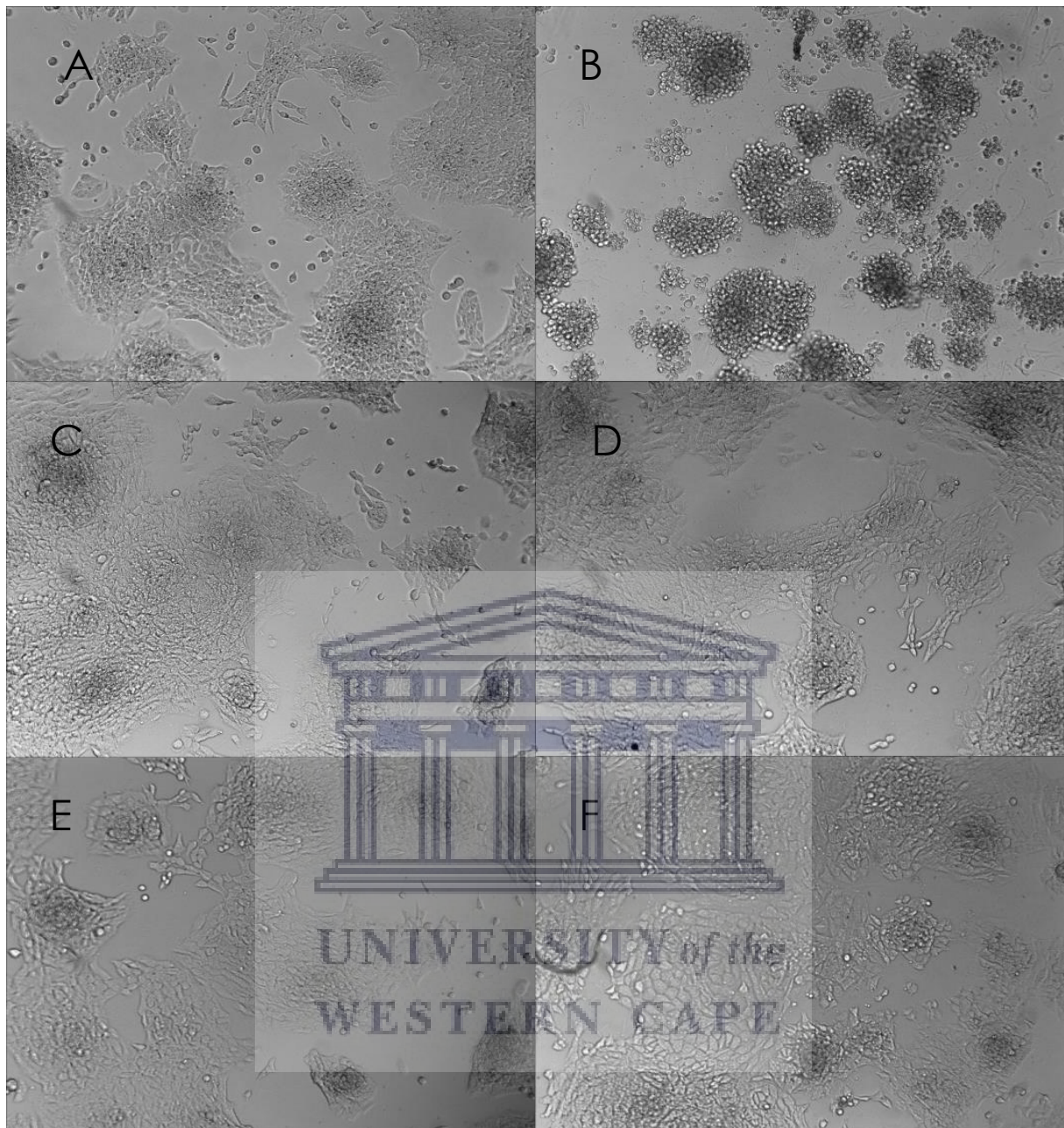


**Figure 3.11. Photomicrographs showing TM3 cell morphology after treatment with green rooibos.** Cells were exposed for 24 hours to controls or varying concentrations of reconstituted green rooibos (without hCG). **A:** negative control (i.e. complete medium); **B:** cell death positive control (i.e. 10 % DMSO); **C:** 50 µg/ml green rooibos; **D:** 100 µg/ml green rooibos; **E:** 200 µg/ml green rooibos; **F:** 400 µg/ml green rooibos. Magnification = 100 ×.

As for the green tea treatments, [Figures 3.11](#) and [3.12](#) showed that green rooibos treatment of TM3 cells (both without and with hCG) produced a similar cell morphology to the corresponding negative control treatment. Once more, the rooibos and negative control cells were elongated and slightly spread laterally, when they had space to do so.

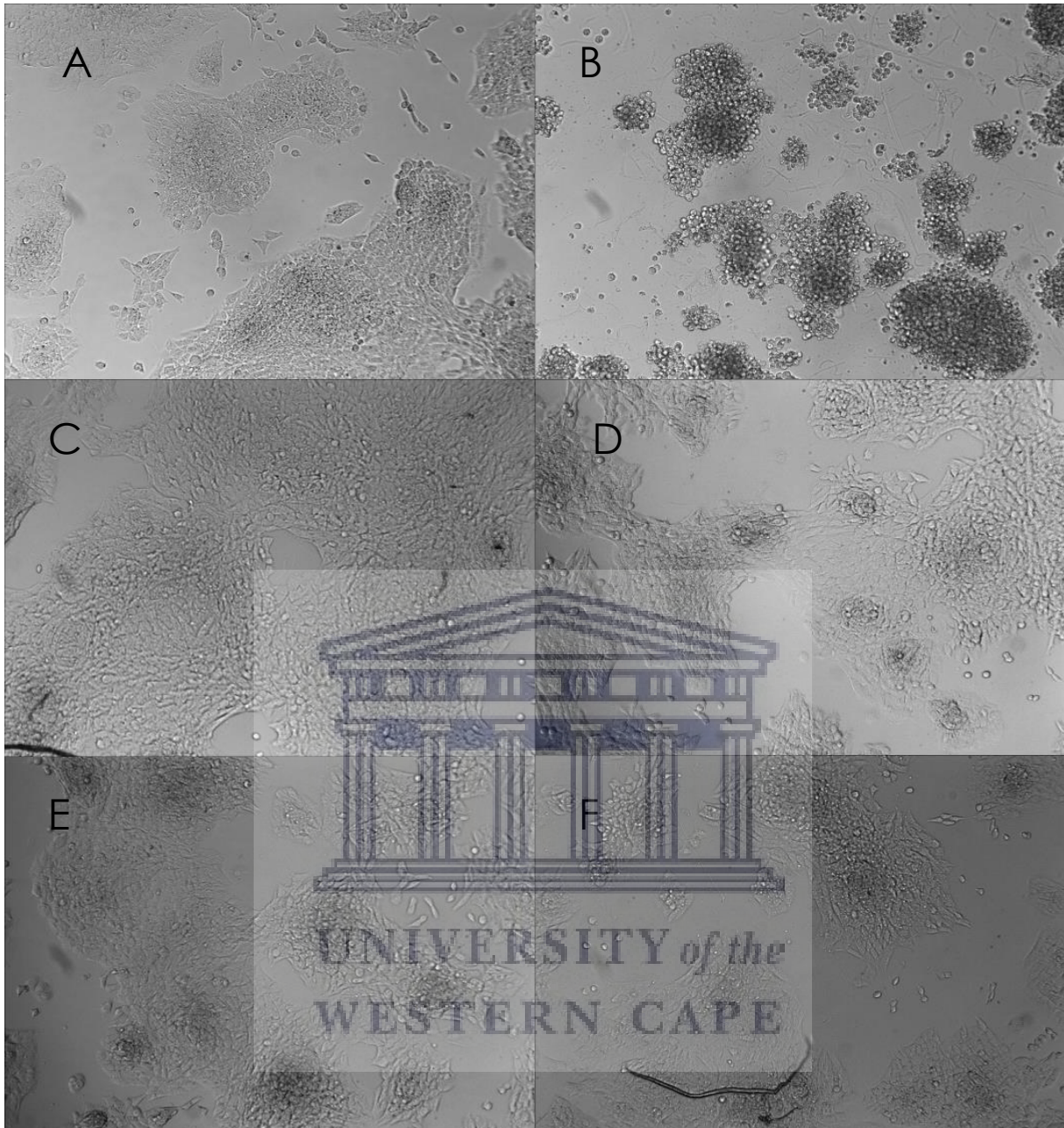


**Figure 3.12. Photomicrographs showing TM3 cell morphology after treatment with green rooibos and hCG.** Cells were exposed for 24 hours to controls or varying concentrations of reconstituted green rooibos as well as hCG at 125 mIU/ml. **A:** negative control (i.e. complete medium); **B:** cell death positive control (i.e. 10 % DMSO); **C:** 50 µg/ml green rooibos; **D:** 100 µg/ml green rooibos; **E:** 200 µg/ml green rooibos; **F:** 400 µg/ml green rooibos. Magnification = 100 ×.

The overcrowded cell clusters were once more present in all treatment groups, but there were no marked differences between the cells that received hCG and those that did not (Figure 3.12). Additionally, the cell death positive control groups had exclusively round shrivelled cells that were detached from the wells.

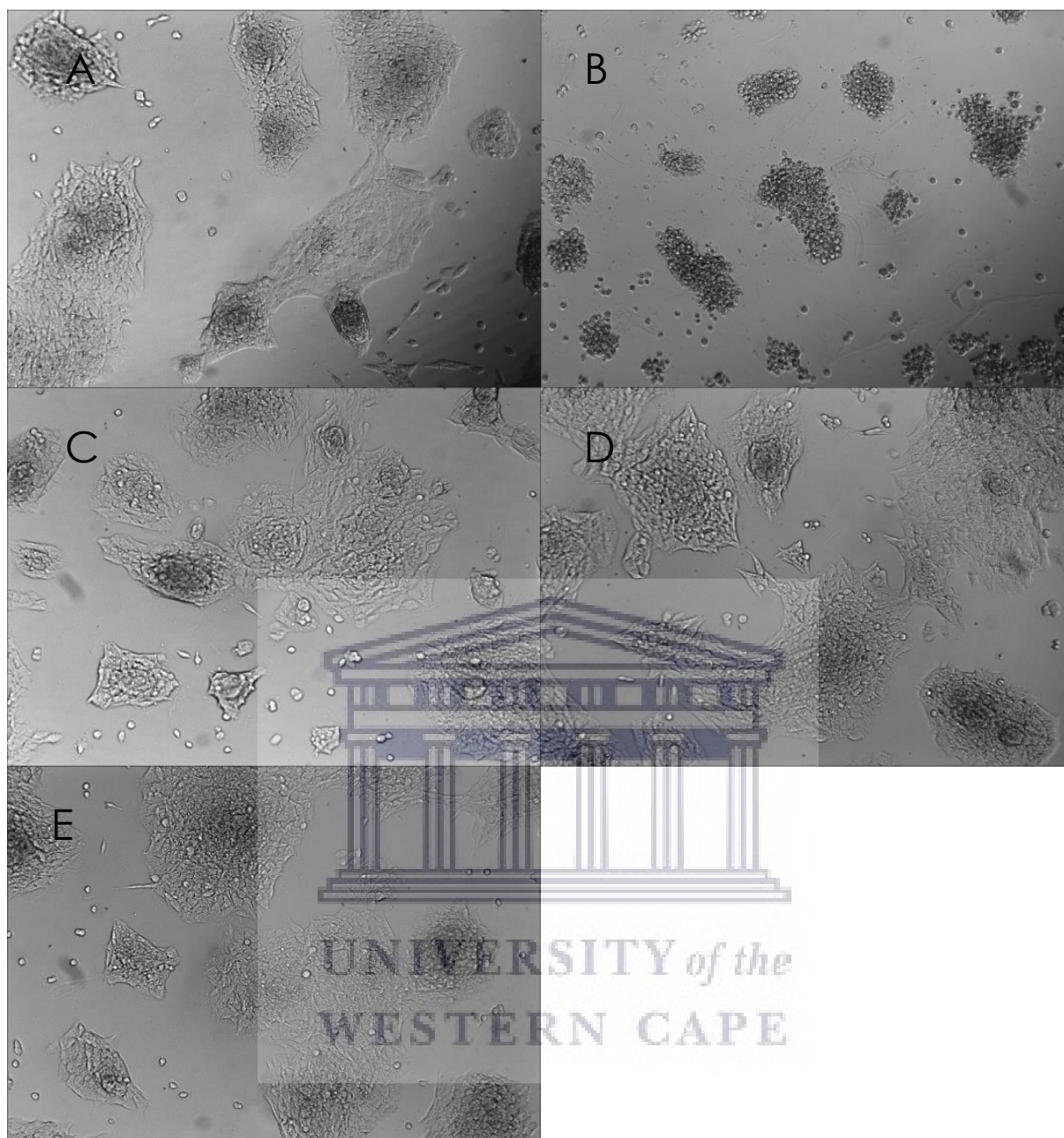


**Figure 3.13. Photomicrographs showing TM3 cell morphology after treatment with EGCG.** Cells were exposed for 24 hours to controls or varying concentrations of EGCG, in DMSO at 0.5 % (without hCG). **A:** negative control (i.e. 0.5 % DMSO); **B:** cell death positive control (i.e. 10 % DMSO); **C:** 0.1  $\mu\text{M}$  EGCG; **D:** 5  $\mu\text{M}$  EGCG; **E:** 10  $\mu\text{M}$  EGCG. Magnification = 100  $\times$ .

The treatment of TM3 cells with EGCG at 0.1  $\mu\text{M}$ , 5  $\mu\text{M}$  and 10  $\mu\text{M}$  also produced cells with good morphology (Figure 3.13). There is no way to easily distinguish between cells given either treatment from each other by their morphology. However, the cell death positive control produced shrunken, rounded, detached cells.

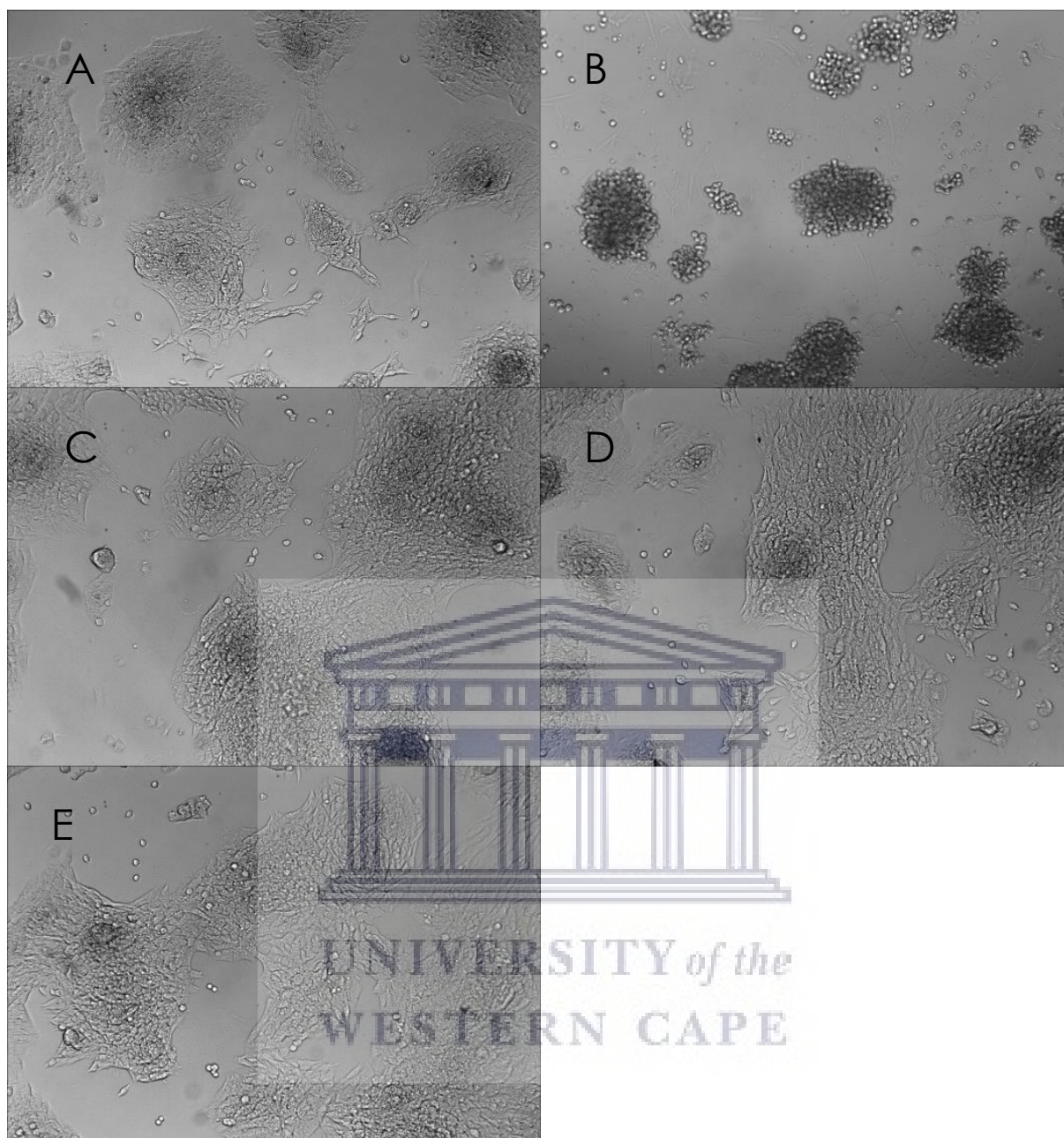


**Figure 3.14. Photomicrographs showing TM3 cell morphology after treatment with EGCG and hCG.** Cells were exposed for 24 hours to controls or varying concentrations of EGCG, in DMSO at 0.5 %, as well as hCG at 125 mIU/ml. **A:** negative control (i.e. 0.5 % DMSO); **B:** cell death positive control (i.e. 10 % DMSO); **C:** 0.1  $\mu\text{M}$  EGCG; **D:** 5  $\mu\text{M}$  EGCG; **E:** 10  $\mu\text{M}$  EGCG. Magnification = 100  $\times$ .

The TM3 cells that received both EGCG and hCG look similar in morphology across the treatment range (from 0  $\mu\text{M}$  to 10  $\mu\text{M}$ ), see [Figure 3.14](#). Furthermore, the morphology of TM3 cells given hCG and EGCG were not really different to those that did not receive hCG (compare [Figures 3.13](#) and [3.14](#)). The cell death control group showed rounded detached shrunken cells, though.



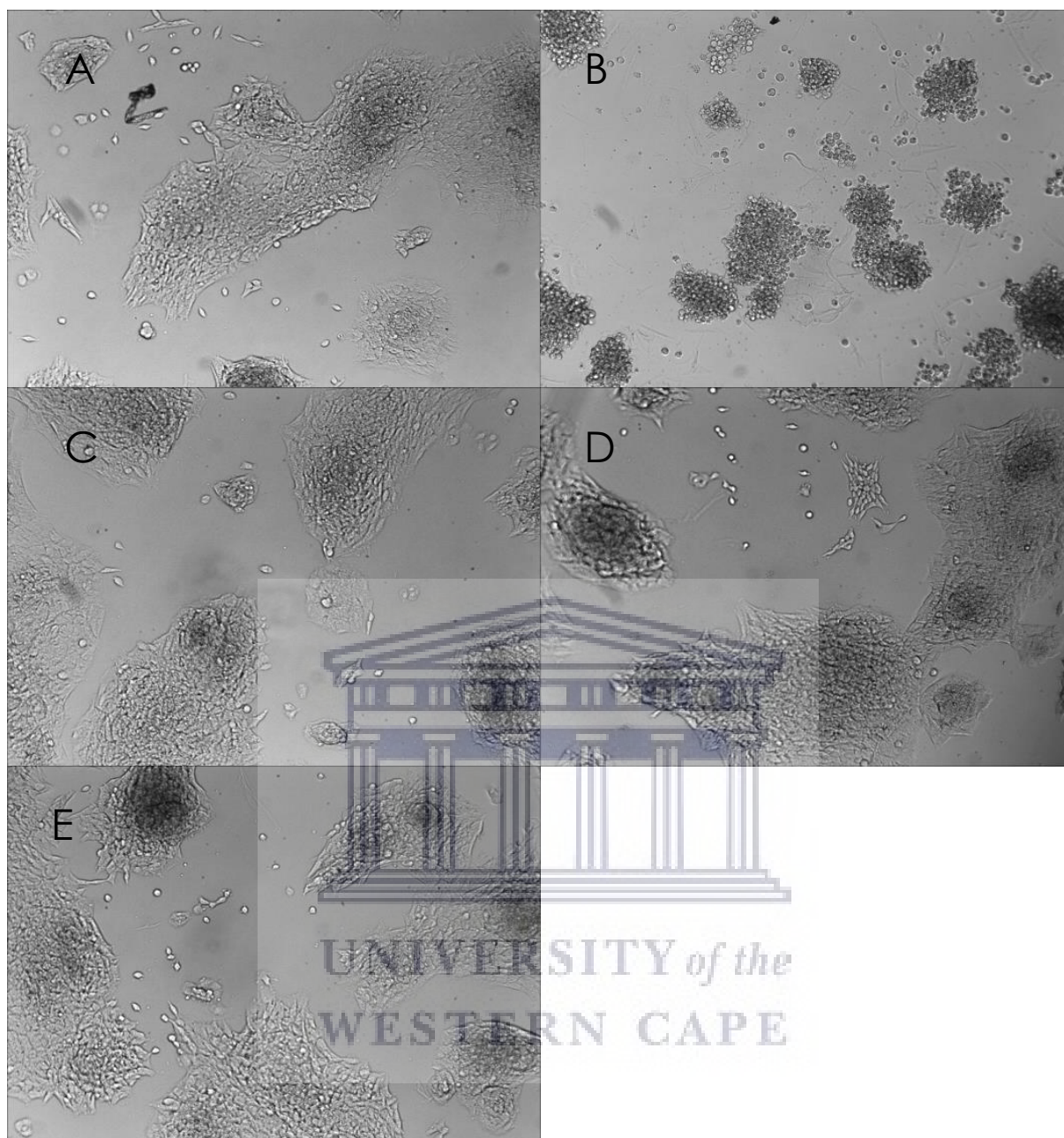


**Figure 3.15. Photomicrographs showing TM3 cell morphology after treatment with aspalathin.** Cells were exposed for 24 hours to controls or varying concentrations of aspalathin, in DMSO at 0.5 % (without hCG). **A:** negative control (i.e. 0.5 % DMSO); **B:** cell death positive control (i.e. 10 % DMSO); **C:** 0.1  $\mu\text{M}$  aspalathin; **D:** 5  $\mu\text{M}$  aspalathin; **E:** 10  $\mu\text{M}$  aspalathin. Magnification = 100  $\times$ .

The treatment of TM3 cells with aspalathin produced no differences in their morphology compared with the negative control group (see [Figure 3.15](#)). However, the cell death control group's cells, were shrunken, rounded and appear detached from the culture well.

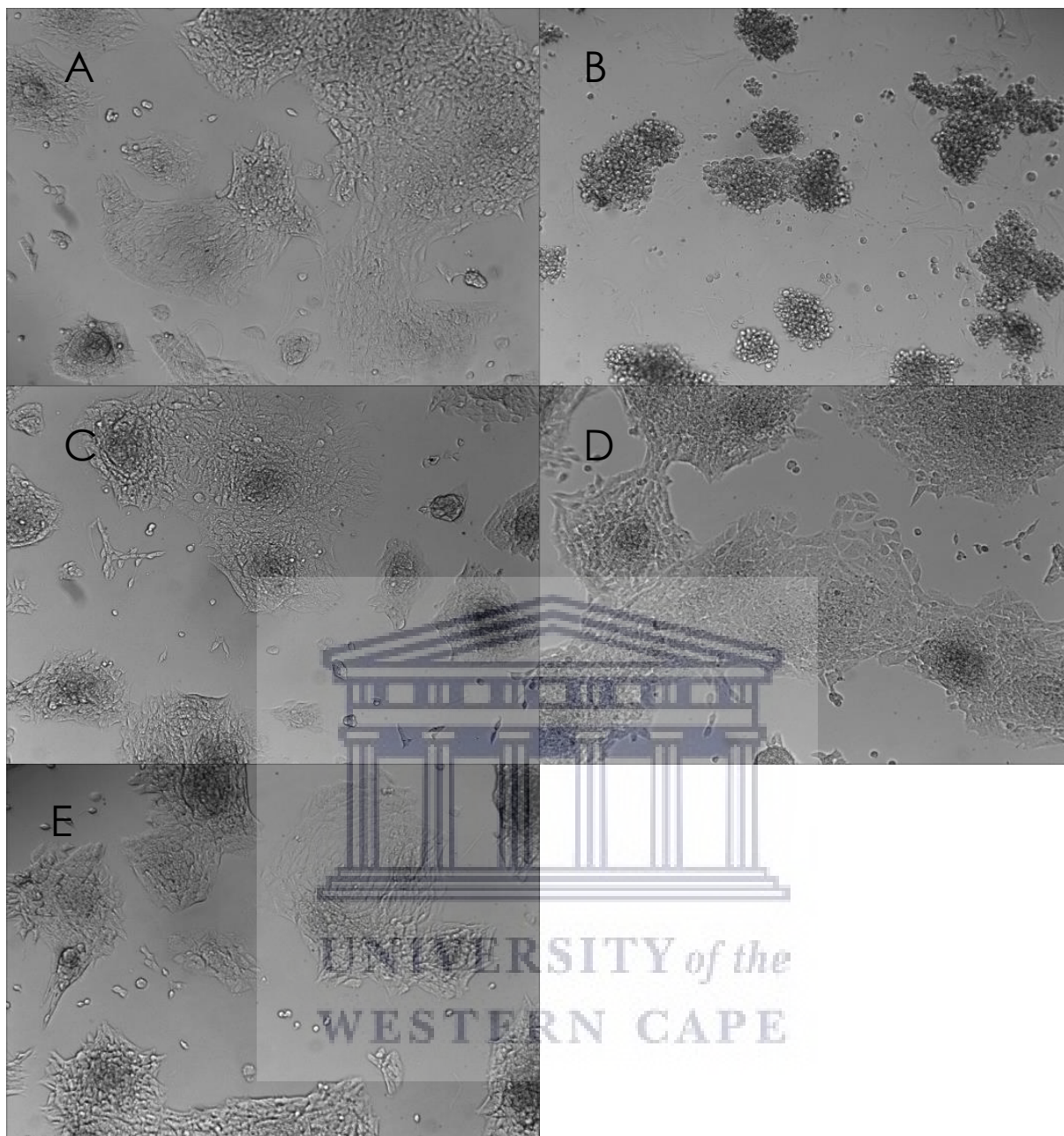


**Figure 3.16. Photomicrographs showing TM3 cell morphology after treatment with aspalathin and hCG.** Cells were exposed for 24 hours to controls or varying concentrations of aspalathin, in DMSO at 0.5 %, as well as hCG at 125 mIU/ml. **A:** negative control (i.e. 0.5 % DMSO); **B:** cell death positive control (i.e. 10 % DMSO); **C:** 0.1  $\mu\text{M}$  aspalathin; **D:** 5  $\mu\text{M}$  aspalathin; **E:** 10  $\mu\text{M}$  aspalathin. Magnification = 100  $\times$ .

As for the EGCG treatments, the aspalathin treatments with hCG revealed TM3 cell morphologies that were no different to those that did not receive hCG (compare [Figures 3.15](#) and [3.16](#)). Here, all treatment groups (except the death positive control) looked similar with attached spindle-shaped cells. The death control cells were rounded, shrunken and detached, though.

When one compares the flavonoid-treated (i.e. EGCG and aspalathin) TM3 cells with those that were treated with the teas (i.e. green tea and green rooibos) no real morphological differences were noted. All treatments except the cell death positive controls produced mostly flattened cells that were spindle shaped (i.e. normal TM3 cell morphology). Even the negative control treatments for the EGCG and aspalathin experiments (0.5% DMSO) appeared to have no noticeable effects on the morphology of the TM3 cells when one compares them to the media-treated negative control cells (Figures 3.9-A, 3.10-A, 3.11-A, 3.12-A, 3.13-A, 3.14-A, 3.15-A and 3.16-A). In all TM3 morphology experiments, the cell death positive controls solely gave shrivelled and round cells that were detached from the culture vessels.

### **3.2.2 TM4 cell morphology**

The negative control group of TM4 cells all showed ideal cell morphology after 24 hours of treatment (Figure 3.17). The cells were stretched and had cellular processes that made them resemble bipolar cells. The cells bodies were mostly spindle shaped, but many were polygonal and tended to take on an almost triangular shape with a cellular process at the apex. A small minority of the cells present were slightly rounded, but remained associated with the culture vessel floor and usually still had cellular processes.

All of the treatments with green tea (i.e. 50 µg/ml, 100 µg/ml, 200 µg/ml and 400 µg/ml) gave cells with similar morphologies to the media control cells. Furthermore, the treatments with green tea produced cells that were morphologically indistinguishable from those given EGCG doses (Figure 3.19).

Nonetheless, the cell death positive control TM4 cells all lacked the aforementioned morphology that the other treated cell groups showed. The treatments with 10 % DMSO produced cells that were round (some appear to have shrunk slightly) and all the cells were detached from the culture wells.

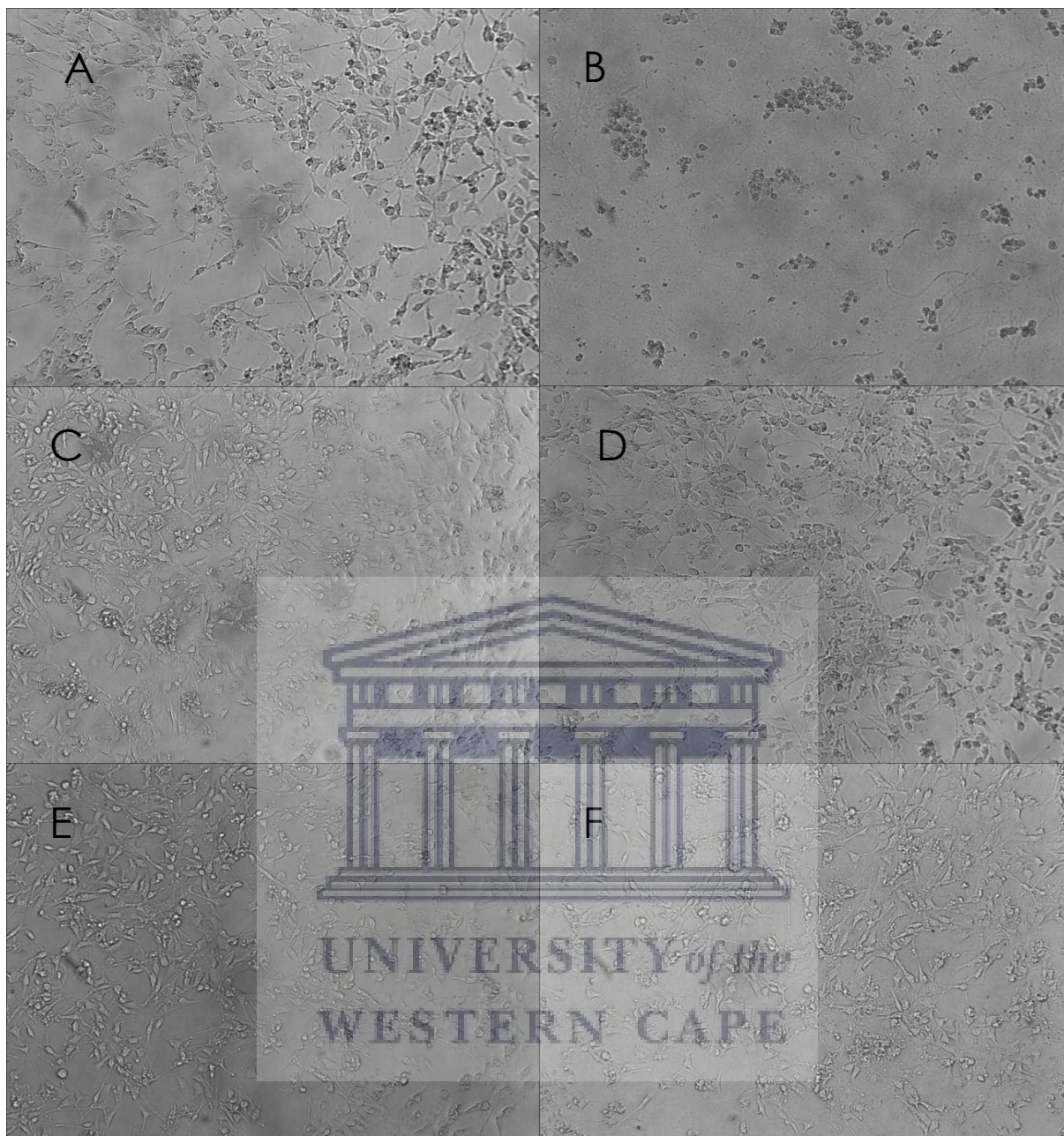


**Figure 3.17. Photomicrographs showing TM4 cell morphology after treatment with green tea.** Cells were exposed for 24 hours to controls or varying concentrations of reconstituted green tea. **A:** negative control (i.e. complete medium); **B:** cell death positive control (i.e. 10 % DMSO); **C:** 50  $\mu\text{g/ml}$  green tea; **D:** 100  $\mu\text{g/ml}$  green tea; **E:** 200  $\mu\text{g/ml}$  green tea; **F:** 400  $\mu\text{g/ml}$  green tea. Magnification = 100  $\times$ .

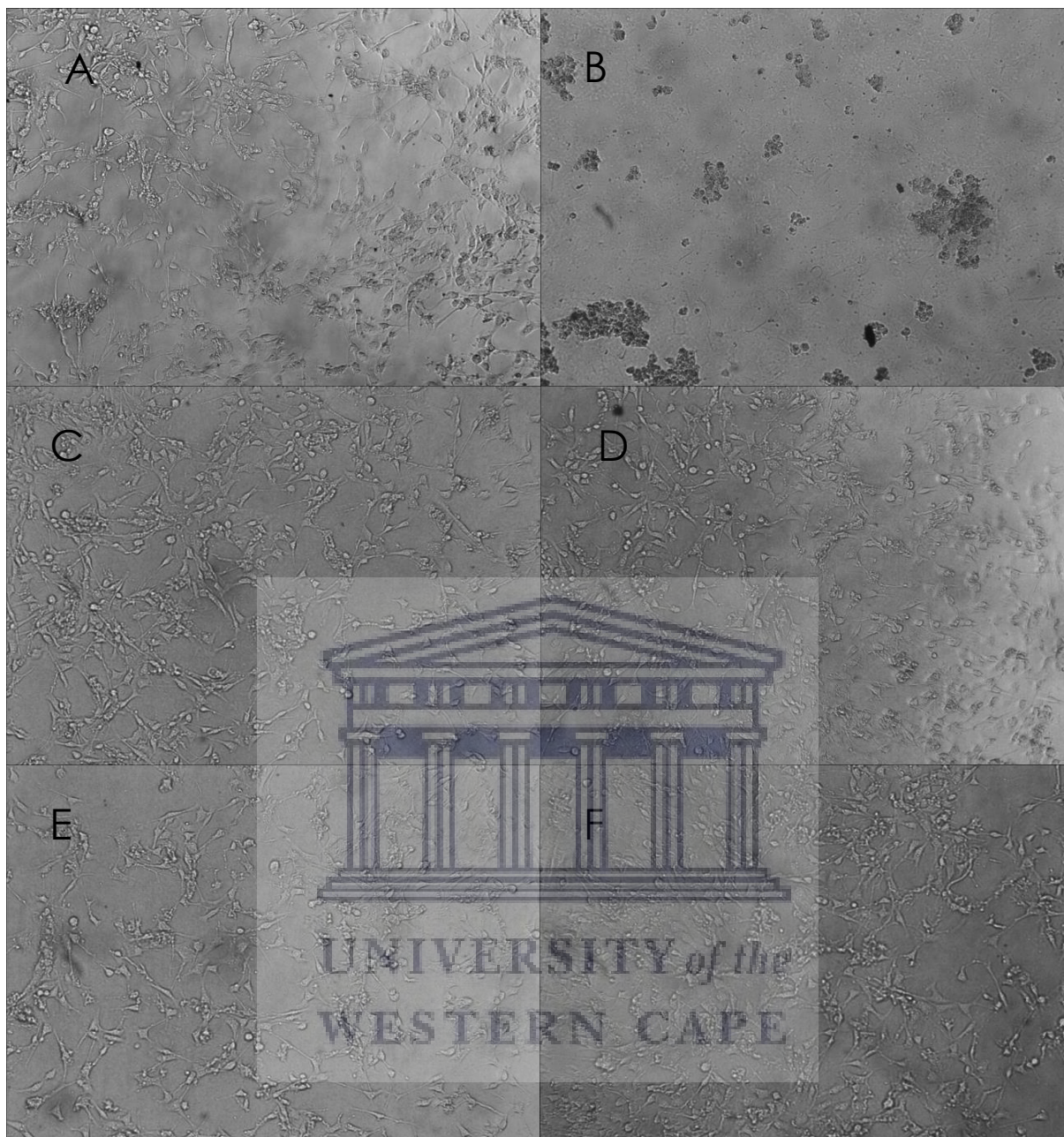


**Figure 3.18. Photomicrographs showing TM4 cell morphology after treatment with green rooibos.** Cells were exposed for 24 hours to controls or varying concentrations of reconstituted green rooibos. **A:** negative control (i.e. complete medium); **B:** cell death positive control (i.e. 10 % DMSO); **C:** 50  $\mu\text{g/ml}$  green rooibos; **D:** 100  $\mu\text{g/ml}$  green rooibos; **E:** 200  $\mu\text{g/ml}$  green rooibos; **F:** 400  $\mu\text{g/ml}$  green rooibos. Magnification = 100  $\times$ .

The treatment of TM4 cells with green rooibos resulted in similar morphologies to the negative control-treated cells (Figure 3.18). On the other hand, the cell death positive control group were all rounded, and detached in clusters.

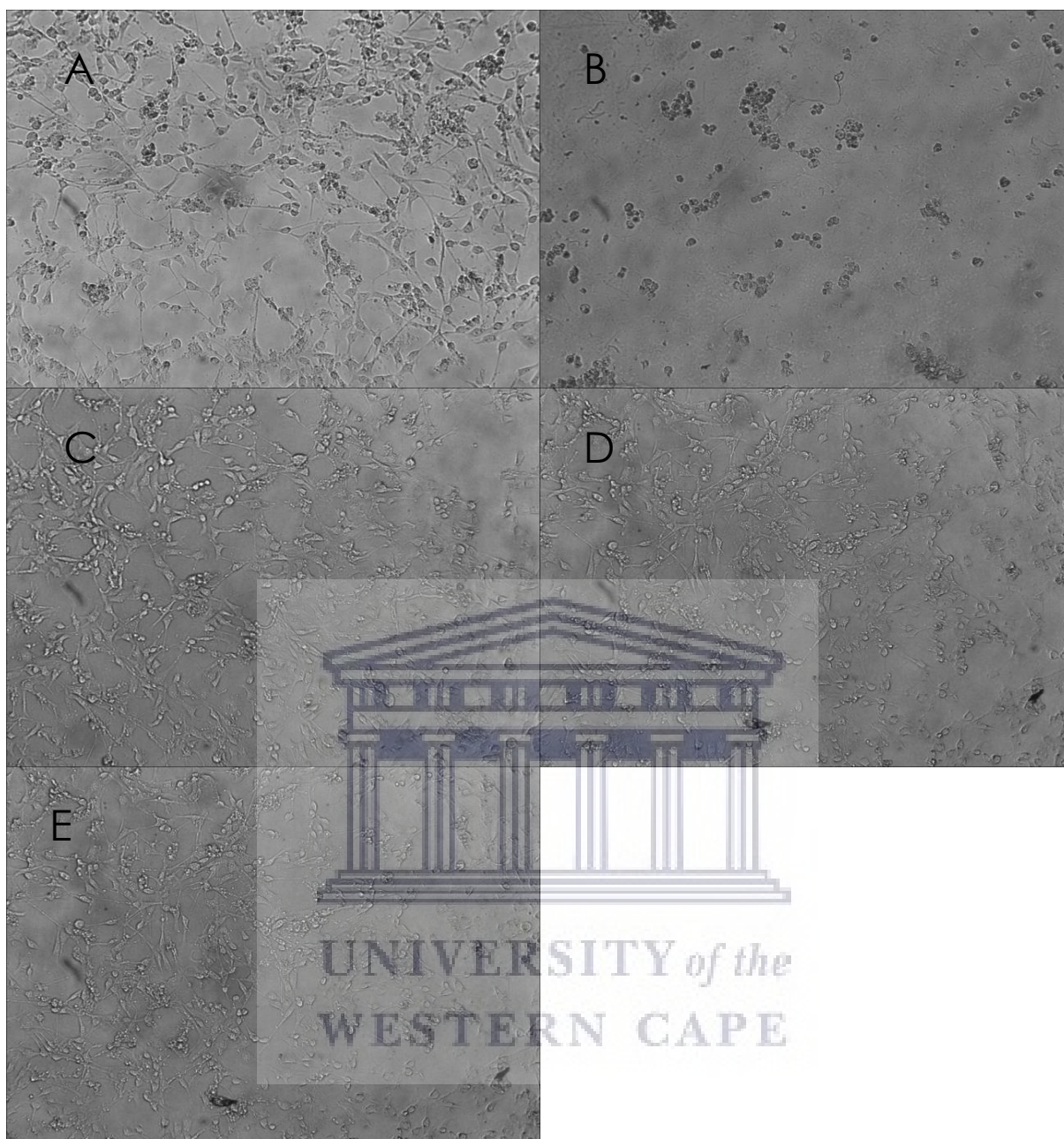


**Figure 3.19. Photomicrographs showing TM4 cell morphology after treatment with EGCG.** Cells were exposed for 24 hours to controls or varying concentrations of EGCG in DMSO at 0.5 %. **A:** negative control (i.e. 0.5 % DMSO); **B:** cell death positive control (i.e. 10 % DMSO); **C:** 0.1  $\mu\text{M}$  EGCG; **D:** 5  $\mu\text{M}$  EGCG; **E:** 10  $\mu\text{M}$  EGCG. Magnification = 100  $\times$ .

The TM4 cells that were treated with 0.5 % DMSO, as the negative control for the EGCG and aspalathin treatments, had good morphology with polygonal shapes and clear cellular processes (Figures 3.19-A and 3.20-A). These results were practically identical to the negative control treated cells shown in Figures 3.17-A and 3.18-A.

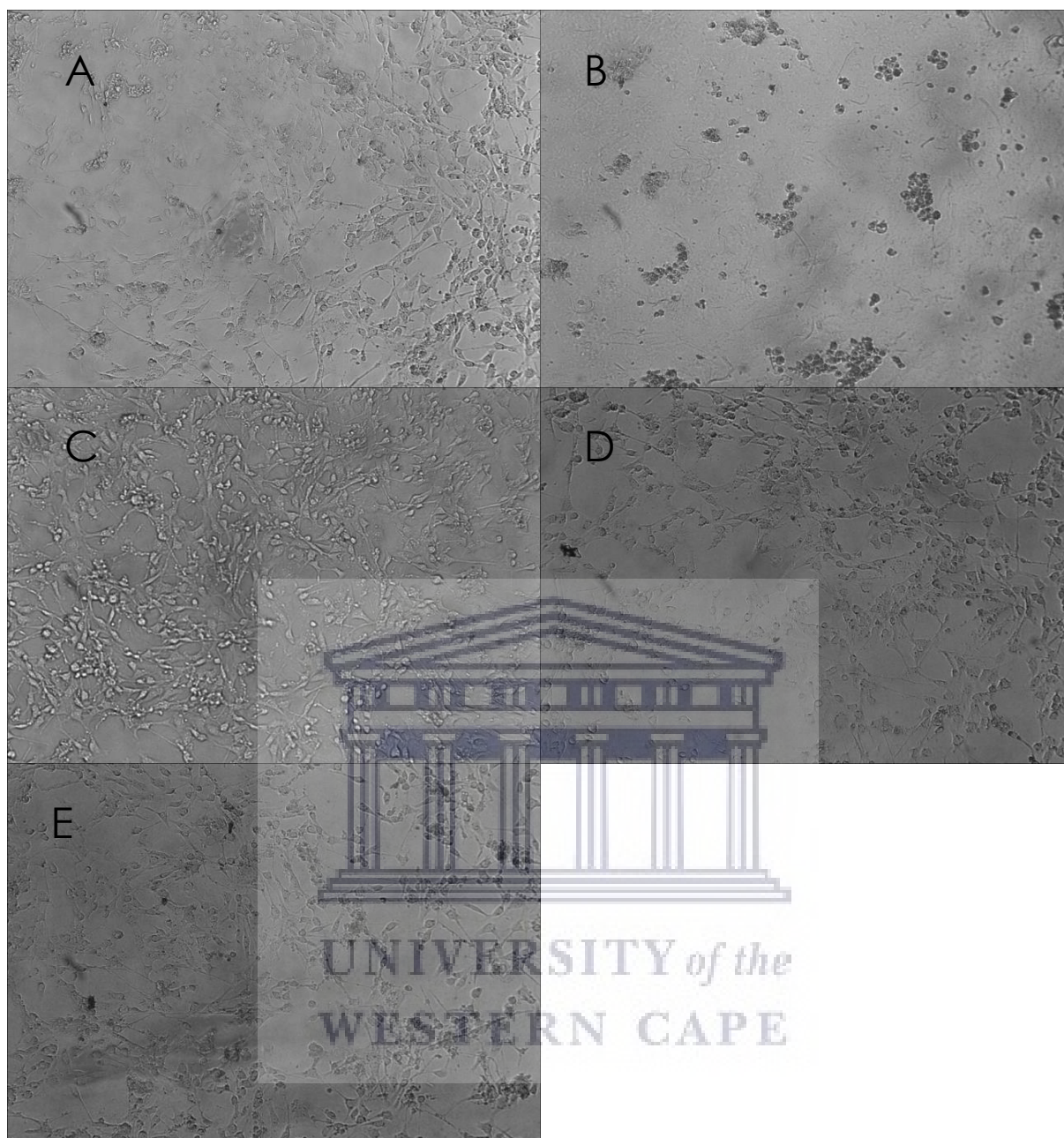


**Figure 3.20. Photomicrographs showing TM4 cell morphology after treatment with aspalathin.** Cells were exposed for 24 hours to controls or varying concentrations of aspalathin in DMSO at 0.5. **A:** negative control (i.e. 0.5 % DMSO); **B:** cell death positive control (i.e. 10 % DMSO); **C:** 0.1  $\mu\text{M}$  aspalathin; **D:** 5  $\mu\text{M}$  aspalathin; **E:** 10  $\mu\text{M}$  aspalathin. Magnification = 100  $\times$ .

The treatments with EGCG and aspalathin (at 0.1  $\mu\text{M}$ , 5  $\mu\text{M}$  and 10  $\mu\text{M}$ ) gave cells that were no different to the negative control groups; they had ideal morphologies for TM4 cells (refer to [Figures 3.19](#) and [3.20](#)).

### 3.3 TMRE assay

Mitochondria play an essential role in cellular metabolism. They maintain a membrane potential that affects (and is affected by) ATP production, as well as cellular  $\text{Ca}^{2+}$  levels. Furthermore, mitochondria are known to produce much of the ROS in cells, play a key role in the intrinsic pathway of apoptosis and they are the site for the first step in steroidogenesis (i.e. the conversion of cholesterol to pregnenolone). All of these traits are related to the mitochondrial membrane potential ( $\Delta\Psi_m$ ), and a change in  $\Delta\Psi_m$  can be a good indicator of cellular pathology. Appropriate fluorophores, like TMRE (tetramethylrhodamine, ethyl ester) can label active mitochondria and hence indicate the health/metabolic status of the cells being examined.

The TMRE probe was used to label active mitochondria and their fluorescence was determined by microplate reader. In order to minimise background fluorescence, black 96 well plates were employed in this study. However, the black plates meant that cell attachment and retention in the wells, at assay time, could not be confirmed by microscope. Consequently, the cells were co-labelled with Hoechst, a membrane permeable fluorescent probe that binds to nuclear material. The Hoechst readings were used to give an indication of cell concentration in each well and were also used to normalise the TMRE readings.



UNIVERSITY of the  
WESTERN CAPE



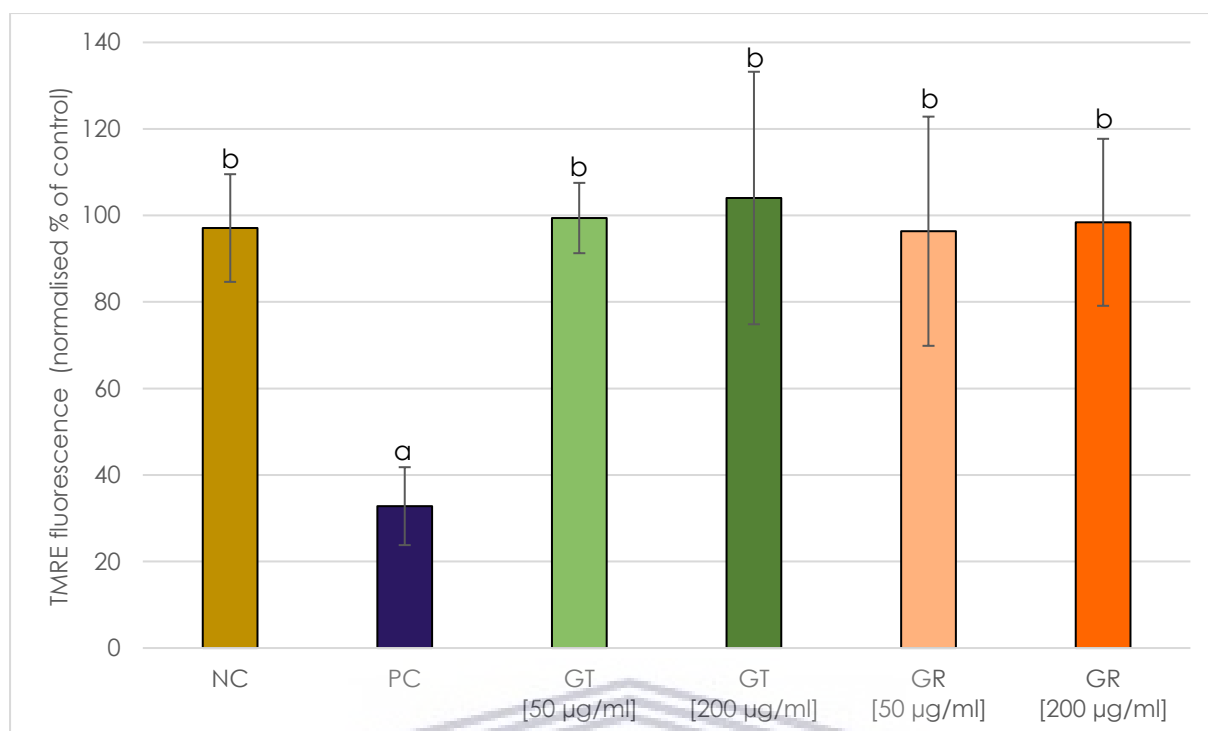


**Figure 3.21. Graph showing the effects of green tea and green rooibos on the mitochondrial membrane potential of TM3 cells.** The cells were treated for 24 hours with either media, reconstituted green tea or reconstituted green rooibos, or for 60 minutes with CCCP. Thereafter the cells were labelled with Hoechst and TMRE; the results here were calculated by dividing the TMRE readings by the Hoechst readings, after subtracting the respective blank readings. Finally, the percentage TMRE fluorescence was calculated on the assumption that the **NC** treatment produced 100 % fluorescence. **NC**: negative control (i.e. complete medium), **PC**: depolarization positive control (i.e. 20 µM CCCP), **GT**: green tea, **GR**: green rooibos. Data are represented as means ± standard deviations. A P value of less than 0.05 was considered significant; a: significantly different to **NC**, b: significantly different to **PC**; c: significantly different to higher/lower concentration of the same treatment; n ≤ 9.

Neither green tea nor green rooibos (at either 50 µg/ml or 200 µg/ml) produced any significant effects on TM3 cell  $\Delta\Psi_m$  compared to the negative control after 24 hours; refer to Figure 3.21. Nonetheless, a one hour exposure to 20 µM of CCCP (carbonyl cyanide 3-chlorophenylhydrazone, i.e. the positive control) produced 32.8 % ± 9 % of the normalised TMRE fluorescence that the media control gave; this was significantly lower ( $P < 0.05$ ) than all other treatments tested. Furthermore, no significant differences were noted when comparing the green tea samples with each other and when comparing the green rooibos samples with each other (i.e. 50 µg/ml vs. 200 µg/ml).

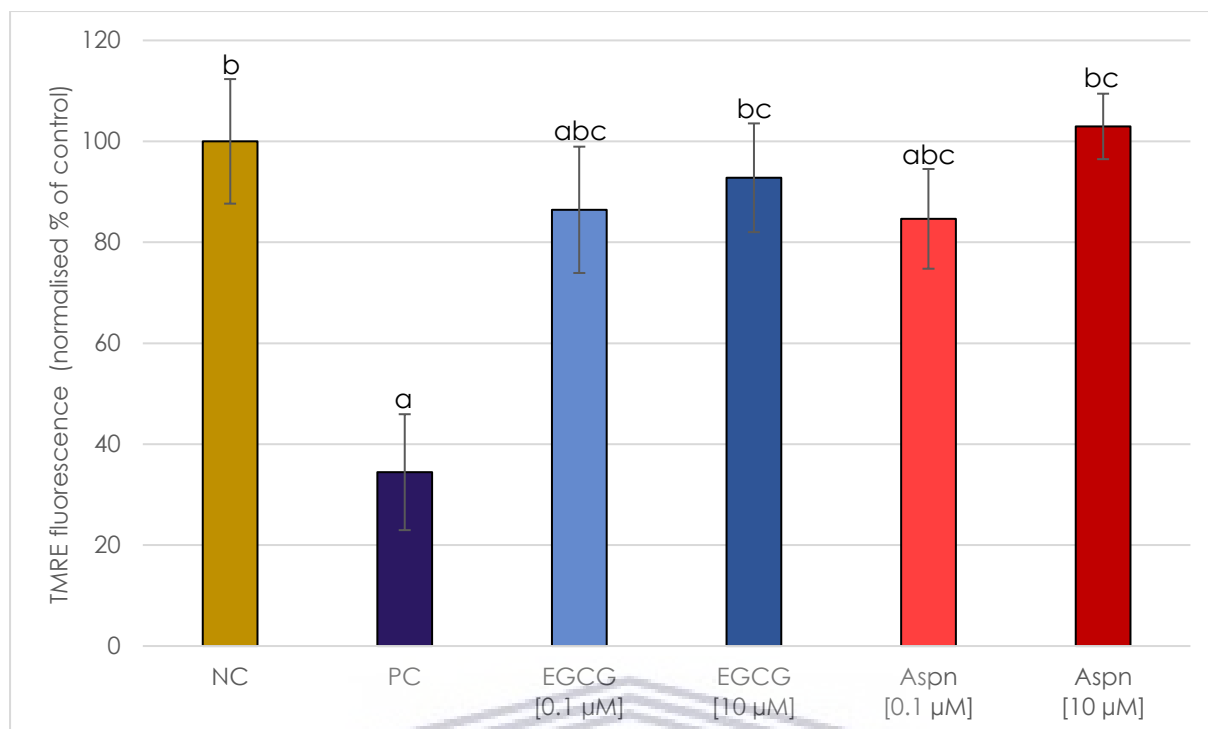


**Figure 3.22. Graph showing the effects of EGCG and aspalathin on the mitochondrial membrane potential of TM3 cells.** The cells were treated for 24 hours with either the vehicle treatment, EGCG (and 0.5 % DMSO) or aspalathin (and 0.5 % DMSO), or for 60 minutes with CCCP. Thereafter the cells were labelled with Hoechst and TMRE; the results here were calculated by dividing the TMRE readings by the Hoechst readings, after subtracting the respective blank readings. Finally, the percentage TMRE fluorescence was calculated on the assumption that the **NC** treatment produced 100 % fluorescence. **NC**: negative control (i.e. 0.5 % DMSO), **PC**: depolarization positive control (i.e. 20 µM CCCP), **Aspn**: aspalathin. Data are represented as means ± standard deviations. A P value of less than 0.05 was considered significant; a: significantly different to **NC**, b: significantly different to **PC**, c: significantly different to higher/lower concentration of the same treatment; n ≤ 9.

In [Figure 3.22](#), one sees that once more, all samples tested produced significantly higher ( $P < 0.05$ ) fluorescence in the TM3 cells than in the positive control-treated cells (i.e. carbonyl cyanide 3-chlorophenylhydrazone: CCCP), which only showed 34.5 % ± 11.5 % of the fluorescence that the vehicle control gave. The high concentrations (i.e. 10 µM) of both EGCG and aspalathin, showed no significant differences to the negative control, with 92.8 % ± 10.8 % and 103 % ± 6.5 % the fluorescence of the negative control. However, 0.1 µM EGCG and 0.1 µM aspalathin both produced significantly lower ( $P < 0.05$ ) fluorescence than the negative control did, at 86.4 % ± 12.5 % and 84.6 % ± 9.9 % that of the negative control respectively. These results were also significantly different ( $P < 0.05$ ) to that of their respective high concentration treatments.

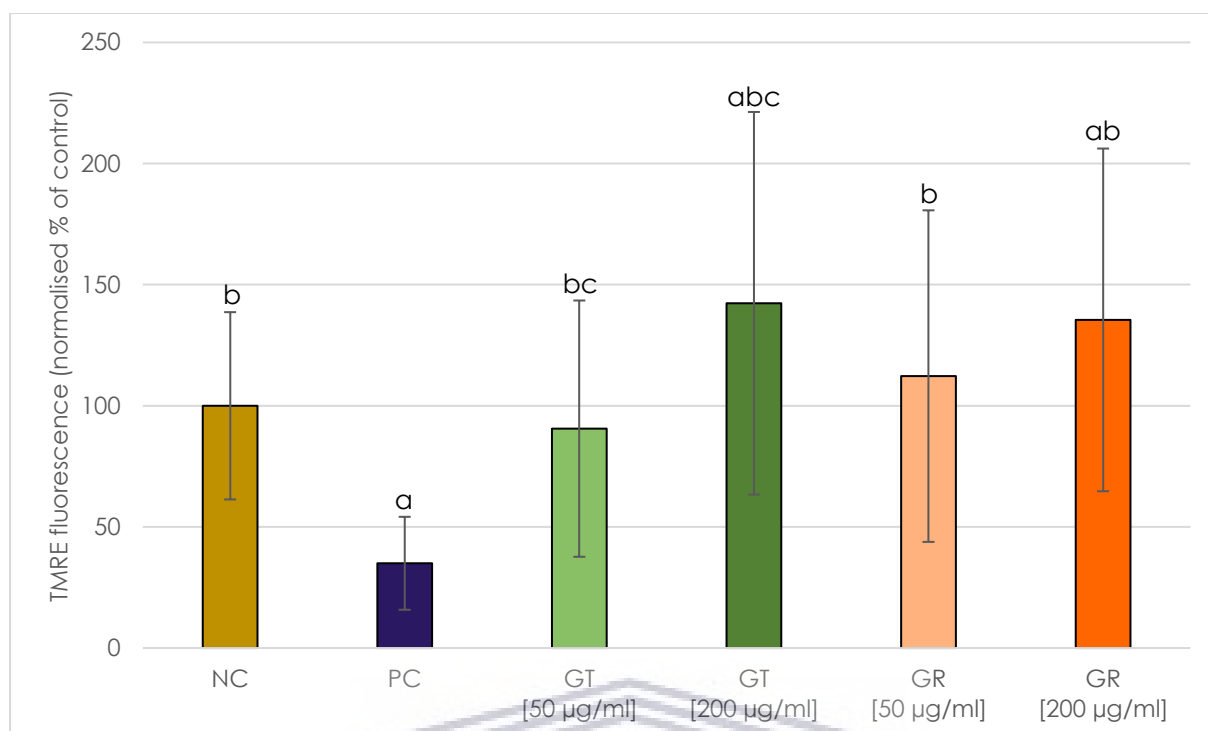


**Figure 3.23. Graph showing the effects of green tea and green rooibos on the mitochondrial membrane potential of TM4 cells.** The cells were treated for 24 hours with either media, reconstituted green tea or reconstituted green rooibos, or for 60 minutes with CCCP. Thereafter the cells were labelled with Hoechst and TMRE; the results here were calculated by dividing the TMRE readings by the Hoechst readings, after subtracting the respective blank readings. Finally, the percentage TMRE fluorescence was calculated on the assumption that the **NC** treatment produced 100 % fluorescence. **NC**: negative control (i.e. complete medium), **PC**: depolarization positive control (i.e. 20 µM CCCP), **GT**: green tea, **GR**: green rooibos. Data are represented as means  $\pm$  standard deviations. A P value of less than 0.05 was considered significant; a: significantly different to **NC**, b: significantly different to **PC**, c: significantly different to higher/lower concentration of the same treatment;  $n \leq 18$ .

Figure 3.23 shows that TM4 cells treated with 20 µM of CCCP (i.e. positive control) gave normalised TMRE fluorescence at 35 %  $\pm$  19.2 % of the negative control, which was a significant reduction ( $P < 0.05$ ) compared to all other treatments tested. Nonetheless, the high concentrations of green tea and green rooibos (i.e. 200 µg/ml) produced significantly more fluorescence ( $P < 0.05$ ) than the negative control did, at 142.3 %  $\pm$  79 % and 135.5 %  $\pm$  70.7 % respectively. Furthermore, there was a significant difference ( $P < 0.05$ ) between the results from the two green tea samples (i.e. 50 µg/ml vs. 200 µg/ml), but not the green rooibos samples.

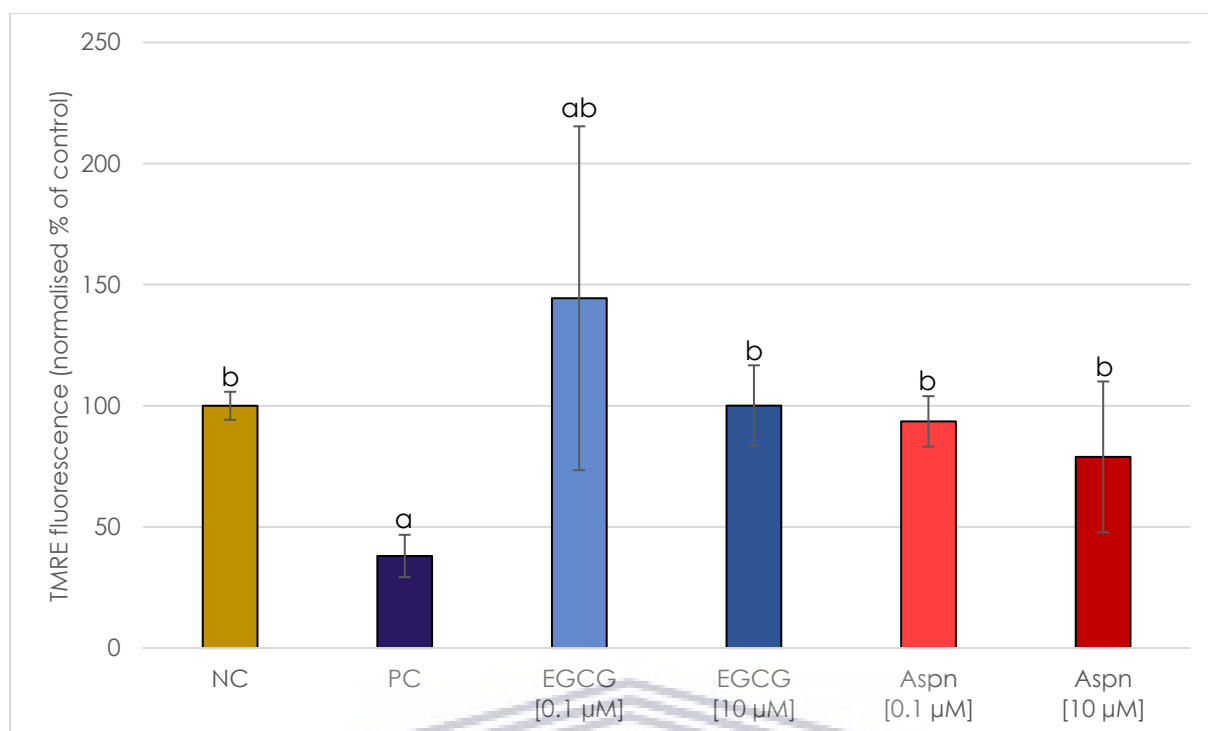


**Figure 3.24. Graph showing the effects of EGCG and aspalathin on the mitochondrial membrane potential of TM4 cells.** The cells were treated for 24 hours with either the vehicle treatment, EGCG (and 0.5 % DMSO) or aspalathin (and 0.5 % DMSO), or for 60 minutes with CCCP. Thereafter the cells were labelled with Hoechst and TMRE; the results here were calculated by dividing the TMRE readings by the Hoechst readings, after subtracting the respective blank readings. Finally, the percentage TMRE fluorescence was calculated on the assumption that the **NC** treatment produced 100 % fluorescence. **NC**: negative control (i.e. 0.5 % DMSO), **PC**: depolarization positive control (i.e. 20 µM CCCP), **Aspnr**: aspalathin. Data are represented as means ± standard deviations. A P value of less than 0.05 was considered significant; a: significantly different to **NC**, b: significantly different to **PC**; c: significantly different to higher/lower concentration of the same treatment;  $n \leq 11$ .

The negative control TM4 cells gave significantly more fluorescence ( $P < 0.05$ ) than the positive control-treated cells did (38 % ± 8.8 % of the negative control; see Figure 3.24). The low EGCG treatment (i.e. 0.1 µM) produced normalised TMRE fluorescence at 144.4 % ± 71 % that of the negative control, which was significantly higher ( $P < 0.05$ ) than all other treatments tested. No significant differences were observed between either of the aspalathin treatments or the 10 µM EGCG treatment and the negative control. There was also no significant difference between the same flavonoid samples (i.e. 0.1 µM vs. 10 µM).

### 3.4 CM-H<sub>2</sub>DCFDA assays

Reactive oxygen species can be either harmful or beneficial to cells. At high concentrations, they can cause lipid peroxidation and oxidative stress. However at low concentration, they may well function in cell signalling. Thus the cellular levels of ROS are deterministic with regards to cell health. Hence, examining cellular ROS levels provides important information about the wellbeing of a cell population.

#### 3.4.1 CM-H<sub>2</sub>DCFDA assay by flow cytometry

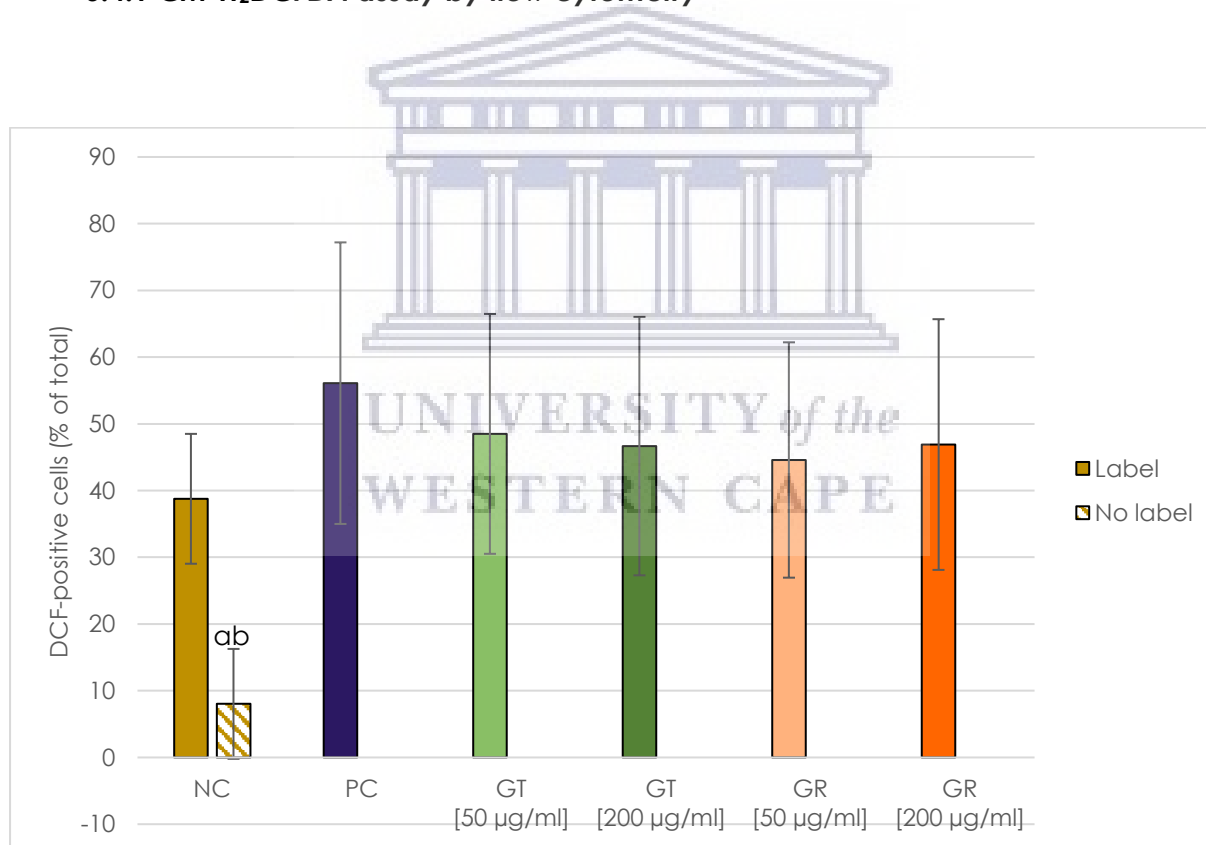


**Figure 3.25. Graph showing the effects of green tea and green rooibos on TM3 cell intracellular ROS, as determined by flow cytometry.** The cells were treated for 24 hours with either a control, reconstituted green tea or reconstituted green rooibos. **NC**: negative control (i.e. complete medium), **PC**: ROS positive control (i.e. 100 µM H<sub>2</sub>O<sub>2</sub>), **GT**: green tea; **GR**: green rooibos, **Label**: cells were labelled with CM-H<sub>2</sub>DCFDA, **No label**: cells were not exposed to CM-H<sub>2</sub>DCFDA. Data are represented as means ± standard deviations. A P value of less than 0.05 was considered significant; a: significantly different to **NC** (with **Label**), b: significantly different to **PC**; n = 6.

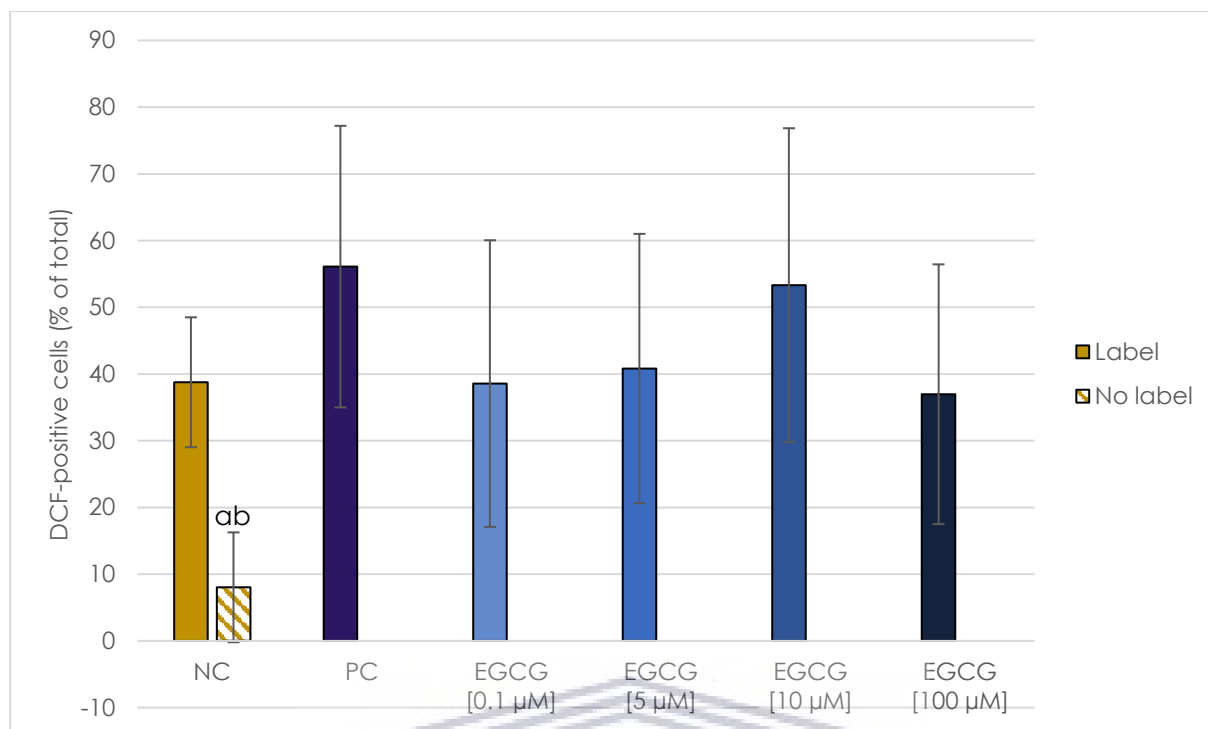


**Figure 3.26. Graph showing the effects of EGCG on TM3 cell intracellular ROS, as determined by flow cytometry.** The cells were treated for 24 hours with either a control or EGCG at the concentrations indicated. **NC**: negative control (i.e. 0.5 % DMSO), **PC**: ROS positive control (i.e. 100 µM H<sub>2</sub>O<sub>2</sub>), **Label**: cells were labelled with CM-H<sub>2</sub>DCFDA, **No label**: cells were not exposed to CM-H<sub>2</sub>DCFDA. Data are represented as means ± standard deviations. A P value of less than 0.05 was considered significant; a: significantly different **NC** (with **Label**), b: significantly different to **PC**; n = 6.

When TM3 cells were assayed for ROS levels by flow cytometry, there were no significant differences noted between any of the treatments and either the positive control (100 µM H<sub>2</sub>O<sub>2</sub>) or the labelled negative control (Figures 3.25, 3.26 and 3.27). This might be due to the high variance between individual measurements. Furthermore, the positive control also did not show significant difference to the labelled negative control. However, both the positive control and the labelled negative control were significantly different to the blank (unlabelled) negative control sample.

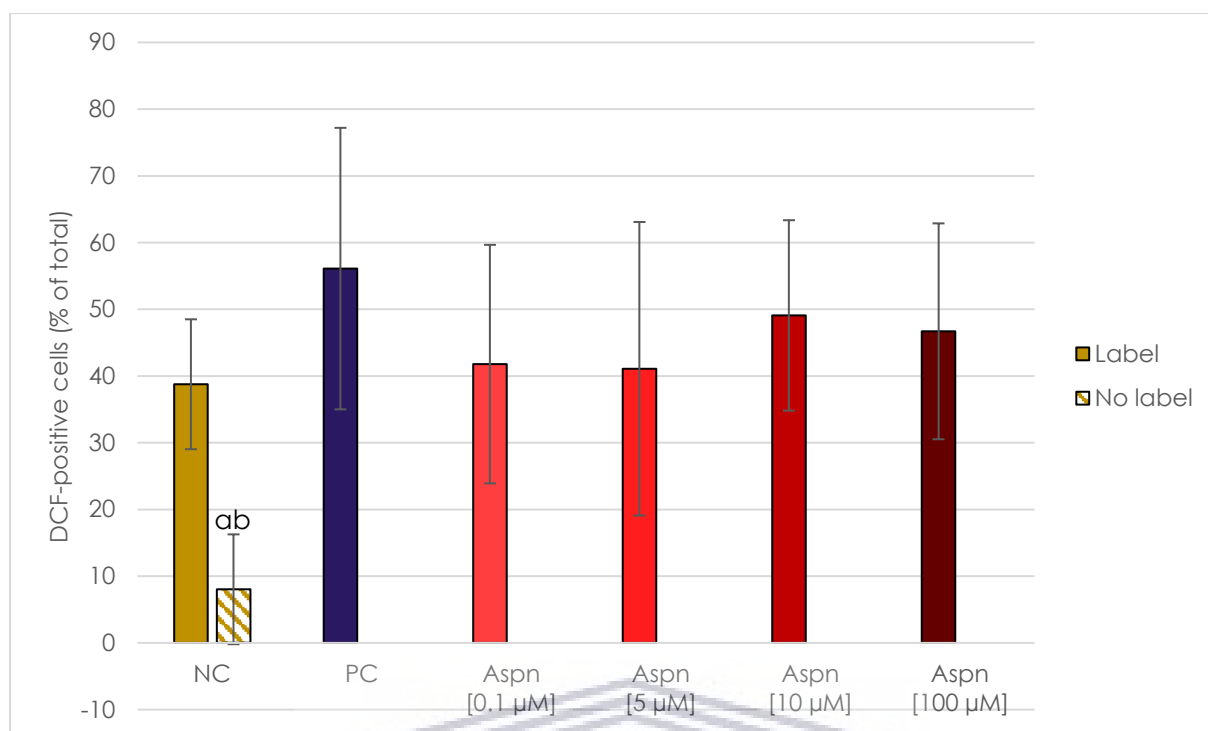


**Figure 3.27. Graph showing the effects of aspalathin on TM3 cell intracellular ROS, as determined by flow cytometry.** The cells were treated for 24 hours with either a control or aspalathin at the concentrations indicated. **NC**: negative control (i.e. 0.5 % DMSO), **PC**: ROS positive control (i.e. 100 µM H<sub>2</sub>O<sub>2</sub>), **Aspn**: aspalathin, **Label**: cells were labelled with CM-H<sub>2</sub>DCFDA, **No label**: cells were not exposed to CM-H<sub>2</sub>DCFDA. Data are represented as means ± standard deviations. A P value of less than 0.05 was considered significant; a: significantly different to **NC** (with **Label**), b: significantly different to **PC**; n = 6.

UNIVERSITY of the  
WESTERN CAPE

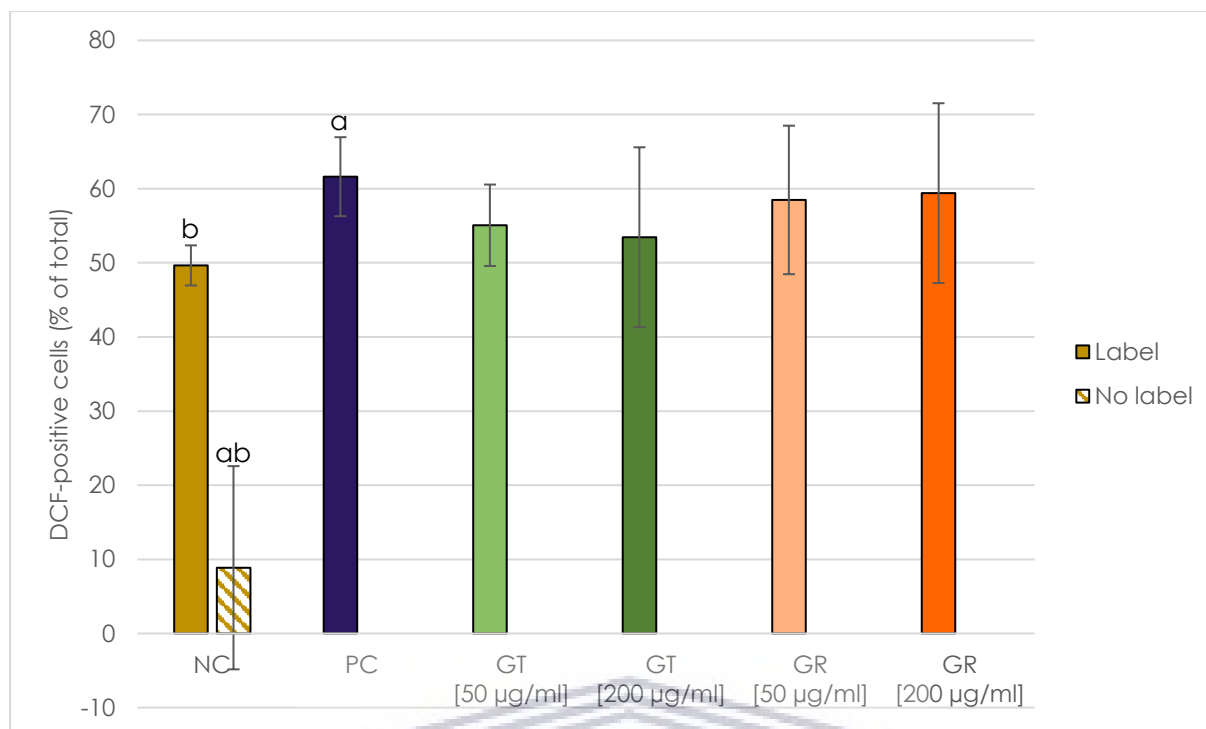


**Figure 3.28. Graph showing the effects of green tea and green rooibos on TM4 cell intracellular ROS, as determined by flow cytometry.** The cells were treated for 24 hours with either a control, reconstituted green tea or reconstituted green rooibos. **NC**: negative control (i.e. complete medium), **PC**: ROS positive control (i.e. 100 µM H<sub>2</sub>O<sub>2</sub>), **GT**: green tea; **GR**: green rooibos, **Label**: cells were labelled with CM-H<sub>2</sub>DCFDA, **No label**: cells were not exposed to CM-H<sub>2</sub>DCFDA. Data are represented as means ± standard deviations. A P value of less than 0.05 was considered significant; a: significantly different to **NC** (with **Label**), b: significantly different to **PC**; n = 6.

When the TM4 cells were assayed for ROS by flow cytometry, the labelled negative control and the positive control showed significantly different ROS levels (Figures 3.28 and 3.29), demonstrating the validity of this assay. Furthermore, both of these controls (the labelled negative control and the positive control) showed significantly higher incidences of ROS-positive cells than the unlabelled negative control (i.e. the blank). Both green tea and green rooibos at 50 µg/ml were no different, statistically, to either the positive control or the negative control (Figure 3.28).



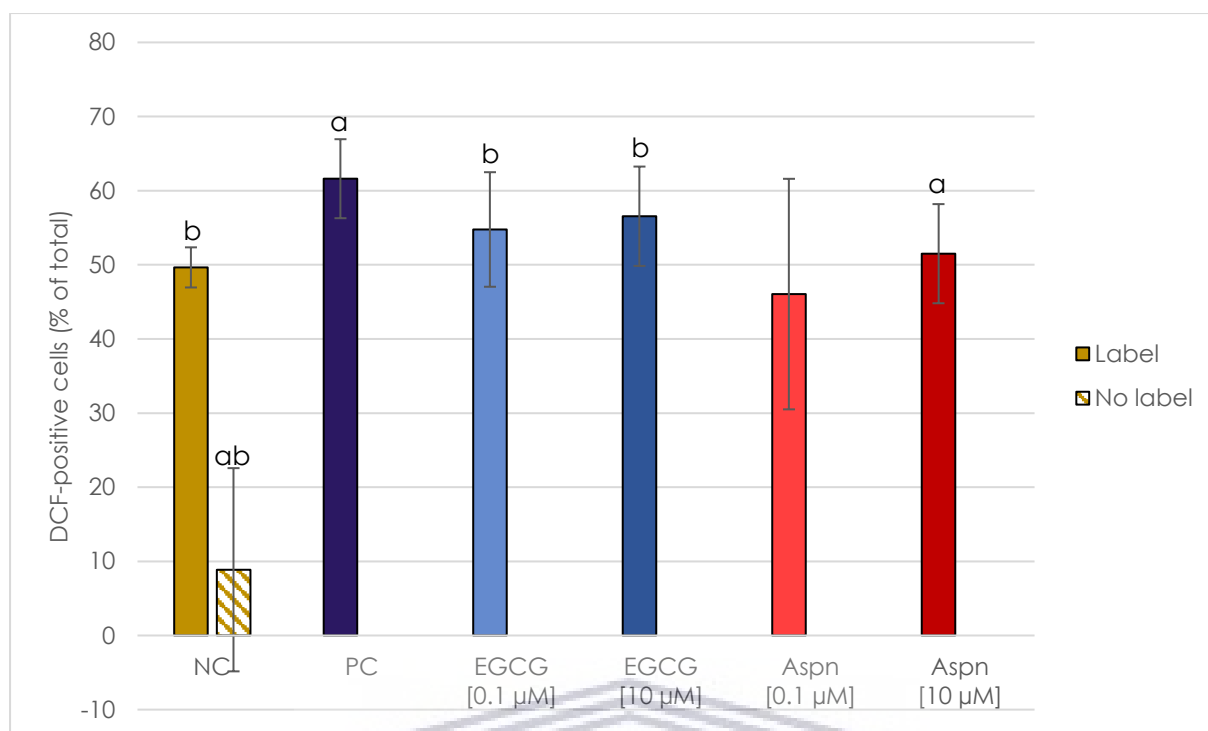


**Figure 3.29. Graph showing the effects of EGCG and aspalathin on TM4 cell intracellular ROS, as determined by flow cytometry.** The cells were treated for 24 hours with either a control, EGCG or aspalathin at the concentrations indicated. **NC**: negative control (i.e. 0.5 % DMSO), **PC**: ROS positive control (i.e. 100  $\mu\text{M}$   $\text{H}_2\text{O}_2$ ), **Aspn**: aspalathin, **Label**: cells were labelled with CM- $\text{H}_2\text{DCFDA}$ , **No label**: cells were not exposed to CM- $\text{H}_2\text{DCFDA}$ . Data are represented as means  $\pm$  standard deviations. A P value of less than 0.05 was considered significant; a: significantly different to **NC** (with **Label**), b: significantly different to **PC**; n = 6.

According to Figure 3.29, the EGCG treatments at either 0.1  $\mu\text{M}$  or 10  $\mu\text{M}$  caused significantly lower ROS levels than the positive control, but was no different to the negative control. Furthermore, the aspalathin treatment at 10  $\mu\text{M}$  caused a significant increase in TM4 ROS levels compared with the negative control.

### 3.4.2 CM-H<sub>2</sub>DCFDA assay trial by plate reader

Due to the failure of the flow cytometry-based ROS assay to produce significant differences between the negative and positive controls in TM3 cells (Figures 3.25, 3.26 and 3.27), a set of trials were performed to determine the optimal label and positive control concentrations to use by microplate reader. There was much variation in the results from the trials with CM-H<sub>2</sub>DCFDA and H<sub>2</sub>O<sub>2</sub> on TM3 cells, see Figure 3.30. There were no trends noted with regards to DCF fluorescence and the H<sub>2</sub>O<sub>2</sub> concentration when labelled with either 10  $\mu$ M or 20  $\mu$ M of CM-D<sub>2</sub>DCFDA.

Once more, when one looks at an individual trial experiment for ROS by microplate reader, one sees a lot of variation in the cell populations that were assayed (Figure 3.31). Looking at Figure 3.31-A, one sees that most of the treatments produced DCF fluorescence within the same range as the blank wells did. The Hoechst fluorescence of most treatment groups were also similar to those of the blanks (Figure 3.31-B).

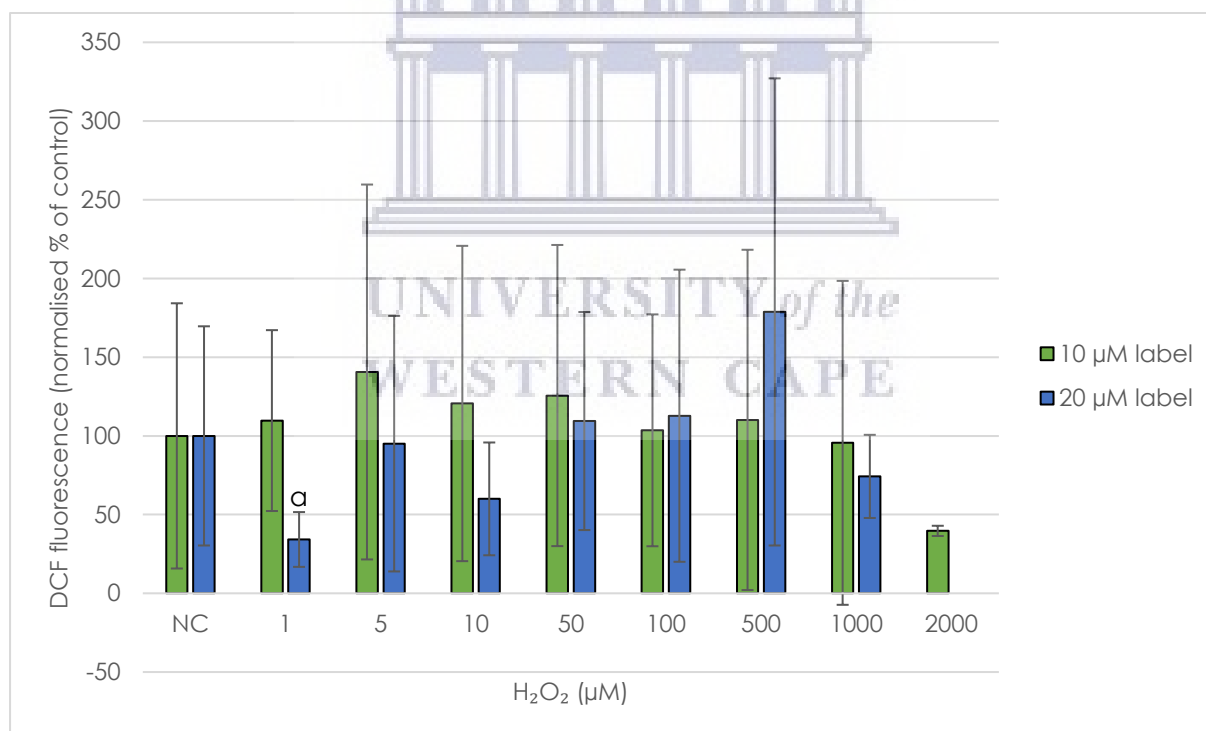


**Figure 3.30.** Graph showing an overview of results from the TM3 cell trials for ROS determination by microplate reader. The cells were treated for 24 hours with varying concentrations of H<sub>2</sub>O<sub>2</sub> and then labelled with Hoechst and CM-H<sub>2</sub>DCFDA, as indicated. The results were calculated by dividing the DCF readings by the Hoechst readings, after subtracting the respective blank readings. The percentage DCF fluorescence was calculated on the assumption that the **NC** treatment produced 100 % fluorescence. **NC:** negative control (i.e. complete medium), **Label:** CM-H<sub>2</sub>DCFDA. Data are shown as means  $\pm$  standard deviations. A P value of less than 0.05 was considered significant; a: significantly different to **NC**; n  $\leq$  6.

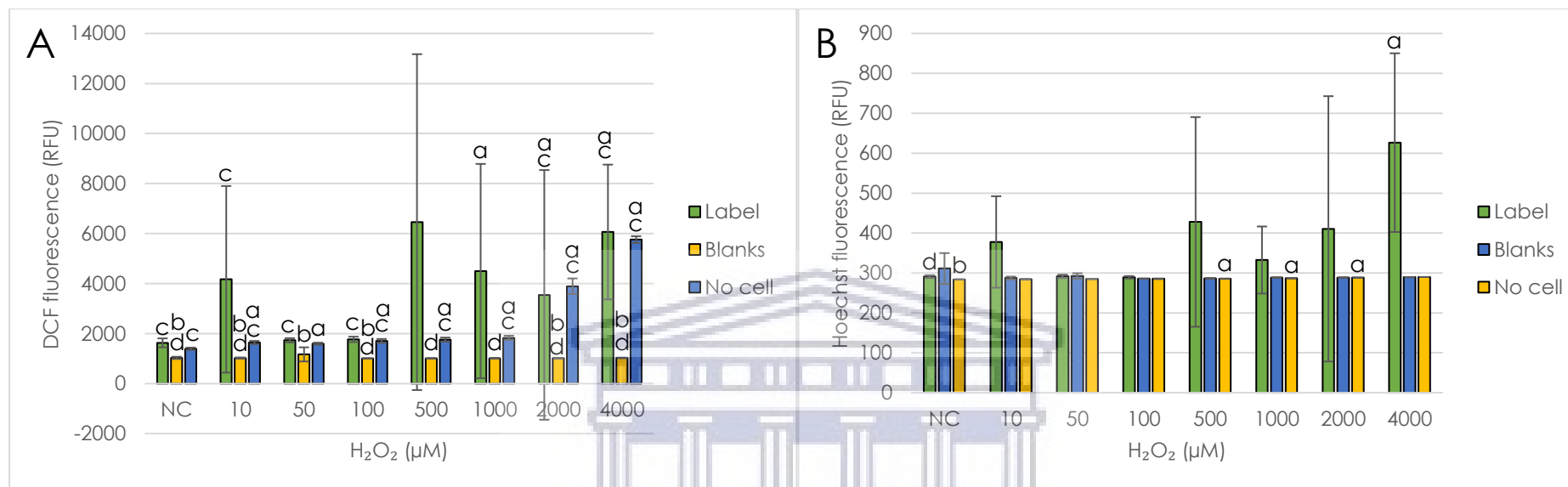


**Figure 3.31. Representative graphs from the trial ROS assay by microplate reader.** **A:** the DCF fluorescence data; **B:** the Hoechst fluorescence data. The cells were treated for 24 hours with varying concentrations of H<sub>2</sub>O<sub>2</sub>. Thereafter the cells were labelled with Hoechst and 30 μM CM-H<sub>2</sub>DCFDA. **NC:** negative control (i.e. complete medium), **Label:** cells were labelled as described, **Blanks:** cells were not exposed to any fluorophores, **No cell:** wells without cells were treated as though they had cells, and were labelled accordingly. Data are represented as means ± standard deviations. A P value of less than 0.05 was considered significant; a: significantly different to corresponding **NC**, b: significantly different to corresponding **Label**, c: significantly different to corresponding **Blank**, d: significantly different to corresponding **No cell**; n = 8.

### 3.5 Leydig cell testosterone secretion experiments

The primary function of Leydig cells is to synthesize and secrete testosterone. This makes testosterone production a good target for assessing any effects substances have on Leydig cells. Furthermore, testosterone is essential for the function of the male reproductive system; making its assessment all the more necessary when evaluating male reproductive toxicology. Lastly, the use of model Leydig cells provide great convenience to researchers for testing these ends, assuming they actually produce testosterone.

As mentioned in [Chapter 1](#), there are studies that have successfully used TM3 cells to test how substances affect testosterone synthesis. These include studies from our very lab, showing that the earlier passages of the TM3 cells used in this thesis did secrete testosterone in response to hCG in the past. This is why TM3 cells were chosen for this study.



UNIVERSITY *of the*  
WESTERN CAPE

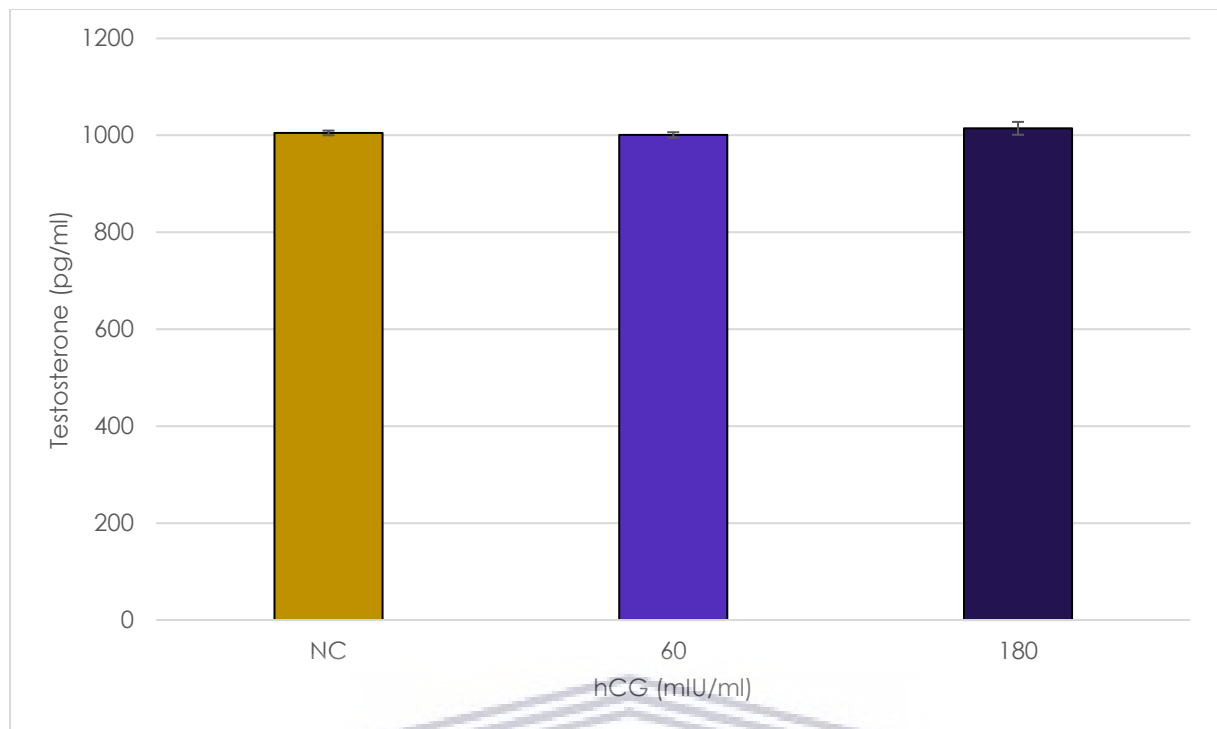


**Figure 3.32. Graph showing the levels of TM3 cell testosterone secretion after 48 hours with complete medium.** The cells were exposed to the indicated hCG levels for 48 hours. **NC:** negative control (i.e. complete medium). Data are represented as means  $\pm$  standard deviations;  $n \leq 3$ .

Some experiments were carried out to establish which concentrations of hCG to use as a positive control for stimulated testosterone production by the TM3 Leydig cells. The results from the first experiment are shown in Figure 3.32. Here one sees that after 48 hours of exposure to hCG at either 60 mIU/ml or 180 mIU/ml, there was no noticeable differences in testosterone levels from TM3 cells. Additionally, the testosterone levels produced were well within the optimal detection range of the ELISA used.

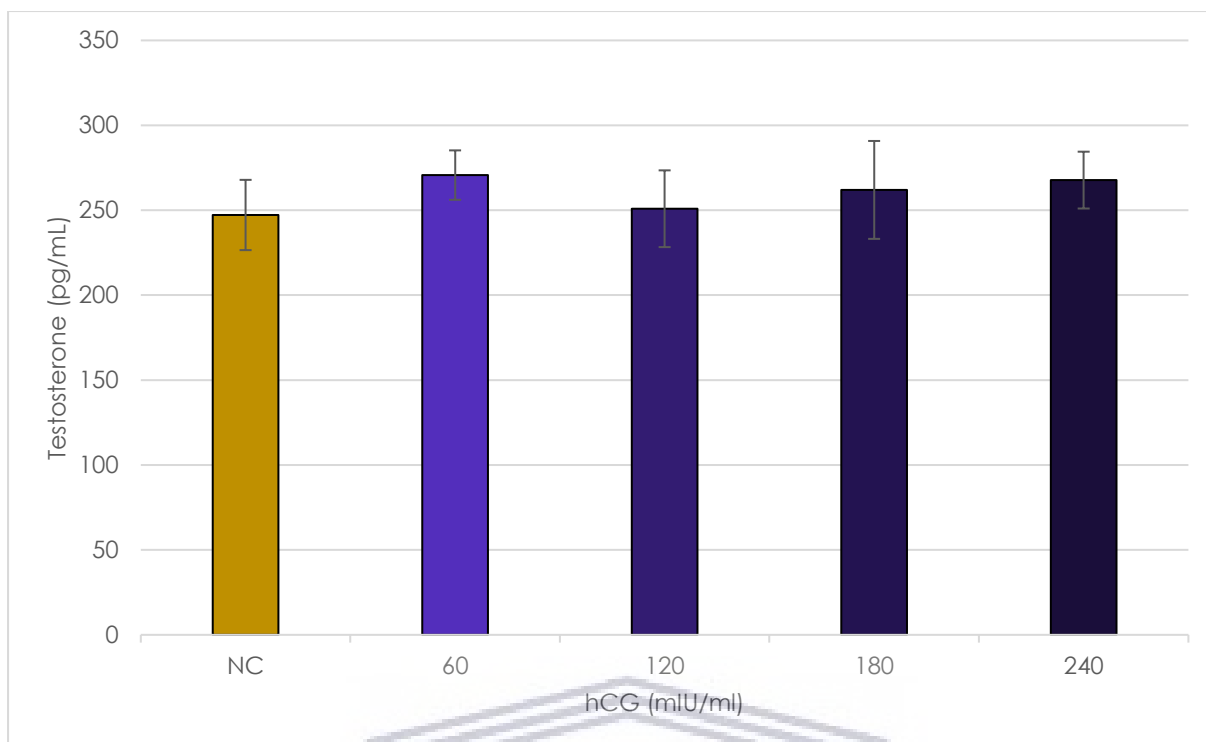


**Figure 3.33.** Graph showing the levels of TM3 cell testosterone secretion after 24 hours with complete medium. The cells were exposed to the indicated hCG levels for 24 hours. **NC:** negative control (i.e. complete medium). Data are represented as means  $\pm$  standard deviations;  $n \leq 4$ .

The second experiment for hCG-stimulated testosterone secretion by TM3 cells was performed for 24 hours (Figure 3.33). Once more, one sees that TM3 cells showed no change in testosterone secretion when exposed to hCG at either 60, 120, 180 or 240 mIU/ml.

Due to the lack of response to hCG, a third experiment was carried out, in which the cells were exposed to hCG without sera for 48 hours. However, the cells were first weaned off the sera for two days before exposing them to the hCG. Figure 3.34 shows the results from the third experiment.

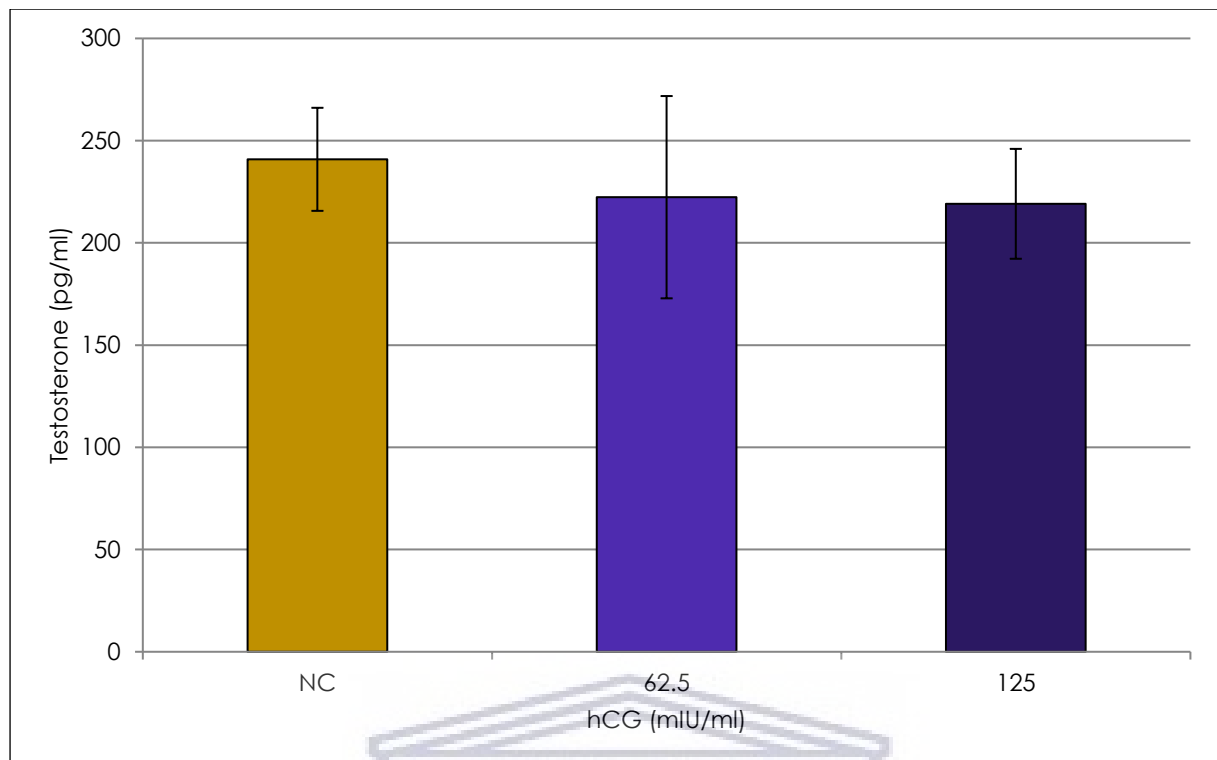


**Figure 3.34.** Graph showing the levels of TM3 cell testosterone secretion in the absence of sera. The TM3 cells were exposed to the indicated hCG levels for 48 hours in the absence of any sera. **NC:** negative control (i.e. complete medium). Data are represented as means  $\pm$  standard deviations;  $n \leq 4$ .

The third experiment showed that culturing the cells with no sera and hCG at 62.5 mIU/ml or 125 mIU/ml produced no noteworthy difference in testosterone levels compared to the negative control (0 mIU/ml; see [Figure 3.34](#)). Furthermore, the testosterone levels detected were near the minimum detection limit of the ELISA used (200 pg/ml).

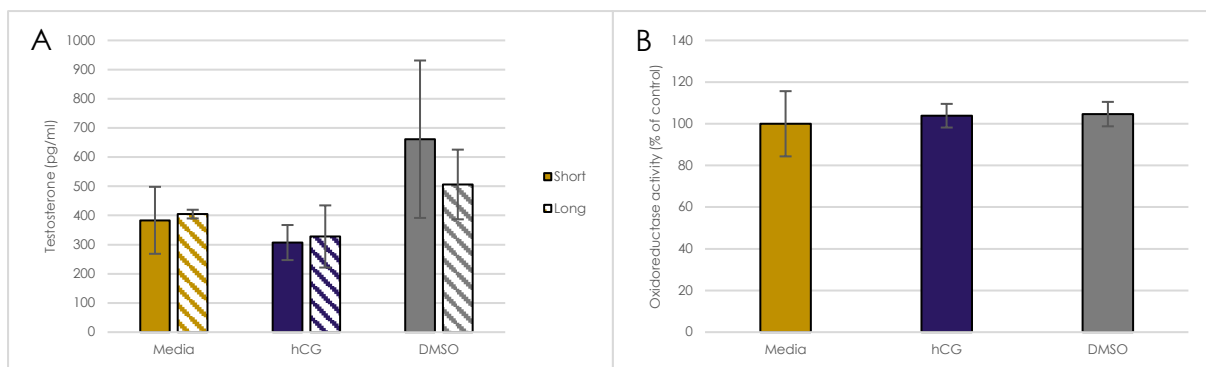


**Figure 3.35. Graphs showing the results from the experiment with the crude boar testes extracts. A:** Testosterone results; **B:** MTT results for the cells that received the long digestion. The cells were extracted by enzymatic digestion using two different digestion periods. Thereafter they were exposed to either media only, hCG or to DMSO for 24 hours. The % oxidoreductase activity was calculated under the assumption that the **Media** treatment produced 100 % activity. **Media:** 0 mIU/ml hCG (i.e. complete medium only); **hCG:** 125 mIU/ml hCG; **DMSO:** 10 % DMSO; **Short:** 20 minute digestion; **Long:** 30 minute digestion. Data are represented as means  $\pm$  standard deviations; n = 8.

A primary crude testis extract from a mature boar was performed in order to determine whether those cultures would provide a better model than TM3 cells for stimulated testosterone production. The crude testis extract was performed using an enzymatic digestion of the testis tissue for two different periods (20 minutes and 30 minutes).

One can see in [Figure 3.35-A](#), that the hCG treatments showed slightly lower testosterone levels than the untreated cells, irrespective of the digestion period used. On the other hand, the DMSO treatment produced the highest testosterone concentrations. Furthermore, the two digestion periods used produced similar testosterone levels.

The MTT data for the tissue that received the longer digestion shows that there was no real difference between the oxidoreductase activities of the untreated, hCG-treated or DMSO-treated cells ([Figure 3.35-B](#)).



## 3.6 AGE results from PCRs for steroidogenic gene expression

### 3.6.1 Conventional PCR AGE results

In order to assess the potential effects of EGCG and aspalathin on the expression of select steroidogenic genes, a set of conventional PCRs were carried out on cDNA from TM3 cells. The first gene of interest (GOI) was the gene for receptor of LH/CG (*Lhcgr*), which stimulates testosterone production in normal Leydig cells. Proteins from the second and third GOIs play roles in controlling the rate-limiting step of steroidogenesis; these GOIs are *Star* and *Tspo*. The last three genes under study play direct roles in steroidogenesis and would give an indication of where along this pathway EGCG or aspalathin might affect steroidogenesis.

The housekeeping gene (*Gapdh*) showed bands at the 241 bp position in all of the cDNA samples tested, whilst the no template control (NTC) produced no bands (Figure 3.36-A). The densitometry data from the AGE for *Gapdh* reveals that *Gapdh* levels were similar amongst the treatments used. However, the presence of non-specific bands indicated that this primer design was not suitable for qPCR. The densitometry data from *Gapdh* was used to normalise the mRNA results from all subsequent conventional PCR experiments.

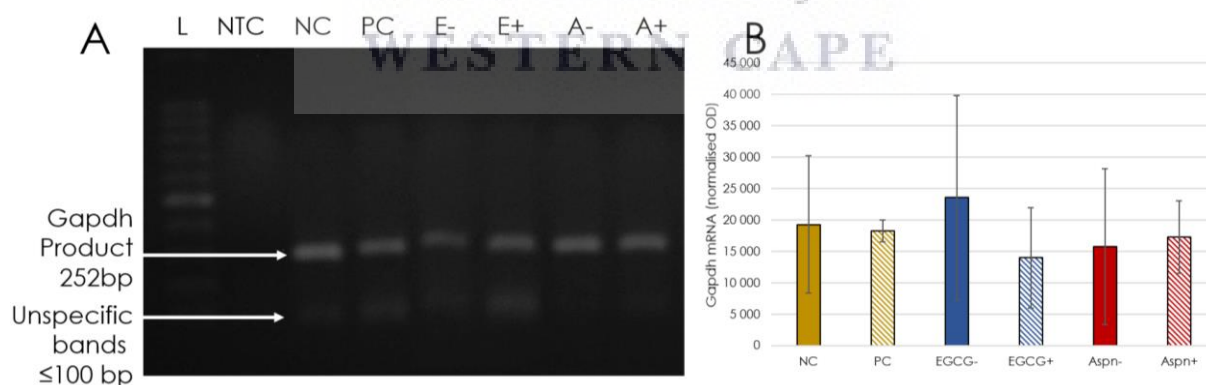


**Figure 3.36. Conventional PCR results for *Gapdh* gene expression.** **A:** Photograph showing a representative AGE result for *Gapdh*; **B:** Graph showing the average densitometry results from the *Gapdh* AGEs. TM3 cells were treated for 24 hours with either a control, 10  $\mu\text{M}$  of EGCG (and 0.5 % DMSO) in media or 10  $\mu\text{M}$  of aspalathin (and 0.5 % DMSO) in media, either with hCG at 125 mIU/ml or without hCG. Thereafter, mRNA was extracted, cDNA synthesized, followed by PCR and AGE. **L:** 100 bp DNA ladder; **NTC:** no template control; **NC:** negative control (i.e. 0.5 % DMSO); **PC:** positive control (i.e. 125 mIU/ml hCG); **E:** EGCG; **A, Apsn:** aspalathin; -: without hCG; +: with hCG. Data are represented as means  $\pm$  standard deviations; n = 2.

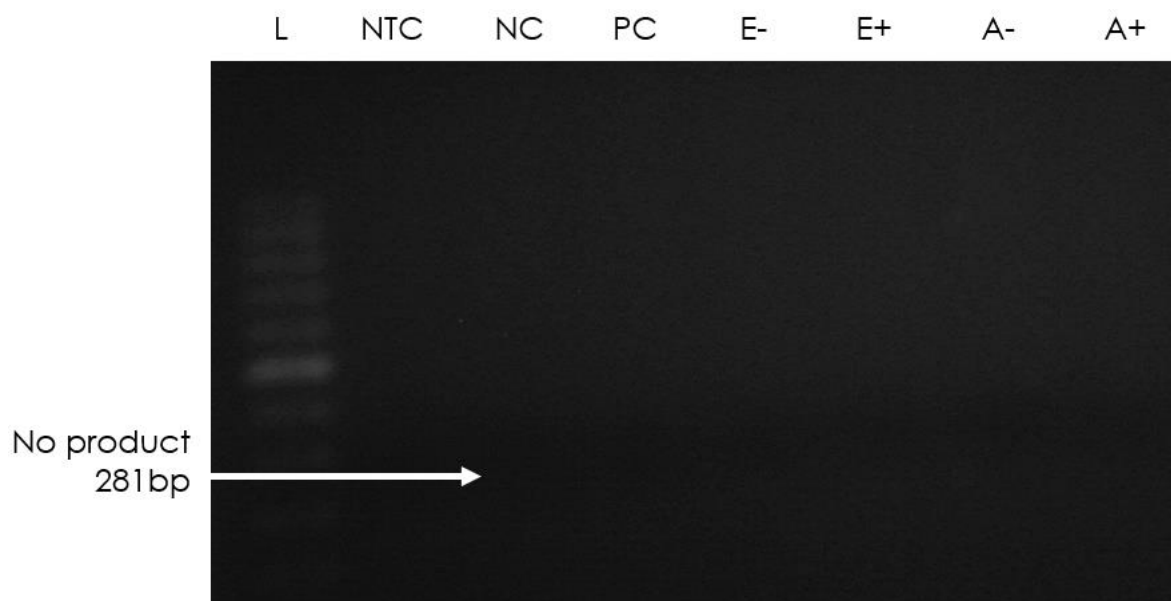


**Figure 3.37. Photograph showing the AGE results for *Lhcgr* gene expression.** TM3 cells were treated for 24 hours with either a control, 10  $\mu$ M of EGCG (and 0.5 % DMSO) in media or 10  $\mu$ M of aspalathin (and 0.5 % DMSO) in media, either with hCG at 125 mIU/ml or without hCG. Thereafter, mRNA was extracted, cDNA synthesized, followed by PCR and AGE. **L:** 100 bp DNA ladder; **NTC:** no template control; **NC:** negative control (i.e. 0.5 % DMSO); **PC:** positive control (i.e. 125 mIU/ml hCG); **E:** EGCG; **A:** aspalathin; **-:** without hCG; **+:** with hCG.

No bands were observed in any lanes after performing the PCR for *Lhcgr*, refer to [Figure 3.37](#). The expected product length was 281 bp. This experiment was repeated (from cell seeding to AGE) and never showed bands in the gels from any of its PCRs.

UNIVERSITY OF  
WESTERN CAPE

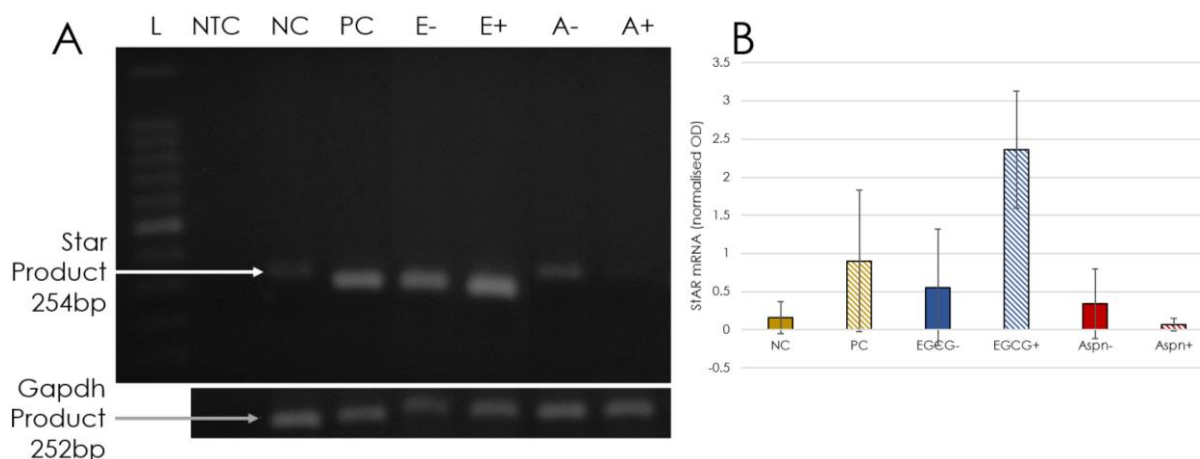


**Figure 3.38. Conventional PCR results for *Star* gene expression.** **A:** Photograph showing a representative AGE result for *Star*; **B:** Graph showing the average densitometry results from the *Star* AGEs. TM3 cells were treated for 24 hours with either a control, 10  $\mu$ M of EGCG (and 0.5 % DMSO) in media or 10  $\mu$ M of aspalathin (and 0.5 % DMSO) in media, either with hCG at 125 mIU/ml or without hCG. Thereafter, mRNA was extracted, cDNA synthesized, followed by PCR and AGE. **L:** 100 bp DNA ladder; **NTC:** no template control; **NC:** negative control (i.e. 0.5 % DMSO); **PC:** positive control (i.e. 125 mIU/ml hCG); **E:** EGCG; **A, Aspn:** aspalathin; -: without hCG; +: with hCG. Data are represented as means  $\pm$  standard deviations; n = 2.

The agarose gel for *Star* cDNA (in Figure 3.38-A) shows no bands in the NTC lane. All the other lanes showed bands at the 254 bp level, albeit at different intensities. The lane for the cells treated with aspalathin and hCG was the faintest, followed by the lane for negative control and the lane for aspalathin without hCG. These findings were confirmed when normalised by *Gapdh* (Figure 3.38-B). Additionally, the 10  $\mu$ M EGCG treatment with hCG showed the highest *Star* cDNA levels.

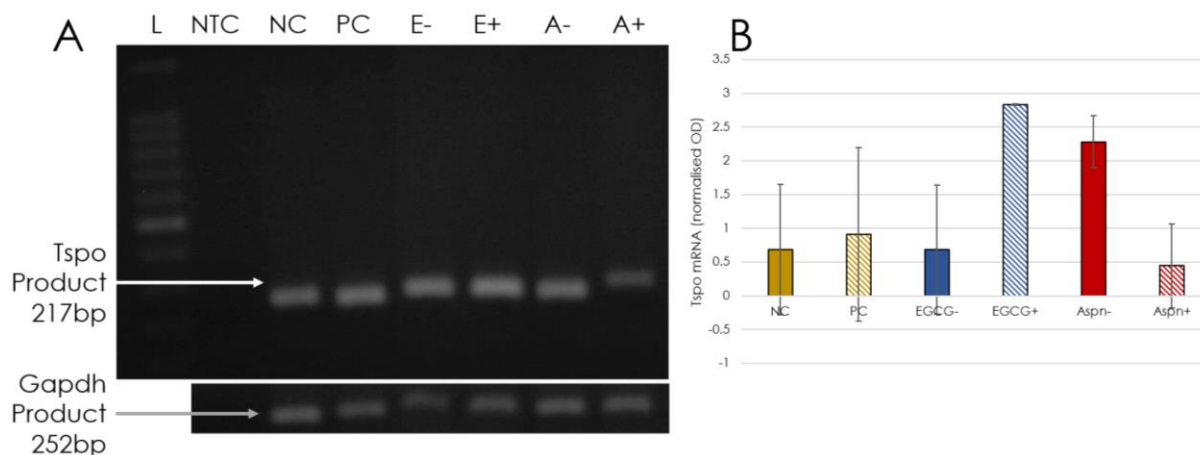


**Figure 3.39. Conventional PCR results for *Tspo* gene expression.** **A:** Photograph showing a representative AGE result for *Tspo*; **B:** Graph showing the average densitometry results from the *Tspo* AGEs. TM3 cells were treated for 24 hours with either a control, 10  $\mu$ M of EGCG (and 0.5 % DMSO) in media or 10  $\mu$ M of aspalathin (and 0.5 % DMSO) in media, either with hCG at 125 mIU/ml or without hCG. Thereafter, mRNA was extracted, cDNA synthesized, followed by PCR and AGE. **L:** 100 bp DNA ladder; **NTC:** no template control; **NC:** negative control (i.e. 0.5 % DMSO); **PC:** positive control (i.e. 125 mIU/ml hCG); **E:** EGCG; **A, Aspn:** aspalathin; -: without hCG; +: with hCG. Data are represented as means  $\pm$  standard deviations; n = 2.

All lanes that received cDNA showed bands at the 217 bp level when using the *Tspo* primer set (Figure 3.39-A). Additionally, the NTC lane showed no bands. Furthermore, all the bands were more or less of similar intensity with the exception of the lane for the cells treated with aspalathin and hCG. The normalised densitometry data show that the aspalathin treatment with hCG and the EGCG treatment without hCG showed the lowest *Tspo* mRNA levels amongst the assayed treatments. On other hand, the EGCG treatment with hCG and the aspalathin treatment without hCG showed the highest *Tspo* mRNA levels.

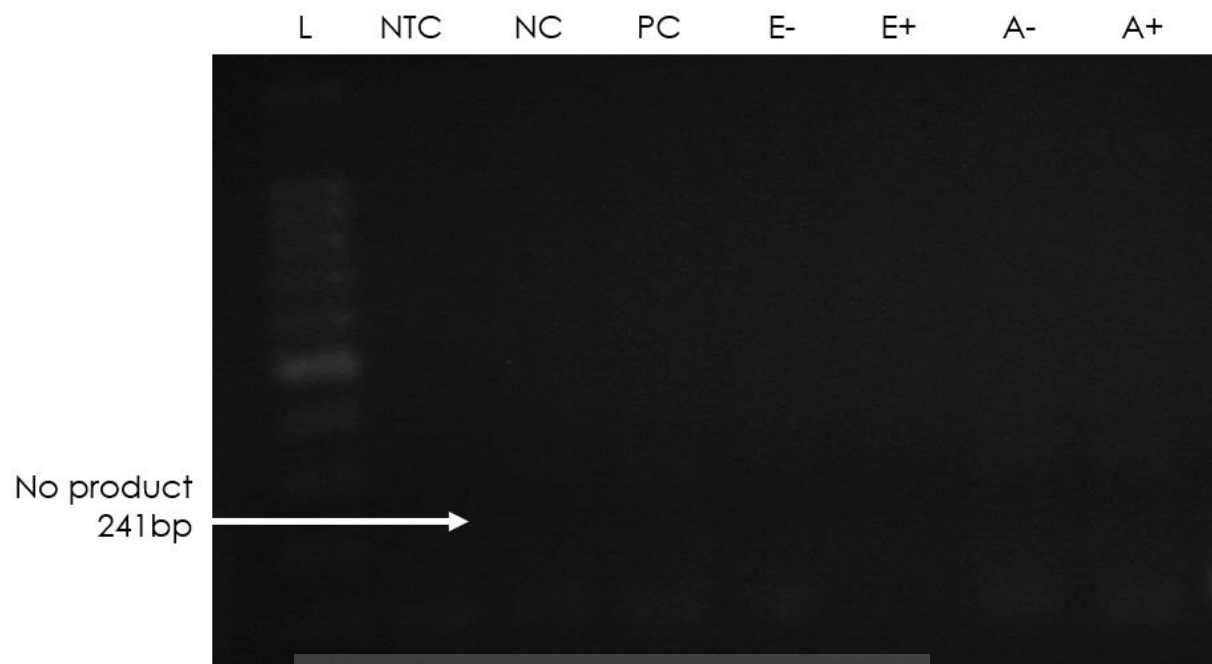


**Figure 3.40. Photograph showing the AGE results for *Cyp11a1* gene expression.** TM3 cells were treated for 24 hours with either a control, 10  $\mu$ M of EGCG (and 0.5 % DMSO) in media or 10  $\mu$ M of aspalathin (and 0.5 % DMSO) in media, either with hCG at 125 mIU/ml or without hCG. Thereafter, mRNA was extracted, cDNA synthesized, followed by PCR and AGE. **L:** 100 bp DNA ladder; **NTC:** no template control; **NC:** negative control (i.e. 0.5 % DMSO); **PC:** positive control (i.e. 125 mIU/ml hCG); **E:** EGCG; **A:** aspalathin; **-:** without hCG; **+:** with hCG.

The AGE on the PCR products from the *Cyp11a1* primers showed no bands in any of the lanes, refer to [Figure 3.40](#).

UNIVERSITY of the  
WESTERN CAPE

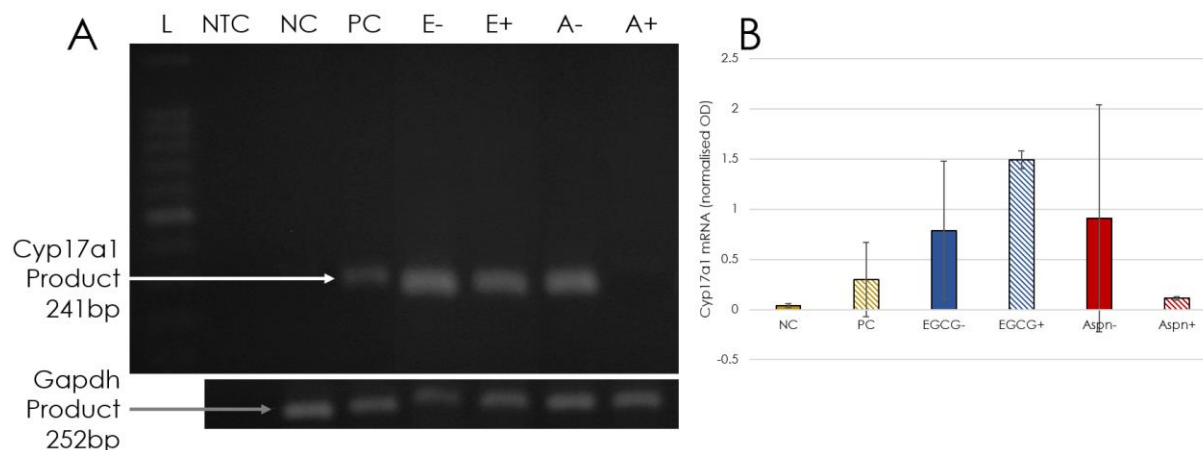


**Figure 3.41. Conventional PCR results for *Cyp17a1* gene expression.** **A:** Photograph showing a representative AGE result for *Cyp17a1*; **B:** Graph showing the average densitometry results from the *Cyp17a1* AGE. TM3 cells were treated for 24 hours with either a control, 10  $\mu$ M of EGCG (and 0.5 % DMSO) in media or 10  $\mu$ M of aspalathin (and 0.5 % DMSO) in media, either with hCG at 125 mIU/ml or without hCG. Thereafter, mRNA was extracted, cDNA synthesized, followed by PCR and AGE. **L:** 100 bp DNA ladder; **NTC:** no template control; **NC:** negative control (i.e. 0.5 % DMSO); **PC:** positive control (i.e. 125 mIU/ml hCG); **E:** EGCG; **A, Asp:** aspalathin; **-:** without hCG; **+:** with hCG. Data are represented as means  $\pm$  standard deviations; n = 2.

The results from the *Cyp17a1* PCR show that the EGCG treated cells, the aspalathin treated cells (without hCG) and the positive control cells all had bands at the 241 bp level (Figure 3.41-A). However, the cells from negative control gave the dimmest of the bands observed. The NTC lane as well as the lanes for the negative control, and for cells treated with aspalathin and hCG showed no visible bands. These results were confirmed by normalised densitometry data (Figure 3.41-B). The aspalathin treatment without hCG and the EGCG treatments (both with and without hCG) all had higher *Cyp17a1* levels than the cells treated with hCG only.

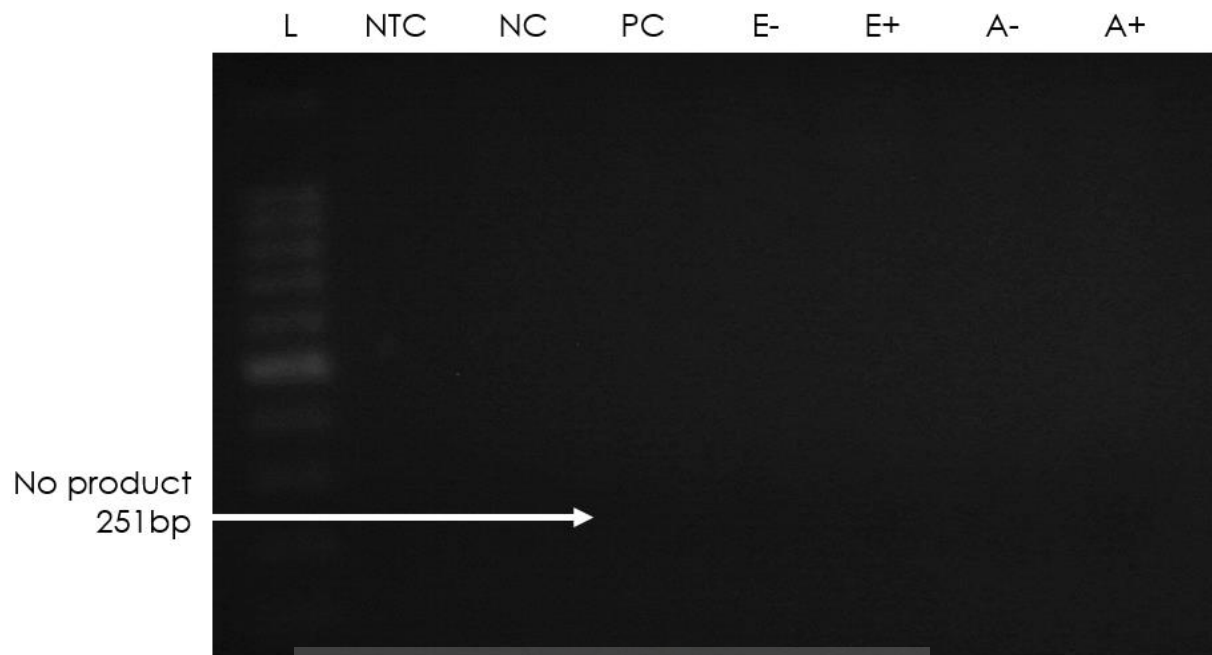


**Figure 3.42. Photograph showing the AGE results for *Hsd17b3* gene expression.** TM3 cells were treated for 24 hours with either a control, 10  $\mu$ M of EGCG (and 0.5 % DMSO) in media or 10  $\mu$ M of aspalathin (and 0.5 % DMSO) in media, either with hCG at 125 mIU/ml or without hCG. Thereafter, mRNA was extracted, cDNA synthesized, followed by PCR and AGE. **L:** 100 bp DNA ladder; **NTC:** no template control; **NC:** negative control (i.e. 0.5 % DMSO); **PC:** positive control (i.e. 125 mIU/ml hCG); **E:** EGCG; **A:** aspalathin; **-:** without hCG; **+:** with hCG.

The PCR and AGE for *Hsd17b3* produced no bands in any of the lanes, refer to [Figure 3.42](#). This experiment was repeated and also showed no bands.

UNIVERSITY of the  
WESTERN CAPE

### 3.6.2 qPCR AGE results

Although each qPCR was followed by a high resolution melt curve analysis, the specificity of each qPCR was also confirmed by AGE. The qPCRs were only performed on the GOIs that successfully amplified when using conventional PCR.

The first primer design for *Gapdh* produced excessive non-specific amplicons and so could not be used for qPCR. Consequently, a second primer design was developed and Figure 3.43 shows that this primer pair only amplified the desired product (97 bp) during the qPCR.

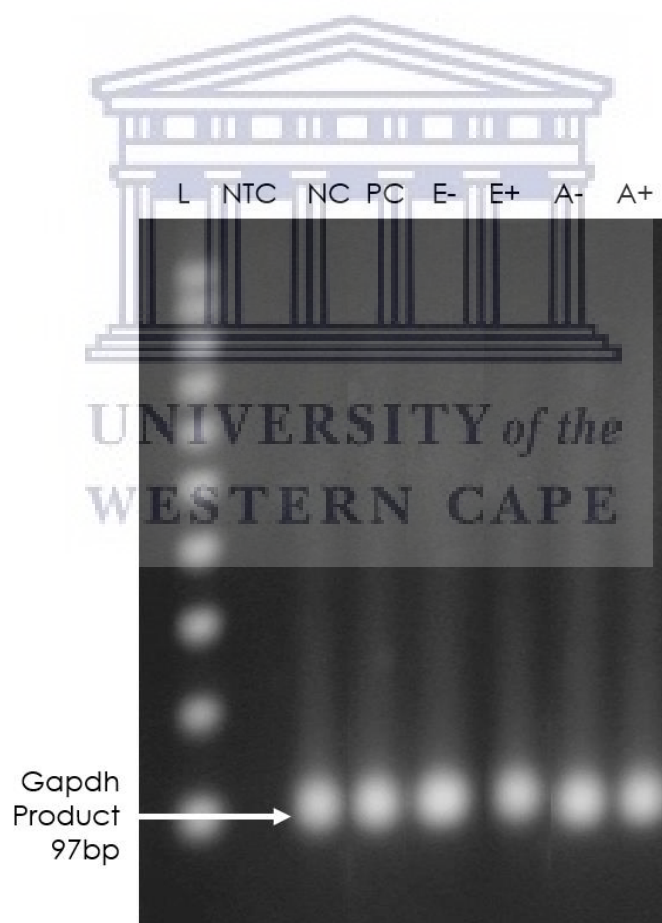


**Figure 3.43. Photograph showing a representative AGE result for *Gapdh* after qPCR.** TM3 cells were treated for 24 hours with either a control, 10  $\mu$ M of EGCG (and 0.5 % DMSO) in media or 10  $\mu$ M of aspalathin (and 0.5 % DMSO) in media, either with hCG at 125 mlU/ml or without hCG. Thereafter, mRNA was extracted, cDNA synthesized, followed by qPCR and AGE. **L**: 100 bp DNA ladder; **NTC**: no template control; **NC**: negative control (i.e. 0.5 % DMSO); **PC**: positive control (i.e. 125 mlU/ml hCG); **E**: EGCG; **A**: aspalathin; **-**: without hCG; **+**: with hCG.



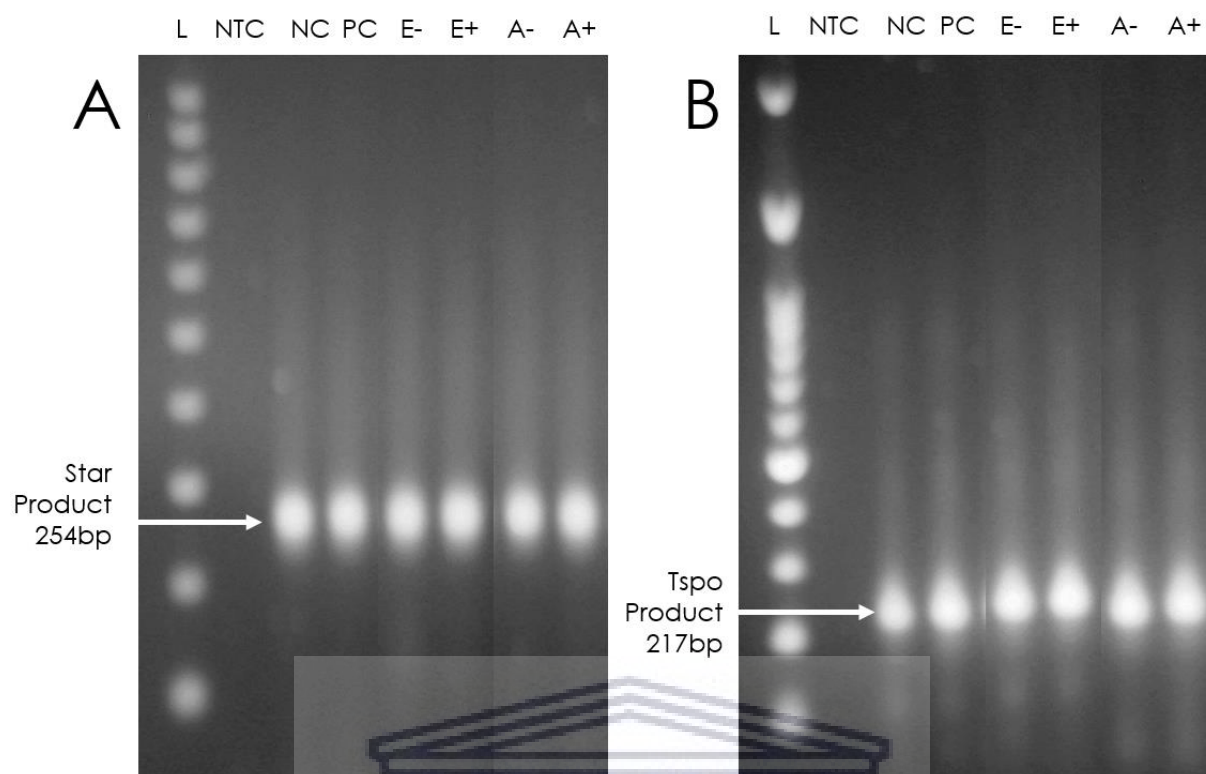


**Figure 3.44.** Photographs showing representative AGE results for *Star* and *Tspo* after qPCR. **A:** the *Star* gel; **B:** the *Tspo* gel. TM3 cells were treated for 24 hours with either a control, 10  $\mu$ M of EGCG (and 0.5 % DMSO) in media or 10  $\mu$ M of aspalathin (and 0.5 % DMSO) in media, either with hCG at 125 mIU/ml or without hCG. Thereafter, mRNA was extracted, cDNA synthesized, followed by qPCR and AGE. **L:** 100 bp DNA ladder; **NTC:** no template control; **NC:** negative control (i.e. 0.5 % DMSO); **PC:** positive control (i.e. 125 mIU/ml hCG); **E:** EGCG; **A:** aspalathin; -: without hCG; +: with hCG.

According to Figure 3.44, the qPCRs for both *Star* and *Tspo* amplified products of 254 bp and 217 bp respectively. These match their respective predicted product lengths.

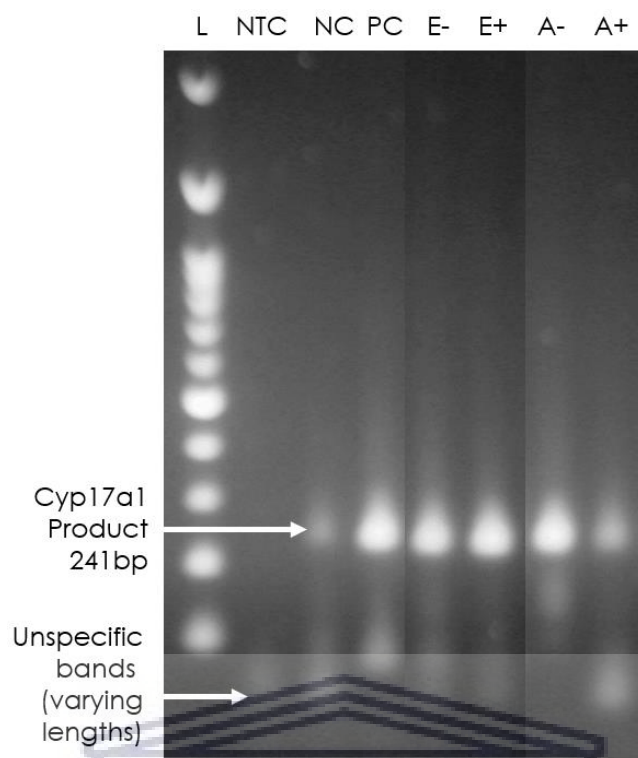


**Figure 3.45. Photograph showing a representative AGE result for *Cyp17a1* after qPCR.** TM3 cells were treated for 24 hours with either a control, 10  $\mu$ M of EGCG (and 0.5 % DMSO) in media or 10  $\mu$ M of aspalathin (and 0.5 % DMSO) in media, either with hCG at 125 mIU/ml or without hCG. Thereafter, mRNA was extracted, cDNA synthesized, followed by qPCR and AGE. **L:** 100 bp DNA ladder; **NTC:** no template control; **NC:** negative control (i.e. 0.5 % DMSO); **PC:** positive control (i.e. 125 mIU/ml hCG); **E:** EGCG; **A:** aspalathin; -: without hCG; +: with hCG.

When *Cyp17a1* underwent qPCR, it showed amplification of nonspecific sequences of varying lengths (see Figure 3.45). Although the desired product was co-amplified (and more abundantly than the unspecific products), this discovery made these primers unusable for qPCR.

### 3.7 Quantitative PCR assay for steroidogenic gene expression

The qPCR data for *Star* and *Tspo* (here) were determined according to Pfaffl (2004).

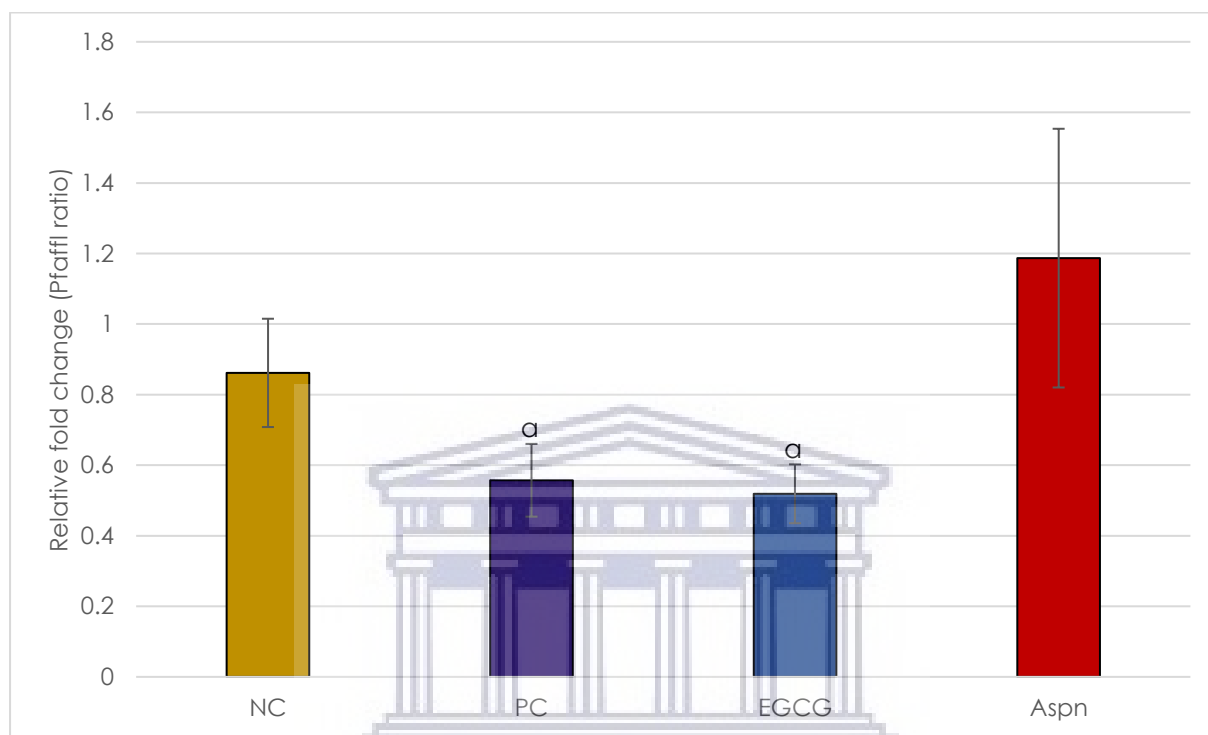


**Figure 3.46.** Graph showing the effects of hCG, EGCG and aspalathin on *Star* relative gene expression.

The cells were treated for 24 hours with either a control, EGCG in media or aspalathin. The Pfaffl ratio was calculated using the formula:  $E_{\text{target}}^{\Delta Ct} \div E_{\text{reference}}^{\Delta Ct}$ ; where  $E_{\text{target}}$  is the PCR efficiency of *Star*,  $E_{\text{reference}}$  is the PCR efficiency of *Gapdh* and  $\Delta Ct$  is  $Ct_{\text{vehicle}} - Ct_{\text{sample}}$ . Here  $Ct_{\text{vehicle}}$  is the  $Ct$  values from cells exposed to the **NC** treatment and  $Ct_{\text{sample}}$  is the corresponding  $Ct$  values for cells exposed to either hCG, aspalathin or EGCG. **NC**: negative control (i.e. 0.5% DMSO); **PC**: positive control (i.e. 125 mlU/ml hCG in 0.5% DMSO); **Aspnl**: 10  $\mu\text{M}$  aspalathin (with 0.5% DMSO); **EGCG**: 10  $\mu\text{M}$  EGCG (with 0.5% DMSO). Data are represented as means  $\pm$  standard deviations. A P value of less than 0.05 was considered significant;  $\alpha$ : significantly different to **NC**,  $n = 3$ .

According to Figure 3.46, cells treated with hCG showed significantly lower ( $P < 0.05$ ) levels of *Star* cDNA than those that were untreated. Similarly, the cells that received EGCG (without hCG) showed significantly lower *Star* cDNA levels than the negative control. The hCG and EGCG treatments showed *Star* expression that was 0.6 and 0.5 fold that of the negative control. Aspalathin produced the highest *Star* cDNA expression (at 1.2 fold that of the negative control), but was not significantly different to the negative control.

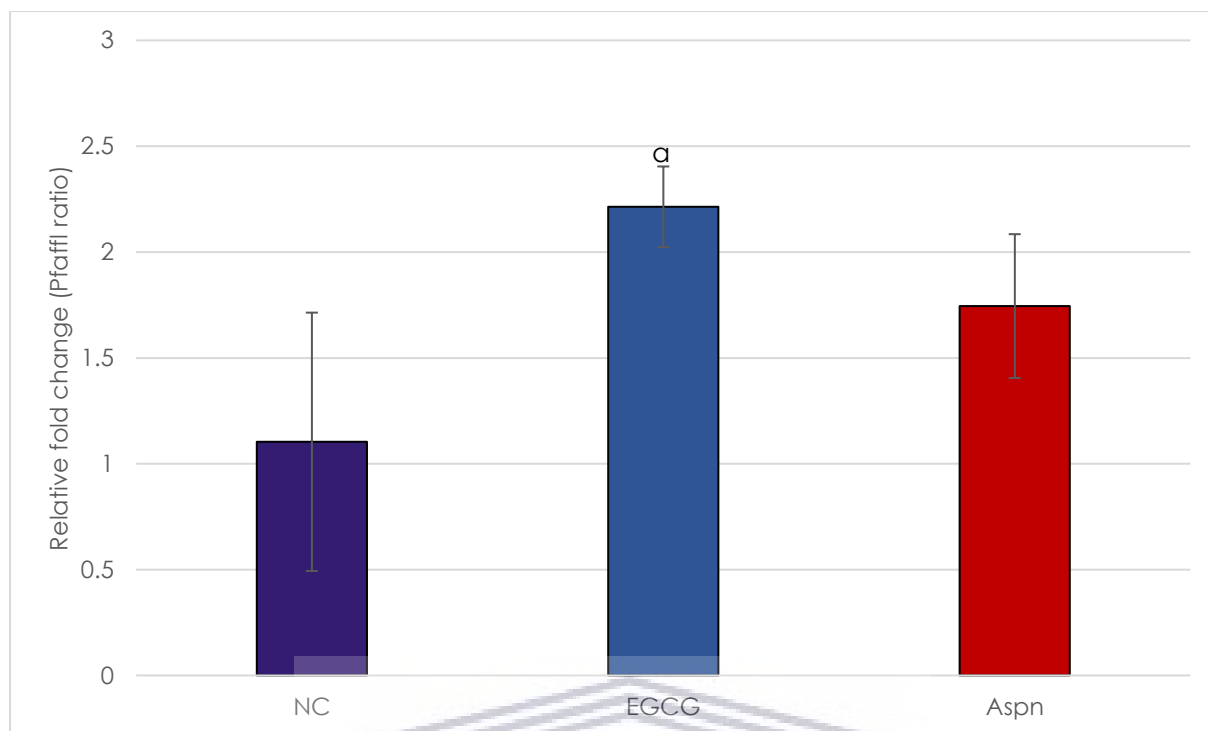


**Figure 3.47. Graph showing the effects of hCG, co-treated with EGCG or aspalathin on *Star* relative gene expression.** The cells were treated for 24 hours with either a control, EGCG (with hCG) or aspalathin (with hCG). The Pfaffli ratio was calculated using the formula:  $E_{\text{target}}^{\Delta Ct} \div E_{\text{reference}}^{\Delta Ct}$ ; where  $E_{\text{target}}$  is the PCR efficiency of *Star*,  $E_{\text{reference}}$  is the PCR efficiency of *Gapdh* and  $\Delta Ct$  is  $Ct_{\text{vehicle}} - Ct_{\text{sample}}$ . Here  $Ct_{\text{vehicle}}$  is the  $Ct$  values from cells exposed to the **NC** treatment and  $Ct_{\text{sample}}$  is the corresponding  $Ct$  values for cells exposed to either hCG, aspalathin or EGCG. **NC**: negative control (i.e. 0.5% DMSO with 125 nIU/ml hCG); **Aspn**: 10  $\mu\text{M}$  aspalathin (with 0.5% DMSO and 125 nIU/ml hCG); **EGCG**: 10  $\mu\text{M}$  EGCG (with 0.5% DMSO and 125 nIU/ml hCG). Data are represented as means  $\pm$  standard deviations. A P value of less than 0.05 was considered significant; a: significantly different to **NC**,  $n = 3$ .

When TM3 cells were co-treated with hCG and 10  $\mu\text{M}$  EGCG, they showed a 2.2 fold elevation in *Star* expression compared to the negative control (Figure 3.47), which was significant ( $P < 0.05$ ). On the other hand the aspalathin treatment with hCG was 1.8 fold higher than the negative control group, but this was not statistically significant.

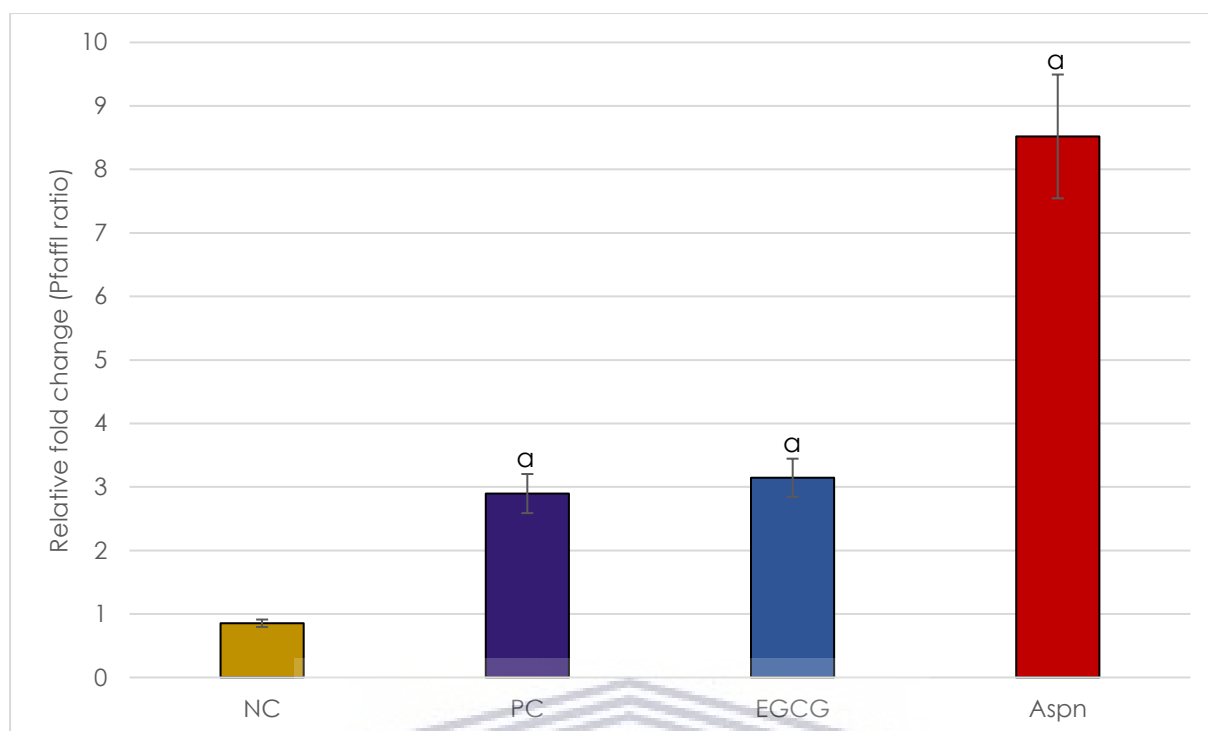


**Figure 3.48. Graph showing the effects of hCG, EGCG and aspalathin on *Tspo* relative gene expression.**

The cells were treated for 24 hours with either a control, EGCG or aspalathin. The Pfaffli ratio was calculated using the formula:  $E_{\text{target}}^{\Delta Ct} \div E_{\text{reference}}^{\Delta Ct}$ ; where  $E_{\text{target}}$  is the PCR efficiency of *Tspo*,  $E_{\text{reference}}$  is the PCR efficiency of *Gapdh* and  $\Delta Ct$  is  $Ct_{\text{vehicle}} - Ct_{\text{sample}}$ . Here  $Ct_{\text{vehicle}}$  is the  $Ct$  values from cells exposed to the **NC** treatment and  $Ct_{\text{sample}}$  is the corresponding  $Ct$  values for cells exposed to either hCG, aspalathin or EGCG. **NC**: negative control (i.e. 0.5% DMSO); **PC**: positive control (i.e. 125 nIU/ml hCG in 0.5% DMSO); **Aspn**: 10  $\mu\text{M}$  aspalathin (with 0.5% DMSO); **EGCG**: 10  $\mu\text{M}$  EGCG (with 0.5% DMSO). Data are represented as means  $\pm$  standard deviations. A P value of less than 0.05 was considered significant; a: significantly different to **NC**, n = 3.

Aspalathin, without hCG, showed the highest *Tspo* expression of the treatments tested and averaged at 8.5 fold higher than the negative control group (Figure 3.48). The hCG treatment and the EGCG treatment (without hCG) showed 2.9 fold and 3.1 fold increases in *Tspo* cDNA levels compared with the negative control, respectively. All three treatments, hCG, aspalathin and EGCG, gave significant increases ( $P < 0.05$ ) in *Tspo* levels.

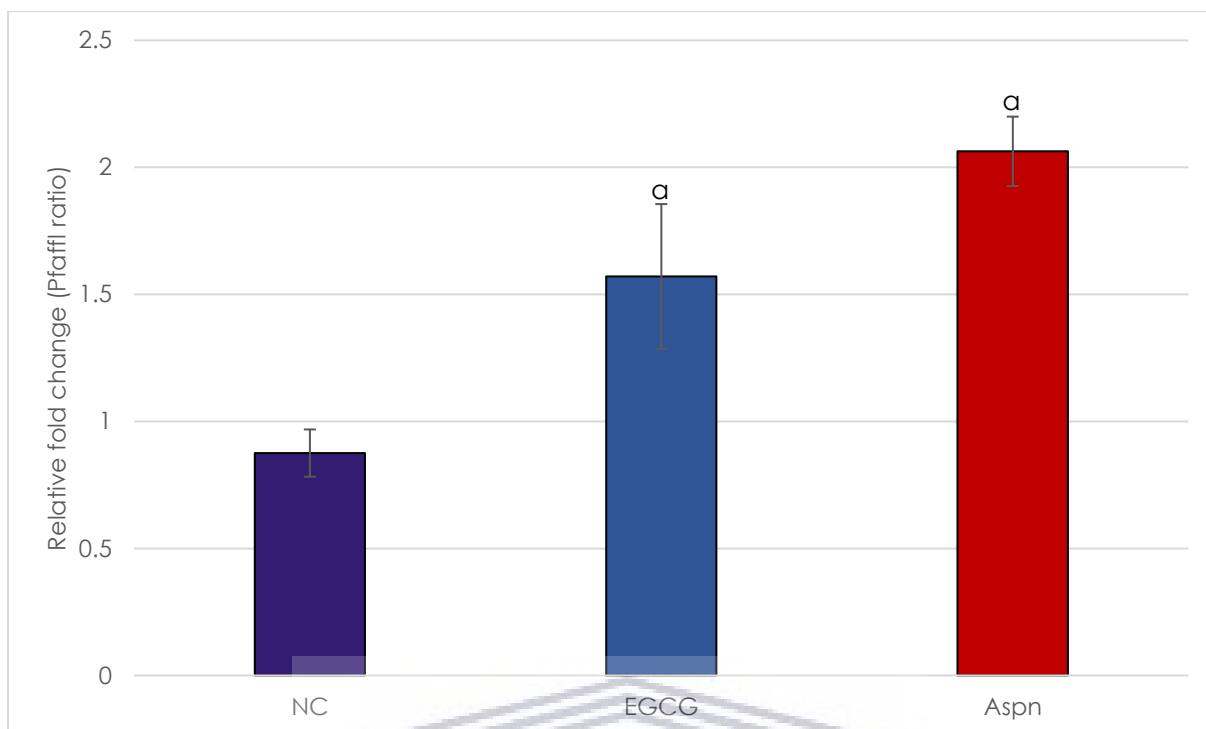


**Figure 3.49. Graph showing the effects of hCG, co-treated with EGCG or aspalathin on *Tspo* relative gene expression.** The cells were treated for 24 hours with either a control, EGCG (with hCG) or aspalathin (with hCG). The Pfaffli ratio was calculated using the formula:  $E_{target}^{\Delta Ct} \div E_{reference}^{\Delta Ct}$ ; where  $E_{target}$  is the PCR efficiency of *Tspo*,  $E_{reference}$  is the PCR efficiency of *Gapdh* and  $\Delta Ct$  is  $Ct_{vehicle} - Ct_{sample}$ . Here  $Ct_{vehicle}$  is the  $Ct$  values from cells exposed to the **NC** treatment and  $Ct_{sample}$  is the corresponding  $Ct$  values for cells exposed to either the vehicle treatment, aspalathin or EGCG. **NC**: negative control (i.e. 0.5 % DMSO with 125 mIU/ml hCG); **Aspn**: 10  $\mu$ M aspalathin (with 0.5% DMSO and 125 mIU/ml hCG); **EGCG**: 10  $\mu$ M EGCG (with 0.5% DMSO and 125 mIU/ml hCG). Data are represented as means  $\pm$  standard deviations. A P value of less than 0.05 was considered significant; a: significantly different to **NC**, n = 3.

Both aspalathin and EGCG showed significant ( $P < 0.05$ ) elevations in *Tspo* cDNA levels when they were co-treated with hCG, compared with cells exposed to hCG alone (Figure 3.49). The aspalathin treatment produced the highest *Tspo* expression at 2.1 fold higher than the negative control, whereas EGCG produced a 1.6 fold increase in *Tspo*.

### 3.8 TM4 cell inhibin B secretion

Inhibin B is produced by Sertoli cells and helps to control testosterone production (via the HPT axis). Hence the secretion of inhibin can be used to help elucidate how a test substance affects Sertoli cell function, as well as the HPT axis.

In order to assess the effects of green tea, green rooibos, EGCG and aspalathin on the function of Sertoli cells, TM4 cells were treated with these teas or flavonoids and the secretion of inhibin B was determined by ELISA. FSH was included as a positive control, because it stimulates Sertoli cell inhibin B secretion (Depuydt *et al.*, 1999).

According to [Figure 3.50](#), it appears that both green tea and green rooibos caused a decrease in TM4 cell inhibin B secretion. However, the levels of inhibin B detected were below the detection minimum of the ELISA, which was 15.63 pg/ml. Furthermore, the treatment of the TM4 cells with 125 mIU/ml FSH (positive control) did not cause an increase in inhibin B secretion.

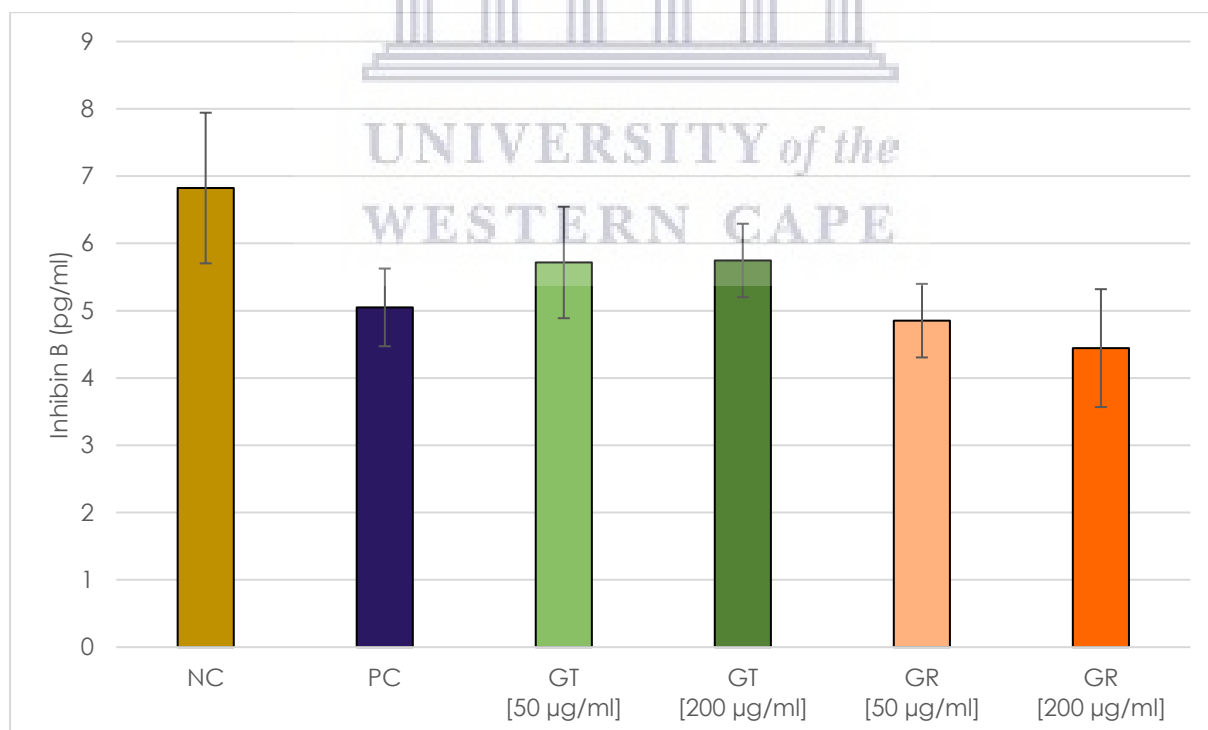


**Figure 3.50.** Graph showing the effects of green tea and green rooibos on inhibin B secretion by TM4 cells.

The cells were treated for 24 hours with either a control, reconstituted green tea or reconstituted green rooibos. **NC**: negative control (i.e. complete medium), **PC**: positive control (i.e. 125 mIU/ml FSH), **GT**: green tea, **GR**: green rooibos. Data are represented as means  $\pm$  standard deviations;  $n = 6$ .

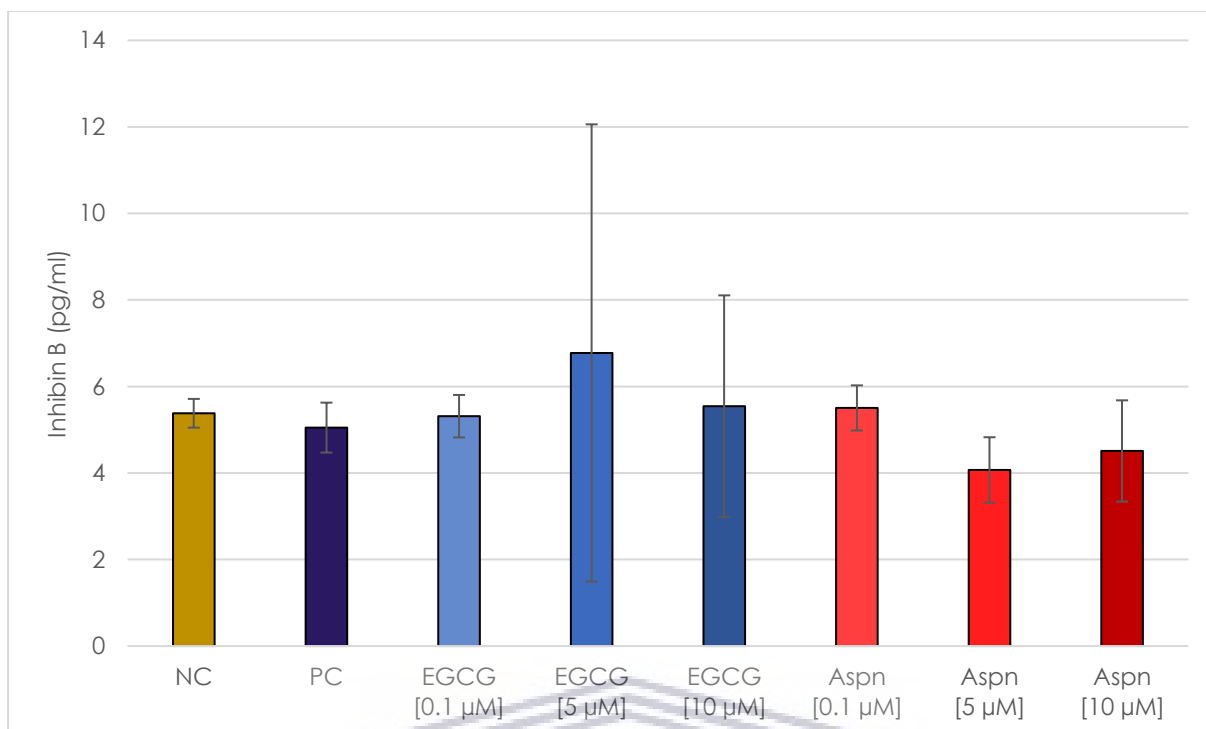


**Figure 3.51. Graph showing the effects of EGCG and aspalathin on inhibin B secretion by TM4 cells.** The cells were treated for 24 hours with either a control, EGCG (and 0.5 % DMSO) or aspalathin (and 0.5 % DMSO). **NC**: negative control (i.e. 0.5 % DMSO), **PC**: positive control (i.e. 125 mIU/ml FSH), **Aspn**: aspalathin. Data are represented as means  $\pm$  standard deviations; n = 6.

The results from [Figure 3.51](#) also show that the treatments with the controls, EGCG and aspalathin all produced inhibin B levels, below the detection threshold of the ELISA. Nonetheless, the inhibin B levels appear to be similar between treatment groups.



### 3.9 TM4 cell lactate secretion

The primary energy source of the spermatogenic series is lactate, which is supplied by the Sertoli cells. This makes lactate a relatively easy product to quantify when one wants to determine the reproductive toxicity of a substance. The lactate levels can indicate Sertoli cell function and also the likely consequences on spermatogenesis.

As for inhibin B secretion, FSH is known to normally stimulate Sertoli cell lactate secretion (Jutte *et al.*, 1983; Riera *et al.*, 2001). Hence, FSH was once more used as a presumptive positive control for this experiment.

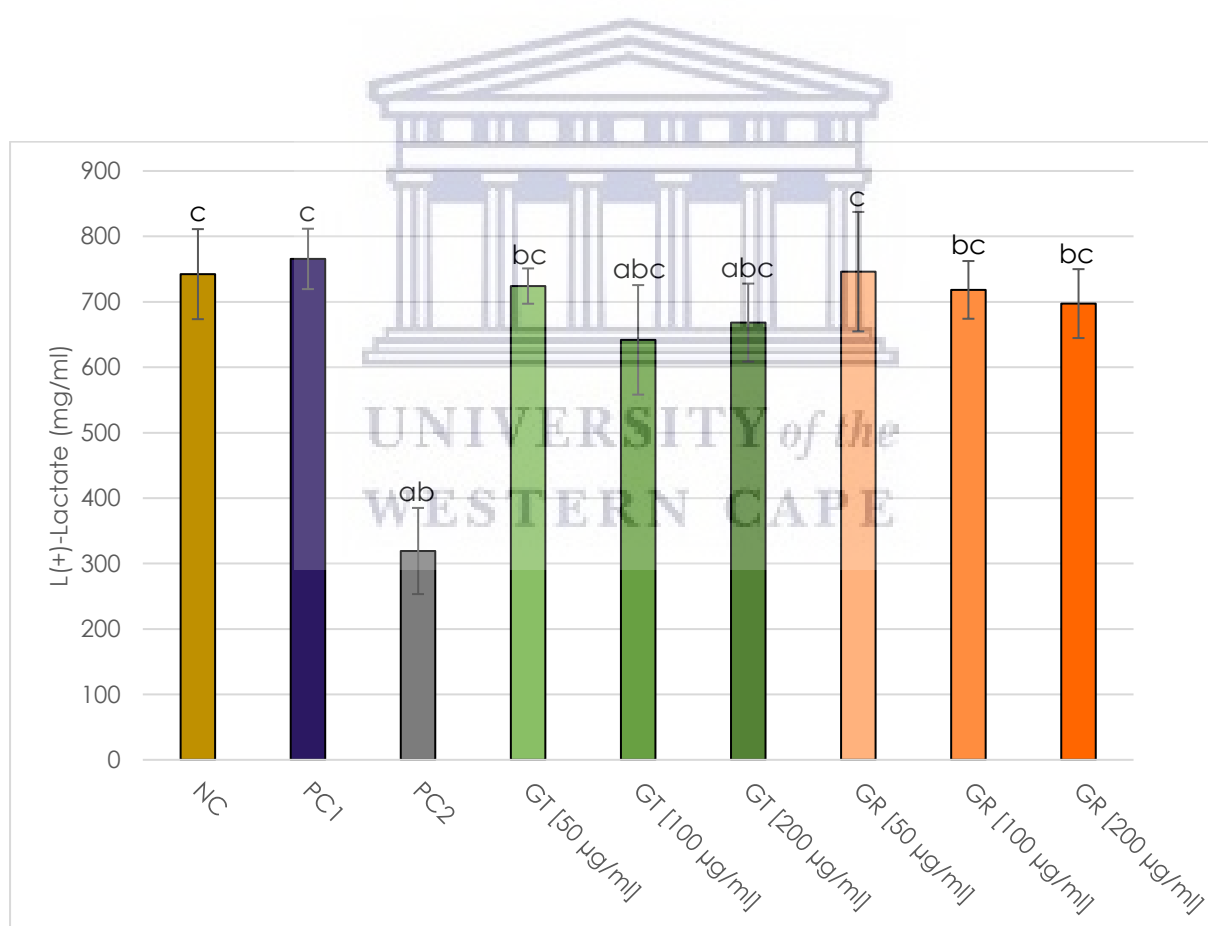


**Figure 3.52.** Graph showing the effects of green tea and green rooibos on lactate secretion by TM4 cells.

The cells were treated for 24 hours with either a control, reconstituted green tea or reconstituted green rooibos. **NC**: negative control (i.e. complete medium), **PC1**: positive control 1: 125 mIU/ml FSH, **PC2**: positive control 2 (cell death) 10 % DMSO, **GT**: green tea, **GR**: green rooibos. Data are represented as means  $\pm$  standard deviations. A P value of less than 0.05 was considered significant; a: significantly different to **NC**, b: significantly different to **PC1**, c: significantly different to **PC2**;  $n \leq 9$ .

According to [Figure 3.52](#), the positive control 2 only produced  $319.2 (\pm 65.9)$  mg/l of lactate, which was significantly lower ( $P < 0.05$ ) than for those treated with either the negative control ( $742.3 \pm 68.8$  mg/l) or positive control 1 ( $765.6 \pm 46.1$  mg/l). In fact, positive control 2 gave significantly lower lactate concentrations ( $P < 0.05$ ) than all the other treatment groups (i.e. all green tea and green rooibos treatments as well). This result was unsurprising, the 10% DMSO treatment served as a positive control for cell death. Additionally, no significant difference was noted between the lactate levels from the negative control and positive control 1 treatments.

The treatment with 50  $\mu\text{g/ml}$  of green tea produced significantly lower lactate levels than positive control 1 did ( $P < 0.05$ ), at  $724.1 (\pm 27.0)$  mg/l. The higher concentrations of green tea, caused a further reduction in lactate levels, such that they were significantly lower than even the negative control ( $P < 0.05$ ). The treatment with 100  $\mu\text{g/ml}$  of green tea showed a lactate concentration of  $641.9 (\pm 83.7)$  mg/l; whereas the treatment with 200  $\mu\text{g/ml}$  of green tea showed a lactate concentration of  $668.2 (\pm 59.6)$  mg/l.

The green rooibos treatments showed a similar trend to that of the green tea, but to a lesser extent. According to [Figure 3.52](#), the 50  $\mu\text{g/ml}$  treatment of green rooibos showed no significant effects on lactate levels when compared to either the negative control or positive control 1. However, both the treatments with 100  $\mu\text{g/ml}$  and 200  $\mu\text{g/ml}$  of green rooibos caused a significant reduction ( $P < 0.05$ ) in lactate concentration compared to positive control 1, but not the negative control. The detected lactate levels were  $746.1 (\pm 91.3)$  mg/l,  $718.3 (\pm 44.1)$  mg/l and  $697.3 (\pm 52.7)$  mg/l for the 50  $\mu\text{g/ml}$ , 100  $\mu\text{g/ml}$  and 200  $\mu\text{g/ml}$  green rooibos treatments respectively.

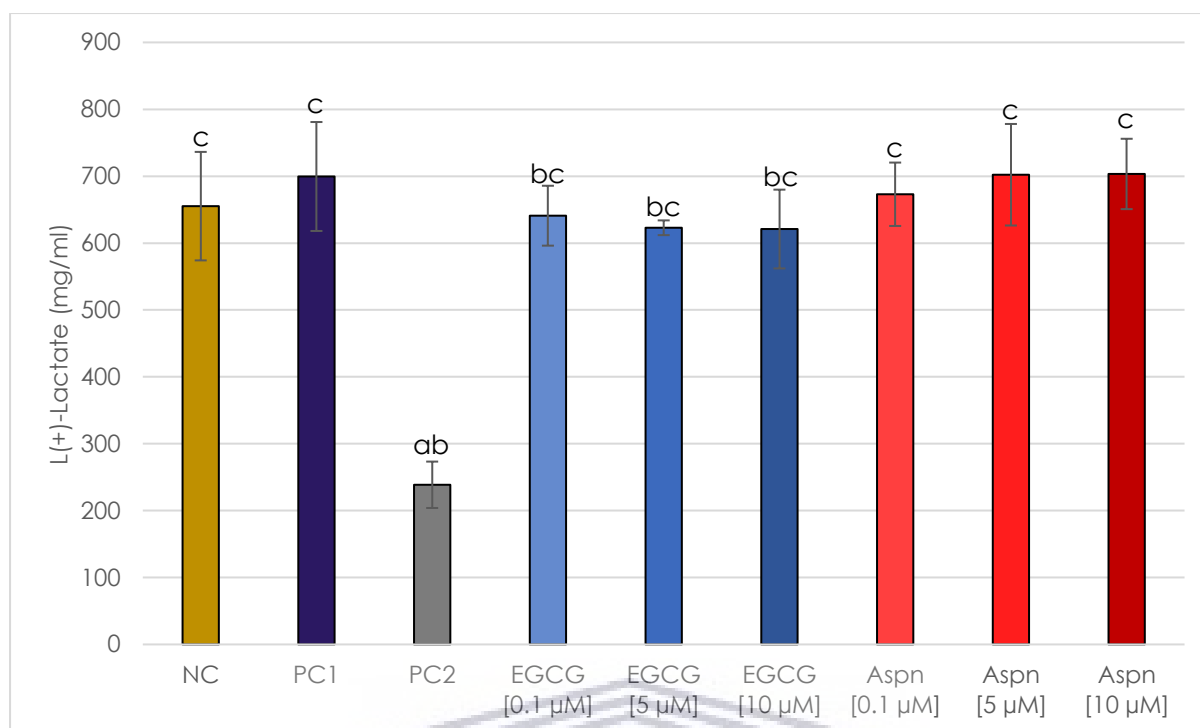


**Figure 3.53.** Graph showing the effects of EGCG and aspalathin on lactate secretion by TM4 cells. The cells were treated for 24 hours with either a control, EGCG (and 0.5 % DMSO) or aspalathin (and 0.5 % DMSO). **NC**: negative control (i.e. 0.5 % DMSO), **PC1**: positive control 1: 125 mIU/ml FSH, **PC2**: positive control 2 (cell death) 10 % DMSO, **Aspn**: aspalathin. Data are represented as means  $\pm$  standard deviations. A P value of less than 0.05 was considered significant; a: significantly different to **NC**, b: significantly different to **PC1**, c: significantly different to **PC2**;  $n \leq 8$ .

The control results in Figure 3.53 agree with that of Figure 3.52. Positive control 2 produced significantly lower lactate levels than all other tested treatments did. Additionally, Figure 3.53 shows no significant difference between the lactate levels of the negative control and positive control 1. However, the values in the graphs (Figures 3.52 and 3.53) are slightly different for the same treatments; in Figure 3.53 they were 238.7 ( $\pm$  34.7) mg/l, 665.2 ( $\pm$  81.1) mg/l and 699.6 ( $\pm$  81.4) mg/l for positive control 2, negative control and positive control 1 respectively.

All the EGCG treatments produced significantly lower lactate concentrations than positive control 1, but not the negative control. The EGCG treatments of 0.1  $\mu$ M, 5  $\mu$ M and 10  $\mu$ M gave lactate levels of 641.0 ( $\pm$  44.8) mg/l, 622.9 ( $\pm$  11.0) mg/l and 621.0 ( $\pm$  58.9) mg/l respectively.

The treatment of TM4 cells with aspalathin at 0.1  $\mu\text{M}$ , 5  $\mu\text{M}$  and 10  $\mu\text{M}$  produced lactate levels of 673.0 ( $\pm$  47.4) mg/l, 702.2 ( $\pm$  76.0) mg/l and 703.4 ( $\pm$  52.6) mg/l respectively. None of the lactate concentrations from the aspalathin treatments were significantly different to those of either the negative control or the positive control 1.



### 3.10 TEER assay

One of the major functions of Sertoli cells is to maintain the immunological privilege of the developing spermatozoa. This is achieved by the Sertoli cell barrier, which is mainly formed by tight junctions between adjacent Sertoli cells. Measuring the transepithelial electrical resistance (TEER) is widely used for studying how various substances affect the integrity of model biological barriers. This thesis also used the TEER assay to test EGCG and aspalathin's effects on the SCB. Green tea and green rooibos were omitted due to a global shortage of the cell culture inserts that were needed for the TEER assay.

According to [Figure 3.54](#), there were no significant differences in TEER between either of the EGCG treatments used (0.1  $\mu\text{M}$ , 5 $\mu\text{M}$  and 10  $\mu\text{M}$ ) and the negative control at 24 hours. However, at the 48 hour mark, the 0.1  $\mu\text{M}$  EGCG treatment showed a significant elevation in TEER compared with the 48 hour negative control. None of the other EGCG treatments showed any significant differences in TEER compared with the negative control at 48 hours. Additionally, after 72 hours, there were no more significant differences in TEER between either of the EGCG treatments and the negative control.

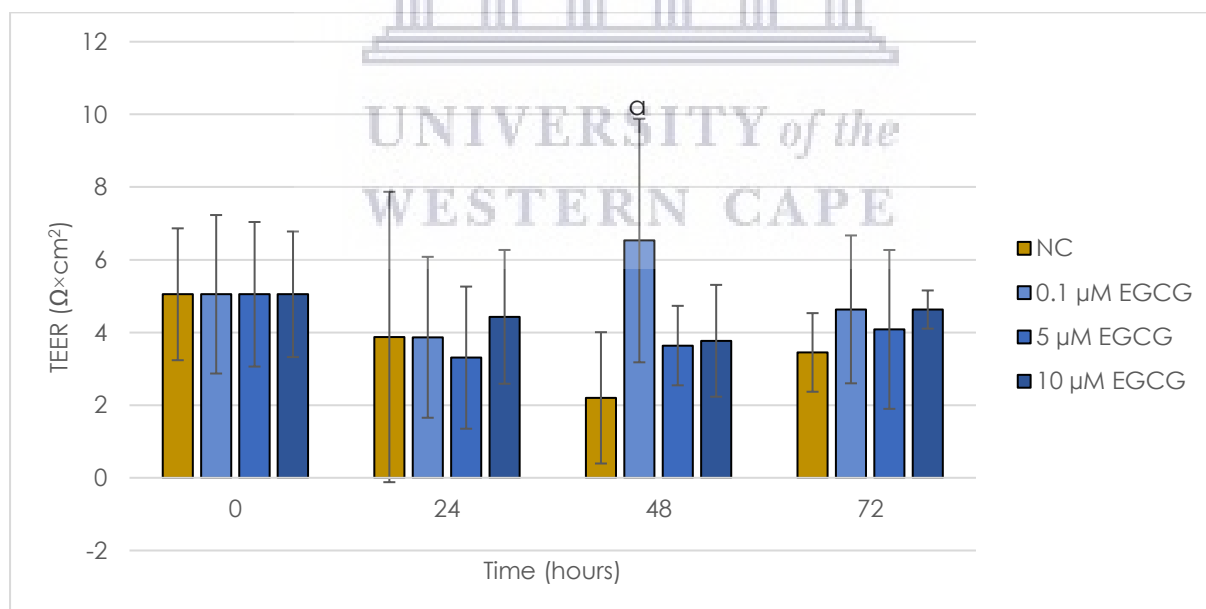


**Figure 3.54. Graph showing the effects of EGCG on TM4 cell transepithelial electrical resistance over a 72 hour period.** The cells were treated with either a vehicle control (0.5 % DMSO) or EGCG (and 0.5 % DMSO) at the indicated concentrations. The TEER values were normalised to **NC** at zero hours of treatment. **NC**: negative control (i.e. 0.5 % DMSO). Data are represented as means  $\pm$  standard deviations. A P value of less than 0.05 was considered significant; a: significantly different to **NC** of the corresponding treatment time;  $n \leq 3$ .

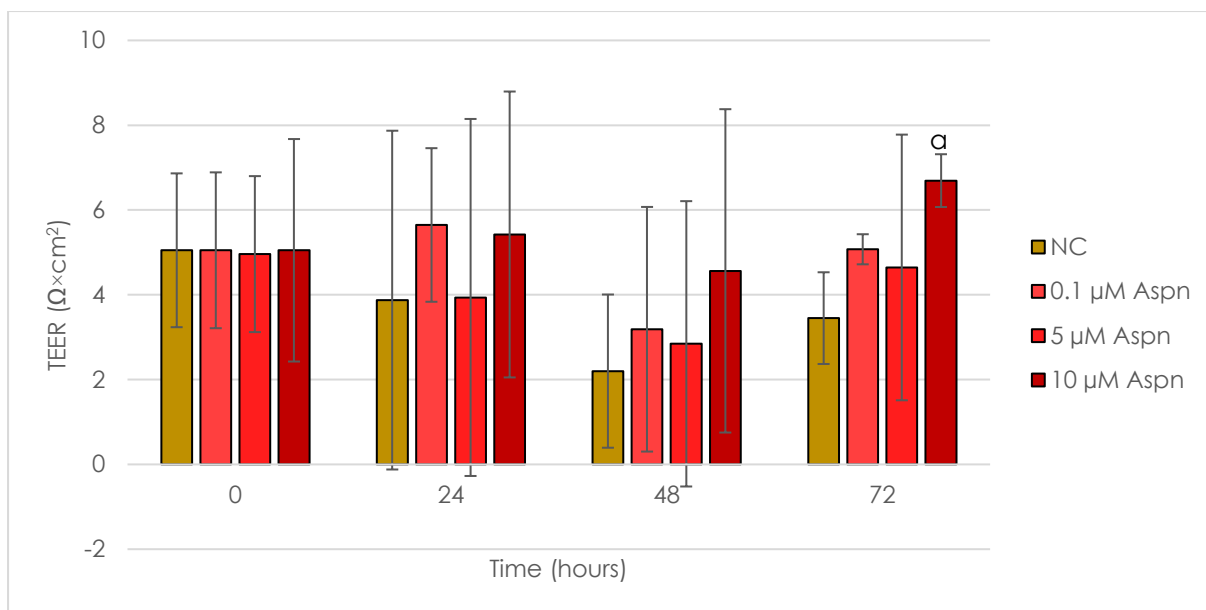


**Figure 3.55. Graph showing the effects of aspalathin on TM4 cell transepithelial electrical resistance over a 72 hour period.** The cells were treated with either a vehicle control (0.5 % DMSO) or aspalathin (and 0.5 % DMSO) in media at the indicated concentrations. The TEER values were normalised to **NC** at zero hours of treatment. **NC**: negative control (i.e. 0.5 % DMSO), **Aspn**: aspalathin. Data are represented as means  $\pm$  standard deviations. A P value of less than 0.05 was considered significant; a: significantly different to **Vehicle** of the corresponding treatment time;  $n \leq 3$ .

In [Figure 3.55](#), one can see that there were no significant difference in TEER between either of the aspalathin treatments and the negative control treatment at either 24 hours or 48 hours. At 72 hours, however, the 10  $\mu\text{M}$  aspalathin treatment gave significantly higher TEER values than the negative control did. None of the other aspalathin treatments showed any significant differences in TEER compared with the negative control at 72 hours of treatment.



# Chapter 4

---

## Discussion



UNIVERSITY *of the*  
WESTERN CAPE

## 4.1 Choosing concentrations for *in vitro* testicular cell studies

The male and female reproductive systems are unique in that neither is needed for the survival of an individual; though both are essential for survival of an animal species. Consequently, the reproductive systems are often overlooked during the toxicological assessment of test substances. However the discovery of endocrine disrupting compounds/chemicals (EDCs), in the 1900s, has revealed that reproductive toxicology actually is important.

Basically, EDCs are chemicals that can interfere with the function of the endocrine system. Research has shown that various chemicals can alter the endocrine functions of vertebrates; and the most often noted EDC activities are those that affect reproduction (Schug *et al.*, 2016; Darbe, 2019). Indeed the recognition of EDC has led to a paradigm shift in toxicology from carcinogenesis as the focus, to including EDC endpoints (Schug *et al.*, 2016). Since the hormone-receptor interaction is highly specific, hormones (and consequently EDCs) can produce physiological effects at very low concentrations (Darbe, 2019). This means that even chemicals that are poorly absorbed into plasma are worth investigating for reproductive toxicity.

Both green tea and green rooibos are reported to show low uptake into plasma after ingestion by humans (see the footnotes<sup>2</sup> on page 22 and<sup>3</sup> on page 24 for my semantics of *green tea* and *green rooibos*). In 1998, Yang *et al.* investigated the uptake and retention of green tea catechins in human plasma after consuming different doses of decaffeinated green tea solids. The Yang *et al.* (1998) study found that consuming either 3 g or 4.5 g of decaffeinated green tea solids lead to a maximal plasma EGCG concentration of 326 ng/ml (i.e. 0.711  $\mu\text{M}$ ) after 1.5 to 2.5 hours. Based on additional information provided by Yang *et al.* (1998), one can calculate that 326 ng/ml is only 0.074 % of the consumed EGCG (for the 3 g dose). Furthermore, Yang *et al.* (1998) could not detect any EGCG in plasma 24 hours after ingestion.

A later study by Henning *et al.* (2005), revealed a similar finding. Henning *et al.* (2005) fed volunteers either 580 mg of EGCG alone or 616 mg of EGCG as part of a green tea extract (Poly E). The Henning *et al.* (2005) EGCG doses were higher than those used by Yang *et al.* (1998), but still gave a similar plasma concentration of about 0.7  $\mu\text{M}$  after 2.5 hours; and was not detectable after 24 hours.



Unfortunately, rooibos is not as widely studied as green tea. To my knowledge only one published study (by Breiter *et al.*, 2011) assessed plasma rooibos absorption and retention after ingestion by humans. The Breiter *et al.* (2011) study reported an average maximum plasma aspalathin concentration at 0.17 % of what was ingested, but they fail to specify the actual aspalathin concentration in plasma. Nonetheless, at 0.17%, it is clear that aspalathin is also poorly absorbed by humans into plasma.

The findings of the three studies mentioned suggest that EGCG and aspalathin are not readily bioavailable to human tissues. However, one must bear in mind that studies such as those only administer a single dose of the tea/tisane, which is not how many people typically consume them. People from tea-loving countries often consume in excess of one kilogram of tea (per person) per annum (Intergovernmental Group on Tea, 2018); which can amount to more than one cup of tea per day. This means that, although poorly absorbed, flavonoids like EGCG and aspalathin could be maintained at their maximal plasma concentrations for extended periods.

Currently it is not possible to study the testicular concentrations of test substances in humans. The testicular determination of substances would likely involve a highly invasive testicular micropuncture, yielding fluid volumes that are too small to ever be justifiable (Setchell, 1986; Clulow and Jones, 2004). Hence, to study how substances affect testicular physiology *in vitro*, one is compelled to guess which concentrations to use.

The best guess would probably be the serum concentration, but it is also useful to employ supraphysiological concentrations. The rationale is that high concentrations of substances would produce more pronounced physiological effects, which are also easier to detect, than low concentrations do. Additionally, should a substance be proven as safe at a supraphysiological concentration, one can be reasonably confident that it is also safe at the lower concentrations expected *in vivo*. So, this thesis focused on green tea and green rooibos concentrations of 50 and 200 µg/ml (roughly 0.5 - 2 % of a cup of tea) as well as EGCG and aspalathin concentrations of 0.1 to 10 µM.

The green tea and green rooibos concentrations used here are within similar ranges to those used by Opuwari and Monsees (2015) and by Abuaniza (2013). In addition the EGCG concentrations correspond to those used by Figueiroa *et al.* (2009) as well as Yu *et al.* (2010); and the aspalathin concentrations are in line with Scholms *et al.* (2012), Scholms and Swart (2014) as well as Mugari (2015).

## 4.2 The effects of green tea on testicular cell physiology

### 4.2.1 Effects of green tea on Leydig cell health

The treatment of TM3 Leydig cells with green tea at a range of 50 to 800 µg/ml gave oxidoreductase activity that was within  $\pm 20\%$  of the negative control. Both the photomicrographs and the TMRE results showed no difference between the green tea treatments and negative controls. Hence, green tea has only a small (and thus nontoxic) effect on general Leydig cell physiology as judged by the methods employed in this thesis. The nontoxic nature of green tea agrees with the findings of Opuwari and Monsees (2015).

Opuwari and Monsees (2015) reveal that TM3 oxidoreductase activity increases when treated with green tea concentrations of 400 to 1000 µg/ml. It should be noted however, that in the MTT experiment of this thesis, three of the concentrations used were lower than what Opuwari and Monsees (2015) used; and revealed no relationship between green tea concentration and oxidoreductase activity. Thus, the effects of green tea on TM3 oxidoreductase activity appears negligible below a concentration of 200 µg/ml.

Data from Opuwari and Monsees (2015) revealed that when co-treated with hCG, the effects of the green tea on TM3 cells appear to have attenuated. Their MTT data show that oxidoreductase activity of TM3 cells that were given green tea and hCG was close to those of cells that received hCG only (Opuwari and Monsees, 2015). Furthermore, the hCG-stimulated green tea treatments resulted in testosterone secretion close to that of the unstimulated control (Opuwari and Monsees, 2015). These findings suggest that hCG might competitively bind to green tea constituents, effectively limiting them (green tea and hCG) from interacting with the cells.

Studies do show that polyphenols interact with proteins directly; and that their binding affinities are determined by the protein structure (Nozaki *et al.*, 2009) as well as the polyphenol's structure (Xiao *et al.*, 2011). The protein-polyphenol interaction can even mask their antioxidant activities (Arts *et al.*, 2002). This suggests that a polyphenol-protein interaction (like the hypothetical hCG-green tea interaction) could influence the physiological activities of each other. Both CG and LH play an important role in initiating Leydig cell steroidogenesis. This means that a hypothetical hCG-green tea interaction might confound the effects of green tea on steroidogenesis. It is regrettable, though, that the TM3 cell model no longer allows one to perform such studies (also see [section 4.3.1.1](#)).

### 4.2.1.1 TM3 cells and testosterone

Three experiments were performed on TM3 Leydig cells in an attempt to stimulate them (with hCG) to secrete testosterone. Unfortunately, all three experiments (one for 48 hours with animal sera, one for 24 hours with animal sera and one for 48 hours without animal sera) revealed that the TM3 cells used for this thesis were insensitive to hCG even at 240 mIU/ml. This was despite the study by Opuwari and Monsees (2015) which showed that 30 mIU/ml of hCG was enough to stimulate TM3 cells. Opuwari and Monsees (2015) do not disclose which passage numbers their cells were from, but theirs very likely came from a lower passage than the cells that I used. In my testosterone experiments, TM3 cells came from the 36<sup>th</sup> to 39<sup>th</sup> passages.

Nonetheless, both my study and that of Opuwari and Monsees (2015) employed antibody-based assays; and according to Engeli *et al.* (2018), these type of assays might overestimate the actual testosterone levels, because they likely show affinity for other steroids as well. Furthermore, Engeli *et al.* (2018) tested for steroids using liquid chromatography-tandem mass spectrometry, and reported that TM3 cells produce "no or only very low" testosterone levels. Ultimately this suggests that the TM3 cell is an unsuitable model for investigating testosterone synthesis. The Engeli *et al.* (2018) study had not been published at the commencement of my project, so I was unaware of any problems with the TM3 model. As previously mentioned, there were studies showing that TM3 cells produced testosterone, including studies from our lab. This is why TM3 cells were used, as the problems with testosterone secretion only became apparent later.

### 4.2.1.2 Boar testis primary culture

Since the TM3 cells could not be used for testosterone secretion studies; a primary culture of boar testicular cells was attempted, in the hopes that they could instead be used for the testosterone secretion studies. Regrettably, the boar testis culture was also unsuccessful, as the hCG treatment did not stimulate testosterone secretion from those cells. The MTT data show that in fact, the boar testis cells must have died during the testis dissociation process (or during culture); as there were no differences noted in the oxidoreductase activities of the cell death positive control (10 % DMSO) and either the negative control (i.e. media treatment) or the testosterone stimulation control (i.e. hCG treatment). Although changes to the testis dissociation protocol might have yielded more viable cells (perhaps with the inclusion of processes to selectively isolate Leydig

cells), optimising those processed would have been costly and without any guarantee of success. Thus the experiments with primary testis cells were also abandoned.

#### 4.2.1.3 Challenges of using flow cytometry

Alas, the effects of green tea on Leydig cell ROS levels could not be established either. This was due to problems with the assay methods used. The flow cytometry-based assay for ROS showed no difference between the controls, and this could easily be explained by assumptions that are made during flow cytometric analyses; discussed below.

Flow cytometry is the choice fluorescence-based assay method for many researches, because of its great strengths. It allows one to separate a population of cells into subgroupings based on multiple parameters, fairly quickly. Furthermore, one can process thousands of cells and potentially profile them at single-cell resolution. Flow cytometry software also employ various charts that reveal a lot about the cells under study.

Flow cytometers channel cells in single file past a laser and photodetectors, allowing one to assay cell suspensions. There is a photodetector placed at the forward scatter position (in line with the laser, but opposite the cell stream) and usually multiple photodetectors at the side scatter position (perpendicular to the forward scatter position, but also facing the cell stream). The forward scatter light gives an indication of how large an object is, and the side scatter indicates how granulated the object is; side scatter detectors usually have optical filters that allow for the detection of various fluorophores, like DCF (Jahan-Tigh *et al.*, 2012).

With all its strengths, it should be stressed that flow cytometry is not perfect. There are a number of challenges that must be overcome to produce reliable unbiased data, and the first challenge regards calibration. Flow cytometers may have different levels of performance throughout a run; this, together with the use of slightly different machine configurations, make calibration an essential component of flow cytometry assessments (Maecker and McCoy Jr, 2010). To accommodate this, flow cytometry manufacturers supply special calibration beads; but for many cell lines, calibration with beads is not enough. One may also need to calibrate the machine with some of the cells to be studied to allow unbiased gating, which can be quite challenging (Cossarizza *et al.*, 2017).

*Gating* is the process of selecting/defining specific cell subpopulations, based on some exclusionary and/or inclusionary criteria. This process has the potential to bias data, as it is

often left to the technician's discretion to decide what the cut-off values should be (Maecker and McCoy Jr, 2010; Jahan-Tigh *et al.*, 2012; van der Strate *et al.*, 2017). The best one can do to mitigate bias is to use appropriate controls, but that also poses its own problems.

One must determine before the time what to use as controls, including the ideal incubation conditions for those controls (concentration and time). Since conventional flow cytometry gating is based on the assumption that controls already work, and since gating is essential for data interpretation, one generally cannot use conventional flow cytometry to prove that a control does work. Thus, the determination of suitable controls must ideally be done using a different platform, like fluorescence microscopy. This also means that failed experiments can be hard to detect sometimes, because a technician can simply adjust gates to match their expectation. In other words, some flow cytometry data may be unfalsifiable.

There is another concern with regards to calibration and gating. When an object passes by the laser of a flow cytometer, it is counted as an 'event'. When using a conventional flow cytometer, one cannot be 100 % sure that any one event actually represents a cell. Some cells naturally die, even in the best culture conditions, and they eventually form a debris. This debris might also be counted as events, so the researcher has to decide what the cut-off values for debris should be. In fact, it is standard practice for flow cytometry technicians to use their debris cut-off values to exclude it from being counted in the first place (Cossarizza *et al.*, 2017). For conventional flow cytometry, the technician often has to take an educated guess where the debris exclusion gates should lie, which opens the door to subjective analyses. Imaging/image-based flow cytometry can overcome this challenge, as it actually allows one to view the cells directly; but the use of conventional flow cytometry is much more common (Cossarizza *et al.*, 2017; McFarlin and Gary, 2017).

Since cells must be in suspension for flow cytometry assessment, anchorage-dependent cells must be subjected to a detachment process before assessment. The detachment process typically is harsh and can alter the levels of target antigens in/on the cells (Kaur and Esau, 2015; Cossarizza *et al.*, 2017), which can seriously compromise the credibility of flow cytometry-acquired data. For decades, researches have known that trypsinisation stresses and harms cells such that it even affects their morphology and physiology (Jensen and Mottet, 1970; Raaphorst *et al.*, 1979; Mersel *et al.*, 1983; Chaudhry, 2008; Sutradhar *et al.*, 2010; Serdiuk *et al.*, 2014). This fact, together with the effects of serial centrifugation

of cells (during preparation), begs the question: how relevant are flow-cytometry based assays (on adherent cells) to the situation *in vivo*?

According to Černe *et al.* (2013), flow cytometry tends to underrepresent the proportion of dead adherent cells compared with fluorescence microscopy. They exposed human umbilical vein endothelial cells to 3.5  $\mu\text{M}$  melittin (a toxin from honeybee venom) and assayed them by haemocytometer (using trypan blue), flow cytometer and by fluorescence microscope (the latter two using 7-aminoactinomycin D). They found that as their exposure time increased (up to 60 minutes) the number of dead cells detected decreased when assayed by flow cytometer and haemocytometer. At the 60 minute mark, the haemocytometer results showed no dead cells, and the flow cytometry results were too low to report. On the other hand, the fluorescence microscopy data indicated a gradual increase in the number and proportion of dead cells detected over time. Černe *et al.* (2013) concluded that the cell processing, in preparation for the haemocytometer and flow cytometer assays (i.e. cell detachment and centrifugation steps), may have eliminated the dead cells from their samples by assay time.

The findings of Černe *et al.* (2013) agree with my personal experience in using flow cytometry. For example, when attempting an apoptosis and necrosis assay by flow cytometer, I was unable to produce a positive control for apoptosis (data not shown). Yet, that very control treatment worked perfectly when I used them in a fluorimeter-based assay. If Černe *et al.* (2013) are correct, then the cell processing caused a bias in my flow cytometry data. This would imply that the less one processes cells before assaying them, the more meaningful one's results would be.

Another concern is that many adherent cells tend to form clumps when detached from their growth surfaces. The proportions of cells in clusters vs single cells vs cellular debris is unknown in any cell sample. This makes it difficult for one to calibrate a conventional flow cytometer to assay a specific cell line for the first time.

The problems of cell debris vs single cells vs clusters of cells, go beyond calibration. If calibration and/or gating is not done correctly, one could count each cell cluster as a single event. If few of the cells in a cluster were positive for a fluorophore (i.e. most were negative), that event would still be counted as positive and one would thus be undercounting the prevalence of the negative phenotype. This can be especially problematic if cells expressing the negative phenotype are more susceptible to clustering.

On the other hand, if most of the cells in a cluster were positive, one would be undercounting the positive phenotype, since the cluster would be one event and not several events. Hence cell clusters present a great deal of uncertainty in conventional flow cytometry analyses. Thus, the cell cluster problem has led to procedures for reducing the incidence of clumping, and the practice of excluding cell clusters from flow cytometry data when suspected (Cossarizza *et al.*, 2017). However, reducing the incidence of cell clumping requires more sample processing; and the exclusion of cell clusters, is once more, usually done at the discretion of the technician.

Almost all of the highlighted problems with flow cytometry pertain to anchorage-dependent cells. Most of these problems would not be encountered when using cells that are not adherent, like those in blood. In fact, many flow cytometry guidebooks use blood as a model for demonstrating the strengths of flow cytometry (Becton, Dickinson and Company, 2002; Rahman, 2006; Wulff, 2006; Bangs Laboratories, Inc, 2020). In many ways, blood is an ideal model for flow cytometry: it is a natural cell suspension, with distinct cell subpopulations that are easily distinguished based on size and granularity.

Yet despite the suitability of blood for flow cytometry, user-defined gating can cause variability in blood assessments of as much as 20 % (Maecker and McCoy Jr, 2010). Since the interpretation of even blood data (from flow cytometry) can be imprecise, surely the data from adherent cells is likely to be even more questionable. Thus, I ultimately agree with Černe *et al.* (2013); and submit that flow cytometry is not a suitable assay platform for anchorage-dependent cells (like TM3 and TM4 cells) on its own. Flow cytometry may be even less suitable for cells that form part of natural barriers, like the blood brain barrier, the SCB or skin, since the integrity of these barriers is dependent on how strongly those cells attach to one another. Hence, barrier cells are probably more likely to form clumps.

#### **4.2.1.4 Leydig cell mitochondrial membrane potential**

It was for these very reasons (discussed in [section 4.2.1.3](#)) that the TMRE assay was performed with a plate fluorimeter. As the data show, the TMRE experiments were successful and could easily discriminate between the positive and negative controls.

There were no differences noted in the mitochondrial membrane potentials ( $\Delta\Psi_m$ ) of green tea treated cells and the controls. This agrees with the assertion that green tea, at the tested concentrations, might have negligible effects on general Leydig cell

physiology. Furthermore, these findings indicate that any effects green tea might have on Leydig cell steroidogenesis are likely mediated by green tea's interaction with specific pathways/reactions; not by general metabolism.

#### **4.2.1.5 Flaw in the ROS assay**

Due to the aforementioned challenges with flow cytometry, it was decided to attempt the ROS assay by plate fluorimeter as well. However, even the plate fluorimeter assay for ROS had some problems. The data show that H<sub>2</sub>O<sub>2</sub> could not cause a reproducible and significant increase in DCF fluorescence in the TM3 cells.

The Hoechst data indicate that the real problem was related to cell detachment from the wells. Both the blank treatments and the wells without cells in them showed similar Hoechst fluorescence, and most of the treated cells that were labelled showed the same fluorescence levels. Hoechst binds to the DNA, and so can indicate relative cell abundance. Thus, the lack of Hoechst fluorescence means that the cells were not present in the wells at assay time. The absence of cells suggests that the positive controls were too harsh, causing detachment or at least weakening cell attachment. On the other hand, the wash steps (which are needed to remove background fluorescence) likely also stressed cell adhesion and caused the actual loss of cells from the wells.

Either way, the ROS trials show that a different assay is needed to test TM3 cell ROS levels. I suggest an assay that does not require any wash steps, and one that can be performed on clear-bottomed plates so that one can visually confirm the presence of cells within the wells.



### 4.2.2 Effects of green tea on Sertoli cell health

Green tea caused a concentration-dependent decrease in TM4 Sertoli cell oxidoreductase activity from 25 to 200  $\mu\text{g/ml}$ . The photo microscopy images indicate that these MTT results were not caused by cell death. Moreover, at 200  $\mu\text{g/ml}$ , green tea caused an increase in  $\Delta\Psi_m$ , which was unexpected. Nonetheless, when one considers what is required for MTT reduction and  $\Delta\Psi_m$ , it actually becomes clear how green tea might affect Sertoli cells.

#### 4.2.2.1 The MTT assay and mitochondria

Mitochondria are important for healthy cell physiology, which is partly why the MTT assay became so popular. The MTT assay was first described by Mosmann (1983), who inferred from Slater *et al.* (1963), that MTT is reduced by mitochondrial succinate dehydrogenase. MTT reduction results in the accumulation of a purple formazan, which can easily be quantified by spectrophotometer. Researchers have reasoned that this assay could give an indication of mitochondrial activity. Since cell line monocultures contain cellular clones, each cell (at a specific stage of the cell cycle) should possess approximately the same number of mitochondria as its neighbours and with the same levels of activity. This means that mitochondrial activity can nicely approximate cell viability as well.

However, in 1993, Berridge and Tan showed that succinate dehydrogenase accounts for less than 10 % of the total cellular MTT reduction, and that most MTT reduction does not occur at the inner mitochondrial membrane. Nearly two decades later, Stockert *et al.* (2012), similarly showed that formazan from MTT does not localise within mitochondria, but instead associates with lipid droplets. Furthermore, Berridge and Tan (1993) discovered that cellular MTT reduction is NAD(P)H-dependent. Hence, according to Berridge *et al.* (2005), MTT is not solely reduced by mitochondrial dehydrogenases, but instead is reduced predominantly by intracellular oxidoreductases. Of course Berridge *et al.* (2005) used a vague term to account for MTT reduction, but this was necessitated by the fact that NADH and NADPH are spectrally indistinguishable from one another (Blacker *et al.*, 2014). This means that it is uncertain whether MTT is predominantly reduced by NADH-dependent or NADPH-dependent enzymes.

Either way, Berridge and Tan (1993) have revealed a link between cellular MTT reduction and the maintenance of  $\Delta\Psi_m$ , namely cytosolic NADH. Both cytosolic and mitochondrial NADH levels are at least partly determined by their  $\text{NAD}^+$  levels (Ying, 2006; Stein and Imai, 2012). Although mitochondrial  $\text{NAD}^+/\text{NADH}$  homeostasis is primarily regulated

internally, it does rely on the shuttling of NAD<sup>+</sup>, NADH and/or their precursors into mitochondria from the cytosol for long term stability (Ying, 2006; Stein and Imai, 2012).

Ultimately, the electron transport system requires NADH to move hydrogen ions from the mitochondrial matrix to the (mitochondrial) intermembrane space. This hydrogen ion concentration gradient produces the mitochondrial membrane potential, which can be revealed with the help of TMRE. Thus, anything which affects cytosolic NADH levels might also affect oxidoreductase activity and  $\Delta\Psi_m$ .

Results from Bernas and Dobrucki (2002) partially support this assertion; they showed that MTT reduction in human hepatoma cells was accompanied by a slight (less than 30 %) drop in  $\Delta\Psi_m$  which then remained stable throughout the MTT reduction process. In the latter study, MTT reduction presumably consumed some cytosolic NADH, resulting in less NADH for mitochondrial use and consequently lowering  $\Delta\Psi_m$ .

#### 4.2.2.2 Green tea and Sertoli cell energy metabolism

A study by Morr e *et al.* (2000) showed that both EGCG and green tea inhibit NADH oxidase activity. These findings were later confirmed by Wu *et al.* (2011) and Li *et al.* (2012); the former even showing that NADH accumulated in the cytosol of EGCG-treated cells. This appears to contradict the findings of this thesis, indicating that a different mechanism may have been active in Sertoli cells.

The increase in  $\Delta\Psi_m$  as a result of green tea treatment may be the key to explaining the MTT results. Instead of being affected by low cytosolic NADH levels, the mitochondria may have been responsible for those levels. Hence, the data from this thesis suggests that green tea (at 25 - 400  $\mu\text{g/ml}$ ) causes an increase in  $\Delta\Psi_m$  which might have increased mitochondrial shuttling of cytosolic NADH. The resulting lower cytosolic NADH levels, in turn may have caused a lower cytosolic oxidoreductase activity (and MTT reduction) in the Sertoli cells. This conclusion is also supported by the lactate experiment, which showed that 100 - 200  $\mu\text{g/ml}$  green tea also caused a reduction in Sertoli cell lactate secretion.

Sertoli cells produce lactate from pyruvate by the enzyme lactate dehydrogenase (LDH), but LDH also oxidises NADH to NAD<sup>+</sup> in the process (Alves *et al.*, 2013). Therefore lower cytosolic NADH levels should result in less lactate secretion, as was the case for green tea. The decline in Sertoli cell lactate secretion due to green tea points to a

negative effect on reproduction, since spermatogenic cells require lactate. However, the difference in lactate levels may still be minor with regards to reproduction, as the lactate levels from the green tea-treated cell were still within 15 % of the negative control.

The academic literature suggest that any negative impact green tea may have on spermatogenesis is outweighed by the positive effects of green tea (see [Table 1.1](#)). Numerous *in vivo* studies show that green tea consumption either improves (Abshenas *et al.*, 2011; Awoniyi *et al.*, 2012; Opuwari, 2013; Sheteifa *et al.*, 2014) or has no effect on sperm quality (Mosbah *et al.*, 2015; Thangapandiyan and Miltonprabu, 2015; Guvvala *et al.*, 2017; Mahmoudi *et al.*, 2018). Sertoli cells play an important role in spermatogenesis, so sperm quality is at least partly determined by the Sertoli cells. Hence, it appears that if the Sertoli cells secrete less lactate in response to green tea *in vivo*, it does not correspondingly lessen/harm spermatogenesis.

Thus, in conclusion, green tea shows a minor shift in Sertoli cell metabolism. This shift appears to be mediated by a stimulation of mitochondrial hyperpolarisation that may lower cytosolic NADH. The consequence thereof is a lower oxidoreductase activity and lactate secretion, though only to within 20 % of the control.

### 4.2.2.3 Green tea and Sertoli cell ROS

Although the ROS assay was unsuccessful for the TM3 cells, the positive and negative controls were significantly different ( $P < 0.05$ ) for the TM4 cells; suggesting a successful assay. This ROS assay showed no difference in the prevalence of ROS-positive cells amongst the green tea-treated cells and the negative control. This suggests that the increased  $\Delta\Psi_m$  observed for 200  $\mu\text{g/ml}$  green tea did not also affect ROS production. Mitochondria are the major producers of cellular ROS, and cells with higher  $\Delta\Psi_m$  are predisposed to producing more ROS (Zorova *et al.*, 2018). Thus, it appears that the antioxidant activity of green tea outweighs any pro-oxidant activity it might have via the mitochondria.

### 4.2.2.4 Problems with the TM4 cell model

The lactate data and the inhibin B data revealed a problem with TM4 cells though; they appear unresponsive to 125 mIU/ml of FSH. This FSH concentration equates to approximately 14  $\mu\text{g/ml}$ , and previous studies showed that 100 ng/ml of FSH was enough to elicit a response in TM4 cells (Musa *et al.*, 2000; Zhang *et al.*, 2012). This means

that the FSH concentration used in the lactate and inhibin secretion experiments were high enough to also have caused a response, but did not. Thus it appears that the TM4 cells (used in this thesis) have lost their sensitivity to FSH.

Furthermore, the TM4 cells may also have lost their ability to secrete inhibin. None of the treatments could produce inhibin levels above 16 pg/ml (the detection limit of the ELISA used). This is despite a study by Liu *et al.* (2014), showing that TM4 cells secreted around 150 pg/ml inhibin after the same treatment period, but with twice as many cells (i.e. 20 000/well).

A study by Alshibani (2016) already gave an indication of potential problems with TM4 cells. Alshibani (2016) showed that TM4 cells could produce more than 200 pg/ml of inhibin (when treated with date palm pollen or a flax seed extract), but required 72 hours of incubation with 50 000 cells per well (in a 24 well plate). Furthermore, Alshibani (2016) showed that even with those adjustments, basal inhibin secretion remained at about 10 pg/ml, which is about 15 times lower than Liu *et al.* (2014) reported. Unfortunately, Alshibani (2016) did not stimulate the cells with FSH (nor did Liu *et al.*, 2014), so we do not know whether the insensitivity to FSH already was apparent or not.

Previous studies show that the TM4 cells express both *Fshr* mRNA (Olugbodi *et al.*, 2019) and FSHR protein (Liu *et al.*, 2014). This suggests that the TM4 cells permit a normal FSH-FSHR interaction. However, it may be possible that a downstream molecule in the FSH-mediated signalling cascade is not functioning properly in the TM4 cells. This molecule must play a role in both inhibin and lactate synthesis/secretion. Alternatively, multiple molecules that affect these processes separately, may be responsible. More studies on the presence and activity of specific signalling molecules would help to elucidate the FSH-insensitivity of the TM4 cells.

### 4.3 The effects of EGCG on testicular cell physiology

#### 4.3.1 Effects of EGCG on Leydig cell health

Almost no EGCG treatments affected TM3 cell oxidoreductase activity compared with the negative control groups. The only exception was the 100  $\mu\text{M}$  EGCG treatment, which produced a significant elevation in oxidoreductase activity. Similarly, the morphology analysis revealed healthy-looking cells that were indistinguishable from the negative control groups. Both lines of evidence suggest that EGCG does not harm Leydig cells within this concentration range.

The EGCG treatment caused a fall in mitochondrial membrane potential at 0.1  $\mu\text{M}$ , but not at 10  $\mu\text{M}$ . Nevertheless, the  $\Delta\Psi_m$  of cells treated with 0.1  $\mu\text{M}$  EGCG were within 20 % of the negative control, implying that it was not harmful to the cells (like the photomicrographs suggest). These findings appear to support those of Webber (2018), who exposed TM3 cells to either 5  $\mu\text{M}$  or 100  $\mu\text{M}$  EGCG and assayed them by flow cytometry. At the concentrations mentioned, Webber (2018) found that EGCG caused an increase in the number of depolarized cells compared to the negative control; though she also noted lower TMRE fluorescence from EGCG-treated cells when observed under microscope. Even so, the percentages of depolarized cells from the EGCG treatments were lower than the depolarization positive control (Webber, 2018), suggesting only a partial depolarization.

Of course, one should bear in mind the drawbacks of using flow cytometry for anchorage-dependent cells (discussed in [section 4.2.1.3](#)). The processing of cells before assaying by flow cytometry may have unintentionally distorted the findings of Webber (2018). This may explain why Webber (2018) found increased depolarization after treatment with 5  $\mu\text{M}$  EGCG, and I found no depolarization from 10  $\mu\text{M}$  EGCG. Nonetheless, Webber's use of fluorescence microscopy adds weight to the validity of her findings. Hence, it appears that EGCG may cause a slight decrease in  $\Delta\Psi_m$  of TM3 cells.

According to Allen *et al.* (2006) and Midzak *et al.* (2011), depolarization of Leydig cell mitochondria leads to a reduction in steroidogenesis. In fact, Allen *et al.* (2006) and Hales *et al.* (2005) both showed that stimulating MA-10 (Leydig) cells with cAMP leads to mitochondrial hyperpolarisation as well as increased steroidogenesis. This suggests that EGCG would similarly decrease steroidogenesis, due to it lowering  $\Delta\Psi_m$ .

According to the qPCR results, EGCG downregulates basal *Star* expression, but also upregulates basal *Tspo* expression. At first, this result may seem contradictory and might also suggest that EGCG produces a net-negative effect on steroidogenesis. According to Fan *et al.* (2018), though, the absolute levels of StAR (protein) might not be as important as its location is; and TPSO appears to mediate StAR localisation at the OMM. In fact, Fan *et al.* (2018) actually found that eliminating TPSO expression from Leydig cells caused an increase in StAR levels, but decreased steroidogenesis. The TPSO-deficient cells may have expressed more StAR protein, but it was confined to the IMM (Fan *et al.*, 2018). On the other hand, the TPSO-expressing cells concentrated their StAR (protein) at the OMM and consequently showed higher steroidogenesis (Fan *et al.*, 2018). This means that EGCG probably produces a net positive effect on basal steroidogenesis, as the increased *Tspo* expression (that should increase TPSO protein levels) would likely result in a better accumulation of StAR where it is most needed.

The fact that the hCG treatment also showed lower *Star* expression with higher *Tspo* expression supports this finding. Furthermore, both conventional and qPCR show that the stimulated expression of both *Star* and *Tspo* were upregulated by EGCG, adding weight to the finding that EGCG is likely pro-steroidogenic. This would agree with Yu *et al.* (2010), who found that EGCG caused an increase in both basal and hCG-stimulated testosterone secretion by rat Leydig cells. In addition, Yu *et al.* (2010) found no significant effects of EGCG on rat StAR protein levels, suggesting that EGCG's effects were not dependent on StAR levels per se. Clearly assessing StAR alone is insufficient to explain the role of EGCG on Leydig cell steroidogenesis.

Unfortunately, as mentioned in [section 4.2.1.1](#), I was unable to measure the effects of EGCG on testosterone steroidogenesis directly. However, the PCR experiments provide some insight into why these TM3 cells were not secreting testosterone.

#### 4.3.1.1 Aberrant TM3 cell gene expression

The conventional PCRs for *Lhcgr*, *Cyp11a1* and *Hsd17b3* all failed to show any amplification, indicating that the TM3 cells might not express mRNA for these genes. Without mRNA expression for these genes (i.e. *Lhcgr*, *Cyp11a1* and *Hsd17b3*), the TM3 cells likely express very little of their proteins, if at all. All three proteins (i.e. LH/CGR, CYP11A1 and 17 $\beta$ HSD3) play essential roles in the normal response of Leydig cells to LH. So the absence of either protein from the TM3 cells could solely explain why they did not release testosterone.

Without LH/CGR, the hCG used to stimulate the TM3 cells would have no way of activating the LH/CGR-mediated signalling cascade for steroidogenesis. Since CYP11A1 (protein) catalyses the first step of steroidogenesis (i.e. the conversion of cholesterol to pregnenolone), its absence would also explain why the basal testosterone secretion from TM3 cells was low. Lastly, 17 $\beta$ HSD3 is responsible for the final step of testosterone synthesis in Leydig cells, so its absence would mean that steroidogenesis would end with dehydroepiandrosterone.

A study by Engeli *et al.* (2018) investigated the mRNA expression of various steroidogenic genes in mouse testis cells (i.e. MA-10 cells, BLTK cells and TM3 cells). Although Engeli *et al.* (2018) did not study *Lhcgr* or *Cyp11a1*, they did investigate *Hsd17b3*, and were also unable to detect any mRNA for *Hsd17b3* from the TM3 cells. However, Engeli *et al.* (2018) could detect *Hsd17b3* from the other cells that they tested, indicating that their primer design was good. This agrees with my findings for *Hsd17b3* and together our studies provide somewhat conclusive evidence that TM3 cells do not express mRNA for *Hsd17b3*. It would be helpful if similar studies were carried out for *Lhcgr* and *Cyp11a1*.

Another observation by Engeli *et al.* (2018) was the detection of mRNA for *Cyp17a1* from TM3 cells. The conventional PCR data of this thesis also detected *Cyp17a1*. However, the qPCR study showed that the primers used gave unacceptable levels of nonspecific amplification. For this reason, those primers could not be used for qPCR study, but another primer design might be helpful for future investigation (perhaps using the same primers as Engeli *et al.*, 2018).

Nonetheless, it is interesting to note that *Cyp17a1*, *Star* and *Tspo* mRNA were all still expressed in the TM3 cells. The proteins of these GOs are normally upregulated by the LH-LH/CGR signal transduction cascade (Stocco *et al.*, 2005); so it is a bit surprising that they were detected, but not *Lhcgr*. This suggests that each of these GOs were expressed as a result of a different process/pathway that does not affect all steroidogenesis proteins equally. It may even be possible that each gene is expressed independently of each other. A review by Andric and Kostic (2019) reveals that the signalling pathways for steroidogenesis are still not fully understood. The revelation, here, that *Star*, *Tspo* and *Cyp17a1* mRNA might be expressed independently of LH/CGR activation may also guide future studies on steroidogenesis.

### 4.3.2 Effects of EGCG on Sertoli cell health

EGCG appears to lower TM4 cell oxidoreductase activity by about 10 % compared with the negative control. Although this lower activity was statistically significant, it remains so close to the control that it might not be physiologically meaningful. At the least, the photo microscopy show that EGCG was not harmful to the cells.

The TMRE experiment showed that 10  $\mu\text{M}$  EGCG produced similar  $\Delta\Psi_m$  to the negative control, and there were no changes in ROS prevalence due to EGCG either. This means that mitochondrial activity could not explain the MTT results for EGCG. Lactate secretion from EGCG-treated cells was also statistically insignificant, indicating that EGCG's effects on MTT reduction were not mediated by NADH either.

As mentioned in [section 4.2.2.2](#), both Morr e *et al.* (2000) and Wu *et al.* (2011) showed that EGCG inhibits NADH oxidase resulting in cytosolic NADH accumulation. One would expect an increase in cytosolic NADH to similarly increase MTT reduction and lactate secretion, but that was not the case here. Wu *et al.* (2011) also showed that EGCG did not inhibit LDH directly, since pyruvate supplementation counteracted EGCG's effect on NADH. Hence, EGCG's effects in Sertoli cell oxidoreductase activity might have been mediated by an effect on its substrate(s).

Interestingly, at 0.1  $\mu\text{M}$  EGCG, the Sertoli cells showed significant ( $P < 0.05$ ) hyperpolarisation. This was not observed in cells exposed to the higher EGCG treatment (i.e. 10  $\mu\text{M}$ ). These TMRE data were normalised to account for the number of cells in each well, so it seems unlikely that this result is an assay artefact. Hence, this result does not reflect the classic toxicology dose-response, where increasing concentrations cause more exaggerated effects (until it causes cell death). Thus, it might be explained by an alternative dose-response model, like hormesis.

Hormesis is a dose-response in which a substance produces a stimulatory effect (usually 30 – 60 % higher than the control) at low dose, but produces no change (compared to the control) at a high dose (usually 10 to 20 times higher dose, but a 100-fold range is not too uncommon) (Calabrese, 2008). According to Calabrese (2008), biological entities overcompensate for the effects of the test substance at low dose, but the mechanism for the hormetic dose-response depends largely on the biological entity under study. Thus, it is unclear how EGCG caused mitochondrial hyperpolarisation at 0.1  $\mu\text{M}$ .



Fortunately, however, Calabrese and Baldwin (1997) have supplied some guidelines for designing studies to investigate hormesis. They recommend using a much larger number of samples, covering a larger range of doses/concentrations, including multiple doses/concentrations within and below the hormetic zone. Later, Calabrese (2008) also recommended studies with multiple time points. Thus, it is inconclusive whether EGCG actually caused a hormetic dose-response or not; but more studies (employing the recommendations of Calabrese and Baldwin, 1997) would go a long way to elucidate these observations.

Whether or not EGCG actually shows hormesis does not change the fact that both the MTT and lactate assays show similar results to the controls. This suggests a potential for EGCG to mildly reduce male fertility. However, the maintenance of the SCB is another important function of Sertoli cells, which also warrants investigation.

The TEER assay revealed that EGCG produced no negative effects on SCB integrity. After 48 hours of exposure, the 0.1  $\mu\text{M}$  EGCG treatment gave significantly higher TEER values than the control. This suggests that the EGCG may have stimulated cell growth and/or the production of tight junctional proteins. At the 72 hour mark, the TEER results were back to being comparable with the control, though.

In general, the EGCG treatments produced similar TEER results to the control group. Therefore EGCG appears to be safe with regards to SCB integrity. These data reveal that EGCG is unlikely to disrupt essential Sertoli cell function *in vivo*.

## 4.4 The effects of green rooibos on testicular cell physiology

### 4.4.1 Effects of green rooibos on Leydig cell health

The TM3 Leydig cells showed a decrease oxidoreductase activity when treated with green rooibos alone, but no change in oxidoreductase activity when co-treated with hCG and green rooibos. These data suggest that hCG interacts directly with green rooibos, offsetting the action of green rooibos on Leydig cells.

Opuwari and Monsees (2015) did not observe statistically significant differences in MTT data for TM3 cells treated with green rooibos. However, they found that co-treatment with green rooibos and hCG produced lower testosterone levels than with hCG alone (Opuwari and Monsees, 2015). This adds weight to the hypothesis that green rooibos constituent interact with hCG directly. Further studies to confirm these findings and to elucidate their interactions are warranted, though.

What is clear from this thesis, is that the lower oxidoreductase activity, caused by green rooibos, was independent of cell death (as revealed by photomicroscopy) as well as  $\Delta\Psi_m$ . Although 200  $\mu\text{g/ml}$  green rooibos produced approximately a 35% decrease in MTT reduction, it produced no effects on  $\Delta\Psi_m$ . This means that it is unlikely that cytosolic NADH levels were affected by the green rooibos, since that would likely have affected the  $\Delta\Psi_m$  as well.

Nonetheless, these experiments show no harmful effects of green rooibos on Leydig cells, which agrees with Opuwari and Monsees (2015). Furthermore, *in vivo* studies with rats generally indicate that green rooibos consumption does not affect serum testosterone levels (Opuwari and Monsees, 2014; Scholms *et al.*, 2014; Manirafasha, 2019). This suggests that the concentration at which Leydig cells were exposed to green rooibos constituents *in vivo* is insufficient to produce noticeable physiological effects on Leydig cells.

### 4.4.2 Effects of green rooibos on Sertoli cell health

Green rooibos showed a decrease in oxidoreductase activity of TM4 cells in the range of 25 to 400 µg/ml. As for the Leydig cell results, the morphology of the TM4 cells was unaffected by green rooibos, indicating that the cells were alive and likely healthy.

However, at 200 µg/ml, the  $\Delta\Psi_m$  showed a significant increase which was not observed in the TM3 cells. The increased  $\Delta\Psi_m$  confirms that the cells were alive at the 200 µg/ml treatment. The lactate secretion showed a decrease in this range, suggesting that mitochondria caused NADH depletion which resulted in lower lactate secretion as well as oxidoreductase activity (just like green tea; [section 4.2.2.2](#)).

According to Opuwari (2013), green rooibos causes an increase in rat sperm concentration, vitality, progressive and total motility; with no change in straight line velocity or average path velocity. However, a subsequent study found that green rooibos had no effect on rat sperm concentration, vitality or total motility; though showing an increase in progressive motility as well as straight line velocity and average path velocity (Manirafasha, 2019). This suggests that, as for green tea, any detrimental effects green rooibos may have on Sertoli cell energy metabolism and lactate secretion are mitigated by other beneficial effects of green rooibos. Alternatively, green rooibos might be so poorly absorbed into plasma that the concentrations (of tea constituents) the testes are exposed to is low enough to produce no effects on physiology.

Furthermore, although the rooibos increased  $\Delta\Psi_m$ , it had no effects on the prevalence of ROS-positive cells. Green rooibos is known for its antioxidant activity and it might have acted as such to counteract ROS accumulation in the TM4 cells.

Thus, green rooibos appears to affect Sertoli cell energy metabolism, causing lower lactate secretion that is unrelated to cell death. Furthermore, it seems unlikely that the aforementioned effects are harmful to reproduction.

## 4.5 The effects of aspalathin on testicular cell physiology

### 4.5.1 Effects of aspalathin on Leydig cell health

Leydig cells showed no change in oxidoreductase activity when treated with aspalathin at most concentrations tested, but showed a significant increase when co-treated with hCG. This, together with the morphology study indicates that there was no drop in cell viability as a result of aspalathin.

However, there was a significant drop in  $\Delta\Psi_m$ , when treated with 0.1  $\mu\text{M}$  aspalathin, which also produced significantly elevated oxidoreductase activity. The inverse relationship between the  $\Delta\Psi_m$  and cytosolic oxidoreductase activity responses to 0.1  $\mu\text{M}$  aspalathin once more suggests a role of NADH. Though in this scenario, cytosolic oxidoreductases (or some other enzymes) might deplete NADH resulting in lower  $\Delta\Psi_m$ .

It should be noted that the MTT and TMRE results for aspalathin are decidedly different to those for green rooibos. Green rooibos produced a decrease in MTT reduction whereas aspalathin showed an increase. On the other hand green rooibos produced no effects on  $\Delta\Psi_m$ , but a low concentration of aspalathin caused some depolarization. This means that aspalathin alone cannot account for the effects of green rooibos on these endpoints. Hence, there appear to be more complex interactions between the green rooibos constituents and the Leydig cells that causes a different physiological response to that of aspalathin alone.

The gene expression experiment revealed that aspalathin has no significant effect on either basal or stimulated *Star* expression. Both aspalathin treatments appear to show increases in *Star* expression, but this was not substantiated by the statistical tests. On the other hand, TM3 cell *Tspo* expression increased significantly ( $P < 0.05$ ) in response to aspalathin. Aspalathin increased basal *Tspo* nine fold and stimulated *Tspo* two fold. This suggests that aspalathin may increase Leydig cell steroidogenesis; since Fan *et al.* (2018), showed that TSPO (protein) levels may be more important than that of StAR.

To my knowledge there are currently no studies on the effects of aspalathin (only) on plasma testosterone levels in either humans or model organisms. In addition, to my knowledge, there are also no conclusive studies on the effects of aspalathin on Leydig cell steroidogenesis (although Webber, 2018 attempted one). However, there are some *in vitro* studies on the effects of aspalathin on other steroidogenic models.

A study by Scholms *et al.* (2012), revealed that aspalathin (and rooibos) caused a decrease in the conversion of pregnenolone by CYP17A1. This was later confirmed by Scholms and Swart (2014) as well as Mugari (2015), suggesting that aspalathin might decrease Leydig cell steroidogenesis. However, Mugari (2015) revealed that aspalathin might not actually inhibit steroidogenesis, it might simply shift steroidogenesis; since it also increased CYP17A1 conversion of progesterone.

Ultimately, though, aspalathin may have no net effect on testosterone synthesis/secretion. One should remember that Mugari (2015) found similar results for rooibos and aspalathin; yet *in vivo* studies show no change in testosterone secretion after rooibos consumption (Opuwari and Monsees, 2014; Scholms *et al.*, 2014; Manirafasha, 2019; Omolaoye, 2020). Furthermore, the increase in *Tspo* mRNA in response to aspalathin indicates that this flavonoid does produce effects on gene expression. Taken together, this suggest that aspalathin might decrease specific enzyme activities, but it might also increase their abundance to counteract its negative effects on enzyme activity.

All in all, these studies largely agree with Webber (2018) that aspalathin is not detrimental to Leydig cells, though they might affect their energy metabolism. Furthermore, these findings indicate that aspalathin alone cannot account for how green rooibos affects Leydig cells. This confirms the assertion that there is a complex interaction between green rooibos constituents and the cells. Lastly, aspalathin appears to increase *Tspo* expression, but not *Star* expression. This suggests that any inhibitory effects aspalathin has on steroidogenic enzymes may be counterbalanced by increasing their expression. Thus, aspalathin appears to cause minor effects on Leydig cell physiology.

#### 4.5.2 Effects of aspalathin on Sertoli cell health

Aspalathin appears to lower TM4 cell oxidoreductase activity within the range of 0.5 to 10  $\mu\text{M}$ . This decrease (in MTT reduction) indicates that aspalathin did affect Sertoli cell physiology, but the lack of a concentration-dependent response makes it unclear how. The photomicroscopy present healthy looking cells, indicating that the decrease in oxidoreductase activity was independent of cell death. This is further supported by the TMRE data, which show no statistical difference in  $\Delta\Psi_m$  as a result of aspalathin. Furthermore, there were no differences in the secretion of lactate when cells were treated with aspalathin or the controls. Altogether, these data indicate that aspalathin –in the tested concentration range– is harmless to Sertoli cells and that its effects on oxidoreductase activity is likely independent of cytosolic NADH, since that would have affected the lactate (and possibly the  $\Delta\Psi_m$ ) results as well.

At first glance, these results appear dissimilar to the effects of green rooibos on the TM4 cells. The high concentration of green rooibos decreased oxidoreductase activity, increased  $\Delta\Psi_m$  and decreased lactate secretion. Only the drop in MTT reduction was common between the green rooibos and aspalathin treatments of TM4 cells. However, the low green rooibos concentration (25  $\mu\text{g/ml}$ ) produced similar MTT results to the aspalathin treatments. This suggests that the aspalathin concentrations used may be too low to illicit any meaningful response in Sertoli cell  $\Delta\Psi_m$  or lactate secretion. This is supported by the fact that even 50  $\mu\text{g/ml}$  green rooibos produced no effect on TMRE and lactate results. Nonetheless, the concentrations used in this thesis are my best guess at the actual concentrations that Sertoli cells are subjected to *in vivo* (see [section 4.1](#)). Thus, one would expect that Sertoli cells would respond similarly after exposure to rooibos.

The 10  $\mu\text{M}$  aspalathin treatment showed a significantly higher prevalence of ROS-positive cells than the negative control cells. This result suggests that aspalathin may have acted as a pro-oxidant in the Sertoli cells. If true, aspalathin might have either activated ROS-producing enzymes (León-González *et al.*, 2015), used metal ions to directly generate ROS (Quideau *et al.*, 2011), or both. However, the 10  $\mu\text{M}$  aspalathin treatment results were no different (statistically) to those of either the EGCG treatments or the 0.1  $\mu\text{M}$  aspalathin treatment; and the latter treatments were no different to the negative control group. This, again, alludes to the problems with using flow cytometry on Sertoli cells ([section 4.2.1.3](#)); suggesting that the 10  $\mu\text{M}$  aspalathin result (for the ROS

assay) was merely an artefact. Thus, the 10  $\mu\text{M}$  aspalathin treatment might not actually increase intracellular ROS.

The TEER data show that aspalathin did not damage the model SCB, similar to the EGCG treatments. Up to 48 hours of treatment, there were no difference in the TEER of the aspalathin treated cells and the negative control cells. Furthermore, at 72 hours, the 10  $\mu\text{M}$  aspalathin treatment produced a significantly higher TEER than the negative control cells did, indicating a potential stimulatory effect on SCB integrity. It is unclear whether aspalathin increased Sertoli cell proliferation or simply increased the abundance of tight junction proteins. Nonetheless, all the experiments indicate a negligible effect of aspalathin on Sertoli cell physiology.



---

(This page was intentionally left blank)



UNIVERSITY *of the*  
WESTERN CAPE



# Chapter 5

---

## Conclusions & Recommendations



UNIVERSITY *of the*  
WESTERN CAPE

## 5.1 General conclusions

In conclusion, there are a lot of studies which indicate that medicinal plant extracts (like green tea and green rooibos) (see the footnotes <sup>2</sup> on page 22 and <sup>3</sup> on page 24 for my semantics of *green tea* and *green rooibos*) show health benefits to humans, and that the health benefits are mediated primarily by their polyphenols (like EGCG and aspalathin). Research on the effects of these teas/flavonoids on male reproduction are sometimes conflicting, and even sparse. Hence, this thesis aimed to study how green tea, green rooibos and their primary polyphenols EGCG and aspalathin affect model Leydig and Sertoli cell physiology.

In general, all the samples (green tea, green rooibos, EGCG and aspalathin) showed mild to no effects on the vitality of either the Leydig or Sertoli cell models. However, the data suggest that both green tea and green rooibos increase mitochondrial activity, resulting in lower cytosolic NADH, consequently decreasing oxidoreductase activity and lactate secretion from Sertoli cells. Contrary to this, their major flavonoids, EGCG and aspalathin did not show the same responses. EGCG showed a general decrease in oxidoreductase activity and lactate secretion, likely via their substrates.

Both EGCG and aspalathin caused slight decreases in mitochondrial membrane polarity without affecting the oxidoreductase activity of Leydig cells. However, the flavonoids alter the expression of certain genes involved in steroidogenesis. EGCG increased both basal and hCG-stimulated *Tspo* expression; as well as hCG-stimulated *Star* expression. On the other hand, aspalathin, showed no effects on *Star* expression, whilst increasing both basal and stimulated *Tspo* expression. All in all, these data suggest that EGCG and aspalathin (alone) show a pro-steroidogenic effect on Leydig cells.

Additionally, this thesis showed problems with the TM3 and TM4 cell models. Although a) several authors reported testosterone secretion in TM3 cells, and b) the TM3 cell population available in the lab also proved to produce testosterone at the start of this study, it seems that those cells lost this ability over time. Namely, TM3 cells were insensitive to hCG; and did not express *Lhcgr*, *Cyp11a1* or *Hsd17b3* mRNA. Moreover, TM4 cells were insensitive to FSH and could not secrete detectable levels of inhibin B.

## 5.2 Recommendations

In light of the discoveries from this thesis, I suggest a few avenues for future study.

Firstly, this thesis showed that energy metabolism may be an important means for EGCG and aspalathin to influence testicular physiology. I thus, recommend a more thorough investigation of this, giving special attention to the role of NADH and LDH in Sertoli cells.

Secondly, research should be done to establish which cell signalling pathways are affected by, especially EGCG and aspalathin; though the study of other polyphenols are also encouraged.

Thirdly, the possibility for a hormetic response was suggested. Therefore, I recommend that future studies consider increasing the number of sample concentrations tested as well as time points.

Fourthly, the discovery that both TM3 and TM4 cells may have changed their physiology over time means that these studies should be performed on different Leydig and Sertoli cell models.

Lastly, the absence of *Lhcgr*, *Cyp11a1* and *Hsd17b3* mRNA from TM3 cells suggests an absence of their proteins; this should be experimentally confirmed. Furthermore, the cell signalling of both TM3 and TM4 cells should be investigated to better understand why and how they deviate from normal testicular cells.



---

(This page was intentionally left blank)



UNIVERSITY *of the*  
WESTERN CAPE

# List of References

---



UNIVERSITY *of the*  
WESTERN CAPE

- Abdelrazek HMA, Helmy SA, Elsayed DH, Ebaid HM, Mohamed RM (2016). Ameliorating effects of green tea extract on cadmium induced reproductive injury in male Wistar rats with respect to androgen receptors and caspase- 3. *Reproductive Biology*; 16: 300-308.
- Abdou HS, Villeneuve G, Tremblay JJ (2013). The calcium signaling pathway regulates Leydig cell steroidogenesis through a transcriptional cascade involving the nuclear receptor NR4A1 and the steroidogenic acute regulatory protein. *Endocrinology*; 154: 511-520.
- Abshenas J, Babaei H, Zare M, Allahbakhshi A, Sharififar F (2011). The effects of green tea (*Camellia sinensis*) extract on mouse semen quality after scrotal heat stress. *Veterinary Research Forum*; 2: 242-247.
- Abuaniza ZAM (2013). Effects of green, black and rooibos tea, coffee and buchu on testosterone production by mouse testicular cultures. MSc Thesis. University of the Western Cape; Cape Town, South Africa.
- Aiyenigba AO, Weeks AD, Rahman A (2019). *African Journal of Reproductive Health*; 23: 76. doi: 10.29063/ajrh2019/v23i2.8.
- Al-Ajmi N, Al-Maghrebi M, Renno WM (2013). (-)-Epigallocatechin-3-gallate modulates the differential expression of survivin splice variants and protects spermatogenesis during testicular torsion. *Korean Journal of Physiology and Pharmacology*; 17: 259-265.
- Allen JA, Shankara T, Janus P, Buck S, Diemer T, Hales KH, Hales DB (2006). Energized, polarized, and actively respiring mitochondria are required for acute Leydig cell steroidogenesis. *Endocrinology*; 147: 3924-3935.
- Al-Maghrebi M, Renno WM, Al-Ajmi N (2012). Epigallocatechin-3-gallate inhibits apoptosis and protects testicular seminiferous tubules from ischemia/reperfusion-induced inflammation. *Biochemical and Biophysical Research Communications*; 420: 434-439.
- Alshibani YA (2016). The effect of Libyan date palm pollen and flax seed on general and specific properties of testicular and breast cancer cells. MSc Thesis. University of the Western Cape; Cape Town, South Africa.
- Alves MG, Rato L, Carvalho RA, Moreira PI, Socorro S, Oliveira PF (2013). Hormonal control of Sertoli cell metabolism regulates spermatogenesis. *Cellular and Molecular Life Sciences*; 70: 777-793.
- Al-Zamely HAN, Al-Maraby NMH (2014). Effect of aqueous green tea extract on male Wistar rats reproductive hormones levels. *Al-Qadisiyah Journal of Veterinary Medicine Sciences*; 14: 98-101.

- Amoako D, Awika JM (2016). Polyphenol interaction with food carbohydrates and consequences on availability of dietary glucose. *Current Opinion in Food Science*; 8: 14-18.
- Andric SA, Kostic TS (2019). Regulation of Leydig cell steroidogenesis: intriguing network of signaling pathways and mitochondrial signalosome. *Current Opinion in Endocrine and Metabolic Research*; 6: 7–20.
- Arts MJTJ, Haenen GRMM, Wilms LC, Beetstra SAJN, Heijnen CGM, Voss H, Bast A (2002). Interactions between flavonoids and proteins: effect on the total antioxidant capacity. *Journal of Agricultural and Food Chemistry*; 50: 1184-1187.
- Awoniyi DO, Aboua YG, Marnewick J, Brooks N (2012). The effects of rooibos (*Aspalathus linearis*), green tea (*Camellia sinensis*) and commercial rooibos and green tea supplements on epididymal sperm in oxidative stress-induced rats. *Phytotherapy Research*; 26: 1231-1239.
- Awoniyi DO, Aboua YG, Marnewick JL, du Plessis SS, Brooks NL (2011). Protective effects of rooibos (*Aspalathus linearis*), green tea (*Camellia sinensis*) and commercial supplements on testicular tissue of oxidative stress-induced rats. *African Journal of Biotechnology*; 10: 17317-17322.
- Ayeleso AO, Oguntibeju OO, Aboua YG, Brooks NL (2014). Effects of red palm oil and rooibos on sperm motility parameters in streptozotocin induced diabetic rats. *African Journal of Traditional, Complement and Alternative Medicines*; 11: 8-15.
- Bangs Laboratories, Inc (2020). *Flow Cytometry Technical Guide*. Fishers, USA: Bangs Laboratories, Inc. 16pp.
- Barrett KE, Barman SM, Boitano S, Brooks HL (2012). *Ganong's review of medical physiology*, 24th edition. New York, USA: McGraw-Hill Medical. 752pp.
- Becton, Dickinson and Company (2002). *Introduction to Flow Cytometry: A Learning Guide*. San Jose, USA: Becton, Dickinson and Company. 52pp.
- Bentes ALA, Borges RS, Monteiro WR, de Macedo LGM, Alves CN (2011). Structure of dihydrochalcones and related derivatives and their scavenging and antioxidant activity against oxygen and nitrogen radical species. *Molecules*; 16: 1749-1760.
- Bergmeyer HU (1975). Neue Werte für die molaren extinktions-koeffizienten von NADH und NADPH zum gebrauch im routine-laboratorium. *Zeitschrift für Klinische Chemie Und Klinische Biochemie*; 11: 507-508.

- Bernas T, Dobrucki J (2002). Mitochondrial and nonmitochondrial reduction of MTT: Interaction of MTT with TMRE, JC-1, and NAO mitochondrial fluorescent probes. *Cytometry*; 47: 236-242.
- Berridge MV, Herst PM, Tan AS (2005). Tetrazolium dyes as tools in cell biology: New insights into their cellular reduction. *Biotechnology Annual Review*; 11: 127-152.
- Berridge MV, Tan AS (1993). Characterization of the cellular reduction of 3-(4,5-dimethylthiazole-2-yl)-2,5-diphenyltetrazolium bromide (MTT): subcellular localization, substrate dependence, and involvement of mitochondrial electron transport in MTT reduction. *Archives of Biochemistry and Biophysics*; 303: 474-478.
- Blacker TS, Mann ZF, Gale JE, Ziegler M, Bain AJ, Szabadkai G, Duchon MR (2014). Separating NADH and NADPH fluorescence in live cells and tissues using FLIM. *Nature Communications*; 5: 3936. doi: 10.1038/ncomms4936
- Blair, TS (1907). A practitioner's handbook of *materia medica* and therapeutics based upon established physiological actions and the indications in small doses. Philadelphia, USA: The Medical Council. 91pp.
- Bloom W, Fawcett DW (1968). A textbook of histology, 9th edition. Philadelphia, USA: W.B. Saunders Company. 858pp.
- Bravo L (1998). Polyphenols: chemistry, dietary sources, metabolism, and nutritional significance. *Nutrition Reviews*; 56: 317-333.
- Breiter T, Laue C, Kressel G, Gröll S, Engelhardt UH, Hahn A (2011). Bioavailability and antioxidant potential of rooibos flavonoids in humans following the consumption of different rooibos formulations. *Food Chemistry*; 128: 338-347.
- Buldan A, Dietze R, Shihan M, Scheiner-Bobis G (2016). Non-classical testosterone signaling mediated through ZIP9 stimulates claudin expression and tight junction formation in Sertoli cells. *Cellular Signalling*; 28: 1075-1085.
- Calabrese EJ (2008). Hormesis: why it is important to toxicology and toxicologists. *Environmental Toxicology and Chemistry*; 27: 1451-474.
- Calabrese EJ, Baldwin LA (1997). The dose determines the stimulation (and poison): development of a chemical hormesis database. *International Journal of Toxicology*; 16: 545-559.
- Černe K, Erman A, Veranič P (2013). Analysis of cytotoxicity of melittin on adherent culture of human endothelial cells reveals advantage of fluorescence microscopy over flow cytometry and haemocytometer assay. *Protoplasma*; 250: 1131-1137.



- Chandra A, Choudhury SR, De N, Sarkar M (2011). Effect of green tea (*Camelia sinensis* L.) extract on morphological and functional changes in adult male gonads of albino rats. *Indian Journal of Experimental Biology*; 49: 689-697.
- Chanphai P, Bourassa P, Kanakis CD, Tarantilis PA, Polissiou MG, Tajmir-Riahi HA (2018). Review on the loading efficacy of dietary tea polyphenols with milk proteins. *Food Hydrocolloids*; 77: 322-328.
- Chaudhry MA (2008). Induction of gene expression alterations by culture medium from trypsinized cells. *Journal of Biological Sciences*; 8: 81-87.
- Chaves LAP, Varanda WA (2008). Volume-activated chloride channels in mice Leydig cells. *Pflügers Archiv - European Journal of Physiology*; 457: 493-504.
- Clulow J, Jones RC (2004). *Biology of Reproduction*; 71: 1508-1516.
- Cooper R, Morr  DJ, Morr  DM (2005). Medicinal benefits of green tea: part i. review of noncancer health benefits. *The Journal of Alternative and Complementary Medicine*; 11: 521-528.
- Cossarizza A, Chang H, Radbruch A, Akdis M, Andr  I, Annunziato F, Bacher P, Barnaba V, Battistini L, Bauer WM, Baumgart S, Becher B, Beisker W, Berek C, Blanco A, Borsellino G, Boulais PE, Brinkman RR, B scher M, Busch DH, Bushnell TP, Cao X, Cavani A, Chattopadhyay PK, Cheng Q, Chow S, Clerici M, Cooke A, Cosma A, Cosmi L, Cumano A, Dang VD, Davies D, De Biasi S, Del Zotto G, Della Bella S, Dellabona P, Deniz G, Dessing M, Diefenbach A, Di Santo J, Dieli F, Dolf A, Donnenberg VS, D rner T, Ehrhardt GRA, Endl E, Engel P, Engelhardt B, Esser C, Everts B, Dreher A, Falk CS, Fehniger TA, Filby A, Fillatreau S, Follo M, F rster I, Foster J, Foulds GA, Frenette PS, Galbraith D, Garbi N, Garc a-Godoy MD, Geginat J, Ghoreschi K, Gibellini L, Goettlinger C, Goodyear CS, Gori A, Grogan J, Gross M, Gr tzkau A, Grummitt D, Hahn J, Hammer Q, Hauser AE, Haviland DL, Hedley D, Herrera G, Herrmann M, Hiepe F, Holland T, Hombrink P, Houston JP, Hoyer BF, Huang B, Hunter CA, Iannone A, J ck H, J vega B, Jonjic S, Juelke K, Jung S, Kaiser T, Kalina T, Keller B, Khan S, Kienh fer D, Kroneis T, Kunkel D, Kurts C, Kvistborg P, Lannigan J, Lantz O, Larbi A, LeibundGut-Landmann S, Leipold MD, Levings MK, Litwin V, Liu Y, Lohoff M, Lombardi G, Lopez L, Lovett-Racke A, Lubberts E, Ludewig B, Lugli E, Maecker HT, Martus G, Matarese G, Mauer der C, McGrath M, McInnes I, Mei HE, Melchers F, Melzer S, Mielenz D, Mills K, Mirrer D, Mj sberg J, Moore J, Moran B, Moretta A, Moretta L, Mosmann TR, M ller S, M ller W, M niz C, Multhoff G, Enrique Munoz L, Murphy KM, Nakayama Y, Nasi M, Neud rfl C, Nolan J, Nourshargh S, O'Connor J, Ouyang W, Oxenius A, Palankar R, Panse I, Peterson P, Peth C,

- Petriz J, Philips D, Pickl W, Piconese S, Pinti M, Pockley AG, Justyna Podolska M, Pucillo C, Quataert SA, Radstake TRDJ, Rajwa B, Rebhahn JA, Recktenwald D, Remmerswaal EBM, Rezvani K, Rico LG, Robinson JP, Romagnani C, Rubartelli A, Ruckert B, Ruland J, Sakaguchi S, Sala-de-Oyanguren F, Samstag Y, Sanderson S, Sawitzki B, Scheffold A, Schiemann M, Schildberg F, Schimisky E, Schmid SA, Schmitt S, Schober K, Schüler T, Ronald Schulz A, Schumacher T, Scotta C, Shankey TV, Shemer A, Simon A, Spidlen J, Stall AM, Stark R, Stehle C, Stein M, Steinmetz T, Stockinger H, Takahama Y, Tarnok A, Tian Z, Toldi G, Tornack J, Traggiai E, Trotter J, Ulrich H, van derBraber M, van Lier RAW, Veldhoen M, Vento-Asturias S, Vieira P, Voehringer D, Volk H, von Volkman K, Waisman A, Walker R, Ward MD, Warnatz K, Warth S, Watson JV, Watzl C, Wegener L, Wiedemann A, Wienands J, Willimsky G, Wing J, Wurst P, Yu L, Yue A, Zhang Q, Zhao Y, Ziegler S, Zimmermann J (2017). Guidelines for the use of flow cytometry and cell sorting in immunological studies. *European Journal of Immunology*; 47: 1584-1797.
- Costa RR, Varanda WA (2007). Intracellular calcium changes in mice Leydig cells are dependent on calcium entry through T-type calcium channels. *The Journal of Physiology*; 585.2: 339-349.
- Costa RR, Varanda WA, Franci CR (2010). A calcium-induced calcium release mechanism supports luteinizing hormone-induced testosterone secretion in mouse Leydig cells. *American Journal of Physiology Cell Physiology*; 299: C316-C323.
- Crespy V, Williamson G (2004). A review of the health effects of green tea catechins in *in vivo* animal models. *The Journal of Nutrition*; 3431S-3440S.
- Crozier A, Del Rio D, Clifford MN (2010). Bioavailability of dietary flavonoids and phenolic compounds. *Molecular Aspects of Medicine*; 31: 446-467.
- Darbre PD (2019). The history of endocrine-disrupting chemicals. *Current Opinion in Endocrine and Metabolic Research*; 7: 26-33.
- Das SK, Karmakar SN (2015). Effect of green tea (*Camellia sinensis* L.) leaf extract on reproductive system of adult male albino rats. *International Journal of Physiology, Pathophysiology and Pharmacology*; 7: 178-184.
- Das S, Thakuria N, Kanodia L (2008). Biological actions and medicinal applications of tea (*Camellia Sinensis*). *Journal of Clinical and Diagnostic Research*; 2: 1215-1225.
- del Corso C, Varanda WA (2003). The resting potential of mouse Leydig cells: role of an electrogenic Na<sup>+</sup>/K<sup>+</sup> pump. *Journal of Membrane Biology*; 191: 123-131.

- Del Rio D, Calani L, Scazzina F, Jechiu L, Cordero C, Brighenti F (2010). Bioavailability of catechins from ready-to-drink tea. *Nutrition*; 26: 528-533.
- Depuydt CE, Mahmoud AM, Dhooge WS, Schoonjans FA, Comhaire FH (1999). Hormonal regulation of inhibin B secretion by immature rat Sertoli cells *in vitro*: possible use as a bioassay for estrogen detection. *Journal of Andrology*; 20: 54-62.
- Diamantina Institute, University of Queensland (2018). Retrieved from: <https://di.uq.edu.au/community-and-alumni/sparq-ed/sparq-ed-services/using-imagej-quantify-blots> [Accessed September, 2018].
- Diamond J (2005). *Guns, germs and steel; a short history of everybody for the last 13,000 years*. London, UK: Vintage. 480pp.
- Ding J, Wang H, Wu Z, Zhao J, Zhang S, Li W (2015). Protection of murine spermatogenesis against ionizing radiation-induced testicular injury by a green tea polyphenol. *Biology of Reproduction*; 92: 1-13.
- Dong Q, Hardy MP (2004). Leydig cell function in man. In: *Male hypogonadism: basic, clinical, and therapeutic principles*. Winters SJ (ed.). Totowa, USA: Humana Press Inc. 396pp.
- Duffy SJ, Keaney JF, Holbrook M, Gokce N, Swerdloff PL, Frei B, Vita JA (2001). Short- and long-term black tea consumption reverses endothelial dysfunction in patients with coronary artery disease. *Circulation*; 104: 151-156.
- Duke JA, Bogenschutz-Godwin MJ, duCellier J, Duke PK (2002). *Handbook of medicinal herbs*, 2nd edition. Boca Raton, USA: CRC Press LLC. 870pp.
- Dyer SJ, Abrahams N, Hoffman M, van der Spuy ZM (2002). Infertility in South Africa: women's reproductive health knowledge and treatment-seeking behaviours for involuntary childlessness. *Human Reproduction*; 17: 1657-1662.
- Dyer SJ, Abrahams N, Mokoena NE van der Spuy ZM (2004). 'You are a man because you have children': experiences, reproductive health knowledge and treatment-seeking behaviour among men suffering from couple infertility in South Africa. *Human Reproduction*; 19: 960-967.
- Dyer SJ (2008). Infertility-related reproductive health knowledge and help-seeking behaviour in African countries. *Human Reproduction*; 2008: 29-33.
- Eldebaky HA, Sabra HA, Abdelaziz SA, Gouda EM, El-Khadrawy HH (2015). Protective effect of green tea (*Camellia sinensis*) extract on p53 gene mutation and reproductive toxicity in male rat. *International Journal of Genetics*; 5: 53-62.
- Engeli RT, Fürstenberger C, Kratschmar DV, Odermatt A (2018). Currently available murine Leydig cell lines can be applied to study early steps of steroidogenesis

- but not testosterone synthesis. *Heliyon*; 4: e00527. doi: 10.1016/j.heliyon.2018.e00527.
- Fan J, Wang K, Zirkin B, Papadopoulos V (2018). CRISPR/Cas9-mediated Tspo gene mutations lead to reduced mitochondrial membrane potential and steroid formation in MA-10 mouse tumor Leydig cells. *Endocrinology*; 159: 1130-1146.
- Ferrazzano GF, Amato I, Ingenito A, Zarrelli A, Pinto G, Pollio A (2011). Plant polyphenols and their anti-cariogenic properties: a review. *Molecules*; 16: 1486-1507.
- Figueiroa MS, Vieira JSBC, Leite DS, Filho RCOA, Ferreira F, Gouveia PS, Udrisar DP, Wanderley MI (2009). Green tea polyphenols inhibit testosterone production in rat Leydig cells. *Asian Journal of Andrology*; 11: 362-370.
- Ge R, Chen G, Hardy MP (2011). The role of the Leydig cell in spermatogenic function. In: *Molecular mechanisms in spermatogenesis*. Cheng CY (ed.). Austin, USA: Landes Bioscience and Springer Science+Business Media, LLC. 274pp.
- Ge J, Han B, Hu H, Liu J, Liu Y (2015). Epigallocatechin-3-O-gallate protects against hepatic damage and testicular toxicity in male mice exposed to di-(2-ethylhexyl) phthalate. *Journal of Medicinal Food*; 18: 753-761.
- Gonçalves GD, Semprebon SC, Biazzi BI, Mantovani MS, Fernandes GSA (2018). Bisphenol A reduces testosterone production in TM3 Leydig cells independently of its effects on cell death and mitochondrial membrane potential. *Reproductive Toxicology*; 76: 26-34.
- Guvvala PR, Ravindra JP, Rajani CV, Sivaram M, Selvaraju S (2017). Protective role of epigallocatechin-3-gallate on arsenic induced testicular toxicity in Swiss albino mice. *Biomedicine & Pharmacotherapy*; 96: 685-694.
- Hales DB, Allen JA, Shankara T, Janus P, Buck S, Diemer T, Hales KH (2005). Mitochondrial function in Leydig cell steroidogenesis. *Annals New York Academy of Sciences*; 1061: 120-134.
- Hassan E, Kahilo K, Kamal T, Hassan M, Elgawish MS (2019). The protective effect of epigallocatechin-3-gallate on testicular oxidative stress in lead-induced toxicity mediated by Cyp19 gene / estradiol level. *Toxicology*; 422: 76-83.
- Hattangady NG, Olala LO, Bollag WB, Rainey WE (2012). Acute and chronic regulation of aldosterone production. *Molecular and Cellular Endocrinology*; 350: 151-162.
- Henning SM, Niu TY, Liu Y, Lee NH, Hara Y, Thames GD, Minutti RR, Carpenter CL, Wang H, Heber D (2005). Bioavailability and antioxidant effect of

- epigallocatechin gallate administered in purified form versus as green tea extract in healthy individuals. *Journal of Nutritional Biochemistry*; 16: 610-616.
- Hess RA, França LR (2005). Structure of the Sertoli Cell. In: *Sertoli cell biology*. Skinner MK, Griswold MD (eds.). San Diego, USA: Elsevier Science. 494pp.
- Hinson J, Raven P, Chew S (2010). The endocrine system, basic science and clinical conditions, 2<sup>nd</sup> edition. Edinburgh, UK: Churchill Livingstone Elsevier. 185pp.
- Hohorst HJ (1957). Enzymatische bestimmung von L(+)-milchsäure. *Biochemische Zeitschrift*; 328: 509-521.
- Iammarrone E, Balet R, Lower AM, Lower C, Grudzinskas JG (2003). Male infertility. *Best Practice & Research Clinical Obstetrics & Gynaecology*; 17: 211-229.
- Intergovernmental Group on Tea (2018). 'Document: CCP:TE 18/2: Emerging trends in tea consumption: informing a generic promotion process'. *Twenty-third session of the Intergovernmental Group on Tea, April 2018, Hangzhou, China*.
- Issop L, Rone MB, Papadopoulos V (2013). Organelle plasticity and interactions in cholesterol transport and steroid biosynthesis. *Molecular and Cellular Endocrinology*; 371: 34-46.
- Jahan-Tigh RR, Ryan C, Obermoser G, Schwarzenberger K (2012). Flow Cytometry. *Journal of Investigative Dermatology*; 132: 1-6.
- Jakobek L (2015). Interactions of polyphenols with carbohydrates, lipids and proteins. *Food Chemistry*; 175: 556-567.
- James PB, Wardle J, Steel A, Adams J (2018). Traditional, complementary and alternative medicine use in Sub-Saharan Africa: a systematic review. *BMJ Glob Health*; 3: e000895. doi: 10.1136/bmjgh-2018-000895.
- Jensen HM, Mottet NK (1970). Ultrastructural changes in keratinizing epithelium following trypsinization, epidermal detachment and apposition to mesenchymes. *Journal of Cell Science*; 6: 511-535.
- Johnson R, Bryant S, Huntley AL (2012). Green tea and green tea catechin extracts: an overview of the clinical evidence. *Maturitas*; 73: 280-287.
- Joubert E, de Beer D (2011). Rooibos (*Aspalathus linearis*) beyond the farm gate: from herbal tea to potential phytopharmaceutical. *South African Journal of Botany*; 77: 869-886.
- Joubert E, Gelderblom WCA, Louw A, de Beer D (2008). South African herbal teas: *Aspalathus linearis*, *Cyclopia* spp. and *Athrixia phylicoides*—a review. *Journal of Ethnopharmacology*; 119: 376-412.
- Jutte NHPM, Jansen R, Grootegoed JA, Rommerts FFG, van der Molen HJ (1983). FSH stimulation of the production of pyruvate and lactate by rat Sertoli cells may

- be involved in hormonal regulation of spermatogenesis. *Journal of Reproduction and Fertility*; 68: 219-226.
- Kang SW, Lee S, Lee EK (2015). ROS and energy metabolism in cancer cells: alliance for fast growth. *Archives of Pharmacal Research*; 38: 338-345.
- Kaur M, Esau L (2015). Two-step protocol for preparing adherent cells for high-throughput flow cytometry. *BioTechniques*; 59: 119-126.
- Khan N, Mukhtar H (2007). Tea polyphenols for health promotion. *Life Sciences*; 81: 519-533.
- Khan WA, Blobe GC, Hannun YA (1995). Arachidonic acid and free fatty acids as second messengers and the role of protein kinase C. *Cellular Signalling*; 7: 171-184.
- Kopera IA, Bilinska B, Cheng CY, Mruk DD (2010). Sertoli-germ cell junctions in the testis: a review of recent data. *Philosophical Transactions of the Royal Society B*; 365: 1593-1605.
- Kraemer FB, Khor VK, Shen W, Azhar S (2013). Cholesterol ester droplets and steroidogenesis. *Molecular and Cellular Endocrinology*; 371: 15-19.
- Krause G, Winkler L, Mueller SL, Haseloff RF, Piontek J, Blasig IE (2008). Structure and function of claudins. *Biochimica et Biophysica Acta*; 1778: 631-645.
- Lambert JD, Yang CS (2003). Cancer chemopreventive activity and bioavailability of tea and tea polyphenols. *Mutation Research*; 523-524: 201-208.
- Leisegang K, Henkel R (2018). The in vitro modulation of steroidogenesis by inflammatory cytokines and insulin in TM3 Leydig cells. *Reproductive Biology and Endocrinology*; 16: 26. doi: <https://doi.org/10.1186/s12958-018-0341-2>.
- León-González AJ, Auger C, Schini-Kerth VB (2015). Pro-oxidant activity of polyphenols and its implication on cancer chemoprevention and chemotherapy. *Biochemical Pharmacology*. Retrieved from: <http://dx.doi.org/10.1016/j.bcp.2015.07.017> [Accessed November, 2015].
- Li B, Vik SB, Tu Y (2012). Theaflavins inhibit the ATP synthase and the respiratory chain without increasing superoxide production. *Journal of Nutritional Biochemistry*; 23: 953-960.
- Liang Y, Ma W, Lu J, Wu Y (2001). Comparison of chemical compositions of *Ilex latifolia* Thumb and *Camellia sinensis* L. *Food Chemistry*; 75: 339-343.
- Liu X, Nie S, Chen Y, Huang D, Xie M (2014). Effects of 4-nonylphenol isomers on cell receptors and mitogen-activated protein kinase pathway in mouse Sertoli TM4 cells. *Toxicology*; 326: 1-8.

- Maecker HT, McCoy Jr JP (2010). A model for harmonizing flow cytometry in clinical trials. *Nature Immunology*; 11: 975-978.
- Mahmoudi R, Azizi A, Abedini S, Jahromi VH, Abidi H, Barmak MJ (2018). Green tea improves rat sperm quality and reduced cadmium chloride damage effect in spermatogenesis cycle. *Journal of Medicine and Life*; 11: 371-380.
- Maloberti P, Cornejo Maciel F, Castillo AF, Castilla R, Duarte A, Toledo MF, Meuli F, Mele P, Paz C, Podestá EJ (2007). Enzymes involved in arachidonic acid release in adrenal and Leydig cells. *Molecular and Cellular Endocrinology*; 265-266: 113-120.
- Manirafasha C (2019). The effects of a green rooibos extract on the reproductive function of obesity-induced insulin resistant or hypertensive male wistar rats. PhD Thesis. Stellenbosch University; Stellenbosch, South Africa.
- Manna PR, Pakarinen P, El-Hefnawy T, Huhtaniemi IT (1999). Functional assessment of the calcium messenger system in cultured mouse Leydig tumor cells: regulation of human chorionic gonadotropin-induced expression of the steroidogenic acute regulatory protein. *Endocrinology*; 140: 1739-1751.
- Marnewick J, Joubert E, Joseph S, Swanevelder S, Swart P, Gelderblom W (2005). Inhibition of tumour promotion in mouse skin by extracts of rooibos (*Aspalathus linearis*) and honeybush (*Cyclopia intermedia*), unique South African herbal teas. *Cancer Letters*; 224: 193-202.
- Martin LJ, Boucher N, El-Asmar B, Tremblay JJ (2009). cAMP-induced expression of the orphan nuclear receptor *Nur77* in MA-10 Leydig cells involves a CaMKI pathway. *Journal of Andrology*; 30: 134-145.
- Martinez-Gonzalez AI, Díaz-Sánchez ÁG, de la Rosa LA, Vargas-Requena CL, Bustos-Jaimes I, Alvarez-Parrilla E (2017). Polyphenolic Compounds and Digestive Enzymes: In Vitro Non-Covalent Interactions. *Molecules*; 22: 669. doi: 10.3390/molecules22040669.
- Mascarenhas MN, Flaxman SR, Boerma T, Vanderpoel S, Stevens GA (2012). National, regional, and global trends in infertility prevalence since 1990: A systematic analysis of 277 health surveys. *PLOS Medicine*; 9: e1001356. doi: 10.1371/journal.pmed.1001356.
- Masuku PN, Unuofin JO, Lebelo SO (2020). Phytochemical content, antioxidant activities and androgenic properties of four South African medicinal plants. *Journal of Herbmед Pharmacology*; 9: 245-256.
- Matzkin ME, Lauf S, Spinnler K, Rossi SP, Köhn FM, Kunz L, Calandra RS, Frungieri MB, Mayerhofer A (2013). The Ca<sup>2+</sup>-activated, large conductance K<sup>+</sup>-channel

- (BK<sub>Ca</sub>) is a player in the LH/hCG signaling cascade in testicular Leydig cells. *Molecular and Cellular Endocrinology*; 367: 41-49.
- McComb RB, Bond LW, Burnett RW, Keech RC, Bowers GN Jr (1976). Determination of the molar absorptivity of NADH. *Clinical Chemistry*; 22: 141-150.
- McFarlin BK, Gary MA (2017). Flow cytometry what you see matters: Enhanced clinical detection using image-based flow cytometry. *Methods*; 112: 1-8.
- Meroni SB, Riera MF, Pellizzari EH, Cigorruga SB (2002). Regulation of rat Sertoli cell function by FSH: possible role of phosphatidylinositol 3-kinase/protein kinase B pathway. *Journal of Endocrinology*; 174: 195-204.
- Mersel M, Benenson A, Delaunoy JP, Devilliers G, Mandel P (1983). Long-term effects of brain trypsinization before cell seeding on cell morphology and surface composition. *Neurochemical Research*; 8: 449-463.
- Midzak AS, Chen H, Aon MA, Papadopoulos V, Zirkin BR (2011). ATP synthesis, mitochondrial function, and steroid biosynthesis in rodent primary and tumor Leydig cells. *Biology of Reproduction*; 84: 976-985.
- Miller WL, Auchus RJ (2011). The molecular biology, biochemistry, and physiology of human steroidogenesis and its disorders. *Endocrine Reviews*; 32: 81-151.
- Morré DJ, Bridge A, Wu LY, Morré DM (2000). Preferential inhibition by (-)-epigallocatechin-3-gallate of the cell surface NADH oxidase and growth of transformed cells in culture. *Biochemical Pharmacology*; 60: 937-946.
- Mosbaha R, Yousef MI, Mantovani A (2015). Nicotine-induced reproductive toxicity, oxidative damage, histological changes and haematotoxicity in male rats: the protective effects of green tea extract. *Experimental and Toxicologic Pathology*; 67: 253-259.
- Mosmann T (1983). Rapid colorimetric assay for cellular growth and survival: application to proliferation and cytotoxicity assays. *Journal of Immunological Methods*; 65: 55-63.
- Moundipa PF, Beboyl NSE, Zelefack F, Ngouela S, Tsamo E, Schill W, Monsees TK (2005). Effects of *Basella alba* and *Hibiscus macranthus* extracts on testosterone production of adult rat and bull Leydig cells. *Asian Journal of Andrology*; 7: 411-417.
- Mruk DD, Cheng CY (2015). The mammalian blood-testis barrier: its biology and regulation. *Endocrine Reviews*; 36: 564-591.
- Mugari MB (2015). The inhibitory effect of Rooibos on cytochromes P450 and downstream *in vitro* modulation of steroid hormones. MSc Thesis. Stellenbosch University; Stellenbosch, South Africa.



- Mukhtar H, Ahmad N (2000). Tea polyphenols: prevention of cancer and optimizing health. *The American Journal of Clinical Nutrition*; 71: 1698S–1702S.
- Muller CJF, Joubert E, de Beer D, Sanderson M, Malherbe CJ, Fey SJ, Louw J (2012). Acute assessment of an aspalathin-enriched green rooibos (*Aspalathus linearis*) extract with hypoglycemic potential. *Phytomedicine*; 20: 32-39.
- Musa FRM, Takenaka I, Konishi R, Tokuda M (2000). Effects of luteinizing hormone, follicle-stimulating hormone, and epidermal growth factor on expression and kinase activity of cyclin-dependent kinase 5 in Leydig TM3 and Sertoli TM4 cell lines. *Journal of Andrology*; 21: 392-402.
- Nahid Z, Tavakol HS, Abolfazl GK, Leila M, Negar M, Hamed F, Akram R (2016). Protective role of green tea on malathion-induced testicular oxidative damage in rats. *Asian Pacific Journal of Reproduction*; 5: 42-45.
- National Center for Biotechnology Information (2016). Retrieved from: at <https://www.ncbi.nlm.nih.gov/gene> [Accessed February, 2016].
- Narotzki B, Reznick AZ, Aizenbud D, Levy Y (2012). Green tea: a promising natural product in oral health. *Archives of Oral Biology*; 57: 429-435.
- Nozaki A, Hori M, Kimura T, Ito H, Hatano T (2009). Interaction of polyphenols with proteins: binding of (-)-epigallocatechin gallate to serum albumin, estimated by induced circular dichroism. *Chemical and Pharmaceutical Bulletin*; 57: 224-228.
- Olugbodi JO, David O, Ojo OA, Akinmoladun AC (2019). Influence of *Glyphaea brevis* twig extract on nucleus, tight junctions and expression of inhibin- $\beta$ , stem cell factor, and androgen binding protein in TM4 Sertoli cells. *Asian Pacific Journal of Reproduction*; 8: 157-166.
- Omolaoye TS (2020). The possible ameliorating effects of rooibos, honeybush and sutherlandia on diabetes-induced reproductive impairment in adult male Wistar rats. PhD Thesis. Stellenbosch University; Stellenbosch, South Africa.
- Opuwari CS (2013). Effect of tea and herbal infusions on mammalian reproduction and fertility. PhD Thesis. University of the Western Cape; Cape Town, South Africa.
- Opuwari CS, Monsees TK (2014). *In vivo* effects of *Aspalathus linearis* (rooibos) on male rat reproductive functions. *Andrologia*; 46: 867-877.
- Opuwari CS, Monsees TK (2015). Reduced testosterone production in TM3 Leydig cells treated with *Aspalathus linearis* (rooibos) or *Camellia sinensis* (tea). *Andrologia*; 47: 52-58

- Opuwari CS, Monsees TK (2020). Green tea consumption increases sperm concentration and viability in male rats and is safe for reproductive, liver and kidney health. *Scientific Reports*; 10: 15269. doi: <https://doi.org/10.1038/s41598-020-72319-6>.
- Pandey AK, Li W, Yin X, Stocco DM, Grammas P, Wang XJ (2010). Blocking L-type calcium channels reduced the threshold of cAMP-induced steroidogenic acute regulatory gene expression in MA-10 mouse Leydig cells. *Journal of Endocrinology*; 204: 67-74.
- Panesar NS, Chan KW (2005). Chloride efflux in unstimulated Leydig cells causes autonomous cAMP production and stimulatory/inhibitory steroidogenesis with an efflux inhibitor. *Steroids*; 70: 652-659.
- Pantsi WG, Marnewick JL, Esterhuyse AJ, Rautenbach F, van Rooyen J (2011). Rooibos (*Aspalathus linearis*) offers cardiac protection against ischaemia/reperfusion in the isolated perfused rat heart. *Phytomedicine*; 18: 1220-1228.
- Pfaffl MW (2004). Quantification strategies in real-time PCR. In: *A-Z of quantitative PCR*. Bustin SA (ed.). La Jolla, USA: International University Line (IUL). 87-112.
- Poderoso C, Duarte A, Cooke M, Orlando U, Gottifredi V, Solano AR, Lemos JR, Podestá EJ (2013). The spatial and temporal regulation of the hormonal signal. Role of mitochondria in the formation of a protein complex required for the activation of cholesterol transport and steroids synthesis. *Molecular and Cellular Endocrinology*; 371: 26-33.
- Quideau S, Deffieux D, Douat-Casassus C, Pouységu L (2011). Plant polyphenols: chemical properties, biological activities, and synthesis. *Angewandte Chemie, International Edition*; 50: 586-621.
- Raaphorst GP, Sapareto SA, Freeman ML, Dewey WC (1979). Changes in cellular heat and/or radiation sensitivity observed at various times after trypsinization and plating. *International Journal of Radiation Biology and Related Studies in Physics, Chemistry and Medicine*; 35: 193-197.
- Rahman M (2006). *Introduction to Flow Cytometry*. Oxford, UK: Serotec Ltd. 33pp.
- Raj Narayana K, Sripal Reddy M, Chaluvadi MR, Krishna DR (2001). Bioflavonoids classification, pharmacological, biochemical effects and therapeutic potential. *Indian Journal of Pharmacology*; 33: 2-16.
- Ramnath HI, Peterson S, Michael AE, Stocco DM, Cooke BA (1997). Modulation of steroidogenesis by chloride ions in MA-10 mouse tumor Leydig cells: roles of

- calcium, protein synthesis, and the steroidogenic acute regulatory protein. *Endocrinology*; 138: 2308-2314.
- Reczek CR, Chandel NS (2015). ROS-dependent signal transduction. *Current Opinion in Cell Biology*; 33: 8-13.
- Rezk HM, Elsherbiny M, Elkashef WF, Taha M (2014). Effect of green tea extract on the interferon-induced testicular apoptosis in the adult albino rat: immunohistochemical and electron microscopic study. *Reproductive System and Sexual Disorders*; 3: doi: 10.4172/2161-038X.1000146.
- Riera MF, Meroni SB, Gómez GE, Schteingart HF, Pellizzari EH, Cigorraga SB (2001). Regulation of lactate production by FSH, IL1 $\beta$ , and TNF $\alpha$  in rat Sertoli cells. *General and Comparative Endocrinology*; 122: 88-97.
- Rio DD, Stewart AJ, Mullen W, Burns J, Lean MEJ, Brighenti F, Crozier A (2004). HPLC-MS<sup>n</sup> analysis of phenolic compounds and purine alkaloids in green and black tea. *Journal of Agricultural and Food Chemistry*; 52: 2807-2815.
- Rowe PJ, Comhaire FH, Hargreave TB, Mellows HJ (1993). WHO manual for the standard investigation and diagnosis of the infertile couple. Cambridge, UK: Cambridge University Press. 50pp.
- Ruxton CHS (2008). Black tea and health. *British Nutrition Foundation Nutrition Bulletin*; 33: 91-101.
- Sandoval-Acuña C, Ferreira J, Speisky H (2014). Polyphenols and mitochondria: An update on their increasingly emerging ROS-scavenging independent actions. *Archives of Biochemistry and Biophysics*; 559: 75-90.
- Satoh K, Sakamoto Y, Ogata A, Nagai F, Mikuriya H, Numazawa M, Yamada K, Aoki N (2002). Inhibition of aromatase activity by green tea extract catechins and their endocrinological effects of oral administration in rats. *Food and Chemical Toxicology*; 40: 925-933.
- Schneider C, Segre T (2009). Green tea: potential health benefits. *American Family Physician*; 79: 591-594.
- Schloms L, Storbeck K, Swart P, Gelderblom WCA, Swart AC (2012). The influence of *Aspalathus linearis* (Rooibos) and dihydrochalcones on adrenal steroidogenesis: quantification of steroid intermediates and end products in H295R cells. *Journal of Steroid Biochemistry & Molecular Biology*; 128: 128-138.
- Schloms L, Swart AC (2014). Rooibos flavonoids inhibit the activity of key adrenal steroidogenic enzymes, modulating steroid hormone levels in H295R cells. *Molecules*; 19: 3681-3695.

- Sewpaul V (1999). Culture religion and infertility: a South African perspective. *British Journal of Social Work*; 29: 741-754.
- Serdiuk T, Alekseev S, Lysenko V, Skryshevsky V, Géloën A (2014). Trypsinization-dependent cell labeling with fluorescent nanoparticles. *Nanoscale Research Letters*; 9: 568. doi: 10.1186/1556-276X-9-568.
- Schug TT, Johnson AF, Birnbaum LS, Colborn T, Guillette LJ Jr., Crews DP, Collins T, Soto AM, vom Saal FS, McLachlan JA, Sonnenschein C, Heindel JJ (2016). Minireview: Endocrine Disruptors: Past Lessons and Future Directions. *Molecular Endocrinology*; 30: 833-847.
- Setchell BP (1986). The movement of fluids and substances in the testis. *Australian Journal of Biological Sciences*; 39: 193-207.
- Sharpe RM (2005). Sertoli cell endocrinology and signal transduction: androgen regulation. In: *Sertoli cell biology*. Skinner MK, Griswold MD (eds.). San Diego, USA: Elsevier Science. 494pp.
- Shen F, Chen H (2008). Element composition of tea leaves and tea infusions and its impact on health. *Bulletin of Environmental Contamination and Toxicology*; 80: 300-304.
- Sheteifa MAM, Morsy WA (2014). Effect of green tea as dietary supplements (*Camellia sinensis*) on semen quality and testosterone profile in rabbits. *Journal of Animal and Poultry Production*; 5: 1-13.
- Slater TF, Sawyer B, Sträuli U (1963). Studies on succinate-tetrazolium reductase systems: III. Points of coupling of four different tetrazolium salts III. *Biochimica et Biophysica Acta*; 77: 383-393.
- Spencer JPE, Abd El Mohsen MM, Rice-Evans C (2004). Cellular uptake and metabolism of flavonoids and their metabolites: implications for their bioactivity. *Archives of Biochemistry and Biophysics*; 423: 148-161.
- Stein LR, Imai S (2012). The dynamic regulation of NAD metabolism in mitochondria. *Trends in Endocrinology and Metabolism*; 23: 420-428.
- Stocco DM, Wang XJ, Jo Y, Manna PR (2005). Multiple signaling pathways regulating steroidogenesis and steroidogenic acute regulatory protein expression: more complicated than we thought. *Molecular Endocrinology*; 19: 2647-2659.
- Stockert JC, Blázquez-Castro A, Cañete M, Horobin RW, Villanueva Á (2012). MTT assay for cell viability: Intracellular localization of the formazan product is in lipid droplets. *Acta Histochemica*; 114: 785-796.

- Sugiyama S, Chiba M, Nakagami T, Kawano S, Sanada Y, Tajiri T, Toki A (2012). Beneficial effects of (-)-epigallocatechin gallate on ischemia-reperfusion testicular injury in rats. *Journal of Pediatric Surgery*; 47: 1427-1432.
- Sutradhar BC, Park J, Hong G, Choi SH, Kim G (2010). Effects of trypsinization on viability of equine chondrocytes in cell culture. *Pakistan Veterinary Journal*; 30: 232-238.
- Tan LC, Koh L, Yuan J, Wang R, Au W, Tan JH, Tan E, Yu MC (2008). Differential effects of black versus green tea on risk of Parkinson's disease in the Singapore Chinese health study. *American Journal of Epidemiology*; 167: 553-560.
- Thangapandian S, Miltonprabu S (2015). Epigallocatechin gallate exacerbates fluoride-induced oxidative stress mediated testicular toxicity in rats through the activation of Nrf2 signaling pathway. *Asian Pacific Journal of Reproduction*; 4: 272-287.
- Tindall DJ, Tash JS, Means AR (1981). Factors affecting Sertoli cell function in the testis. *Environmental Health Perspectives*; 38: 5-10.
- Tsao R (2010). Chemistry and biochemistry of dietary polyphenols. *Nutrients*; 2: 1231-1246.
- Valcic S, Muders A, Jacobsen NE, Liebler DC, Timmermann BN (1999). Antioxidant chemistry of green tea catechins. Identification of products of the reaction of (-)-epigallocatechin gallate with peroxy radicals. *Chemical Research in Toxicology*; 12: 382-386.
- van der Merwe JD, Joubert E, Richards ES, Manley M, Snijman PW, Marnewick JL, Gelderblom WCA (2006). A comparative study on the antimutagenic properties of aqueous extracts of *Aspalathus linearis* (rooibos), different *Cyclopia* spp. (honeybush) and *Camellia sinensis* teas. *Mutation Research*; 611: 42-53.
- van der Strate B, Longdin R, Geerlings M, Bachmayer N, Cavallin M, Litwin V, Patel M, Passe-Coutrin W, Schoelch C, Companjen A, Fjording MS (2017). Best practices in performing flow cytometry in a regulated environment: feedback from experience within the European Bioanalysis Forum. *Bioanalysis*; 9: 1253-1264.
- van Vliet AR, Verfaillie T, Agostinis P (2014). New functions of mitochondria associated membranes in cellular signaling. *Biochimica et Biophysica Acta*; 1843: 2253-2262.
- van Wyk BE (2008). A broad review of commercially important southern African medicinal plants. *Journal of Ethnopharmacology*; 119: 342-355.

- Van Wyk BE, Gorelik B (2017). The history and ethnobotany of Cape herbal teas. *South African Journal of Botany*; 110: 18-38.
- Velayutham P, Babu A, Liu D (2008). Green tea catechins and cardiovascular health: an update. *Current Medical Chemistry*; 15: 1840-1850.
- Vogl AW, Vaid KS, Guttman JA (2011). The Sertoli cell cytoskeleton. In: *Molecular mechanisms in spermatogenesis*. Cheng CY (ed.). Austin, USA: Landes Bioscience and Springer Science+Business Media, LLC. 274pp.
- von Gadow A, Joubert E, Hansmann CF (1997). Comparison of the antioxidant activity of rooibos tea (*Aspalathus linearis*) with green, oolong and black tea. *Food Chemistry*; 60: 73-77.
- Walker WH, Cheng J (2005). FSH and testosterone signaling in Sertoli cells. *Reproduction*; 130: 15-28.
- Walker WH (2009). Molecular mechanisms of testosterone action in spermatogenesis. *Steroids*; 74: 602-607.
- Walton JR (1975). The systematic appraisal of cellular injury. *Agents and Actions*; 5: 394-400.
- Wang H, Provan GJ, Helliwell K (2003). HPLC determination of catechins in tea leaves and tea extracts using relative response factors. *Food Chemistry*; 81: 307-312.
- Wang XJ, Dyson MT, Mondillo C, Patrignani Z, Pignataro O, Stocco DM (2002). Interaction between arachidonic acid and cAMP signaling pathways enhances steroidogenesis and StAR gene expression in MA-10 Leydig tumor cells. *Molecular and Cellular Endocrinology*; 188: 55-63.
- Webber TJ (2018). The effect of rooibos and green tea flavonoids on the physiology of TM3 Leydig cells. MSc Thesis. University of the Western Cape; Cape Town, South Africa.
- Weinbauer GF, Luetjens CM, Simoni M, Nieschlag E (2010). Physiology of Testicular Function. In: *Andrology, male reproductive health and dysfunction*. Nieschlag E, Behre HM, Nieschlag S (eds.). Berlin, Germany: Springer. 629pp.
- World Health Organization (2002). WHO Traditional medicine strategy 2005-2005. Geneva, Switzerland: WHO. 61pp.
- World Health Organization (2013). WHO traditional medicine strategy 2014-2023. Geneva, Switzerland: WHO. 76pp.
- Wright JS, Johnson ER, DiLabio GA (2001). Predicting the activity of phenolic antioxidants: theoretical method, analysis of substituent effects, and application to major families of antioxidants. *Journal of the American Chemical Society*; 123: 1173-1183.

## List of References

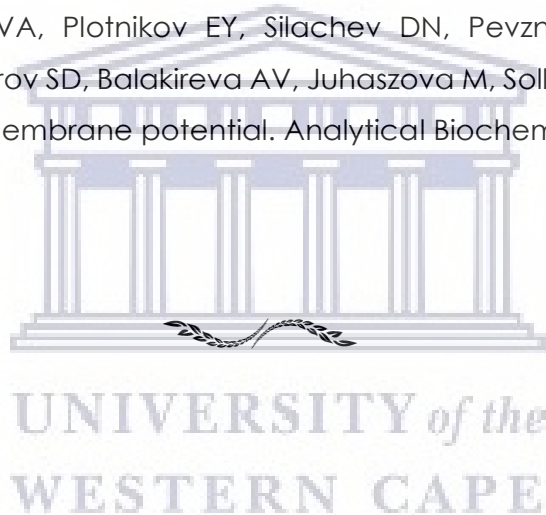
---

- Wu LY, De Luca T, Watanabe T, Morr  DM, Morr  DJ (2011). Metabolite modulation of HeLa cell response to ENOX2 inhibitors EGCG and phenoxodiol. *Biochimica et Biophysica Acta*; 1810: 784-789.
- Wulff S (2006). *Flow Cytometry Educational Guide*, 2<sup>nd</sup> edition. Carpinteria, USA: Dako. 120pp.
- www.ensembl.org (2020a). Retrieved from: [https://www.ensembl.org/Mus\\_musculus/Gene/Summary?db=core;g=ENSMUSG00000057666;r=6:125161715-125166467](https://www.ensembl.org/Mus_musculus/Gene/Summary?db=core;g=ENSMUSG00000057666;r=6:125161715-125166467) [Accessed March, 2020]
- www.ensembl.org (2020b). Retrieved from: [http://www.ensembl.org/Mus\\_musculus/Gene/Summary?db=core;g=ENSMUSG00000024107;r=17:88716481-88791990](http://www.ensembl.org/Mus_musculus/Gene/Summary?db=core;g=ENSMUSG00000024107;r=17:88716481-88791990) [Accessed March, 2020]
- www.ensembl.org (2020c). Retrieved from: [http://www.ensembl.org/Mus\\_musculus/Gene/Summary?g=ENSMUSG00000031574;r=8:25806555-25815982](http://www.ensembl.org/Mus_musculus/Gene/Summary?g=ENSMUSG00000031574;r=8:25806555-25815982) [Accessed March, 2020]
- www.ensembl.org (2020d). Retrieved from: [http://www.ensembl.org/Mus\\_musculus/Gene/Summary?g=ENSMUSG00000041736;r=15:83563592-83574203](http://www.ensembl.org/Mus_musculus/Gene/Summary?g=ENSMUSG00000041736;r=15:83563592-83574203) [Accessed March, 2020]
- www.ensembl.org (2020e). Retrieved from: [http://www.ensembl.org/Mus\\_musculus/Gene/Summary?g=ENSMUSG00000032323;r=9:58006411-58027023](http://www.ensembl.org/Mus_musculus/Gene/Summary?g=ENSMUSG00000032323;r=9:58006411-58027023) [Accessed March, 2020]
- www.ensembl.org (2020f). Retrieved from: [http://www.ensembl.org/Mus\\_musculus/Gene/Summary?g=ENSMUSG00000003555;r=19:46667165-46673172](http://www.ensembl.org/Mus_musculus/Gene/Summary?g=ENSMUSG00000003555;r=19:46667165-46673172) [Accessed March, 2020]
- www.ensembl.org (2020g). Retrieved from: [http://www.ensembl.org/Mus\\_musculus/Gene/Summary?g=ENSMUSG00000033122;r=13:64058266-64089230](http://www.ensembl.org/Mus_musculus/Gene/Summary?g=ENSMUSG00000033122;r=13:64058266-64089230) [Accessed March, 2020]
- www.gulliverstea.com (2016). Retrieved from: <https://www.gulliverstea.com.au/wp-content/uploads/2015/01/green-red-rooibos.jpg> [Accessed January, 2016]
- www.maultasch.us (2016). Retrieved from: <http://www.maultasch.us/wp-content/uploads/2014/01/green-tea-plant.jpg> [Accessed January, 2016]
- www.nexcesscdn.net (2016). Retrieved from: <http://lghttp.32478.nexcesscdn.net/80E972/organiclifestylemagazine/wp-content/uploads/2013/10/Green-Tea-Leaves.jpg> [Accessed January, 2016]

- www.s3.amazonaws.com (2015). Retrieved from:  
<https://s3.amazonaws.com/classconnection/682/flashcards/3453682/jpg/picture1-14ADA3A98F4237AE697.jpg> [Accessed October, 2015].
- www.tumblr.com (2016). Retrieved from:  
[http://41.media.tumblr.com/3b7ea5b7386ee15c54751d6ee4957db8/tumblr\\_nhd8qaUpXZ1sbs2szo1\\_1280.jpg](http://41.media.tumblr.com/3b7ea5b7386ee15c54751d6ee4957db8/tumblr_nhd8qaUpXZ1sbs2szo1_1280.jpg) [Accessed January, 2016]
- www.virtualslides.med.umich.edu (2015). Retrieved from:  
[http://virtualslides.med.umich.edu/Histology/Male%20Reproductive%20System/275\\_HISTO\\_40X.svs/view.apml?cwidth=800&cheight=485&chost=virtualslides.med.umich.edu&csis=1](http://virtualslides.med.umich.edu/Histology/Male%20Reproductive%20System/275_HISTO_40X.svs/view.apml?cwidth=800&cheight=485&chost=virtualslides.med.umich.edu&csis=1) [Accessed October, 2015].
- www.wordpress.com (2016). Retrieved from:  
<https://sociorocketnewsen.files.wordpress.com/2013/09/nj-1.jpg?w=580&h=524> [Accessed January, 2016]
- Xiao J, Zhao Y, Wang H, Yuan Y, Yang F, Zhang C, Yamamoto K (2011). Noncovalent interaction of dietary polyphenols with common human plasma proteins. *Journal of Agricultural and Food Chemistry*; 59: 10747-10754.
- Yang CS, Chen L, Lee M, Balentine D, Kuo MC, Schantz SP (1998). Blood and urine levels of tea catechins after ingestion of different amounts of green tea by human volunteers. *Cancer Epidemiology, Biomarkers & Prevention*; 7: 351-354.
- Yang CS, Wang H, Li GX, Yang Z, Guan F, Jin H (2011). Cancer prevention by tea: evidence from laboratory studies. *Pharmacological Research*; 64: 113-122.
- Yang XR, Ye CX, Xu JK, Jiang YM (2007). Simultaneous analysis of purine alkaloids and catechins in *Camellia sinensis*, *Camellia ptilophylla* and *Camellia assamica* var. *kucha* by HPLC. *Food Chemistry*; 100: 1132-1136.
- Ying W (2006). NAD<sup>+</sup> and NADH in cellular functions and cell death. *Frontiers in Bioscience*; 11: 3129-3148.
- Young B, Heath JW (2000). Wheater's functional histology, 4<sup>th</sup> edition. Edinburgh, UK: Churchill Livingstone. 413pp.
- Yu P, Pu H, Chen S, Wang S, Wang PS (2010). Effects of catechin, epicatechin and epigallocatechin gallate on testosterone production in rat Leydig cells. *Journal of Cellular Biochemistry*; 110: 333-342.
- Zaher KS, Ahmed WM, Zerizer SN (2008). Observations on the biological effects of black cumin seed (*Nigella sativa*) and green tea (*Camellia sinensis*). *Global Veterinaria*; 2: 198-204.
- Zanchi MM, Manfredini V, dos Santos Brum D, Vargas LM, Spiazzi CC, Soares MB, Izaguirry AP, Santos FW (2015). Green tea infusion improves



- cyclophosphamide-induced damage on male mice reproductive system. *Toxicology Reports*; 2: 252-260.
- Zaveri NT (2006). Green tea and its polyphenolic catechins: medicinal uses in cancer and noncancer applications. *Life Sciences*; 78: 2073-2080.
- Zhang S (1999). *An atlas of histology*. New York, USA: Springer-Verlag. 426pp.
- Zhang S, Li W, Zhu C, Wang X, Li Z, Zhang J, Zhao J, Hu J, Li Y, Zhang Y (2012). Sertoli cell-specific expression of metastasis-associated protein 2 (MTA2) is required for transcriptional regulation of the follicle-stimulating hormone receptor (FSHR) gene during spermatogenesis. *The Journal of Biological Chemistry*; 287: 40471-40483.
- Zhu Y, Huang H, Tu Y (2006). A review of recent studies in China on the possible beneficial health effects of tea. *International Journal of Food Science and Technology*; 41: 333-340.
- Zorova LD, Popkov VA, Plotnikov EY, Silachev DN, Pevzner IB, Jankauskas SS, Babenko VA, Zorov SD, Balakireva AV, Juhaszova M, Sollott SJ, Zorov DB (2018). Mitochondrial membrane potential. *Analytical Biochemistry*; 552: 50-59.



---

(This page was intentionally left blank)



UNIVERSITY *of the*  
WESTERN CAPE

# Appendices

---



UNIVERSITY *of the*  
WESTERN CAPE

## Appendix I

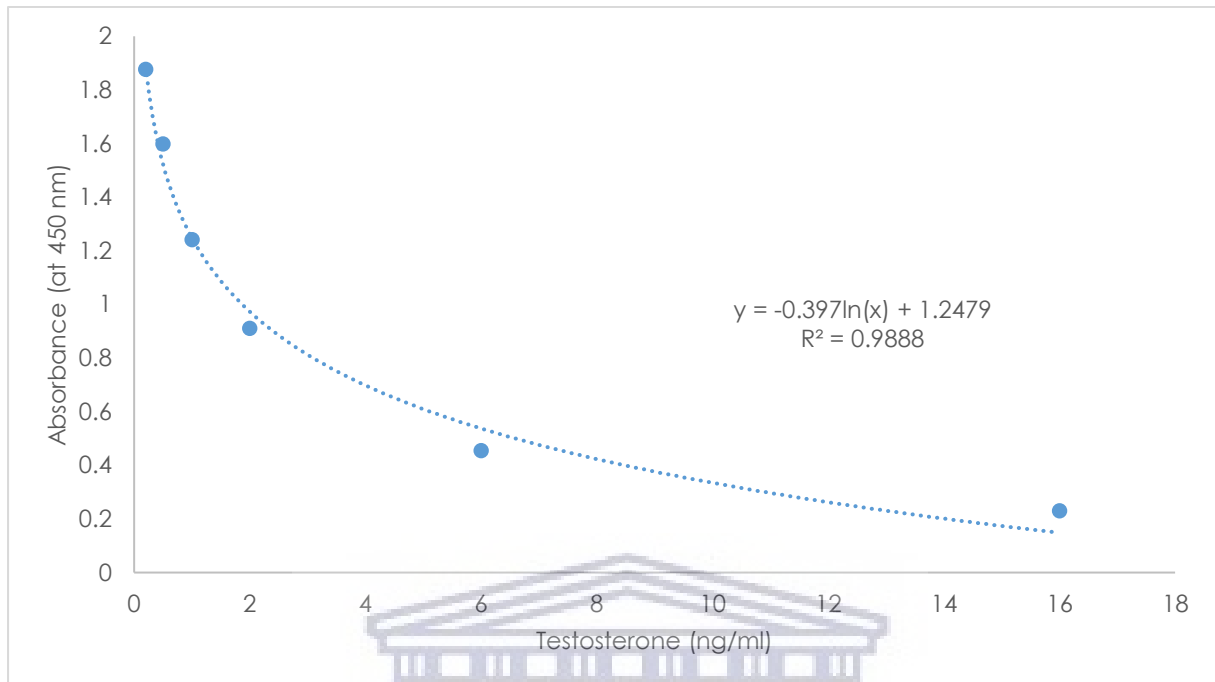


Figure I. Graph showing a standard curve used for testosterone quantitation via ELISA.

## Appendix II

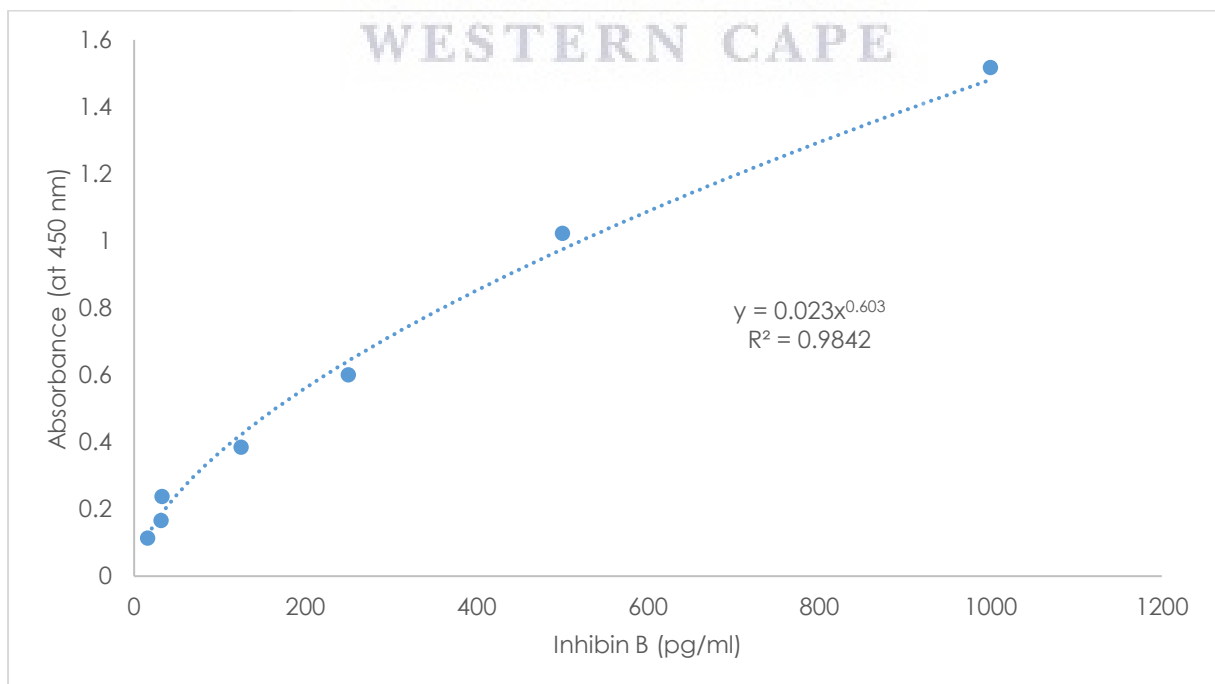
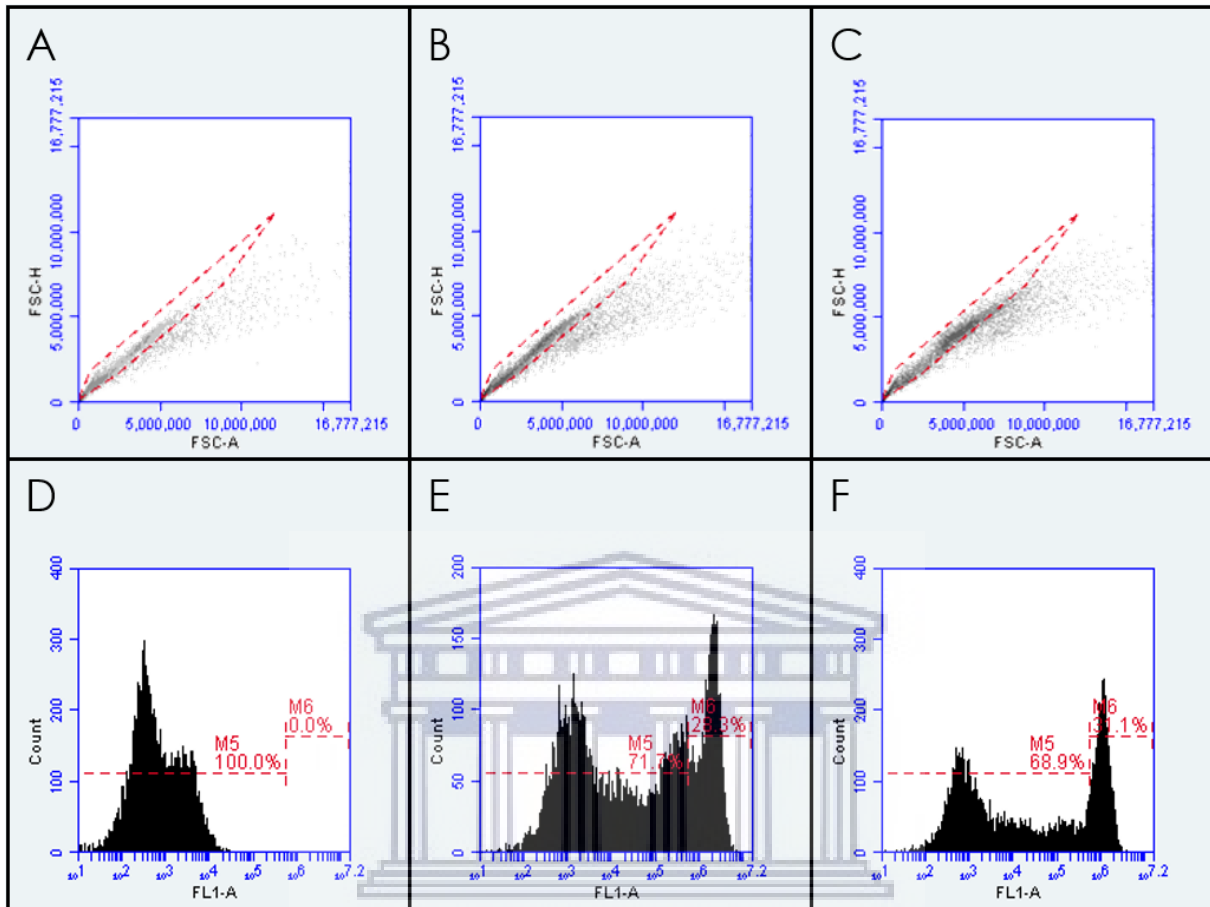


Figure II. Graph showing the standard curve used for inhibin B quantitation via ELISA.

Appendix III



**Figure III. Representative scatter plots and histograms showing the gating strategy for TM3 cell ROS determination.** **A:** scatter plot for unlabelled negative control cells, **B:** scatter plot for labelled negative control cells; **C:** scatter plot for cells treated with 100 µM H<sub>2</sub>O<sub>2</sub> (positive control), **D:** histogram for ROS determination of the unlabelled negative control; **E:** histogram for ROS determination of the negative control; **F:** histogram for ROS determination of the positive control. The cells were exposed to the indicated treatment for 24 hours and were subsequently labelled with CM-H<sub>2</sub>DCFDA, except for the unlabelled cells.

## Appendix IV

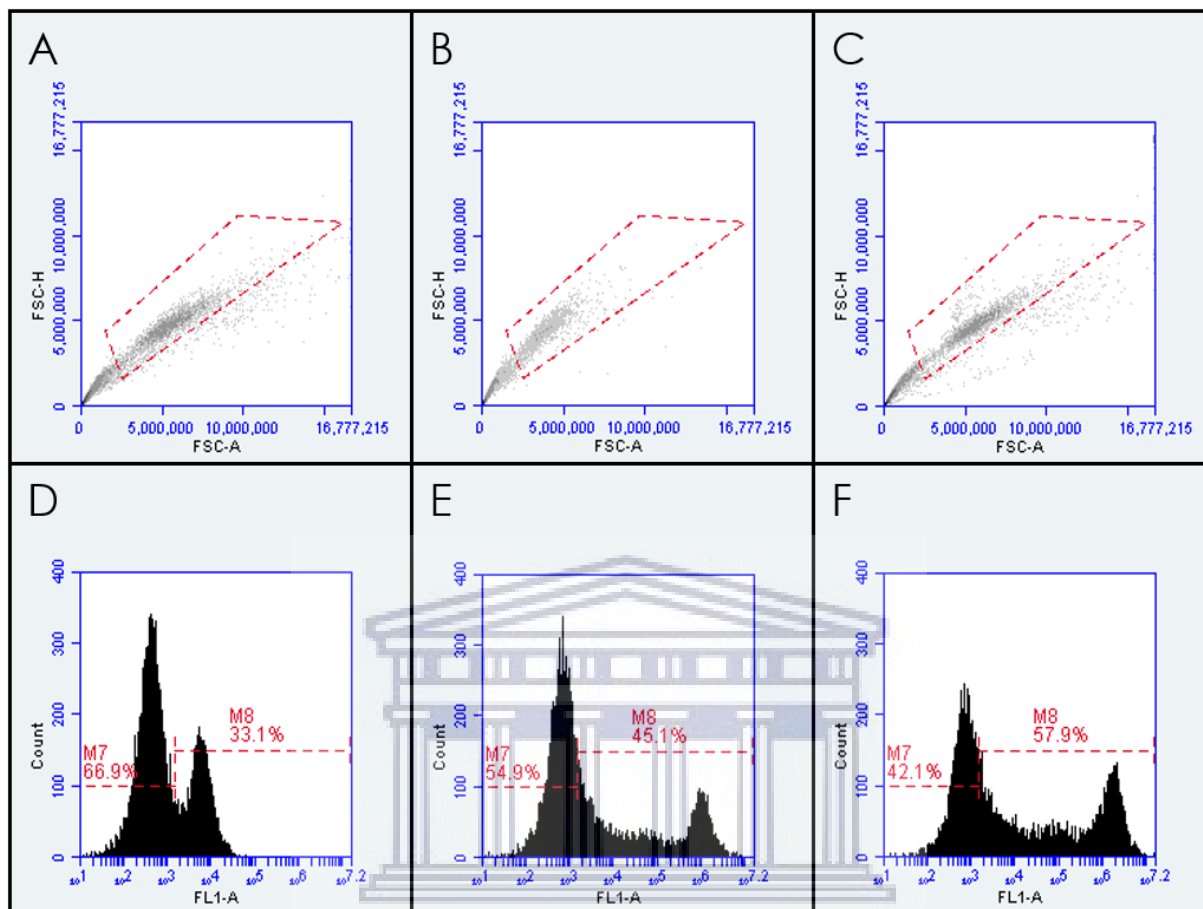


**Figure IV. Representative scatter plots and histograms showing the gating strategy for TM4 cell ROS determination.** **A:** scatter plot for unlabelled negative control cells, **B:** scatter plot for labelled negative control cells; **C:** scatter plot for cells treated with 100  $\mu\text{M}$   $\text{H}_2\text{O}_2$  (positive control), **D:** histogram for ROS determination of the unlabelled negative control; **E:** histogram for ROS determination of the negative control; **F:** histogram for ROS determination of the positive control. The cells were exposed to the indicated treatment for 24 hours and were subsequently labelled with CM- $\text{H}_2\text{DCFDA}$ , except for the unlabelled cells.

## Appendix V

### Information on the target gene: *Gapdh* (*Mus musculus*)

Official full name: glyceraldehyde-3-phosphate dehydrogenase

NCBI Reference Sequence: NM\_001289726.1

Location: Chromosome 6 (125161852-125166467, complement)

Length: 1296 bp

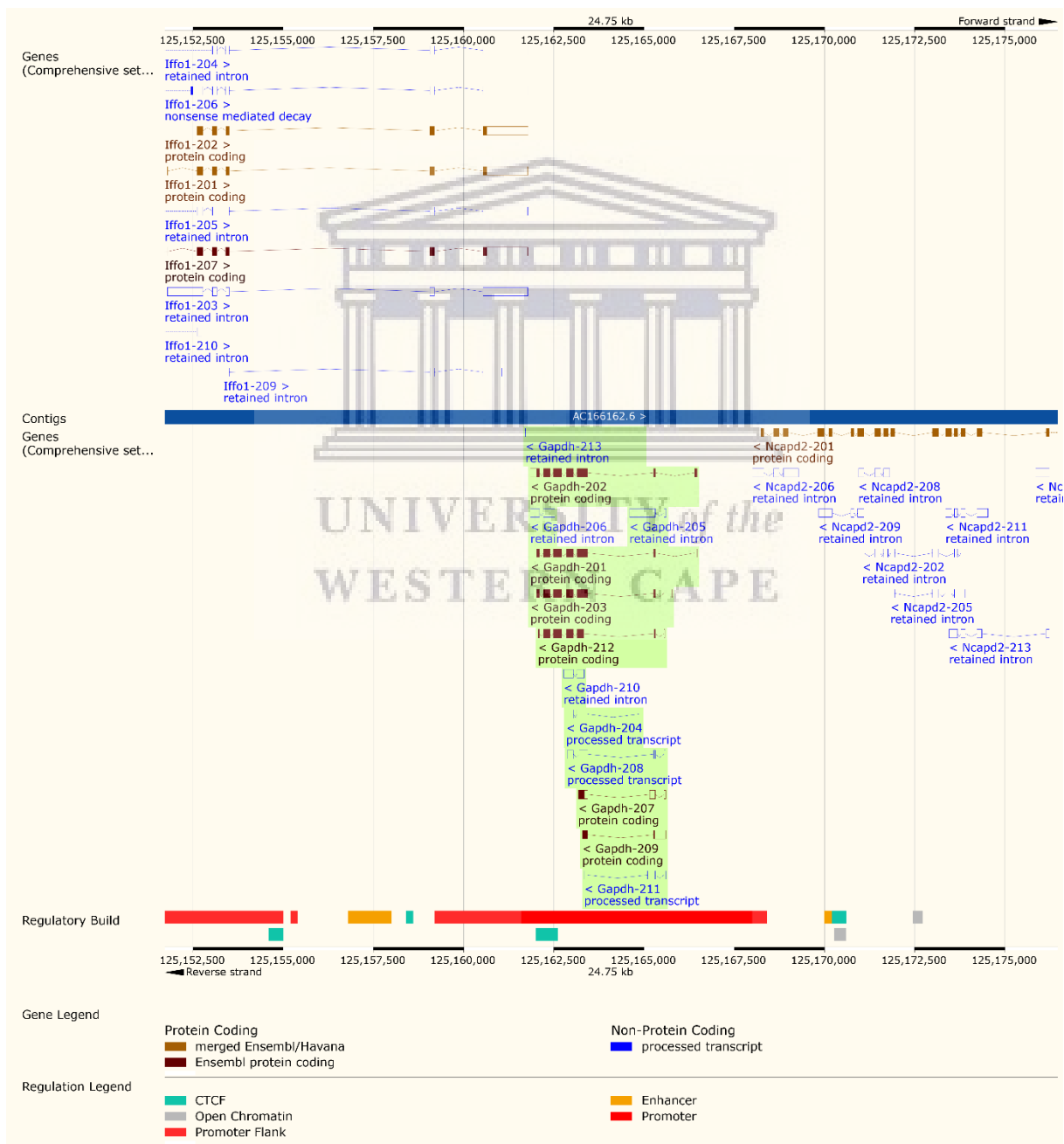


Figure V. Graphic representation of the *Gapdh* gene features (from [www.ensembl.org](http://www.ensembl.org), 2020a).

Primers used for conventional PCR

**Forward Primer** 5'-AACTCAGGAGAGTGTTTCCTCG-3'

**Reverse Primer** 5'-TGATGGGCTCCCGTTGATG-3'

Product length: 252 bp

Primers used for qPCR

**Forward Primer** 5'-GTCCCAGCTTAGGTTTCATCAGGT-3'

**Reverse Primer** 5'-CCAATACGGCCAAATCCGTTTC-3'

Product length: 97 bp

ORIGIN

```

1  aacccttaag agggatgctg cccttaccac ggggctccag cttaggtca tcaggtaac
61  tcaggagagt gtttcctcgt cccgtagaca aatggtgaa ggtcgggtg g aacggattg
121 gccgtattgg ggcgctggtc accagggctg ccattgacag tggcaaagtg gagattgttg
181 ccatcaacga cccttcatt gacctcaact acatgggteta catgttccag tatgactcca
241 ctacggcaa attcaacggc acagtcaagg ccgagaatgg gaagcttgt c atcaacggga
301 agcccatcac catcttcag gagcgagacc ccaetaacat caaatggggg gaggccggg
361 ctgagtatgt cgtggagtct actggtgtct tcaccaccat ggagaaggcc ggggcccact
421 tgaaggggtg agccaaaagg gtcacatct ccgcccttc tgccgatgcc ccatgtttg
481 tgatgggtgt gaaccacgag aatatgaca actactcaaa gattgtcage aatgcatct
541 gcaccaccaa ctgcttagcc ccctggcca aggtcateca tgacaacttt ggcatgtgg
601 aagggtcat gaccacagtc catgccaatca ctgccacca gaagactgtg gatggcccct
661 ctggaaagct gtggcgtgat ggccgtgggg ctgccagaa catcatecct gcatccactg
721 gtgtgccaa ggctgtgggc aaggtcatec cagagctgaa cgggaagctc actggcatgg
781 ccttccgtgt tctaccccc aatgtgtccg tegtggatct gacgtgccgc ctggagaaac
841 ctgccaagta tgatgacatc aagaagggtg tgaagcaggc atctgagggc cactgaagg
901 gcatcttggg ctacactgag gaccaggtg tctcctgca ctcaacagc aactcccact
961 ctccacctt cgatgccggg gctggcattg ctctcaatga caacttgtc aagctcatt
1021 cctggtatga caatgaatac ggctacagca acaggggtgt ggacctcatg gctacatgg
1081 cctccaagga gtaagaaacc ctggaccacc caccacagca aggacactga gcaagagagg
1141 ccctatecca actcgcccc caacactgag catctccctc acaatttcca tcccagacct
1201 ccataataac aggaggggccc tagggagccc tccctactct ctggaatacc atcaataaag
1261 ttcgctgcac ccacaaaaaa aaaaaaaaaa aaaaaa

```



## Appendix VI

### Information on the target gene: *Lhcgr* (*Lh/cgR*) (*Mus musculus*)

Official full name: luteinizing hormone/choriogonadotropin receptor

NCBI Reference Sequence: NM\_013582.2

Location: Chromosome 17 (88716481-88791990, complement)

Length: 2553 bp

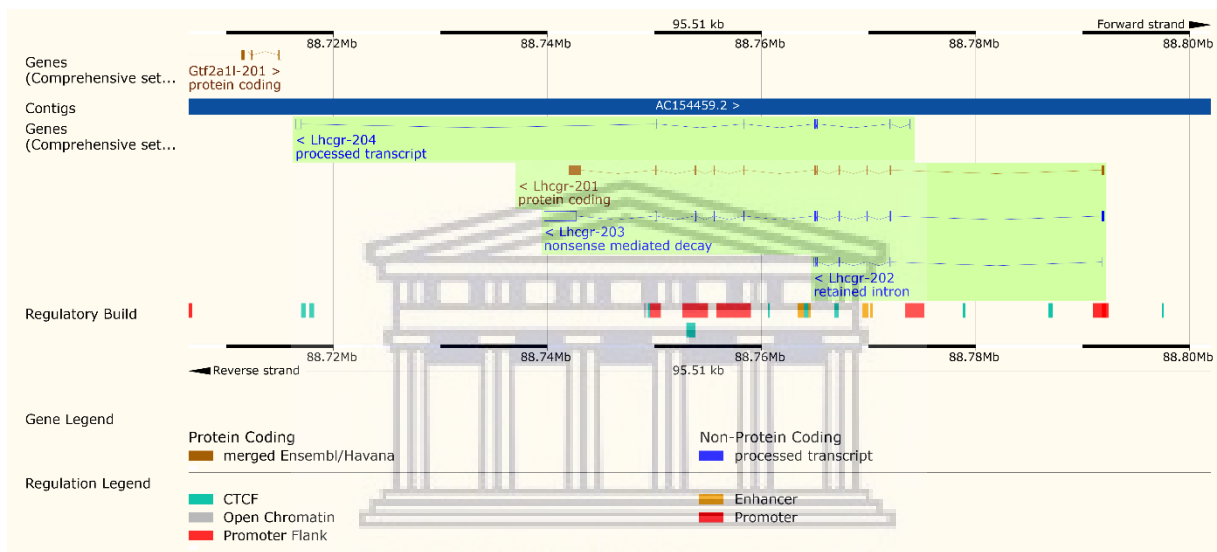


Figure VI. Graphic representation of the *Lhcgr* gene features (from [www.ensembl.org](http://www.ensembl.org), 2020b).

**Forward Primer** 5'-AGAAGCTAATGCCTTTGACA-3'

**Reverse Primer** 5'-CATACAGTTTCAGCGTGATG-3'

Product length: 281 bp

#### ORIGIN

```

1  gggccatggg gcggcgggtc ccggctctga gacagctgct ggtgctggca atgctggtgc
61  tgaagcagtc acagctgcac tctccagagt tgtcagggtc gcgctgccct gagccctgcg
121 actgcgcgcc ggatggtgcc ctgctgctcc ctggccctcg agctggcctc gcccgactat
181 ctctcaccta tctccctgtc aaagtaatcc catcacaagc ttfcagggga cttaatgagg
241 tcgtaaaaat tgaatctct cagagtgatt ccttggaag gatagaagct aatgcctttg
301  accacctcct caatctgtct gaatactga tccagaacac caaaaacctg ctatacattg
361  aaccgggtgc ttttacaac ctccctcggg taaaatacct gagcatctgt aacacaggca
421  tccggaccct ccagatggt tcgaagatct ctctctgga atftaatttc attctggaaa
481  tctgtgataa ctatacata accaccatac cagggaaacg ttccaaggg atgaataatg
    
```

541 agtc **catcac gctgaaactg tatg** gaaatg ggtttgaaga agtacaagc catgcattca  
601 atgggacgac gctaatctcg ctggagttaa aagaaaacat ctacctggag aagatgcaca  
661 gtggcacctt ccagggggcc acggggccca gcctcctgga tgtctcttcc accaaattgc  
721 aggcctgcc gagccacggg ctggagtcca ttcagacgct catcgccaag tcactctact  
781 cactgaaaac tetgcectcc agagaaaaat tcaccagcct actggttgcc acgctgacct  
841 accctagcca ctgctgtgct ttcaggaatt tgccgaagaa agaacagaat tttcatttt  
901 ccattttga aaactttcc aaacaatgtg aaagcacagt tagagaagcg aataacgaga  
961 cgctttatc tgccatctt gaggagaatg aactcagtgg ctgggattac gattatgact  
1021 tctgttacc caagacactc caatgtactc cagaaccaga tgcattcaat cctgtgaag  
1081 atattatggg ctatgccttc cttaggggtg tgattggct aattaatata ctagccatct  
1141 ttggcaactt gacagtctc tttgttctc tgaccagtgc ttataaactg acggtgcccc  
1201 gcttctcat gtgtaatctc tctttgcag acttttgcac ggggctctac ctgctgctca  
1261 ttgcctcagt agactccca acaaaaggcc agtactataa ccatgccata gactggcaga  
1321 cagggagtgg ctgcagtgca gctggcttct ttactgtgtt cgccagtga ctttctgtct  
1381 ataccttac agtcatcact ctggaaagggt ggcacacat cacctatgct gttcagctgg  
1441 accaaaagct gaggetgaga catgccatcc caattatgct cggaggatgg atttttcta  
1501 cctgatggc cacattgccc ctgtgggtg tcagcagtta catgaaagtc agcatctgcc  
1561 tccccatgga tgtggaatcc actctgtcac aagtctacat attatccatc ttgctcctca  
1621 atgcagtggc cttgtctgc atctgtgctt gctacgttag gatatacttt gcagttcaaa  
1681 atccagagct gacggctcct aacaaggaca caaaaattgc taagaagatg gccatcctca  
1741 tcttcacaga ctccacatgc atggcaccca tctcattctt tgccatctca gctgcttca  
1801 aagtaccct tctactgtc accaactcaa aagttctgct ggtcctttt tctctgtca  
1861 attctgtgc caaccattt ctgtacgcag tgttcagaa ggcatttcag agagatttct  
1921 ttctcttgc gagcagattt ggttgctgta agcaccgggc tgaactttac agaaggaagg  
1981 aattttctgc atgtacctc aactccaaa acggtttcc aagatcaagt aagccttccc  
2041 aggetgccct gaagttatcc atagtgcact gcaacaacc tacacctcca agagtgttaa  
2101 ttcagtaact gcattactga attgtatcta aatatgttcc ccccaaaaaa gtccaccaa  
2161 attagtcact ttaatataat gtgttttga aaaaatatt atctttaagc acttcaggtg  
2221 aattgaaacc tgcattcaag ggtggcccaa gacactggg gacataaatt tcagaagggt  
2281 ttgaaaaatt tttataata atttagaaag aatagttttt gttgttgaa tctaatatta  
2341 agaaaatcta agttgtgtc atttccatg tctcttgatc ttttactt caatctgtga  
2401 ttcatgttgc catctctaaa tatatattca taacagactg gaaatttaa gtggtctttg  
2461 tctcagata gttgataaa tacattcaag agatgcactg tgcagcgtga tagctgttag  
2521 ccttacatgg taataaaaag tttcttagcc ata

## Appendix VII

### Information on the target gene: *Star* (*Mus musculus*)

Official full name: steroidogenic acute regulatory protein

NCBI Reference Sequence: NM\_011485.4

Location: Chromosome 8 (25808474-25815982)

Length: 4007 bp

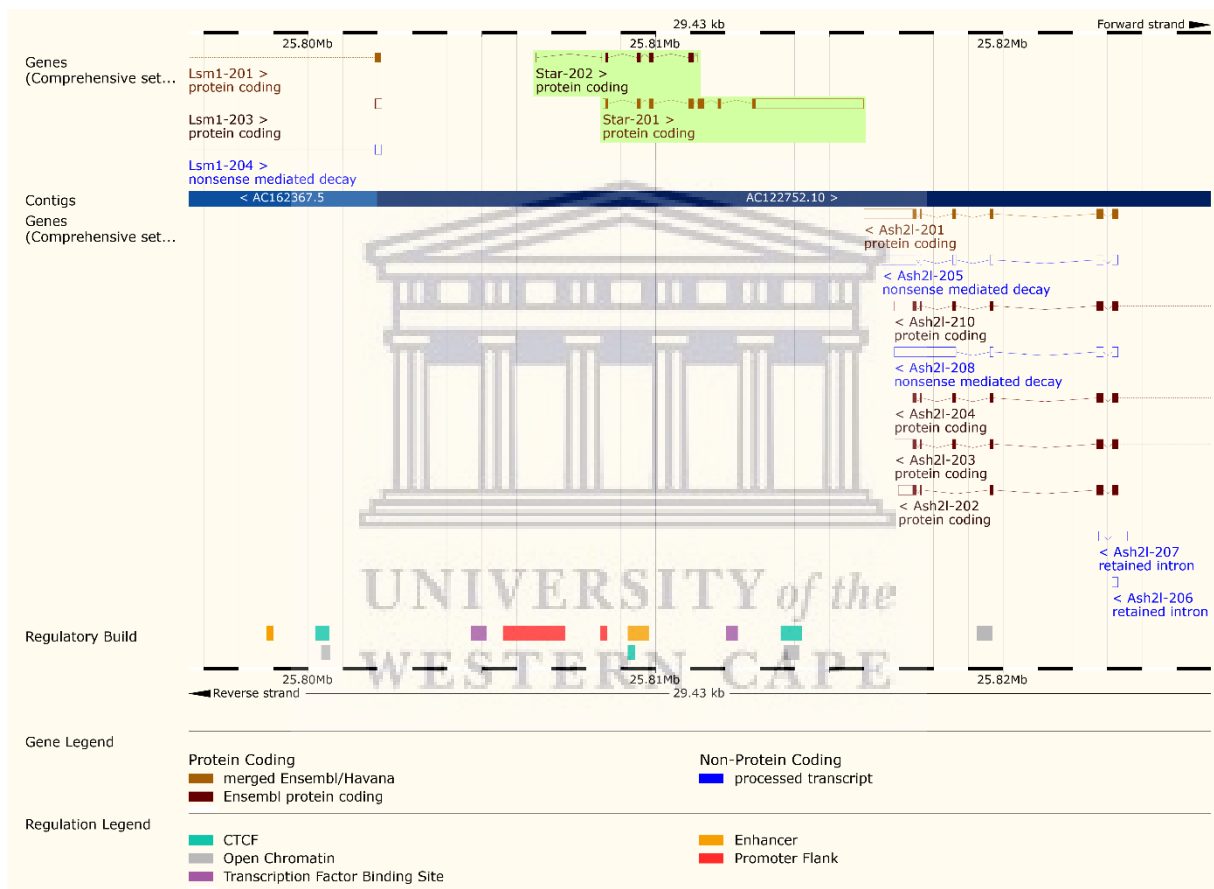


Figure VII. Graphic representation of the *Star* gene features (from www.ensembl.org, 2020c).

**Forward Primer** 5'-AGTATTGACCTGAAGGGGT-3'

**Reverse Primer** 5'-TTACCAGTCAGTCCTAGTGT-3'

Product length: 254 bp

ORIGIN

1 actcaggacc ttgaaaggct caggaagaac aacccttgag cacctcagca ctcagcatgt

61 tcctcgctac gttcaagctg tgtgctggaa gctcctatag acatatgcgg aatatgaaag  
121 gattaaggca ccaagctgtg ctggccattg gccaaagagct caactggaga gcaactggggg  
181 attccagtc cgggtggatg ggtcaagttc gacgtcggag ctctctgctt gggtctcaac  
241 tggaaagcaac actctatagt gaccaggagc tgtcctacat ccagcagggg gaggtggcta  
301 tgcagaaggc ctggggcata ctcaacaacc aggaaggctg gaagaaggaa agccagcagg  
361 agaacggggg cgaagtgcta agtaagatgg tgccagatgt gggcaaggtg ttctgcttgg  
421 aggtgggtgg agaccagccc atggacagac tctatgaaga acttgtggac cgcattggagg  
481 ccatggggaga gtggaacca aatgtcaagg agatcaaggt cctgcagagg attggaanaag  
541 acacggatc cactcatgag ctggctgcgg cggcagcagg caacctgggt gggcctcgag  
601 acttctgtgag cgtgcgctgt accaagcgcg gaggttccac ctgtgtgctg gcaggcatgg  
661 ccacacattt tggggagatg cgggagcaga gtgggtgcat cagagctgaa cacggcccca  
721 cctgcatggt gcttcatcca ctggctggaa gtcctccaa gactaaactc acttggctgc  
781 tcagattga cctgaagggg tggctgccga agacaatcat caaccaggte ctatcgcaga  
841 cccagataga gttcgccaac cacctgcgca agcgcctgga agccagccct gcctctgagg  
901 cccagtgtta aggactgtcc accacattga cctgcaaatc attggaagct ctacacaggaa  
961 gcctgcaagt ctgtccatct tcagetaaca gcatcggggag ggggtgtagt caggagacac  
1021 taggactgac tggtaaac aate aggatcagca aatagaaat gaggcttaga ataaaagttc  
1081 tctagtgtct cccactgcat agctgtgaag gctaagggat aagtagctat gaaaccttc  
1141 atctaggctt gtatatgctg acctaaaaga caccagcagc tacgaacagg ggatgctaag  
1201 gatcgggaac tgtgtctta ccagctcca atgtcactac ctgaaggcag tgtgcacaca  
1261 aagcaaggte ttgcctagga aactctgtaa aagttctct ctgtaaagg ccagaacttg  
1321 aatgaaacta cctacaagg gcctttccag agtattccaa ctttctctg aggagaaatg  
1381 aaaccatcat tgtgccgact tccctactaa tcccatgaca ataaagaaca tacatgcaca  
1441 cttcagcctg tacatgtcag gtcccagcct gaggaatcac agcttcagca gaactctgcg  
1501 cttaaatec ctagctcaca aaaggggaca aaacgtccgg agatttatgt catttgactg  
1561 tttagattct ttctaaaaa ggcaatctca taattaaagg cacgtgcctt taatcccaac  
1621 actcaagtgg cagaggcagg tggattttt ctaatactga ggctaacctg gtctacacag  
1681 aaggatagcc agagctacat aatgagactg tctcaaaacc acaaaacca gggattgaa  
1741 agatggctga cctgttggga gcacaagctg ctcttccaag gaatccaggg tcaatctcca  
1801 gcatccacac agcagctccc aactctaatt ctagtcccag ggaacctgat gccctctgt  
1861 ggccgcatg gggaccagg atgcaagtgg tacatagaca tacagatag taggctgaac  
1921 accattaac attaacaaca aaaccttgt cgggcacggg ggctcaacag cttaaatctc  
1981 aacactgca atggtgacac cagtgaatcg ctccaagttc caggccagct tggaccccag  
2041 tgagaccgtc tcacaaaagc aggaacaaaa tcttggggag tggtagtta gattaacagc  
2101 atcctggcag gaagattatg acgggattt catttaccta tactgatcaa ataatactga  
2161 ccaataatgt taagataaag tgaactgtct attgtttata gacagattag atgccagcct  
2221 ggctcagagc tagcagcttc ctatttgaa aaggttaaa tgttatgta cttctagga  
2281 agacaaatag ctagaagtca gtagagctat aacattctg ttccaggatt tggagatatt  
2341 acacttaag ggtataaatt gggagccagg tgacgggtggc acacgacttt aatcccagta  
2401 gaggcagggt gatctctga gtttgaagtc agcctggttt acagagtaag ttccagga  
2461 gtcagggctg taaatagag aatgctgct caaaaacata aaaaataaa aatgacaaaa  
2521 atataagtgt gaccagcaaa atgactcagg gtgtaagtgc ttgccacca gtctgatgat

2581 ggcagaagcc acagagatgg aaggagagag atgaaaaaca gaggtcctta tggctgctta  
2641 tctacactaa gtaccttaca cacataaata ctggtatata ttggaattcc ttccgaatg  
2701 tgtaaggat gaacaattct aacaaccgaa agcttttcat tctaagcatg aaaaaaaaaa  
2761 aaagtaatgt ctgtgtgagt gtgcatgggc cccagcagac acgtggaggf cagaggacaa  
2821 cttcaggagt gtgccttca cccccaccg ggtcttgggt cctggattgt tagggtaggc  
2881 agcaagcact tcatccgca gtgccatfff gctggcccac tttctgtcc cttatcgtgt  
2941 gggtaacccc catcatttgc aaagaactga gcttattat gaatagaaca atgtggaaca  
3001 tgtacttatt tattgaagtc ttaagccttc actgatattt attgctcacc tcggtgcttt  
3061 aaggtgagcg agggcagctg tagagtgttt ctgatagaac catcccggga atcagttaag  
3121 agagcagcca cttgggtgct gaaagacca tgtgtgccgg cctcgagaca acaggctgcc  
3181 agtggagaag cgccttcagc aaacactgtg gctttgattg gattagtgtt tgctcctata  
3241 cacaccgta ctctatctct gccgtctggg atgtttgacc cttttgta atcttatatt  
3301 ttaataaaag cagtgtcacc tggcattctg atacctatag atgggtagta gttcttttt  
3361 aatctttcaa acgaacctta ttaacacatt caagtttaca actgtacaca ctttttttt  
3421 ttcttglttc actcaattg ttcttttgag acaggatctt ctactcatt ctgtagccca  
3481 agatggcctg gaacttatat caacccttct gcctctgcct ctcaagtgtt gggattaatg  
3541 gtggggcctg caggcatctg ggcatttttt tcagacactg ctaagtactg tcaagcacct  
3601 tgataacttc taatgcagga aagccaggta cacaaacag taggtagaca ggagacctgg  
3661 gcatggttat gtgccaacac ccaactatac ttcttccaag accatcactt cactttcttc  
3721 agagtcttc gaacaccgat gagctcattc tacaagctgg cttgttcttt cttggactag  
3781 tccttgcatf agtggttatc tagcagctgg taggctgtga ccccagcttt aataatgca  
3841 gacaccccaa agaaggcata gcaagacaga tttctgtcag ttggaagcca gtcaggctat  
3901 atggacagac cttgcctcaa aaaagcaaaa aaagatattc aatgtatgaa agaagtttgg  
3961 gggattcagc agcagacaag tatattaat tgtgtaata gtcattc



(This page was intentionally left blank)



UNIVERSITY *of the*  
WESTERN CAPE

## Appendix VIII

### Information on the target gene: *Tspo* (i.e. *Pbr*) (*Mus musculus*)

Official full name: translocator protein

NCBI Reference Sequence: NM\_009775.4

Location: Chromosome 15 (83563592-83574203)

Length: 871 bp

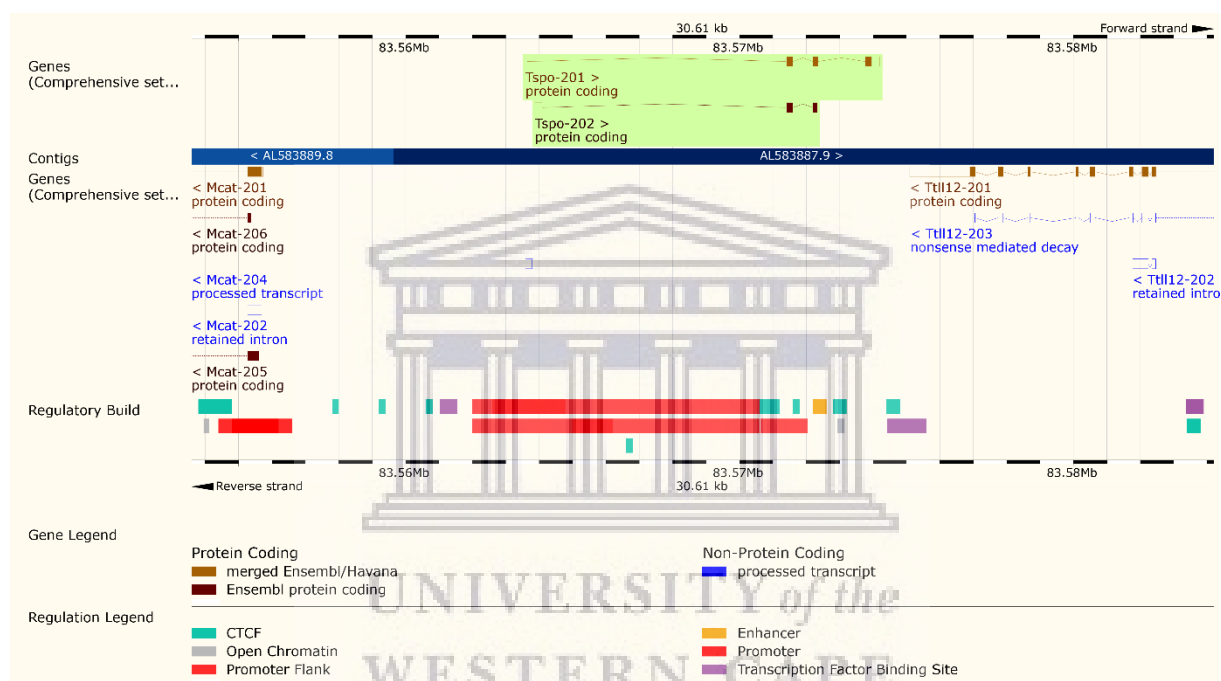


Figure VIII. Graphic representation of the *Tspo* gene features (from www.ensembl.org, 2020d).

**Forward Primer** 5'-AACATCAGTTGCAATCACCA-3'

**Reverse Primer** 5'-TATGTAGGAGCCATACCCCAT-3'

Product length: 217 bp

### ORIGIN

```

1  gtcagcggct accaacctct gtgcgcagtg tccttcacgg aacaaccagc gactgcgtga
61  gcggggctgt ggatctttcc agaacatcag ttgcaatcac caatgcctgaa tcttgggtgc
121 ctgccgtggg cctcactctg gtgccagacc tggggggcct catgggagcc tactttgtac
181 gtggcgaggg cctccggtgg tatgctagct tgcagaacc ctcttggcat ccgcctcget
241 ggacactggc tccatctgg ggcacactgt attcagcc atggggtatggc tctacatag
301 tctggaaaga gctgggaggt ttacagagg acgctatggt tccttgggt ctctacactg
    
```

361 gtcagctggc tctgaactgg gcgtggcccc ccatcttctt tgggccccgg cagatgggct  
421 gggccttggc cgatcttctg cttgtcagtg ggggtggcgac tgccacaacc ctggcttggc  
481 accgagtgag cccgcccggct gcccgcttgc tgtaccctta cctggcctgg ctggcttttg  
541 ccaccgtgct caactactat gtatggcgtg ataactctgg ccggcgaggg ggctcccggc  
601 tcccagagtg aaggcaccca gccatcagga atgcagccct gccagccagg caccatgggt  
661 ggcagccatc atgcttttat gaccattggg cctgctggtc tacctggtct tagcccagga  
721 agccaccagg taggttaggg tggtcagtgc cgagtctct gcagacacag ttatactgc  
781 ctttctgcac tgcctcaggc atgcccttag agcatgggtt ttaaaagcta aataaagtct  
841 ctaacttcat gtgtaaaaaa aaaaaaaaaa a



UNIVERSITY *of the*  
WESTERN CAPE



## Appendix IX

### Information on the target gene: *Cyp11a1* (i.e. *P450scc*) (*Mus musculus*)

Official full name: cytochrome P450, family 11, subfamily a, polypeptide 1

NCBI Reference Sequence: NM\_019779.3

Location: Chromosome 9 (58006411-58027023)

Length: 1774 bp

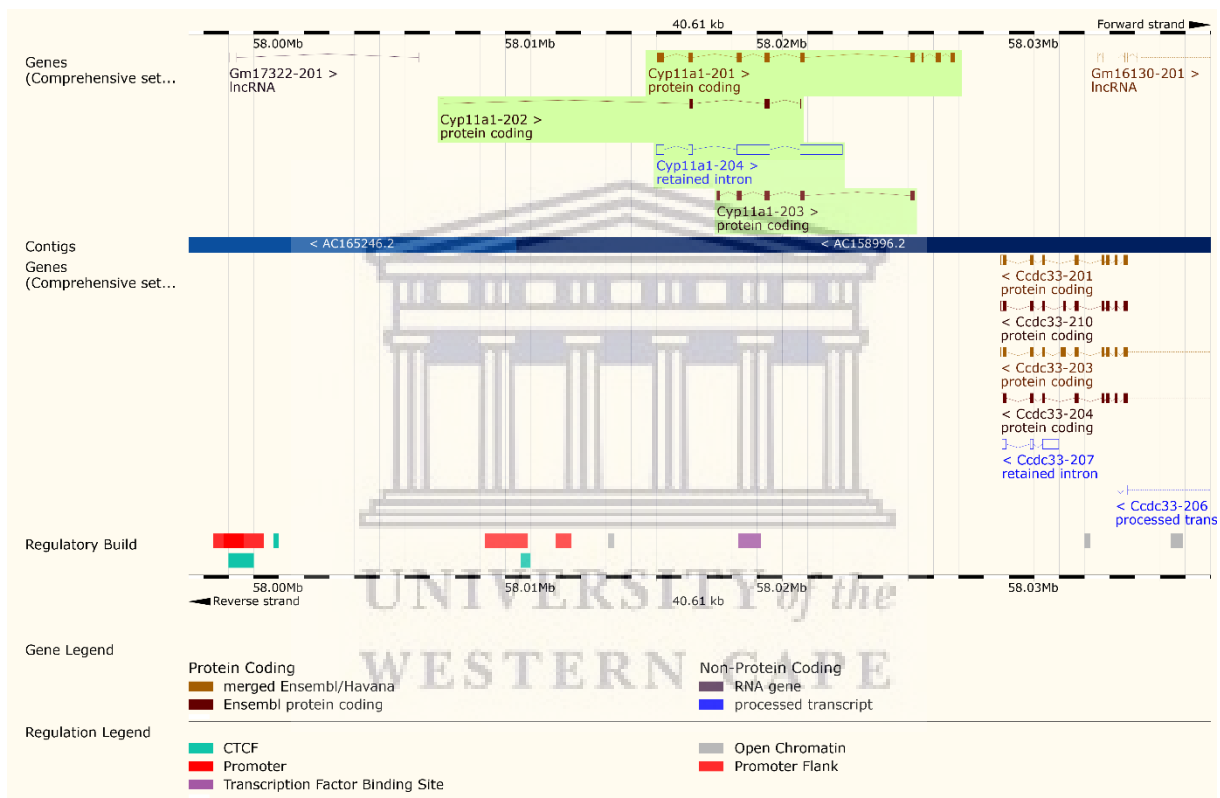


Figure IX. Graphic representation of the *Cyp11a1* gene features (from www.ensembl.org, 2020e).

**Forward Primer** 5'-GGGTCCTGTTAAGAGTTCA-3'

**Reverse Primer** 5'-CGCTCCCCAAATATAACACT-3'

Product length: 241 bp

#### ORIGIN

```

1  aagtggcagt cgtggggaca gtatgctggc taaaggactt tccctgcgct cagtgctgg
61  caaaggctgc caaccttcc tgagccctac gtggcagggt ccagtgctga gtactggaaa
121 gggagctggg accttacta gcagtcctag gtcctcaat gagatccctt ccctggcga
    
```

181 caatggttgg ctaaacctgt accacttctg gagggagagt ggcacacaga aatccatta  
241 ccatcagatg cagagtttcc aaaagtatgg ccccatftac agggagaagc tgggcacttt  
301 ggagtcagtt tacatcgtgg accccaagga tgcgtcgata ctcttctcat gcgagggctc  
361 caaccggag cggttccttg tgccccctg ggtggcctat caccagtatt atcagaggcc  
421 cattggggtc ctgtttaaga gttcagatgc ctggaagaaa gaccgaatcg tctaaacca  
481 agaggtgatg gcgcctggag ccatcaagaa cttcgtgcc ctgctggaag gtgtagetca  
541 ggacttcac aaagtcttac acagacgcat caagcagcaa aattctggaa atttctcagg  
601 ggtcatcagt gatgacctat tccgctttc ctttgagtcc atcagc agtg ttatatttg  
661 ggagcgc catg gggatgctgg aggagatcgt ggatcccag gcccagcggg tcatcaatgc  
721 tgtctaccag atgttccaca ccagtgtccc catgctcaac ctgcctccag acttcttctg  
781 actctcaga actaagacct ggaaggacca tgcagctgcc tgggatgtga tttcaataa  
841 agctgatgag tacaccaga acttctactg ggacttaagg cagaagcag acttcagcca  
901 gtaccctggg gtctttata gctctctggg gggcaacaag ctgcccctca agaacatcca  
961 ggccaacatt accgagatgc tggcaggagg ggtggacacg acctccatga cctgcagtg  
1021 gaacctttat gagatggcac acaactttaa ggtacaggag atgctgcggg ctgaagtcct  
1081 ggtgcccgg cgccaggccc agggagacat ggccaagatg gtacagttgg ttccactct  
1141 caaagccage atcaaggaga cactgagact ccacccatc tccgtgacct tgcagagga  
1201 cactgtgaat gacctggtgc ttcgtaatta caagattcca gccaaagactt tggtagcgg  
1261 ggctagcttt gccatgggtc gagatccggg ctctttccc aatccaaaca agtttgacc  
1321 aactcgttg ctggaaaaa gccaaatac caccacttc cggacttgg gctttggctg  
1381 ggggttccg cagtgtctg gccggcggat tgcggagctg gagatgacca tctctctat  
1441 caatctgctg gagaacttca gaattgaagt tcaaatctc cgtgatgtgg ggaccaagtt  
1501 cagctcatc ctgatgctg agaaccccat cctcttcaac ttccagcctc tcaagcagga  
1561 cctgggcca gccgtgacca gaaagacaa cactgtgaac tgaaggctgg agtcacatgg  
1621 ggaggtggcc catggggcat ttgaggggtg tctctctgta tctcagaaa cagcactctg  
1681 tgattacctg cccaggttag ctgggctctc ctctcttca tctctttcc ctcttccct  
1741 accagggag ttaataaaca cttgaacact gagg

## Appendix X

### Information on the target gene: *Cyp17a1* (*Mus musculus*)

Official full name: cytochrome P450, family 17, subfamily a, polypeptide 1

NCBI Reference Sequence: NM\_007809.3

Location: Chromosome 19 (46667165-46673000, complement)

Length: 1841 bp

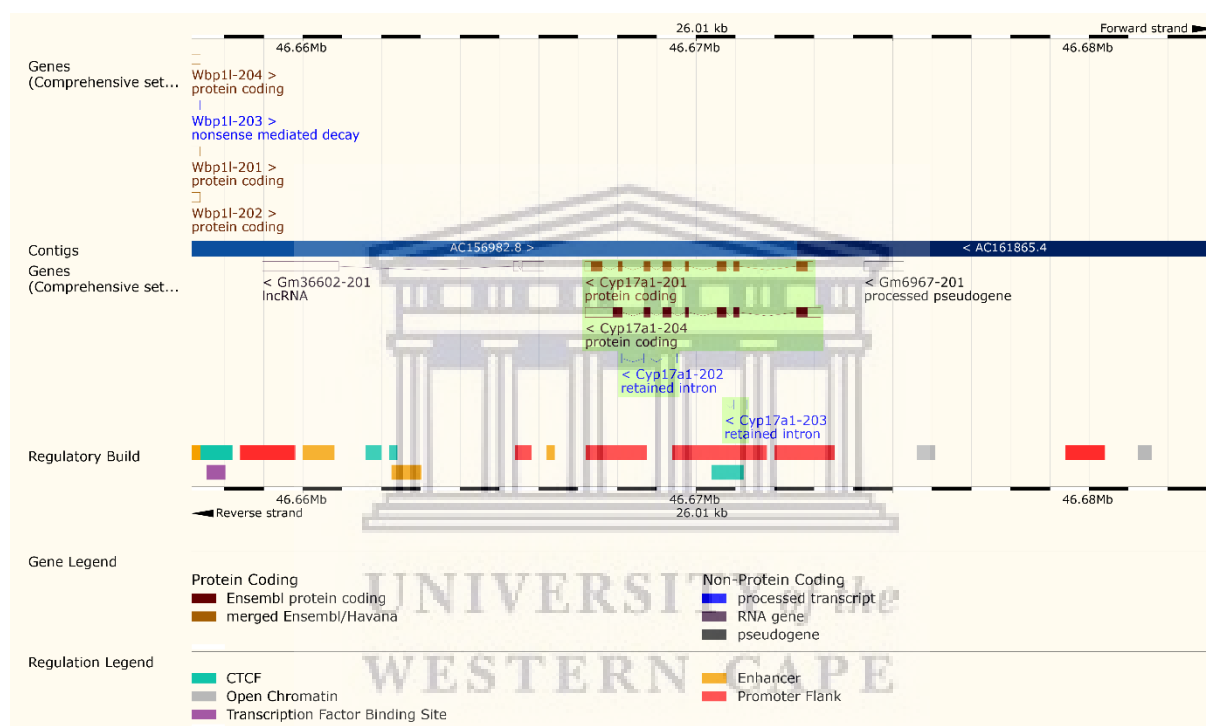


Figure X. Graphic representation of the *Cyp17a1* gene features (from [www.ensembl.org](http://www.ensembl.org), 2020f).

Forward Primer 5'-TGATATGTCAGGAAGCCAAC-3'

Reverse Primer 5'-GGAAAATCTCAACCACGG-3'

Product length: 241 bp

### ORIGIN

```

1  caggcttggg gacactccag gataaacttc tgcaggccaa gagataacac gtcttcaagg
61  tgacaatcag aaacgccttt taaagttct ccttctctgc tgaattgct gtagcttctc
121 cactccacag ctggccatct gcctacacct ggctgcatg tgggaacttg tgggtctctt
181  gctgctcacc ctggcctatt tctttggcc caagtcaag acacctaag ccaagttccc
241  caggagcctt ccattcctgc cctgggtggg tagtctaccg ttctccca gacgtggtca
    
```

301 tatgcatgcc aacttctca agctgcagga aaagtatggt cccatctatt ctcttcgct  
361 gggfaccaca actgcagtga ttgtcggtea ctatcagctg gccagagaag tgctcgtgaa  
421 gaaggggaaa gaattctctg gtcggcccca gatggtgact ctaggcctct tgcggacca  
481 aggaaaagge gtcgcctttg cggatagtag tagctctgg cagctgcacc ggaagctggt  
541 attcagcacc tttccctgt tcagggatga ccagaaactg gagaagatga tatgtcagga  
601 agccaactca ctgtgtgact tgatacttac atacgacggg gagtcccag atctgtctac  
661 gctcatcttc aagtcagtaa tcaatatacat ctgtaccatc tgcttcaaca tctctttga  
721 gaacaaggat ccgatactga ctaccataca gacctttaca gagggtattg tggatgtcct  
781 gggccacage gatctggtgg acatattc ccgtggfgaag attttccca ataaaaactt  
841 ggaaatgata aaggaacaca ctaaaattcg agaaaaaaca ctggttgaaa tgtttgaaaa  
901 atgcaaggag aattcaata gtgaatctct ctccagcctg acagacattc tgatacaagc  
961 caagatgaat gcagaaaata ataacttg ggaaggccag gaccaagtg tgttctcaga  
1021 taagcatatc ctgtcaccg tgggagacat cttggggca ggcatagaga caactagctc  
1081 tgtgctgaac tggatcctgg ctttctggt gcacaatcct gaggtgaaga ggaagatcca  
1141 aaaggagatt gaccagtatg taggcttcag tcgaacaccg tcttcaatg accggactca  
1201 cctctcatg ctggaggcca ctatccgaga agtgcttctg atcaggccgg tggccccctt  
1261 gctcatecca cacaaggeta acattgactc cagcattgga gagttgcca tcccgaagga  
1321 cacacatgtg atcatcaatc tctgggcact gcatacagat aaaaatgaat gggaccagcc  
1381 agatcggttt atgctgagc gcttcttga tccaacagga agccatctca ttacaccac  
1441 accagttat ttgccctcg gagctggtcc ccgacgtgc attggagagg ctctggcccg  
1501 gcaggagctc ttatcttca tggccttget gctgcagagg ttgactttg atgtgcaga  
1561 tgacaaacag ctgccctgtc tgggtgggtga cccaaggtg gctttctga tcgaccctt  
1621 caaagtgaat atcacagtgc gacaagcatg gaaggatgca caggttgagg tttagcacta  
1681 gaggcgaat ctaacgtccc ggateccatg ccttgacacc cacagccca tcttagaggt  
1741 gctccaaca atctctctca ctctatccc gtttctact tggcagcaat gaagggtgag  
1801 acacatatta aaggtttcc aataaacatc tctgagctgt c

## Appendix XI

### Information on the target gene: *Hsd17b3* (17 $\beta$ -hsd 3) (*Mus musculus*)

Official full name: hydroxysteroid (17-beta) dehydrogenase 3

NCBI Reference Sequence: NM\_008291.3

Location: Chromosome 13 (64058266-64089230, complement)

Length: 1286 bp

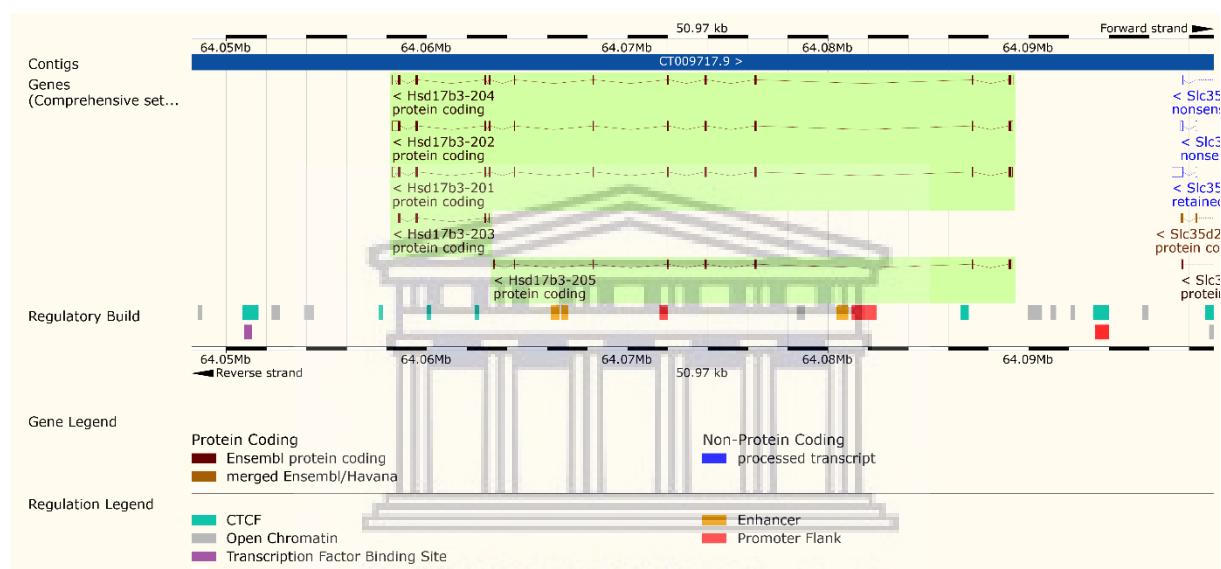


Figure XI. Graphic representation of the *Hsd17b3* gene features (from www.ensembl.org, 2020g).

**Forward Primer** 5'-TATTCAGGTGCTGACCCCTTA-3'

**Reverse Primer** 5'-TGTTGCGTTTGAGGTAATCT-3'

Product length: 251 bp

#### ORIGIN

```

1  ttgcctggg aatcacacgg ggataaagac caggtccagc agcatctcca gcaagacagc
61  tccagaggag gccatggaga agctcttcat tgctgcaggg ctcttcgtgg gctctggttg
121  cctggtgaag tgcatgaggt tctcgcagca ccttttctg aggttctgca aggctttgcc
181  aagctcttc ctgcgatcaa tgggacaatg ggcagtgatt accggagcag gcgatggcat
241  cgggaagcc tattcattg agttggccag acatggactc aatggtgtac ttattagtcg
301  gacactggaa aagctacaga ccattgcaga agagattgag aggaccactg gaagctgtgt
361  gaagattgta caagcagatt ttaccagaga agacatctat gaccatatta aagaacacct
421  tgaaggctta gaaataggaa ttttagtcaa caacgttga atgctcccca gcttttccc
    
```

481 aagccatttc ctgagcaactt ccggtgagag ccagaatctc atccactgca acattacctc  
541 cgtagtcaag atgacacagc ttgttctcaa acacatggag tcaaggagga aaggcctcat  
601 cttgaatatt tcttcaggcg cagcccttcg tcctggcct ctttacagcc tgtactcagc  
661 ttccaaggct tttgtgtaca cttttccaa ggctctgagt gtggaataca gagataaagg  
721 aatcattatt caggtgctga ccccttattc ttttcaacc ccaatgaca agtacctaaa  
781 taacaagatg accaagaccg ccgatgagtt tgttaaagaa tccttgaat atgtcacgat  
841 cggagctgaa tcctgtggct gccttgctca tgaatcatt gcaataattc tgaaccggat  
901 ccttccaga atcttctata gcagcaccgc tcaacgattc ctctgacac gatactcaga  
961 ttacctcaaa cgcaacatca gcaacagata gtgggggaag ggtgtgtgtg ggggggtaga  
1021 gttaggggtg ggtgggggta gggtgagggtg gggctggagg gagagttgag aaggacatcc  
1081 agagctcttc attggtagta gtggccagag ggtggtgacc cttgacctcc tgaaggagg  
1141 cttccatgc cacaggcaca gtgtgcagtt gttggaattc agagatctta ggaaaagctg  
1201 ggggtaaag gctgtgttcc tataaaaggg aggctggcat caagggaaat gctggaagaa  
1261 cccctcccc caataataa atatac



UNIVERSITY *of the*  
WESTERN CAPE

## Appendix XII

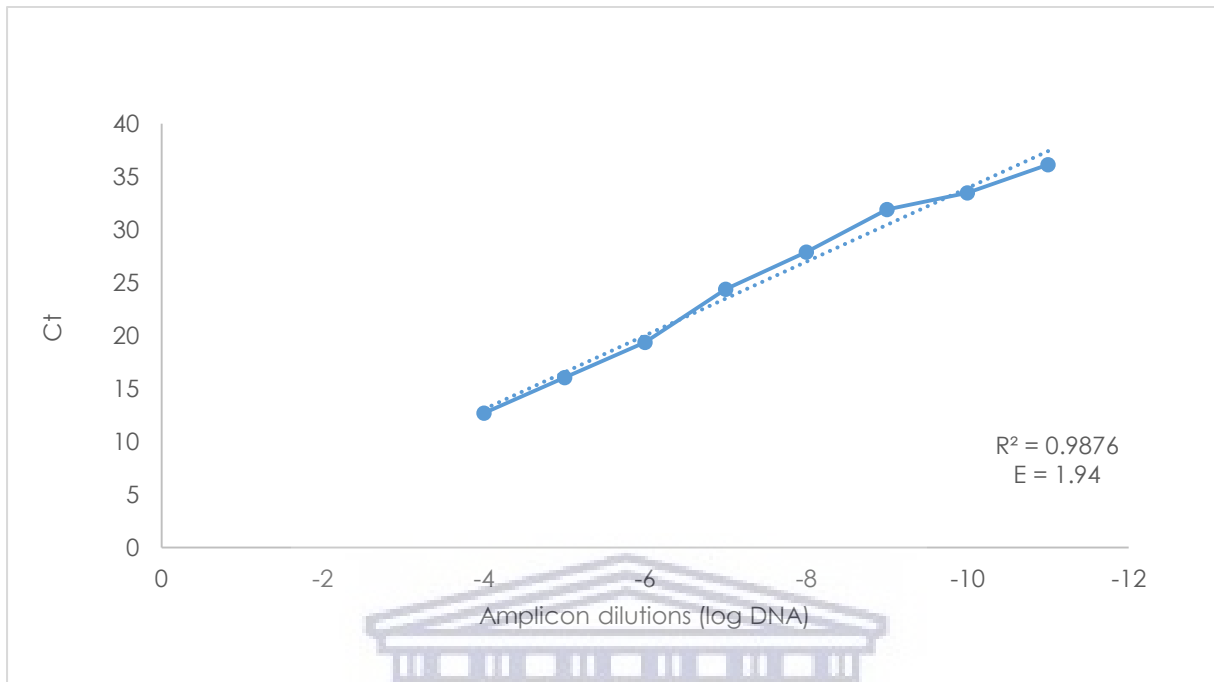


Figure XII. Graph showing the standard curve used for *Gapdh* quantitation by qPCR.

## Appendix XIII

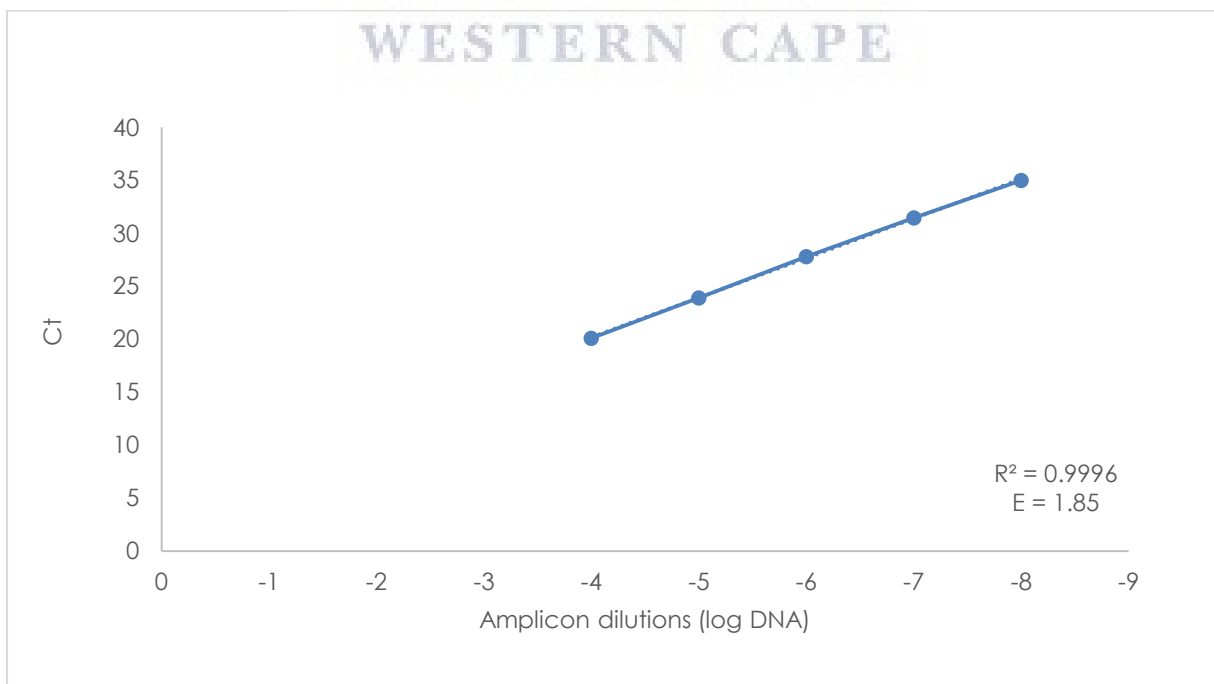


Figure XIII. Graph showing the standard curve used for *Star* quantitation by qPCR.

## Appendix XIV

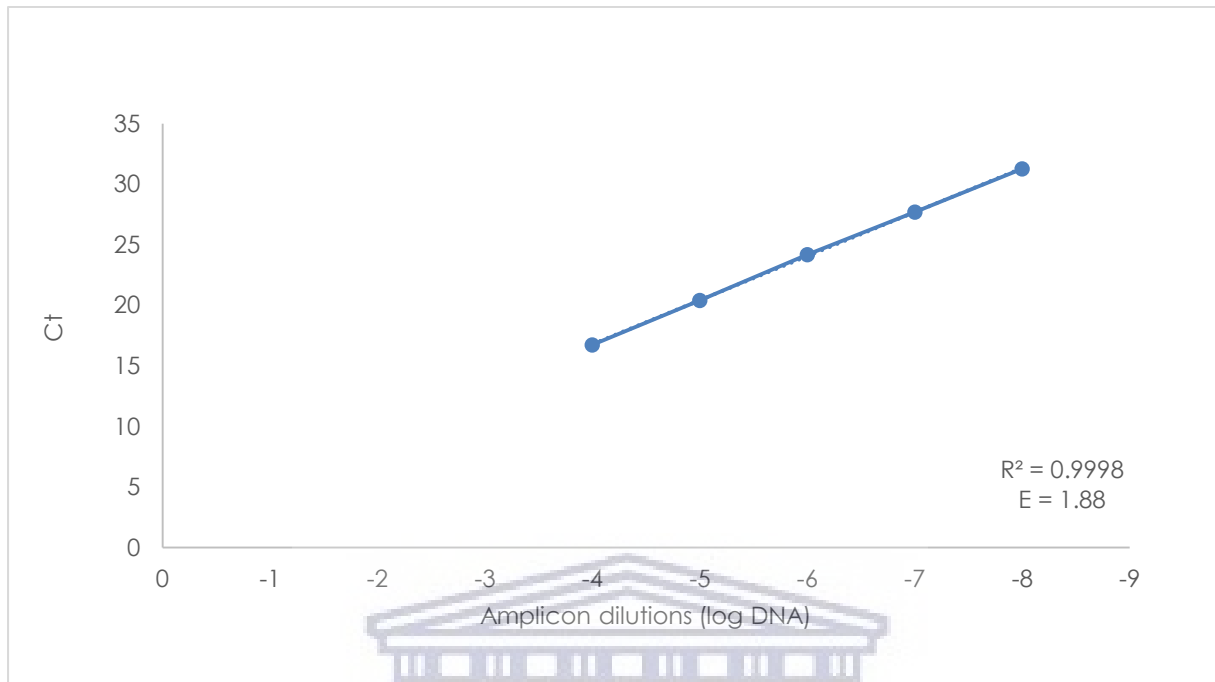


Figure XIV. Graph showing the standard curve used for *Tspo* quantitation by qPCR.

## Appendix XV

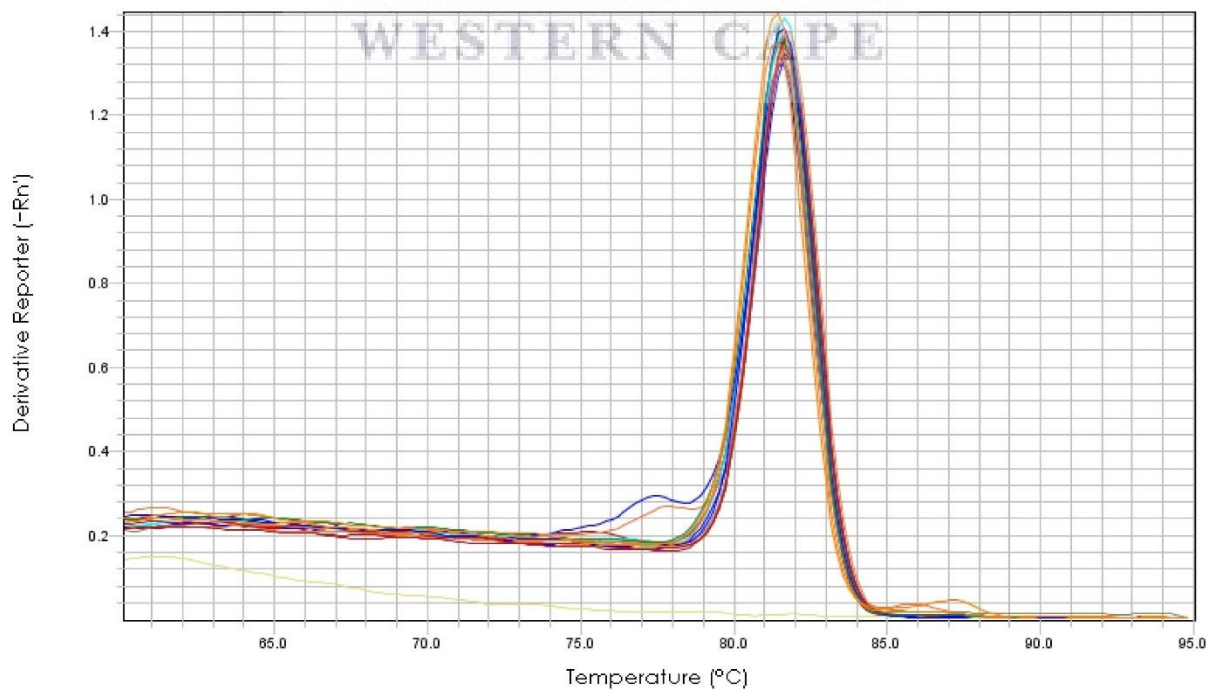


Figure XV. Graph showing a melting curve for *Gapdh* qPCR.



## Appendix XVI

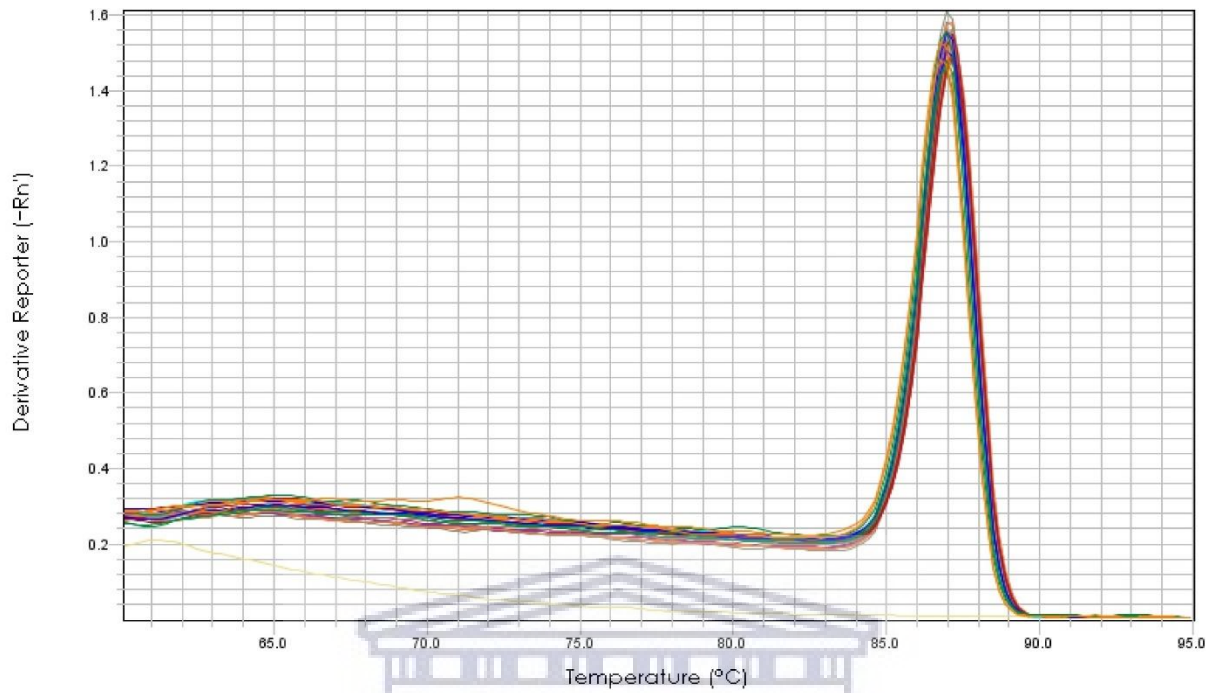


Figure XVI. Graph showing a melting curve for *Star* qPCR.

## Appendix XVII

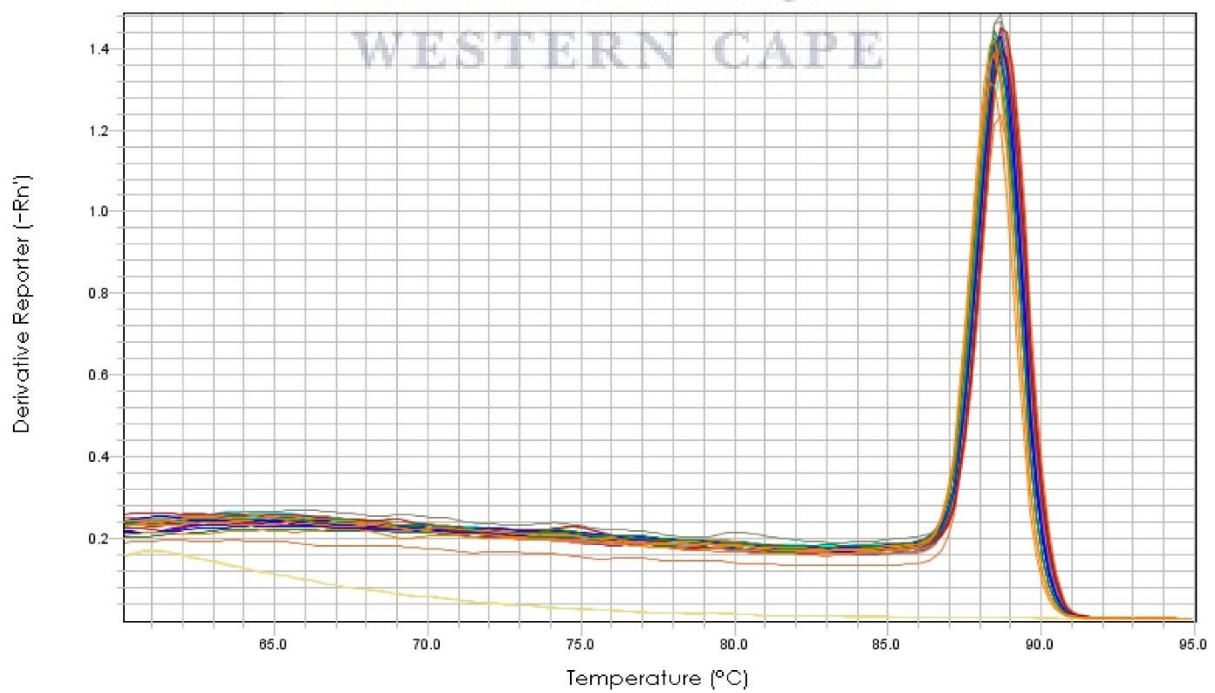
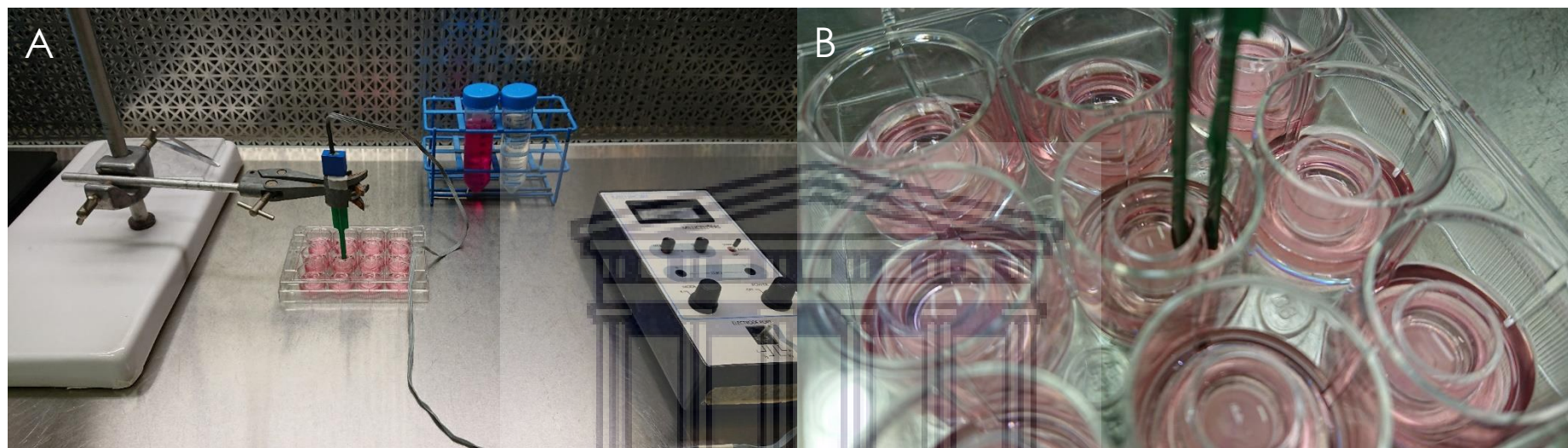


Figure XVII. Graph showing a melting curve for *Tspo* qPCR.

## Appendix XVIII



**Figure XVIII.** Photographs of the apparatus used for measuring transepithelial electrical resistance. **A:** An overview of the TEER setup, **B:** A close-up view showing how the chopstick electrodes were positioned during a TEER measurement.

UNIVERSITY of the  
WESTERN CAPE

